THE UNIVERSITY OF QUEENSLAND

AUSTRALIA

Bayesian methods to treat geotechnical uncertainty in risk-based design of open pit slopes

Luis-Fernando Contreras

A thesis submitted for the degree of Doctor of Philosophy at The University of Queensland in 2019

School of Civil Engineering

Geotechnical Engineering Centre

Abstract

Common questions asked during the process of mine design are “how much geotechnical information is required for an acceptable design” and “how to measure its confidence”. These are key aspects associated not only with the determination of parameters but more generally with the definition of the geotechnical model for design.

The definition of the geotechnical model for slope design is based on four main components including the geological, structural, rock mass and hydrogeological models. Each model is described by different sets of information and parameters and is defined at a scale of interest for the purpose of the analysis of slope behaviour. In the area of slope design in particular, the estimation of geotechnical parameters is normally supported by small data sets, which are evaluated with simple statistical procedures based on frequentist concepts. The geotechnical model defined in this manner lacks a proper measure of its confidence levels, which in turn complicates judging the sufficiency of data and precludes planning the data collection based on strategy at the various stages of project development.

The Bayesian approach is an alternative route to the conventional probabilistic methods used in slope design. The approach is based on a particular interpretation of probability and provides a suitable framework to treat uncertainty in the geotechnical model for slope design. Two important features of the approach are the possibility of combining data with subjective information and the ability to quantify the uncertainty of the parameters or models given the available data. The first point is especially relevant in the area of mine slope design considering that subjective information such as expert opinion or engineering judgement is a common element present in the geotechnical design process. The second point provides a contrast with the situation within the frequentist approach where the uncertainty measures apply to the data rather than to the parameters or models, which are the objects of interest to the analyst.

The first part of the research focused on reviewing the concepts of uncertainty and probability to derive the arguments supporting the statement that the Bayesian approach offers a better framework for the quantification of uncertainty in the slope design process. The result of this work is illustrated with simple examples and is described in detail in the two papers included as Chapters 3 and 4. The second part of the research was aimed at

demonstrating the use of the Bayesian approach for the inference of geotechnical parameters in typical situations encountered during the design of rock slopes. The examples presented in the papers included as Chapters 3 to 6 refer to the rock mass strength parameters of the Hoek-Brown criterion. These examples were used to highlight the advantages of the methodology for the quantification of geotechnical uncertainty.

The core procedure of the Bayesian approach for the inference of parameters is the evaluation of the posterior probability function. There are various methods to evaluate this function as described briefly in Chapter 2. However, the specific method used in the research is the Markov Chain Monte Carlo (MCMC) simulation. This method was selected because it can be easily applied by the geotechnical practitioner using existing tools, without relying too much on the use of intricate mathematical procedures. Chapter 2 presents a summary of the principles of this technique and describes the more common MCMC algorithms. Nevertheless, all the analyses included in the thesis were carried out with a powerful MCMC sampler named 'emcee', which was developed and is used extensively by the astrophysics community. The sampler, as well as the models presented in the thesis, are coded in the Python programming language.

The cases of Bayesian interference of parameters covered by the research include the intact rock strength parameters σ_{ci} and m_i, and the geological strength index (*GSI*) from the Hoek-Brown strength criterion. The analysis of *GSI* was based on a correlation commonly used in the design of mine slopes that relates *GSI* with the rock mass factors block volume (V_b) and joint condition (J_c). Moreover, the research also included the use of the geotechnical parameters inferred with the Bayesian approach for the analysis of the reliability of the slope and the back-analysis of slope failure to illustrate how the observed performance of the slope could be used to update the parameters. The Bayesian analysis involving the stability of the slope require an explicit representation of the slope model that can be incorporated into the posterior function. Therefore, the topic of construction of a surrogate model using the response surface (RS) methodology is also discussed in detail.

The research served to identify the main features of the Bayesian methodology that make it a suitable approach for the quantification of the geotechnical uncertainty in the slope design process in mining projects. The examples presented showed the benefits of the approach by contrasting the results with those from conventional frequentist methods.

Declaration by author

This thesis is composed of my original work, and contains no material previously published or written by another person except where due reference has been made in the text. I have clearly stated the contribution by others to jointly-authored works that I have included in my thesis.

I have clearly stated the contribution of others to my thesis as a whole, including statistical assistance, survey design, data analysis, significant technical procedures, professional editorial advice, financial support and any other original research work used or reported in my thesis. The content of my thesis is the result of work I have carried out since the commencement of my higher degree by research candidature and does not include a substantial part of work that has been submitted to qualify for the award of any other degree or diploma in any university or other tertiary institution. I have clearly stated which parts of my thesis, if any, have been submitted to qualify for another award.

I acknowledge that an electronic copy of my thesis must be lodged with the University Library and, subject to the policy and procedures of The University of Queensland, the thesis be made available for research and study in accordance with the Copyright Act 1968 unless a period of embargo has been approved by the Dean of the Graduate School.

I acknowledge that copyright of all material contained in my thesis resides with the copyright holder(s) of that material. Where appropriate I have obtained copyright permission from the copyright holder to reproduce material in this thesis and have sought permission from co-authors for any jointly authored works included in the thesis.

Publications during candidature

Published peer-reviewed journal papers:

Contreras, L.F., Brown, E.T., Ruest, M., 2018. Bayesian data analysis to quantify the uncertainty of intact rock strength. *Journal of Rock Mechanics and Geotechnical Engineering*, 10(1), 11-31.

Contreras, L.F., Brown, E.T., 2019. Slope reliability and back analysis of failure with geotechnical parameters estimated using Bayesian inference. *Journal of Rock Mechanics and Geotechnical Engineering*, 11(3), 628-643.

Llano-Serna, M.A., **Contreras, L.F.**, 2019. The effect of surface roughness and shear rate during fall-cone calibration. Geotechnique, article number 18-P-222R1, (accepted for publication).

Published peer-reviewed conference papers:

Contreras, L.F., Ruest, M., 2016. Unconventional methods to treat geotechnical uncertainty in slope design. In: Dight P, editor. *Proceedings of the First Asia- Pacific Slope Stability in Mining Conference*, Brisbane, Australia. Perth: Australian Centre for Geomechanics, 315-330.

Contreras, L.F., Brown, E.T., 2018. Bayesian inference of geotechnical parameters for slope reliability analysis. *Slope Stability Symposium 2018*, Seville, Spain. Bco Congresos, 1998-2026.

Contreras, L.F., Hormazabal, E., Ledezma, R., Arellano, M., 2019. Geotechnical risk analysis for the closure alternatives of the Chuquicamata open pit. In: Wesseloo J, editor. *Proceedings of the First International Conference on Mining Geomechanical Risk*, Perth, Australia. Perth: Australian Centre for Geomechanics, 373-388.

Publications included in this thesis

Contreras, L.F., Ruest, M., 2016. Unconventional methods to treat geotechnical uncertainty in slope design. In: Dight P, editor. *Proceedings of the First Asia-Pacific Slope Stability in Mining Conference*, Brisbane, Australia. Perth: Australian Centre for Geomechanics, 315-330. – incorporated as Chapter 3.

Contributor	Statement of contribution
Contreras, L.F. (Candidate)	Conception and layout (100%) Analysis and interpretation (100%) Drafting and production (95%)
Ruest, M.	Drafting and production (5%)

Contreras, L.F., Brown, E.T., Ruest, M., 2018. Bayesian data analysis to quantify the uncertainty of intact rock strength. *Journal of Rock Mechanics and Geotechnical Engineering*, 10(1), 11-31. – incorporated as Chapter 4.

Contributor	Statement of contribution
Contreras, L.F. (Candidate)	Conception and layout (100%) Analysis and interpretation (95%) Drafting and production (90%)
Brown, E.T.	Analysis and interpretation (5%) Drafting and production (5%)
Ruest, M.	Drafting and production (5%)

Contreras, L.F., Brown, E.T., 2018. Bayesian inference of geotechnical parameters for slope reliability analysis. *Slope Stability Symposium 2018*, Seville, Spain. Bco Congresos, 1998-2026. – incorporated as Chapter 5.

Contributor	Statement of contribution
Contreras, L.F. (Candidate)	Conception and layout (100%) Analysis and interpretation (100%) Drafting and production (90%)
Brown, E.T.	Drafting and production (10%)

Contreras, L.F., Brown, E.T., 2019. Slope reliability and back analysis of failure with geotechnical parameters estimated using Bayesian inference. *Journal of Rock Mechanics and Geotechnical Engineering*, 11(3), 628-643. – incorporated as Chapter 6.

Contributor	Statement of contribution
Contreras, L.F. (Candidate)	Conception and layout (95%) Analysis and interpretation (95%) Drafting and production (95%)
Brown, E.T.	Conception and layout (5%) Analysis and interpretation (5%) Drafting and production (5%)

Contributions by others to the thesis

Professor Ted Brown critically reviewed the journal and conference papers included with this PhD thesis. Professor Marc Ruest contributed to the production of the first two papers.

Statement of parts of the thesis submitted to qualify for the award of another degree

None.

Research involving human or animal subjects

None.

Acknowledgements

I would like to express my gratitude to Professor Marc Ruest for making possible my participation in this research and for his support as Principal Advisor during the first stage of the study and to Professor David Williams who acted as Principal Advisor during the final stage of the research. Special thanks are extended to Dr Tony Dutton and Dr Alan Huang for their assistance as Associate Advisors. Special thanks are due to Emeritus Professor Ted Brown for his encouragement, advice and review of the manuscripts. Finally, I would like to express my gratitude to my friends and colleagues in SRK and UQ for their encouragement during the whole research period.

Financial support

The research on which this thesis is based was funded by the Large Open Pit II Project through contract no. 019799 with the Geotechnical Engineering Centre (GEC) of the University of Queensland (UQ). This support was canalised through the Research Higher Degree Scholarship providing a living allowance stipend. I also would like to acknowledge the tuition fees award provided by the UQ International Scholarship. Finally, I want to acknowledge the financial support provided by SRK Consulting South Africa.

Keywords

Geotechnical uncertainty, probabilistic methods, Bayesian updating, Hoek-Brown criterion, rock slope reliability, back analysis of failure.

Australian and New Zealand Standard Research Classifications (ANZSRC)

ANZSRC code: 090501, Civil Geotechnical Engineering, 100%

Fields of Research (FoR) Classification

FoR code: 0905, Civil Engineering, 100%

Table of Contents

List of figures

List of tables

List of abbreviations

BTS	Brazilian tensile strength
CC	Coefficient of correlation
CDF	Cumulative distribution function
CI	Confidence interval
DTS	Direct tensile strength
DSS	Direct shear strength
ESS	Effective sample size (in an MCMC analysis)
FORM	First order reliability method
FS	Factor of safety
H-B	Hoek-Brown (strength criterion or parameters)
HDI	Highest density interval
HMC	Hamiltonian Monte Carlo
LEM	Limit equilibrium method
LSS	Limit state surface
M-C	Mohr-Coulomb (strength criterion or parameters)
MC	Monte Carlo
MCMC	Markov chain Monte Carlo
MCSE	Monte Carlo standard error (in an MCMC analysis)
M-H	Metropolis-Hastings (MCMC procedure)
NLLS	Nonlinear least squares
pdf	Probability density function
PF	Probability of failure
PI	Prediction interval
PLT	Point load test
RS	Response surface
SORM	Second order reliability method
TCS	Triaxial compression strength
TSS	Total sample size (in an MCMC analysis)
UCS	Uniaxial compression strength

List of notations

α, α_1	Correlation factors between BTS and DTS and between PLT and UCS
β	Reliability index
$\Gamma()$	Gamma function
Δ_{PF}, Δ_{β}	Maximum absolute errors in the estimation of *PF* and β in a reliability analysis
δ_i	Response factor of variable *i* to define a response surface
ε	Error to account for model uncertainty in the generic formulation of the Bayesian model for inference of parameters
θ	Vector with the uncertain parameters in the generic formulation of the Bayesian model for inference of parameters
v	Normality parameter of t-distribution
ξ_i	Input factor of variable *i* to define a response surface
ρ_i	Coefficients for calibration of the GSI chart (*i* = 0 to 2 for a three-parameter model and *i* = 0 to 4 for a five parameter model)
σ	Standard deviation of the normal distribution or scale parameter of t-distribution
σ_1, σ_3	Major and minor principal stresses
σ_{ci}, m_i, a	Parameters of the Hoek-Brown intact rock strength criterion
σ_t	Tensile strength in the Hoek-Brown strength envelope
$\Phi^{-1}[\ ]$	Inverse of the standard normal cumulative distribution function
ϕ_b	Basic friction angle of rock discontinuities
ϕ_p	Peak friction angle of rock discontinuities
c, ϕ	Cohesion and friction angle parameters of the Mohr-Coulomb strength criterion
D	Rock mass disturbance factor of the Hoek-Brown strength criterion
GSI	Geological strength index of the Hoek-Brown strength criterion
IS_{50}	Point load index
JC	Joint condition rating as used in the GSI chart from Hoek et al. (2013)
J_c	Joint condition factor from Palmström (1996)
JRC	Joint roughness coefficient of the Barton-Bandis joint strength criterion
JCS	Joint compression strength of the Barton-Bandis joint strength criterion
$\boldsymbol{R}$	Correlation matrix for the calculation of β with the FORM

r	Vector with the certain parameters in the generic formulation of the Bayesian model for inference of parameters
RQD	Rock quality designation index as used in the GSI chart from Hoek et al. (2013)
RMR	Rock mass rating as defined by Bieniawski (1989)
u, h, d	Universe, hypothesis and data sets in the definition of Bayes' rule
V_b	Block volume of rock mass
x^*	Value of variable x at the design point in a reliability analysis

Chapter 1 - Introduction

1.1 Background

Probabilistic methods are used to quantify uncertainty in engineering design. However, there are two approaches of analysis known as frequentist and Bayesian, which are based on different interpretations of probability (Christian, 2004). The frequentist approach relies on repeated sampling and produces point estimates and error measures of parameters. In comparison, the Bayesian approach uses prior knowledge and data to define posterior probability distributions to represent the uncertainty of parameters. The first part of the research was devoted to contrast the two approaches and to gather the arguments supporting the statement that Bayesian methods provide a better framework for the quantification of uncertainty in slope design. The second part of the research was aimed at demonstrating the use of the Bayesian approach for the inference of geotechnical parameters in typical situations encountered during the design of rock slopes.

1.2 Statement of the problem

A notable drawback of the design process of mine slopes is the lack of a suitable approach to quantify the confidence of the geotechnical information, including data, parameters and models used in the design. Probabilistic methods are commonly used to represent and quantify uncertainty in the slope design process. However, there are no clear guidelines with regard to the appropriate methods to use in specific situations, and most of the techniques of analysis used correspond to the frequentist approach, which has limitations when data is scarce and engineering judgement is required. A consequence of this situation is that the geotechnical engineer does not have the appropriate tools to judge the sufficiency of the available data, nor to define strategies for collection of additional data on a rational basis, as the project progresses.

The research is guided by the argument that Bayesian statistical methods are a better option to quantify the uncertainty of the geotechnical model for slope design. Methods of Bayesian statistics have been applied in many scientific fields such as physics, astronomy, biology, and social sciences, and in areas of engineering such as the oil and gas industries and in the dam and foundation design disciplines. However, these methods are not used in the area of geotechnical analysis for mine design, either because they are unknown to this geotechnical community or because they are perceived as complicated and difficult to apply.

Notable advantages of Bayesian methods over conventional frequentist methods in terms of the problems confronted in the geotechnical design process are:

(1) Bayesian methods provide the answer to the question of interest to the geotechnical engineer, i.e. “what is the probability of the hypothesis (or model) being true given the data?” Frequentist methods address the reverse question, i.e. “what is the probability of the data given the hypothesis?”

(2) Bayesian methods make use of both, prior information on the hypothesis (or model) being examined and the likelihood of data, to provide a balanced answer to the question of interest. Frequentist methods on the other hand only use the data, which is assumed to be the result of a random process.

(3) The results of the Bayesian analysis are richer, including probability distributions and correlation characteristics of the parameters investigated. The frequentist results consist of a point estimate and an error measure of the parameters.

1.3 Research objectives

The purpose of the research is to examine the use of Bayesian methods to deal with geotechnical uncertainty in the design of mine slopes and to provide recommendations in terms of procedures of analysis that could be incorporated into routine practices of slope design. The evaluation of these techniques shall focus on the ability of the approach to:

(1) Quantify the confidence of the geotechnical parameters at different stages of the open pit development.

(2) Combine in a rational way data from geotechnical investigations with subjective information from engineering judgment to produce a balanced result between the two inputs.

(3) Facilitate judging the sufficiency and quality of data at different stages of open pit development.

1.4 Methodology

The definition of the geotechnical model for slope design is based on four main components; including the geological, structural, rock mass and hydrogeological models (Stacey, 2009). Due to the extent and variety of aspects of the uncertainty map in the slope design process, the research focuses on those items used in routine slope design tasks, which are under the direct control of the geotechnical engineer. In particular, the research includes the intact rock and the rock mass quality parameters that form part of the rock mass model. The research also considers some aspects of the slope stability model required to incorporate performance measurements as an additional source of data to update the geotechnical parameters.

The method of analysis is based on constructing a probability distribution function called a posterior function using the Bayes rule, and the evaluation of this function for the inference of the parameters of interest contained in the function. The posterior distribution function combines a model representing a particular behaviour of interest, data corresponding to measurements of this behaviour, and the prior information on the parameters defining the model. The inference of parameters requires the evaluation of the posterior function. The objective is to find the sets of values that produce the minimum differences between model predictions and data, i.e. minimum errors. This condition corresponds to the maximum values of the posterior function.

There are various methods to evaluate the posterior function as described briefly in Chapter 2. However, the specific method used in the research is the Markov Chain Monte Carlo (MCMC) simulation. This method was selected because it can be easily applied by the geotechnical practitioner using existing tools, without relying too much on the use of intricate mathematical procedures. Chapter 2 presents a summary of the principles of this technique and describes the more common MCMC algorithms. The analyses included in the thesis were carried out with a powerful MCMC sampler named ‘emcee’, which was developed and it is used extensively by the astrophysics community (Foreman-Mackey et al., 2013). The sampler, as well as the models presented in the thesis, are coded in the Python programming language (Phyton Software Foundation, 2001). The sampler with the characteristics described was selected in order to focus the research on the applications rather than on the intricacies of the MCMC algorithm. The MCMC analysis is used to draw representative samples of the parameters investigated, providing information on their best estimate values, variability and correlations.

1.5 Thesis structure

This thesis uses a format that incorporates published papers produced during the PhD candidature. It consists of seven chapters, with four of them containing the four papers covering the subject of the thesis. The papers included in Chapters 3 to 6 are arranged in a logical sequence consistent with the development of the topics studied. However, there is some degree of overlapping of the topics presented in these chapters because the papers were originally structured to be self-contained units for independent publication. This means that the papers contain basic concepts from the literature review required to build threads that facilitate the presentation of the subjects.

The format of the published versions of the papers was slightly modified to be consistent with the format of the thesis. These changes include the numbering of the sections, figures, tables and equations, and the format of the references. Similarly, minor changes in the text of the first paper (Chapter 3) were required to maintain the coherence with the content of the subsequent papers.

The first chapter introduces the thesis and includes the background of the subject, statement of the problem, research objectives, methodology, and thesis structure.

The second chapter presents the literature review, including discussions on the nature of uncertainty, the probabilistic approaches to deal with uncertainty in geotechnical engineering, the Bayesian approach of statistical analysis and the Markov chain Monte Carlo (MCMC) algorithm used in Bayesian analysis. More specific aspects of the literature review are covered in the papers included in Chapters 3 to 6.

The chapters third to sixth include the four papers produced during the PhD candidature. The purpose of these chapters is to present the topics covered during the research, highlighting the benefits of the proposed methods relative to the current approach, and giving a general perspective of the issue of the handling of uncertainty in slope design with the Bayesian approach of statistical analysis. The examples included in the papers only cover the rock mass strength part of the geotechnical model for slope design, as a large part of the manuscripts were devoted to discussing the concepts of uncertainty quantification and the contrast between the Bayesian and classical approaches of statistical analysis.

The seventh chapter presents a summary of the most significant findings and conclusions from the research, and discuss the aspects requiring a future study that serve as suggested topics for further research. These include the assessment of sufficiency of data and the hierarchical model for inference of parameters from slope performance, including the Bayesian analysis of the rock joint strength parameters.

1.6 Links between included papers

The thesis includes four papers presented in a logical and coherent order, supporting the objectives of the research. Table 1.1 shows the connection between the papers and the topics covered in the thesis.

Table 1.1 Links between thesis topics and included papers

Topic	Paper description
Geotechnical uncertainty in slope design	**Contreras, L.F.**, Ruest, M., 2016. Unconventional methods to treat geotechnical uncertainty in slope design. In: Dight P, editor. *Proceedings of the First Asia-Pacific Slope Stability in Mining Conference*, Brisbane, Australia. Perth: Australian Centre for Geomechanics, 315-330.
Bayesian inference of intact rock strength parameters	**Contreras,** L.F., Brown, E.T., Ruest, M., 2018. Bayesian data analysis to quantify the uncertainty of intact rock strength. *Journal of Rock Mechanics and Geotechnical Engineering*, 10(1), 11-31.
Slope reliability using rock mass parameters from Bayesian analysis	**Contreras, L.F.,** Brown, E.T., 2018. Bayesian inference of geotechnical parameters for slope reliability analysis. *Slope Stability Symposium 2018*, Seville, Spain. Bco Congresos, 1998-2026.
Updating of geotechnical parameters from back analysis of slope failure	**Contreras,** L.F., Brown, E.T., 2019. Slope reliability and back analysis of failure with geotechnical parameters estimated using Bayesian inference. *Journal of Rock Mechanics and Geotechnical Engineering*, 11(3), 628-643.

Paper-I in Chapter 3 presents a general discussion on the types of uncertainty found in geotechnical engineering and describes two classes of unconventional approaches to deal with uncertainty in engineering design. The first corresponds to the Bayesian inference of parameters, highlighting the advantages of this approach over the conventional frequentist methods used in slope design. This is the approach treated in more detail in the remaining chapters. The second consists of non-probabilistic approaches especially suited to deal with uncertainty related to imprecision due to incompleteness of information. These methods include interval analysis and procedures based on the possibility and evidence theories.

Paper-II in Chapter 4 presents a detailed description of the Bayesian method for inference of parameters applied to the analysis of the intact rock strength using the Hoek-Brown (H-B) strength criterion. The paper includes two case examples to illustrate different aspects of the Bayesian methodology and to contrast the approach with frequentist techniques. These include the nonlinear least-squares method of regression and the use of confidence and prediction intervals to measure uncertainty. The work for this paper was developed in 2017 and for this reason, the regression analysis used tensile strength data, which was allowed with the 2002 edition of the H-B strength criterion (Hoek et al., 2002) valid at the time. The updated version of the H-B strength criterion published in 2019 (Hoek and Brown, 2019) excludes the use of data in the tensile region, which is a change that was incorporated in the example presented in Paper-IV. Nevertheless, the essence of the arguments and conclusions presented in Paper-II remain relevant, and the analyses using tensile strength data serve to show the capability of the Bayesian regression method to handle situations where the errors are defined in different directions of the model space.

Paper-III in Chapter 5 describes a Bayesian methodology in which typical data from laboratory tests and site investigations are used to define representative distributions of the geotechnical parameters, and the use of these results for the evaluation of the reliability of a slope using the first-order reliability method (FORM). In addition to the estimation of the intact rock strength parameters described in the previous chapter, the paper also describes a methodology for the inference of the geological strength index (GSI) reflecting the rock mass quality. The Bayesian reliability procedure requires the use of a surrogate slope model constructed with the response surface (RS) methodology. The paper presents an example of a slope evaluated with an RS based on limit equilibrium analyses with the slope model, using H-B strength parameters as well as equivalent Mohr-Coulomb (M-C) parameters. This example serves to highlight the advantages of using the posterior distributions from the Bayesian analysis for the assessment of the slope reliability using the FORM approach.

Paper-IV in Chapter 6 extends the methodology presented in Paper-III for the analysis of the reliability of the slope, which is considered a forward analysis of stability, to include a back-analysis of slope failure. The back analysis is used within the Bayesian approach to update the estimation of the input parameters according to their uncertainty, which is determined by the amount of data supporting them. The methodology is illustrated using the same example of a rock slope described in the previous chapter, incorporating updates for the inference of the intact rock strength parameters according to the latest edition of the H-B strength criterion, as well as for the analysis of GSI data. This example is used to highlight the advantages of using Bayesian methods for the slope reliability analysis and to demonstrate the ability of the Bayesian approach to incorporate information from slope performance for the updating of the geotechnical parameters. In particular, the example shows how the amount of data from the geotechnical investigations affect the results of the updating process from the back analysis of failure.

References

Christian, J.T., 2004. Geotechnical Engineering Reliability: How Well Do We Know What We Are Doing? *Journal of Geotechnical and Geoenvironmental Engineering*, 130(10), 985–1003.

Foreman-Mackey, D., Hogg, D.W., Lang, D. and Goodman, J., 2013. emcee: The MCMC Hammer. *Publications of the Astronomical Society of Pacific*, 125(925), 306–312.

Hoek, E. and Brown, E.T., 2019. The Hoek – Brown failure criterion and GSI – 2018 edition. *Journal of Rock Mechanics and Geotechnical Engineering*, 11(3), 445-463.

Hoek E., Carranza-Torres C.T. and Corkum B., 2002. Hoek–Brown failure criterion—2002 edition. In R. Hammah, W. Bawden, J. Curran, M. Telesnicki (eds), *Proceedings of the Fifth North American Rock Mechanics Symposium (NARMS-TAC)*, University of Toronto Press, Toronto. 267–273.

Python Software Foundation, 2001. *Python language reference*, version 3.4 [on line]. [Accessed 20/01/2015]. https://www.python.org/.

Stacey, P., 2009. Fundamentals of Slope Design. In J. Read and P. Stacey (eds), *Guidelines for Open Pit Slope Design*, CSIRO Publishing, Collingwood, Victoria. 1–14.

Chapter 2 - Literature Review

2.1 Introduction

This chapter presents a summary of fundamental concepts from the literature review on uncertainty in general and with regard to the geotechnical model for slope design in particular. The topics discussed include the approaches to deal with uncertainty in geotechnical engineering design and the contrast between classical (frequentist) and Bayesian probabilistic methods of analysis. A description of the fundamental concepts of the Bayesian approach is presented, including an overview of the methods to solve the posterior distribution function, which is a central element of the approach. The chapter also discusses the Markov Chain Monte Carlo (MCMC) procedure, which is the method selected for the evaluation of the posterior function in the research. Finally, a discussion is presented on the available software packages to perform this type of analysis and the recommendations to verify the quality of the MCMC samples from a Bayesian analysis.

2.2 The geotechnical model for slope design

The geotechnical model for slope design is particularly complex because it incorporates information from different already complex models. The slope design model is based on the geological, structural, rock mass and hydrogeological models (Stacey, 2009). Each model is described by different sets of information and parameters and is defined at a scale of interest for the analysis of slope behaviour. Figure 2.1 describes the contribution of the component models used in the slope design process. The components under the direct control of the geotechnical engineer are the rock mass model and the aspects associated with systematic structures of the structural model. These elements are described briefly hereinbelow; however, the focus of the research was primarily on the application of the Bayesian approach for the analysis of data, and only the rock mass strength aspects were covered in the scope.

2.2.1 Rock mass strength

The methodology followed for the rock mass strength characterisation is based on the Hoek-Brown (H-B) strength criterion (Hoek et al., 2002) as illustrated in the diagram of Figure 2.2. The H-B strength criterion includes the intact rock strength defined by the parameters σ_{ci}

and m_i, the rock mass quality described by the geological strength index (*GSI*) and the rock disturbance factor (*D*).

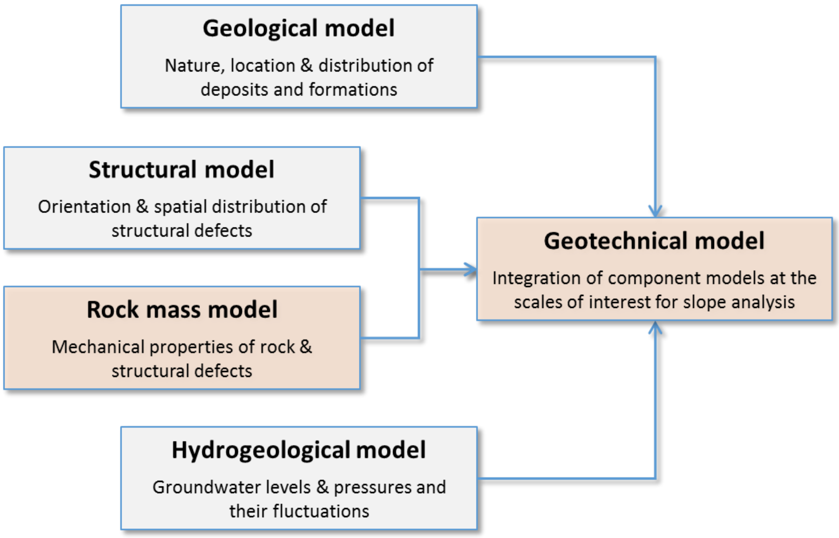

Figure 2.1 Components of the geotechnical model for mine slope design

The estimation of σ_{ci} and m_i is based on fitting Hoek-Brown failure envelopes to measurements of uniaxial (UCS) and triaxial (TCS) compression tests results. Occasionally, UCS data is estimated indirectly from point load test (PLT) results. The intact rock strength characterisation according to the latest version of the H-B strength criterion (Hoek and Brown, 2019) no longer uses tensile strength data.

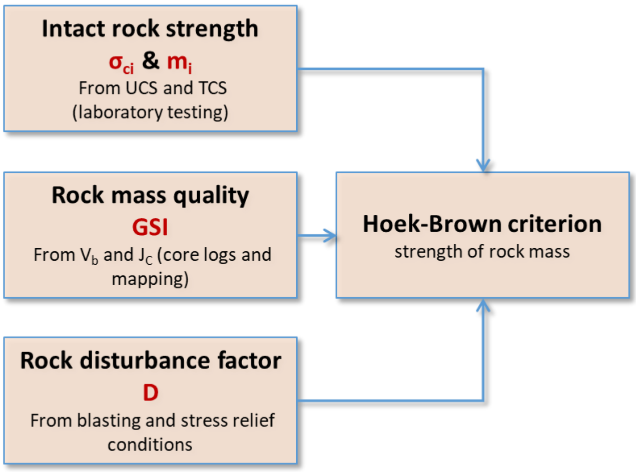

Figure 2.2 Rock mass strength estimation methodology

The estimation of GSI is based on charts describing the structural characteristics of the rock mass on the vertical axis and the joint conditions on the horizontal axis. The original chart proposed by Hoek and Brown (1997) was based on qualitative descriptions of the rock mass; however, various authors have proposed alternative charts based on measured factors to reduce the uncertainty of the estimation (Sonmez and Ulusay, 1999; Cai et al., 2004; Russo, 2009; Hoek et al., 2013). The chart selected in this research for the Bayesian analysis is based on the block volume (V_b) and the joint condition rating from Palmström (1996), as described by Cai et al. (2004).

The *D* factor is based on the assessment of the damage from blasting close to the surface of the excavation (Hoek, 2012). At deeper levels, the *D* factor is associated with the disturbance from the stress relief caused by the excavation of the slopes. The *D* factor can take values from 0.7 to 1.0 in slopes, with the larger values assigned to zones closer to the surface of the excavation.

2.2.2 Rock joint strength

The methodology followed for the joint strength characterisation is based on the Barton-Bandis (1982) criterion as illustrated in the diagram of Figure 2.3. The system is a refinement of the original criterion described by Barton and Choubey (1977).

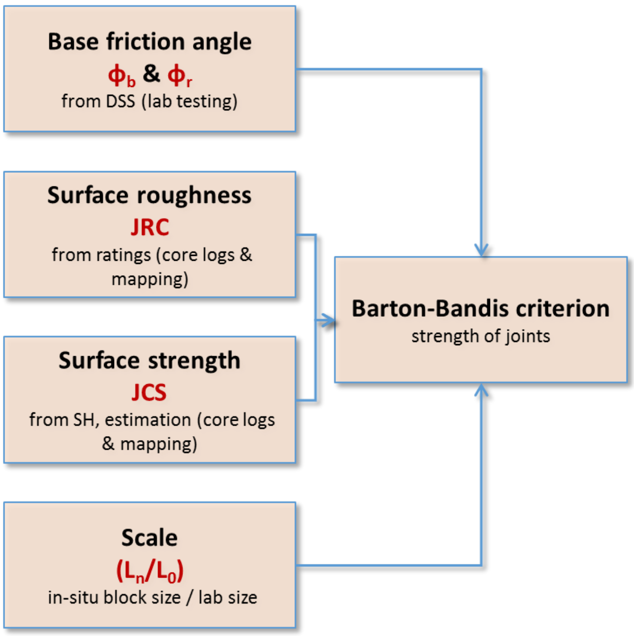

Figure 2.3 Rock joint strength estimation methodology

The base friction angle (Φ_b) and the residual friction angle (Φ_r) are derived from direct shear strength (DSS) tests on rock surfaces. Saw cut planes in unaltered rock are used for the determination of Φ_b, whereas weathered surfaces subject to large shear deformations provide the measurements of Φ_r.

The joint roughness coefficient (*JRC*) and the joint compression strength (*JCS*) are derived from borehole logs and mapping data. The *JRC* is based on the comparison of the observed roughness of the surfaces with rated profiles of reference. The *JCS* is based on rebound values from a Schmidt hammer acted on the surfaces. The hammer calibration graphs relate the rebound number with the compressive strength of the material tested.

A scale factor (L_n/L_0) based on the ratio between the estimated in-situ block size (L_n) and the reference size of specimens in the laboratory (L_0), typically 10 cm, is used to adjust the *JRC* and *JCS* parameters to represent field conditions.

2.2.3 Structural patterns

The characteristics of the systematic structural patterns include the identification of the rock joint systems and the estimation of their orientation and spatial distribution characteristics as illustrated in the diagram of Figure 2.4.

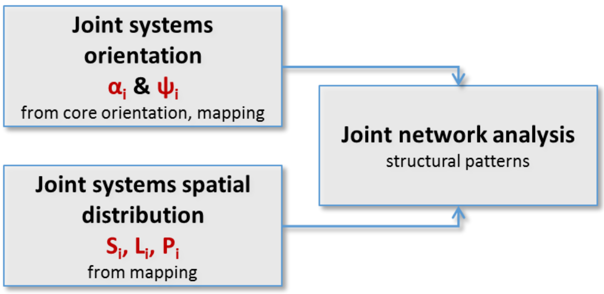

Figure 2.4 Joint structure estimation methodology

The orientation of the joint systems is described by the dip direction (α_i) and dip (ψ_i), which are derived from core orientation measurements and face mapping data. The data collected is represented in stereographic projection plots to facilitate the visualization of patterns and the analysis of the information (Hoek and Bray, 1981).

The spatial distribution characteristics of the joint systems are based on data collected from the mapping of rock exposures (Priest and Hudson, 1981). The data include measurements of spacing (S_i), length (L_i) and persistence (P_i = length of joint / length of joint and rock bridge) for each discontinuity system.

The orientation and spatial distribution properties of the joint systems are used to define three-dimensional structural patterns that can be used for kinematic analysis of stability and for the direct representation of the structural systems in slope stability models.

2.3 Uncertainty in the geotechnical model for slope design

The discussion on the types of uncertainty and their occurrence in the geotechnical model for slope design was included in Paper-I (Section 3.2) and Paper-II (Section 4.2), and only a brief summary of key points is presented in this section.

The concept of uncertainty refers to the attribute of being unpredictable, imprecise, variable, and similar concepts denoting lack of certainty. The uncertainty occurring in the geotechnical model for slope design, in particular, has various sources including: (1) approximations in the component sub-models, (2) inherent variability of properties assumed as random variables, (3) errors in the measurement of properties, and (4) approximations in the statistical representation of parameters. However, at a fundamental level, the uncertainty is due to lack of knowledge on the subject model and to the natural variability of the properties represented within it. This consideration defines the two basic types of uncertainty known as epistemic and aleatory, respectively.

An important aspect of contrast between these two types of uncertainty is that the knowledge uncertainty (epistemic) can be reduced with the addition of information (i.e. data collection, model refinement), whereas the uncertainty due to natural variability (aleatory) is irreducible (Baecher and Christian, 2003). The amount of data supporting the geotechnical model for slope design in open pits is relatively small compared with the situation in other geotechnical fields. For this reason, the main type of uncertainty present in this area of design corresponds to epistemic uncertainty, which is susceptible to reduction with the availability of more data.

2.4 Slope design approaches to deal with uncertainty

There are three main approaches commonly used to account for the uncertainties in slope design: the factor of safety, the probability of failure and the risk analysis. Contreras (2015) describes the approaches, highlighting their benefits and limitations as summarised below.

2.4.1 The factor of safety approach

In the slope design context, the factor of safety (FS) can be considered as the ratio between the resisting forces (strength) and the driving forces (loading) along a potential failure surface. Therefore, FS values larger than, equal to, or less than unity, correspond to slopes in stable, limit equilibrium, or unstable conditions, respectively. The FS is calculated with a deterministic model using the best estimate values, typically the mean, of the uncertain variables. Hence, the combined effect of the uncertainties on the stability evaluation is taken into account by using an FS for design larger than unity. Typical design values of FS in mining applications range between 1.2 and 2.0 (Wesseloo and Read, 2009).

The more relevant benefit of the FS approach is its simplicity. In contrast, their main drawbacks are the difficulty of selecting the appropriate acceptability criterion in a particular geomechanical environment, and the fact that the FS does not vary linearly with the likelihood of slope failure.

2.4.2 The probability of failure approach

The Probability of Failure (PF) of the slope is generally based on the probability distribution of the FS, which is estimated with a deterministic slope model that uses probability distributions rather than point values to represent the uncertain parameters. The PF can be calculated as the ratio between the area of the FS distribution representing failure i.e. FS<1.0 and the total area of the distribution representing all the cases of stability. The Monte Carlo (MC) simulation is a technique commonly used to construct the distribution of FS values. Wesseloo and Read (2009) present a summary of acceptability criteria for PF from different sources, although these authors highlight the difficulty of prescribing general recommendations on the appropriate values to use in particular situations.

A benefit of using the PF as a stability indicator is that it varies linearly with the likelihood of failure e.g. a slope with a PF of 5% is twice as stable as one with a PF of 10%. In contrast, the FS does not offer this useful reference. This means that a larger FS does not necessarily represent a safer slope, as the magnitude of the implicit uncertainties is not captured by the FS value e.g. a slope with an FS of 3 is not twice as stable as one with an FS of 1.5. The main drawbacks of the PF approach are the difficulties to select adequate acceptability criterion for design and the limitations in predicting failure with the underlying deterministic model.

2.4.3 The risk analysis approach

In the context of slope design, risk is defined as the combined effect of the probability of failure of the slope and the consequence of the failure in terms of safety and economic impacts. The risk methodology attempts to solve the problem of defining the acceptability criteria present in the FS and PF approaches. In this case, the definition of acceptability is more intuitive because it is set directly on the impacts of failure. The calculation of the PF for a rick analysis requires a thorough evaluation because it should reflect the actual likelihood of failure of the slope. The conventional PF calculated with the slope stability model normally accounts for part of the uncertainties, hence, other sources of uncertainty not accounted for need to be included in the calculation. It is common to use information derived from engineering judgement and expert opinion for the estimation of the PF of the slope and for the evaluation of failure impacts. This type of analysis is carried out with methods based on the use of logic diagrams and event trees. Baecher and Christian (2003) describe these techniques with reference to dam and foundation engineering problems. Steffen et al (2008) and Contreras (2015) demonstrate the use of these methods in the context of the mine slope design.

2.5 Strategies to treat uncertainty in geotechnical design

The more common strategies to deal with uncertainty in geotechnical engineering are described by Christian (2004) and a brief summary is included here to provide the general framework to place the Bayesian approach proposed in the research.

2.5.1 Conservative design

A conservative design consists in the selection of high FS or low PF values as the acceptability criteria of the slope design. However, the difficulty to define the acceptability criteria with these design approaches is still present, which complicates the use of the strategy efficiently. This strategy is particularly inconsistent with the concept of design in mining projects where the steepest or highest slopes are often required to achieve the sought economic benefit of the project.

2.5.2 Observational method

The observational method is based on measuring the slope performance as the project progresses, in order to verify the design assumptions and to implement the required adjustments that will ensure the achievement of the design objectives. However, the successful application of this strategy requires that the project has sufficient flexibility to accommodate the adjustments, but this attribute might not be present in mine slope situations. For example, when the observation of the slope performance suggests that the flattening of a slope is required to prevent a ramp failure, it may be too late to implement this measure.

2.5.3 Quantification of uncertainty

A straightforward strategy to treat uncertainty is to include it explicitly in the design. The Bayesian approach subject of the research fits into this strategy. In this case, probability measures are used to quantify uncertainties as they express the likelihood of occurrence of events. However, there are two main interpretations of probability, one as frequencies in a series of similar random trials, and the other as degrees of belief assigned directly to situations. There are various types of uncertainties in geotechnical engineering, which are better represented by either of these interpretations. For example, the uncertainty of a property determined from sampling results corresponds to a frequency situation, whereas any form of expert opinion represents a degree of belief case. Baecher and Christian (2003) provide a detailed discussion on the topic of duality in the interpretation of uncertainty and probability in geotechnical engineering.

The epistemic uncertainty can be associated with different aspects of lack of knowledge, some of which are not compatible with a representation based on conventional probability values (Helton et al. 2004). Examples of these special cases of epistemic uncertainty include vagueness and various types of ambiguity, which are better treated with alternative approaches outside the classical probability theory (e.g. possibility theory and evidence theory). These methods are briefly discussed in Section 3.5 to illustrate the variety of aspects that need to be considered when dealing with knowledge uncertainty. However, the topic is not treated any further as the focus of the research is on the contrast between the classical and Bayesian perspectives of probabilistic analysis to represent uncertainty.

2.6 Probabilistic methods to treat uncertainty

There are two main approaches of statistical analysis known as frequentist (or classical) and Bayesian. These methodologies refer in particular to statistical inference analysis where data is used to draw conclusions on the characteristics of the population represented by the data. The objects of the inference analysis are the parameters used to describe the population. This process has uncertainty, which is measured with probability values. The conceptual basis of the two approaches differ in terms of what is considered uncertain (data or parameters), and on the interpretation of probability (VanderPlas, 2014a).

2.6.1 The frequentist approach of statistical analysis

The frequentist approach is based on the concept of data, which is used to characterise the population from which it is drawn, as being the result of a random sampling process. Therefore, in this approach data is considered uncertain whereas the parameters investigated are unknown fixed quantities. In this case, probabilities are interpreted as relative frequencies of outcomes from randomised trials or samples. Meaningful probabilities require to be based on numerous trials; hence, it is implicit in the approach that many samples (data) are necessary for accurate characterisation of the population.

The results of the inference analysis of parameters consist of point estimates (e.g. the mean) and error measures (e.g. the confidence interval) of the parameters investigated. Frequentist statistical methods are used by default in many areas of engineering design, including the geotechnical design of mine slopes; however, the implications of the conceptual basis are rarely comprehended by the analysis, leading to misinterpretation of results, as discussed in detail in Section 4.3.4.

2.6.2 The Bayesian approach of statistical analysis

In the Bayesian approach, data is combined with the existing prior knowledge on the parameters investigated into a so-called posterior distribution using the Bayes' rule. In this case, data represents a particular state of information on the population and therefore are considered fixed, whereas the parameters sought to characterise the population are uncertain and represented by random variables. The posterior distribution reflects the probabilities of the parameters investigated for the particular state of knowledge included in the data and priors used in the analysis. In this case, probabilities are interpreted as degrees of belief that can be assigned directly to situations or events. The posterior distributions are normally complicated functions that require special methods of evaluation.

The results of the Bayesian inference of parameters are probability distributions reflecting their likelihood and uncertainty. The analysis also provides information on the correlation between these parameters. A description of the elements of the Bayesian approach for the inference of parameters is included in Section 4.3.2. However, a summary is presented below for completeness to introduce the methods of evaluation of the posterior function described later in this chapter.

There are many books on Bayesian analysis with different levels of complexity in the presentation of the topic. Stone (2013) gives an introductory description of the subject including simple examples aimed at providing intuition on fundamental concepts. Hoff (2009), Kruschke (2015), and Sivia and Skilling (2006) give detailed presentations of the topic including mathematical descriptions and practical examples developed with specialized software. Gregory (2005) provides a good description of underlying concepts with examples from the physical sciences. The book by Gelman et al. (2013) is considered a classic textbook on the subject, contains practical examples mainly from the social sciences fields and includes detailed mathematical descriptions of the topic.

2.6.3 Fundamentals of the Bayesian approach

The Bayesian approach of statistical analysis refers to the method of statistical inference based on the Bayes' rule, which describes a construct using the concept of conditional probability. The rule takes its name from the English mathematician Thomas Bayes who described it in his work published in 1763, two years after his death (Bayes, 1763). Figure 2.5 shows the derivation of Bayes' rule using Venn diagrams to have intuitive representations of the conditional probabilities. The three sets represented with the diagrams in Figure 2.5 correspond to the universe set (*u*) that contains the hypothesis (*h*) and data (*d*) sets. The probabilities of the hypothesis (*p[h]*) and data (*p[d]*) are defined with reference to the universe set. However, the conditional probabilities of the hypothesis given the data (*p[h|d]*) or the data given the hypothesis (*p[d|h]*) are based on resizing the universe and making it equal to the respective conditional set.

The general form of the Bayes' equation, using the definition of terms in Figure 2.5 is:

$$p(h|d) = \frac{p(d|h)p(h)}{p(d)} \tag{2.1}$$

which can also be interpreted in the following manner (Kruschke, 2015):

$$posterior = \frac{likelihood \times prior}{evidence} \tag{2.2}$$

The Bayes rule is used to update the knowledge of a hypothesis (i.e. a model or a set of parameters) from observations represented by the data, and from the available prior knowledge on the hypothesis (i.e. subjective information or older data sets). The following sections present a brief description of the four components of the Bayes' rule shown in Eq. (2.2).

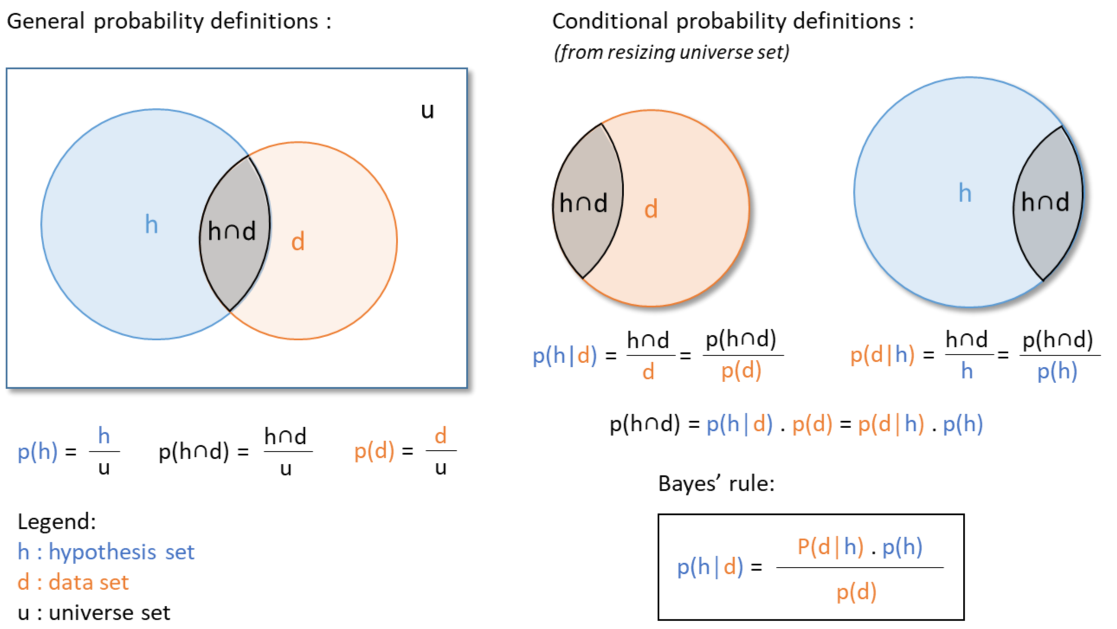

Figure 2.5 Derivation of Bayes' rule from definitions of conditional probability visualized with Venn diagrams

2.6.3.1 *The posterior distribution*

The "posterior" is a probability distribution that reflects the uncertainty of the hypothesis examined (e.g. the set of parameters of a regression model) after taking into account the relevant data and prior knowledge on the hypothesis. The posterior is the answer sought by the analyst, reflecting the balance between the knowledge provided by the data and prior components. For this reason, the posterior is useful to gauge the sufficiency of data, as a strong data set outbalances the effect of the prior.

2.6.3.2 The likelihood function

The "likelihood" function defines the probability of obtaining the observations included in the data set given the hypothesis under examination (e.g. the set of parameters of a regression model). The likelihood is the answer given by classical statistical methods and reflects the likelihood of the hypothesis (i.e. the set of parameters) for that particular data set.

Figure 2.6 shows an example extracted from Kruschke (2015) of the calculation of the likelihood of parameters of a normal distribution for a data set of three points, d = [85, 100, 115]. In this case, the data points represent a variable x, which is assumed to follow a normal distribution with mean μ and standard deviation σ, hence:

$$p(x|\mu,\sigma) = \frac{1}{\sqrt{2\sigma^2\pi}} e^{-\frac{(x-\mu)^2}{2\sigma^2}} \tag{2.3}$$

The likelihood of a particular set of parameters [μ, σ] for a data set of three points d = [x_1, x_2, x_3] corresponds to the product of the three probabilities of the data points as expressed by the likelihood function:

$$p(d|\mu,\sigma) = \prod_{i=1}^{3} \frac{1}{\sqrt{2\sigma^2\pi}} e^{-\frac{(x_i-\mu)^2}{2\sigma^2}} \tag{2.4}$$

Therefore, the likelihood of an arbitrary chosen normal distribution with parameters μ = 87.8 and σ = 18.4, represented in blue in Figure 2.6, is 2.70E^{-06} for the data set of three points shown in this figure. It is possible to verify that the likelihood of the calculated mean and standard deviation of the data points (μ = 100, σ = 12.2), represented in grey in Figure 2.6, corresponds to the maximum possible likelihood value, which is a known attribute of these parameters from classical statistics.

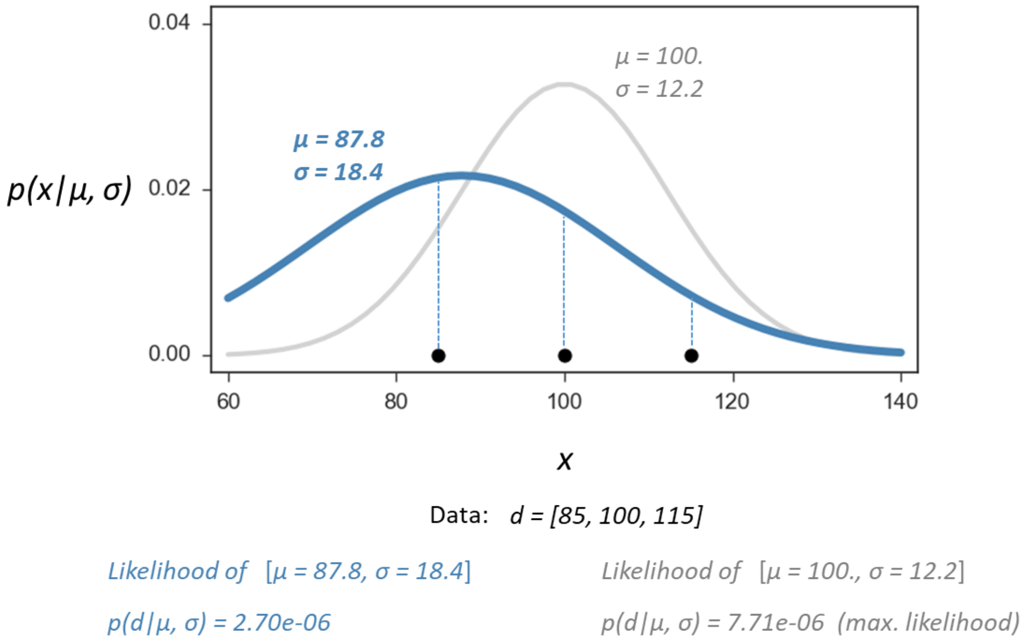

Figure 2.6 Example of calculation of the likelihood of the mean (μ) and standard deviation (σ) of a normal distribution assumed to represent the variability of a data set of three points

2.6.3.3 The prior distribution

The "prior" represents the initial knowledge on the hypothesis, and it can be informative or vague. Informative priors can be any type of distribution that represents adequately the existing knowledge of the model or parameter examined. Before the widespread availability of numerical methods to sample the posterior distributions, the selection of informative priors was based on their affinity with the likelihood function to facilitate the analytical calculation of the posterior. These priors are known as conjugate distributions.

The non-informative priors to express ignorance about a parameter value, are based on the range of the parameter domain, with the uniform distribution among the more commonly used for this purpose. However, there are situations where a uniform distribution might not be the best option to represent the lack of information because it could constrain the results of the analysis. In these cases, the definition of the prior distribution could be based on the principle of maximum entropy, also known as the principle of minimum prejudice, developed by E. T. Jaynes in 1957.

Gregory (2005) provides a detailed presentation of the concept of maximum entropy probabilities. The maximum entropy principle states that "the least prejudiced assignment of probabilities is that which maximizes Shannon's measure and agrees with the given information" (Tribus, 1988, p. 48). Shannon's measure refers to the measure of entropy or disorder in information and it was described by C. Shannon as part of his mathematical theory of communication published in 1948 (Shannon, 1948). According to this theory, "entropy measures what we do not know when we have encoded our knowledge in a probability distribution. It measures what is left to learn when you are uncertain" (Tribus, 1988, p. 45). Table 2.1 shows a list of common maximum entropy probability distributions for various constraints, adapted from Harr, 1987.

Table 2.1 Maximum entropy probability distributions

Constraints	**Maximum entropy probability distribution**
$a \leq x \leq b$	Uniform
$x \geq 0$, mean known	Exponential
$-\infty \leq x \leq +\infty$, mean and standard deviation known	Normal
$a \leq x \leq b$, mean and standard deviation known	Beta
$0 \leq x \leq n$, mean occurrence rate of independent events known	Poisson

The selection of the prior is an important step in a Bayesian analysis. The prior could add valuable available information to the posterior if selected adequately, or it could bias the results if it over-constrains the data. Figure 2.7 shows a conceptual representation of the influence of the prior on the posterior. The left column plots illustrate the situation of a vague prior having no influence on the posterior regardless of the size of the data set. The middle column plots show the strong influence of an informative prior on the posterior when the data set is small. The right column plots represent the case of an informative prior out weighted by the strong influence of a large data set. The selection of inappropriate priors could result in over-constrained posterior distributions, in particular when data is scarce.

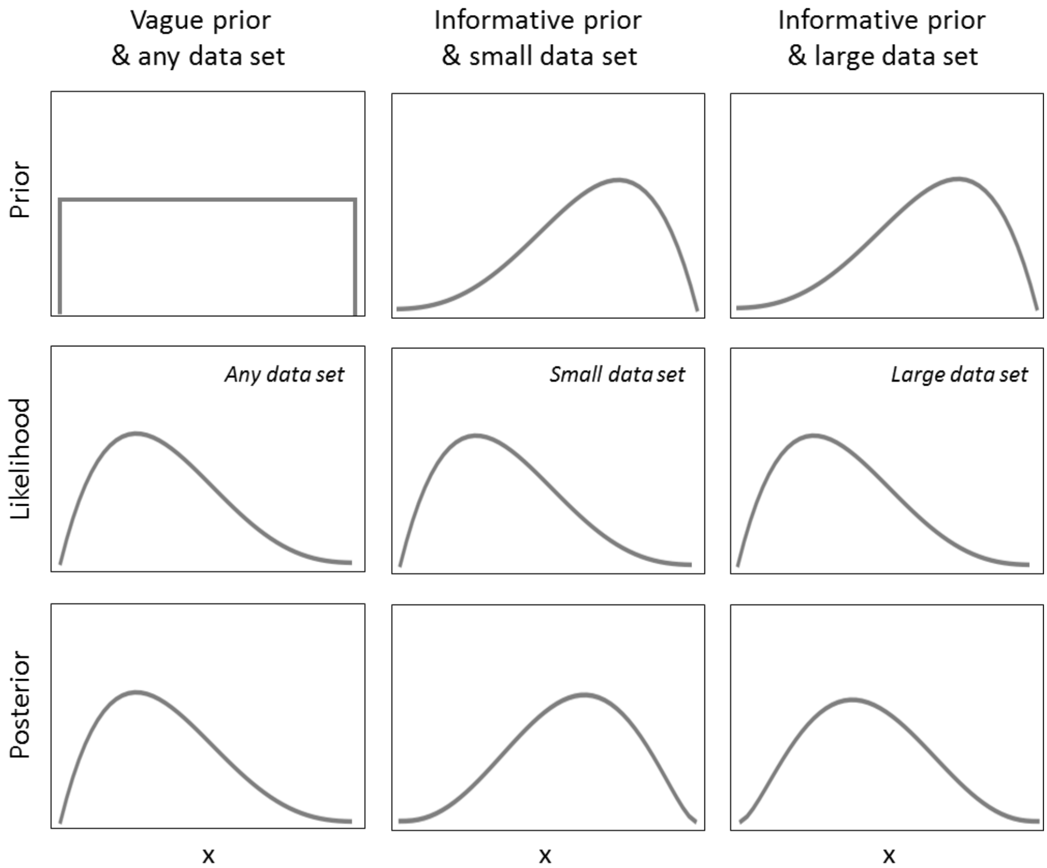

Figure 2.7 Conceptual representation of the influence of vague and informative priors on the posteriors depending on the size of the data set

Siu and Kelly (1998) summarise the concepts of Bayesian analysis and maximum entropy and provide practical recommendations to define prior distributions in the context of risk analysis. Bozorgzadeh and Harrison (2014) discuss a practical example to illustrate the effect of informative and non-informative priors on the estimation of UCS values using different sizes of data sets. Cao et al. (2016) discuss approaches to define non-informative and informative prior distributions of soil parameters for the Bayesian analysis of site characterisation.

2.6.3.4 The evidence function

The “evidence” part in the denominator of Bayes equation (Eq. 2.1) is normally treated as a normalisation factor so that the posterior integrates to one. It is calculated as the integral of the numerator over the whole parameter space. The posterior distribution does not need to be normalized when the purpose of the Bayesian analysis is the inference of parameters and the posterior is evaluated using the Markov chain Monte Carlo (MCMC) method. In this case, the calculation of the typically complex integral in the denominator of the Bayes equation can be skipped. However, the denominator is required when the objective of the analysis is the comparison of two alternative models, which is done through the calculation of the Bayes factor that relates the posteriors of the two models.

2.6.4 Contrast between the frequentist and Bayesian approaches

The comparison of key aspects of the two approaches was presented initially in Paper-I (Table 3.1) and was emphasised again in Paper-II (Table 4.1). The summary of contrasting features presented in these tables was a necessary element to explain the subtle differences in the interpretation of results of the inference analysis with both methods, which seems to coincide in many cases.

A fundamental difference consists in the interpretation of probability, which is associated with a frequency of outcomes in a series of repeated random trials in the frequentist approach, as opposed to a degree of belief assigned directly to a situation in the Bayesian approach. Another fundamental difference is that in the Bayesian approach data is considered a fixed entity whereas the parameters investigated are the uncertain objects represented by random variables. This assumption is reversed in the frequentist approach where data is random and the parameters sought are fixed, although intractable objects.

Methodologically, the Bayesian method uses in addition to the data, which is the only input in a frequentist analysis, any prior knowledge available on the parameters investigated, including subjective information such as expert opinion. The result of a Bayesian analysis applied to the inference of parameters consists of a probability distribution of the parameters that reflects the balance between the prior information and data. This type of analysis is known as Bayesian updating because it can be applied in successive stages as more data is available, which is a feature that suits well the typical process followed in geotechnical design. In contrast, the frequentist analysis for the inference of parameters provides a point estimate (e.g. the mean) and an error measure (e.g. the confidence interval) of the parameter investigated, although the true value of the parameter is a fixed entity, and cannot be known.

A consequence of the differences indicated above is that the Bayesian approach addresses the question of interest to the analyst, which is what is the probability of the parameter (or model) given the data. The frequentist approach, in contrast, can only answer the reverse question, i.e. what is the probability of the data given the parameter (or model), which clearly is of less interest to the analyst (VanderPlas, 2014a).

A common misinterpretation of the confidence interval (CI) in the frequentist approach is discussed in detail in Paper-I (Section 3.4.2) and Paper-II (Section 4.3.4), including an example to illustrate this point. In general, the CI is mistakenly used to quantify the uncertainty of parameters such as the mean value of a rock property, when in fact the CI really measures the uncertainty of the data supporting the parameter estimate. The confusion is the result of the intuitive interpretation by the analyst of data as fixed and parameters as random entities, which is inconsistent with the assumptions of the approach. However, this intuitive interpretation of data and parameters is consistent with the assumptions of the Bayesian approach, which suits better the interest of the analyst as a result.

2.6.5 Arguments for using the Bayesian approach for the geotechnical design of mine slopes

The main arguments supporting the use of the Bayesian approach for the geotechnical design of mine slopes include:

- The suitability of the approach to represent the epistemic uncertainty, which is the prevailing type of uncertainty in the geotechnical model for slope design. This aspect contrast with the inconsistency of the frequentist approach to model this type of uncertainty as discussed in Paper-I (Section 3.4.3).

- The ability of the approach to combine information from various sources to provide the best possible estimates of design parameters. The types of information that can be used with the approach include prior knowledge and data from different sources such as site and laboratory investigations and measurements of slope performance. This aspect is described in Paper-III (Section 5.2.6).

Although the Bayesian methods of analysis have been known for more than two centuries, their use for practical applications involving multidimensional models was limited due to the difficulties of solving the posterior distributions. In contrast, the frequentist methods used with large sample sizes have known asymptotic properties that made probabilistic inference easy (Zyphur and Oswald, 2015). However, the rapid development of modern computers and computing algorithms that have occurred during the past 50 years have made the Bayesian solutions equally attainable. The situation today is that the flexibility of the Bayesian methods allow the estimation of parameters in situations where traditional methods cannot provide a solution (Zyphur and Oswald, 2015).

2.7 Methods of evaluating the posterior distribution

The posterior distribution in a Bayesian analysis is generally difficult to evaluate because combines two different distributions representing the prior and likelihood components of the Bayes equation. In addition, the likelihood part contains the function that represents the model under examination, contributing to the complexity of the distribution. There are several methods used to evaluate the posterior distribution as described hereinafter.

2.7.1 Conjugate prior

This method corresponds to the case where the prior distribution is a function that can be easily multiplied by the likelihood function to obtain analytically a posterior distribution of the same type as the prior. The prior distribution is then called a conjugate prior for the likelihood function (Baecher and Christian, 2003). The posterior distribution obtained in this way is represented by a closed function whose evaluation is straightforward. The main limitation of this method is that in many real case situations the likelihood functions have no conjugate priors and the method is not applicable. The method is better illustrated with a simple example of inference of the mean (μ) and standard deviation (σ) of UCS based on a data set of n = 15 values in MPa (x = [130.7, 144.4, 121.8, 114.4, 95.8, 76.6, 144.0, 110.7, 113.0, 172.0, 140.5, 131.1, 124.3, 165.6, 171.6]). The UCS is considered a random variable that follows a normal distribution for the solution of this problem. The available information on the parameter values indicates a prior mean μ_0 = 100 MPa and a prior standard deviation σ_0 = 20 MPa. In this case, the prior parameters represent a single observation (v_0 = 1).

The inference of the joint distribution of μ and σ is based on the posterior distribution of these parameters given the data according to Bayes' rule as follows:

$$p(\mu,\sigma|data) = \frac{p(\mu,\sigma)\,p(data|\mu,\sigma)}{p(data)} = \frac{p(\mu,\sigma)\,p(data|\mu,\sigma)}{\iint p(\mu,\sigma)\,p(data|\mu,\sigma)d\mu\,d\sigma} \qquad (2.5)$$

The denominator in Eq. (2.5) acts as a normalisation constant and corresponds to the integral over the whole parameter space of the product of the prior and likelihood terms in the numerator. The use of conjugate priors allows the analytical solution of this integral.

The prior term *p(μ,σ)* in Eq. (2.5) corresponds to a bivariate distribution and can be represented as the product of a conditional probability and a marginal probability (Hoff, 2009) as follows:

$$p(\mu,\sigma) = p(\mu|\sigma)\,p(\sigma) \qquad (2.6)$$

The conjugate prior for the probability of μ conditioned to σ is the normal distribution with parameters μ_0, σ (i.e. $\mu \sim Normal\ [\mu_0,\ \sigma]$). The conjugate prior for the probability of the variance (σ^2) is the inverse-gamma distribution with parameters $v_0/2$, $v_0\sigma_0^2/2$ (i.e. $\sigma^2 \sim Inv.Gamma\ [v_0/2,\ v_0\sigma_0^2/2]$). Therefore, the informative prior distribution in Eq. (2.6) can be expressed as follows:

$$p(\mu,\sigma|\mu_0,\sigma_0,\nu_0) = \left[\frac{1}{\sqrt{2\pi\sigma^2}}e^{-\frac{(\mu-\mu_0)^2}{2\sigma^2}}\right]\left[\frac{\left(\frac{\nu_0{\sigma_0}^2}{2}\right)^{\frac{\nu_0}{2}}}{\Gamma\left(\frac{\nu_0}{2}\right)}\left(\frac{1}{\sigma^2}\right)^{\left(\frac{\nu_0}{2}+1\right)} e^{-\frac{\nu_0{\sigma_0}^2}{2\sigma^2}}\right] \qquad (2.7)$$

The likelihood term *p(data| μ,σ)* in Eq. (2.5) is calculated from the data set as follows:

$$p(data|\mu,\sigma) = p(x_1,\ldots x_n|\mu,\sigma) = \prod_{i=1}^{n}\left(\frac{1}{\sqrt{2\pi\sigma^2}}e^{-\frac{(x_i-\mu)^2}{2\sigma^2}}\right) \qquad (2.8)$$

The posterior probability distribution function can be decomposed into the mean and standard deviation parts, in the same way as it was done with the prior distribution in Eq. (2.6) as follows:

$$p(\mu,\sigma|x_1,\ldots x_n) = p(\mu|\sigma,x_1,\ldots x_n)\,p(\sigma|x_1,\ldots x_n) \qquad (2.9)$$

The result from applying the Bayes theorem and performing the mathematical analysis to the terms in Eq. (2.9) is that the posterior distribution is of the same type as the prior, i.e.

normal and inverse-gamma for the mean and variance parameters, respectively. In this case, the posterior distribution is defined by the following expression:

$$p(\mu,\sigma|x_1,\dots x_n,\mu_n,\sigma_n,\nu_n) = \left[\frac{1}{\sqrt{2\pi\sigma^2}}e^{-\frac{(\mu-\mu_n)^2}{2\sigma^2}}\right]\left[\frac{(\frac{\nu_n{\sigma_n}^2}{2})^{\frac{\nu_n}{2}}}{\Gamma\left(\frac{\nu_n}{2}\right)}\left(\frac{1}{\sigma^2}\right)^{\left(\frac{\nu_n}{2}+1\right)}e^{-\frac{\nu_n{\sigma_n}^2}{2\sigma^2}}\right] \tag{2.10}$$

where:

$\nu_n = \nu_0 + n$

$\mu_n = \dfrac{\nu_0\mu_0 + n\bar{x}}{\nu_n}$

$\sigma_n = \sqrt{\dfrac{1}{\nu_n}\left[\nu_0{\sigma_0}^2 + (n-1)s^2 + \dfrac{\nu_0 n}{\nu_n}(\bar{x}-\mu_0)^2\right]}$

$\bar{x} = mean\ of\ data\ set$

$s^2 = variance\ of\ data\ set$

The mean parameters of the posterior distribution in Eq. (2.10) are:

$$Mean\ \mu = \mu_n \tag{2.11}$$

$$Mean\ \sigma = \sqrt{\frac{2{\sigma_n}^2}{\nu_n\left(\frac{\nu_n}{2}-1\right)}} \tag{2.12}$$

Details of the mathematical analysis to derive the posterior function for the normal-inverse gamma prior case can be found in Hoff (2009). Although this analytical process can be tedious, the benefit of the method is that the result is a closed-form expression of the posterior distribution of parameters that can be easily evaluated. The graph in Figure 2.8 shows the joint prior and posterior distributions of parameters (*μ, σ*) representing the mean and standard deviation of UCS, for the example of the data set of 15 values. The prior distribution is constructed with Eq. (2.7) using the available information on the parameters. The posterior distribution is based on Eq. (2.10) using the prior parameters and the data set.

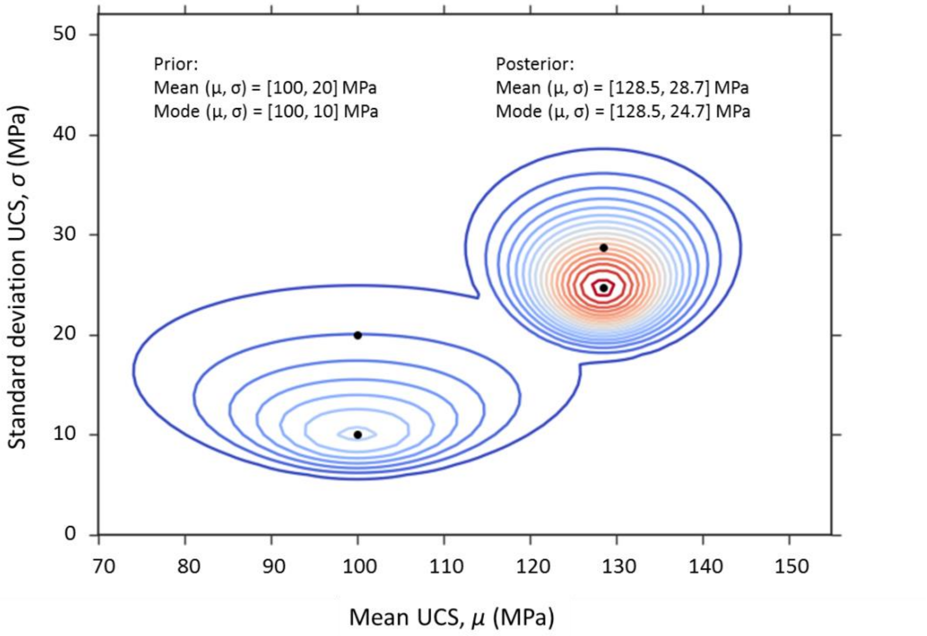

Figure 2.8 Joint prior and posterior distributions of (μ, σ) corresponding to the mean and standard deviation of UCS for the example of a data set of 15 values and information on prior parameters

The method of conjugate priors to solve the posterior is applicable to specific problems where the likelihood function has a conjugate prior, which in addition should be suitable to represent the available prior knowledge. In general, the range of applicability of this method is restricted to simple low dimensional problems. Therefore, this method is not used for the problems pertaining to the geotechnical model for slope design treated in the research.

2.7.2 Direct integration

This method consists in the use of numerical integration procedures to evaluate the integrals required to define the statistics of the posterior distribution. If $\boldsymbol{\theta}$ is a vector containing the uncertain parameters in the posterior distribution, the statistics of these parameters are given by the following equations:

$$Mean\ \theta_i = \int \theta_i\, f(\theta_i|data)\, d\theta_i \tag{2.13}$$

$$Stdev\ \theta_i = \sqrt{\int (\theta_i - Mean\ \theta_i)^2\, f(\theta_i|data)\, d\theta_i} \tag{2.14}$$

where *Mean* θ_i is the posterior mean of θ_i, *Stdev* θ_i is the posterior standard deviation of θ_i and $f(\theta_i|data)$ corresponds to the posterior PDF of the ith element of $\boldsymbol{\theta}$.

There are different numerical procedures for the calculation of these integrals, but in general, the computational cost of these methods increases significantly with the dimension of **θ**. For this reason, direct integration methods are used for low dimensional problems. Juang and Zhang (2017) describe a simple method to solve the integrals for two-dimensional problems based on a grid calculation procedure. The method is based on dividing the domain of the two uncertain variables in **θ** = [θ_1, θ_2] into a grid of points where the unnormalised posterior distribution is evaluated. The summation of all the values of the function calculated at the grid points is the numerical approximation of the integral of the posterior. Hence, the statistics of the parameters of the posterior distribution are calculated with the following equations:

$$Mean\ \theta_1 = \Delta_1 \sum_{i=1}^{n1} \theta_{1i}\, f(\theta_{1i}|data) \tag{2.15}$$

$$Stdev\ \theta_1 = \sqrt{\Delta_1 \sum_{i=1}^{n1} (\theta_{1i} - Mean\ \theta_1)^2\, f(\theta_{1i}|data)} \tag{2.16}$$

$$Mean\ \theta_2 = \Delta_2 \sum_{j=1}^{n2} \theta_{2j}\, f\left(\theta_{2j}|data\right) \tag{2.17}$$

$$Stdev\ \theta_2 = \sqrt{\Delta_2 \sum_{j=1}^{n2} \left(\theta_{2j} - Mean\ \theta_2\right)^2 f\left(\theta_{2j}|data\right)} \tag{2.18}$$

$$f(\theta_{1i}|data) = \frac{\sum_{j=1}^{n2} q\left(\theta_{1ij}, \theta_{2ij}\right)}{\Delta_1 \sum_{j=1}^{n2} \sum_{i=1}^{n1} q\left(\theta_{1ij}, \theta_{2ij}\right)} \tag{2.19}$$

$$f\left(\theta_{2j}|data\right) = \frac{\sum_{i=1}^{n1} q\left(\theta_{1ij}, \theta_{2ij}\right)}{\Delta_2 \sum_{j=1}^{n2} \sum_{i=1}^{n1} q\left(\theta_{1ij}, \theta_{2ij}\right)} \tag{2.20}$$

where:

n1, *n2* = number of grid points along the θ_1 and θ_2 axes, respectively

Δ_1, Δ_2 = grid spacing along the θ_1 and θ_2 axes, respectively

θ_{1i}, θ_{2j} = i^{th} point of θ_1 and j^{th} point of θ_2

$q(\theta_{1ij}, \theta_{2ij})$ = unnormalised posterior function evaluated at the point $[\theta_{1i}, \theta_{2j}]$

In the example presented in the previous section, the posterior is defined by the parameters (μ, σ). Furthermore, the product of the prior in Eq. (2.7) and the likelihood in Eq. (2.8) defines the unnormalised posterior distribution function. For comparison purposes, the grid calculation method was used with the data and prior information from that example and the results are presented in Figure 2.9.

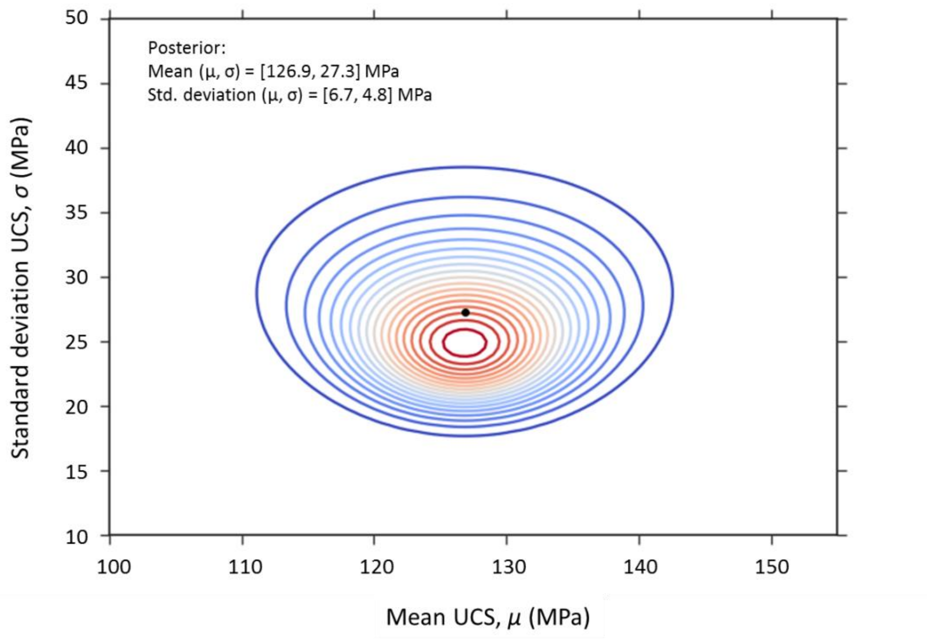

Figure 2.9 Contours of the unnormalised posterior distribution of parameters (μ, σ) representing the mean and standard deviation of UCS for the example in Section 2.7.1, showing the statistics of the posterior evaluated with the grid calculation method

The grid spacing used for the numerical calculation of the unnormalised posterior was $\Delta_1 = \Delta_2 = 0.5$, with μ varying between 70 and 160 and σ between 0 and 50, to include the domain of the prior distribution as indicated in Figure 2.8. The conjugate prior from the example presented in the previous section was used for comparison purposes; however, there are no restrictions in terms of the prior used for the grid calculation method. Typically, a non-informative prior represented by a uniform distribution would be used for this type of analysis. The main limitation of the direct integration methods is that their applicability is restricted to low dimensional problems and in particular, the grid calculation method is limited to two-dimensional problems. This method was not considered for the problems studied in the research due to the advantages offered by the sampling-based methods described in the following sections.

2.7.3 Markov chain Monte Carlo (MCMC) sampling

The MCMC method to evaluate the posterior distribution consists of drawing samples of the uncertain parameters in the posterior function by means of an iterative random process called a Markov chain. The samples from the Markov chain can be used for inferring the properties of the posterior distribution, and as a representation of the uncertain parameters in subsequent probabilistic analysis.

The more common algorithms used to implement an MCMC process are the Metropolis, Gibbs and Hamiltonian algorithms. There are other procedures developed as refinements of the previously mentioned, but in general, all the algorithms share common basic steps as follows:

(1) Start with an initial guess of the set of parameters to sample

(2) Evaluate a random jump of the set of parameters from their current values

(3) Evaluate the probabilities of the proposed and current sets of values with the target distribution

(4) Use the ratio between the probabilities of the proposed and current sets of values to define a criterion of acceptance of the jump. The criterion should favour moves towards the regions of higher probability, but should not eliminate the possibility of moves towards the regions of lower probability.

(5) Apply the acceptance criterion to update or retain the current values and repeat the process from step 2 until a sufficient number of sets of values (samples) is defined.

The main differences between the various algorithms are related to the way of defining the proposed jumps and the acceptance criteria of the jumps. The example of the UCS data set presented in Section 2.7.1 was used to illustrate the evaluation of the posterior distribution with the MCMC method. The method works with the unnormalised posterior; therefore, the posterior is calculated as the product of the prior in Eq. (2.7) and the likelihood in Eq. (2.8).

A simple Metropolis algorithm was implemented with reference to the generic MCMC procedure. In this case, the evaluation of the random jump in step (2) was based on a normal distribution centred at each location, and the acceptance criterion of the jump in step (4) consisting of acceptance proportional to the ratio of probabilities. Figure 2.10 shows the scatter plot of the 50,000 samples of the parameters (*μ, σ*) corresponding to the mean and standard deviation of UCS. The contour lines in the plot fine the regions containing 68% and 95% of the sampled points, which were also used to calculate the mean and standard deviation of the distribution. These results are consistent with those from the conjugate prior (Figure 2.8) and grid calculation (Figure 2.9) methods.

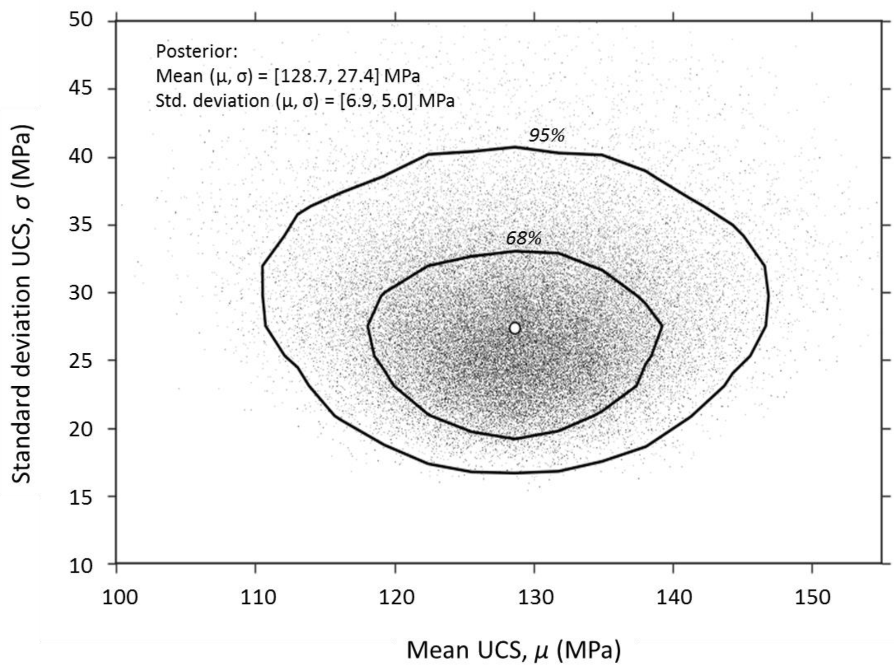

Figure 2.10 Scatter plot of parameters (*μ, σ*) sampled from the posterior distribution using the Metropolis MCMC procedure. The samples represent the mean and standard deviation of UCS for the example in Section 2.7.1. The contour lines define 68% and 95% high-density regions

The increased use of MCMC methods during the last 20 years is related to the advances in computer hardware and numerical algorithms facilitating the use of these methods. MCMC sampling is the method selected in the research for evaluating the posterior distribution. The method is efficient, powerful and simple, and its use does not require special skills in mathematical analysis. The regular geotechnical practitioner, already familiar with the conventional Monte Carlo analysis, can easily apply the method for the inference of geotechnical parameters in slope design. The MCMC procedure is described in more detail in Section 2.8 because it is the method selected for the Bayesian analysis included in the research.

2.7.4 Other methods

The evaluation of the posterior distribution using conjugate priors or direct integration techniques is limited to simple low-dimensional problems. The MCMC procedures are a simple and powerful tool normally used for the analysis of more complicated models with multiple dimensions. There are other methods based on mathematical procedures used to define the location of the maximum posterior densities or to construct simpler approximations of the posterior distribution that can be used for the inference of parameters. Some of these methods include the modal approximation technique, the expectation maximisation method and the variational Bayes method, which are described in detail in Gelman et al. (2013). In general, these methods are used to provide inferences utilised for verification of the results from simulation analysis. However, these methods are not discussed in the thesis, considering that the aim of the research is to focus on a simple method such as the MCMC simulation that can be applied by the regular geotechnical practitioner.

2.8 The Markov chain Monte Carlo (MCMC) method

The MCMC sampling is the method of choice for the evaluation of the posterior distribution in the research, and for that reason, this section provides more details on this methodology. The section includes a brief description of the more common algorithms, provides some guidelines for the assessment of the quality of the MCMC results and describe software alternatives to carry out MCMC analysis.

The rapid developments of MCMC techniques during the last 20 years has extended the range of application of the Bayesian approach for data analysis. Diaconis (2009) presents some examples of formerly intractable problems that can be solved today with this technique. Robert and Casella (2011) provide a brief history of MCMC, and Kruschke (2015) describes the basic concepts of the algorithms. A comprehensive treatment of MCMC techniques is presented in Robert and Casella (2004) and Gelman et al. (2013).

2.8.1 The Metropolis algorithm

The Metropolis algorithm is a method to carry out a random walk through the parameter space of a target distribution in order to obtain representative samples of the parameters. The procedure is based on defining the possibility of moving the parameter value from the current location to a neighbouring location selected randomly with a proposal distribution. The acceptance of the move depends on the relative values of the target distribution at the current and proposed locations. The move is accepted if the value of the target distribution at the proposed location is larger than the value at the current location. However, if the value of the distribution at the proposed location is less than the value at the current location, the move is accepted with a probability that is proportional to the ratio of the two distribution values. For example, if a distribution has a value of five at the current location and a value of six at the proposed location, the move will be accepted. On the other hand, if the value of the distribution at the proposed location is four, the move will be accepted with an 80% probability reflecting the ratio 4/5 of the distribution values at the two locations. The current position will be maintained with the remaining 20% probability.

The steps of the Metropolis algorithm to sample a variable x from a target distribution p, can be summarised as follows:

(1) Initialize x_t: x_0 for $t = 0$

(2) Define a proposed position y from a symmetric probability distribution q centred at current position x_t: $q(y|x_t)$

(3) Evaluate the ratio r: $r = p(y) / p(x_t)$

(4) Sample a uniform variable u in the range (0, 1),

if $u \leq r$, accept proposed location: $x_{t+1} = y$

if $u > r$, reject proposed location: $x_{t+1} = x_t$

(5) Increment t and repeat steps (2) to (5) until a representative number of samples of x has been collected.

An example adapted from Kruschke (2015) illustrates the Metropolis sampling algorithm applied to a simple discrete distribution of a variable with 10 possible values. Figure 2.11 shows the results of the process for two cases of the target function. The case shown to the left corresponds to a distribution with a single maximum in the middle of the range, whereas in the case to the right, the distribution has two local maxima. The plots at the bottom correspond to the target distribution to be sampled, the middle plots show the traces of the random walks of 3,000 steps followed by the Metropolis algorithm, and the plots at the top correspond to the resulting histograms of sampled values, which mimic the respective target distributions.

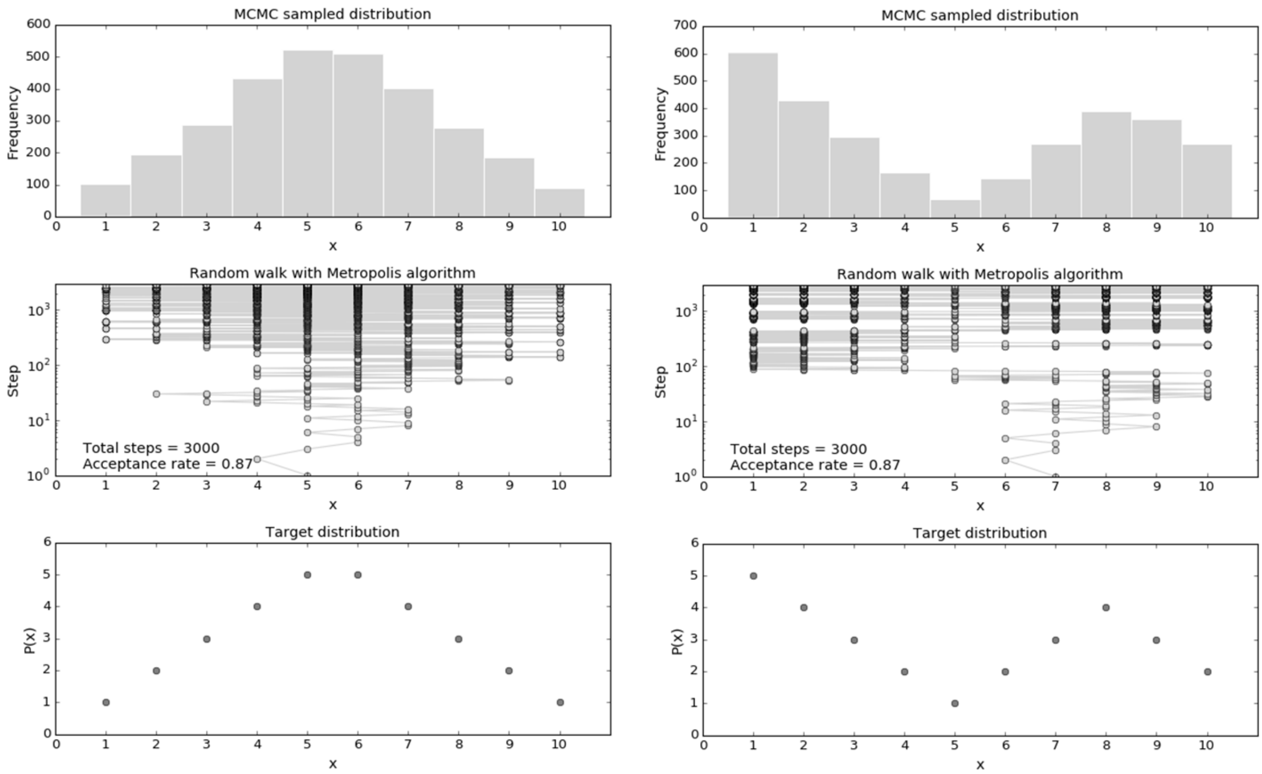

Figure 2.11 Example of the Metropolis sampling algorithm applied to two cases of a discrete target function. The case of a function with a single maximum (left) is compared with the case of a function with two local maxima (right) (adapted from Kruschke 2015)

The proposed moves at each position during the walk are easy to define for the simple discrete distribution shown in Figure 2.11. They correspond to a 50% chance of moving to the neighbouring location on either side of the current location. However, when the target distribution is continuous, the definition of a proposed jump is not that simple. To achieve a proper sampling of the target distribution with a Metropolis algorithm, it is necessary to select an appropriate proposal distribution to cover efficiently the domain of representative values of the parameters investigated. The acceptance rate of proposed locations is one of the various indicators used to verify the quality of the sample. Proposal distributions with small jumps have a high acceptance rate and require a large number of steps to produce an adequate sample. Proposal distributions with large jumps result in small acceptance rates and also require long chains to achieve proper coverage of the representative domain.

2.8.2 The Metropolis-Hasting algorithm

The Metropolis algorithm uses a symmetrical proposal distribution; however, a generalization of the method considers a non-symmetrical proposal distribution, which favours the incorporation of adjustments to achieve the efficiency of the process in particular problems. The generic method is known as the Metropolis-Hastings algorithm. In this case, the probability of acceptance of a move depends not only on the ratio between values of the target distribution at the two locations (proposed upon current) but also on the ratio between the probabilities of the move in the two directions (proposed to current upon current to proposed).

The steps of the Metropolis-Hastings algorithm to sample a variable x from a target distribution p, can be summarised as follows:

(1) Initialize x_t: x_0 for $t = 0$

(2) Define a proposed position y from a probability distribution q centred at current position x_t: $q(y|x_t)$

(3) Evaluate the ratio r: $r = [p(y) \, . \, q(x_t|y)] \, / \, [p(x_t) \, . \, q(y|x_t)]$

(4) Sample a uniform variable u in the range (0, 1),

if $u \leq r$, accept proposed location: $x_{t+1} = y$

if $u > r$, reject proposed location: $x_{t+1} = x_t$

(5) Increment t and repeat steps (2) to (5) until a representative number of samples of x has been collected.

Figure 2.12 illustrates how the Metropolis-Hastings algorithm handles the acceptance of proposed moves in the Markov chain process. In this example, it is possible to visualize the consequence of using a symmetrical proposal distribution, which reduces the method to the simple Metropolis algorithm. In this case, the acceptance of the move depends only on the value of the target distribution at the proposed and current locations.

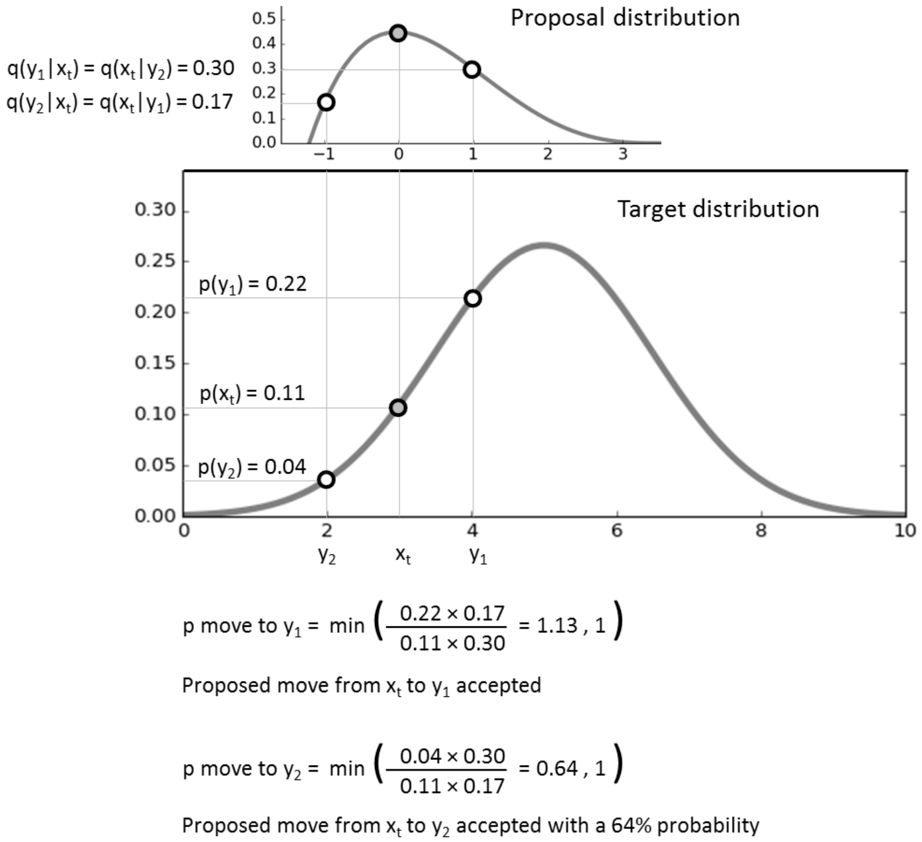

Figure 2.12 Illustration of the acceptance criteria in the Metropolis-Hastings algorithm for two opposite proposed moves in the Markov chain

In the example illustrated in Figure 2.12 the value of the target function at the current location *x=3* is 0.11, if a move is proposed say with probability 0.30 to location *x=4* where the function has a value of 0.22, the probability of that move would be 1.13 and the move would always be accepted. On the other hand, if the proposal distribution suggests a move say with probability 0.17 to location *x=2* where the target function has a value of 0.04, then the probability of the move would be 0.64 and the move would be rejected with a 36% probability. The non-symmetrical proposal distribution provides an additional mechanism to tune the random walk in order to achieve the efficient sampling of particular target distributions.

2.8.3 The Gibbs algorithm

One drawback of the Metropolis algorithm is that the proposal distribution must be properly tuned to the target distribution for the algorithm to be efficient. The Gibbs algorithm is a more efficient variation of the Metropolis algorithm suited for probability functions with many parameters. In this case, the jumps with the proposal distribution are defined for each parameter separately and the conditional probability distribution of the parameter evaluated is used as the proposal distribution. The moves are always accepted with these proposal distributions and the procedure is applied cyclically through all the parameters in an organized manner. Kruschke (2015) explains in detail the method and only a brief description is included hereinafter.

Figure 2.13 illustrates the two steps used with the Gibbs algorithm to sample a two-dimensional target distribution. The current location is at *a0* (*x1=7*, *x2=3*). First, a proposed *x1* value (*x1=6*) is defined conditioned on the current *x2* value (*x2=3*) using the respective probability distribution shown in red in Figure 2.12. Next, a proposed *x2* value (*x2=6*) is defined conditioned to the newly defined *x1* value (*x1=6*) with the distribution shown in blue in the figure. In this way, a move from the current position *a0* to the new position *a1* is completed in two steps.

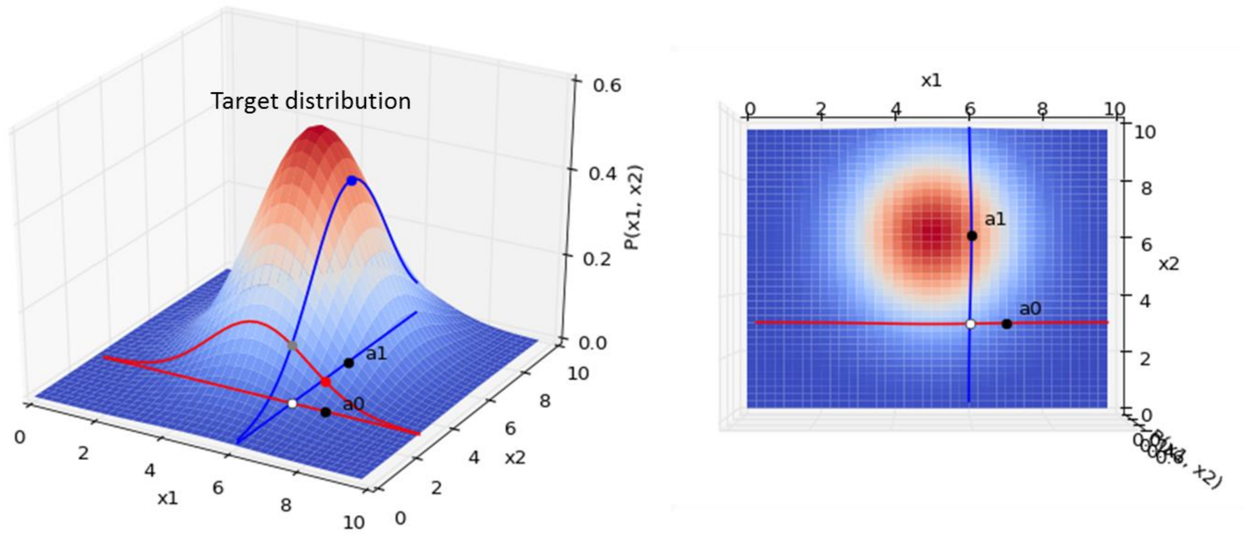

Figure 2.13 Illustration of the double-step used with the Gibbs algorithm for the sampling of a two-dimensional target distribution. The walk from the initial position *a0* to position *a1* is defined with the proposal distributions for the variables *x1* (red) and *x2* (blue)

One limitation of the Gibbs algorithm is that it is inefficient with highly correlated parameters because the progress of the walk can get trapped in narrow regions of the function, requiring small steps to achieve a proper coverage of the parameter space. Figure 2.14 shows an example of a probability distribution of two highly correlated variables that would be difficult to sample efficiently with the Gibbs algorithm.

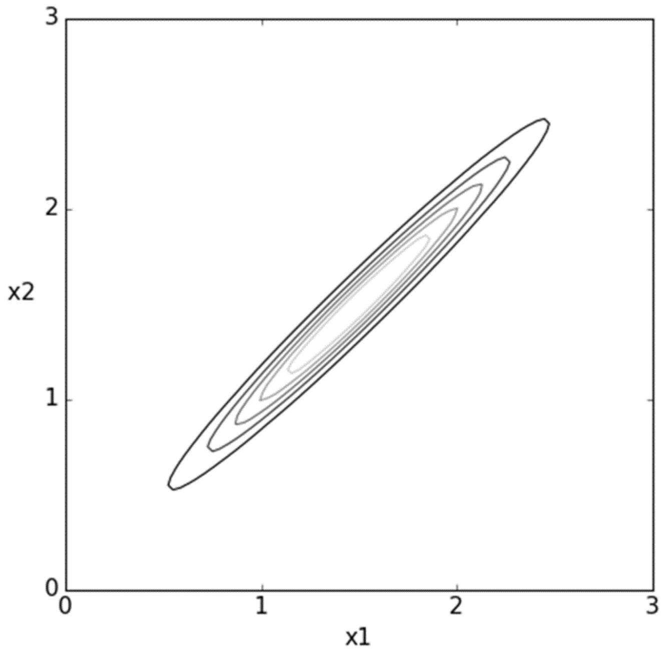

Figure 2.14 Example of a target distribution of two highly correlated variables *x1* and *x2* that would be difficult to sample efficiently with the Gibbs algorithm

2.8.4 The Hamiltonian algorithm

The Hamiltonian Monte Carlo (HMC) is a variation of the Metropolis algorithm where the proposal distribution changes depending on the current position. The algorithm shifts the proposal distribution in the direction in which the target distribution increases. This direction is called the gradient of the function. Kruschke (2015) provides a detailed description of the procedure from a practical perspective and Neal (2011) offers a more rigorous and comprehensive presentation of the method.

Figure 2.15 illustrates the principles of the HMC sampling with the move from point *a0* to *a1* in the domain of a two-dimensional target distribution with variables *x1* and *x2* (top left). The generation of proposal positions with this method is based on the analogy to the dynamics of a frictionless rolling marble on a concave surface, where the surface corresponds to the negative logarithm of the target distribution (bottom left). A new proposed position *a1* is generated by giving a random momentum to the marble and letting it roll on the surface for a certain defined duration (top right). The marble positions define sample points in the space *x1*, *x2* reflecting the probabilities of the target distribution. The position of the marble at the end of the time step is the proposed position, which is accepted or rejected according to a defined criterion. The dynamics of the marble on the surface results in proposal distributions shifted towards the region of higher probabilities at every location (bottom right).

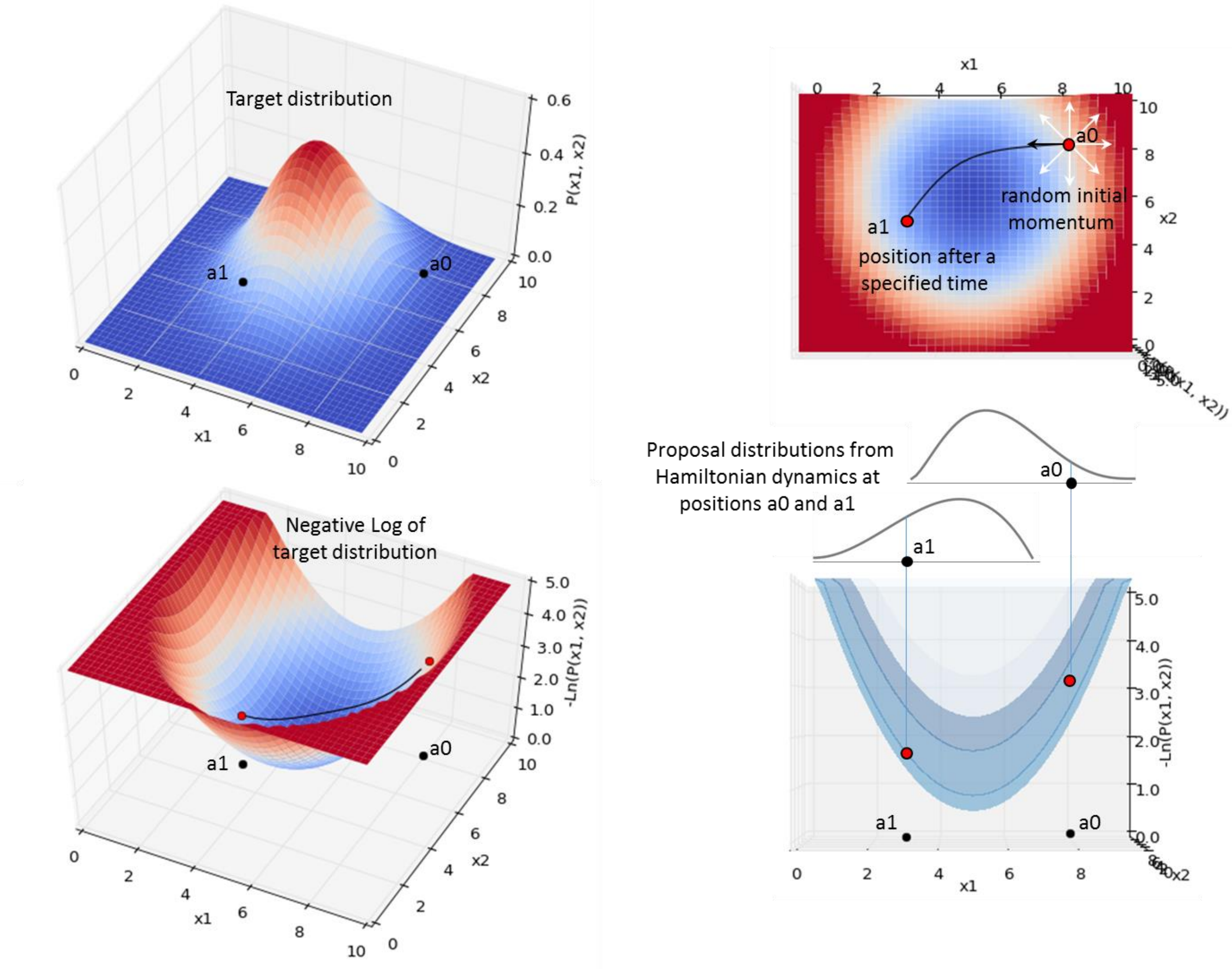

Figure 2.15 Illustration of the principles of the Hamiltonian Monte Carlo. Target distribution (top left). Potential energy of an analogous physical system of frictionless marble rolling on this surface (bottom left). The positions of the rolling marble after a specified time define reflect the probabilities of the target distribution (top right). Proposal distributions shifted towards the region of higher probabilities at every location (bottom right)

The product between the probabilities of the position and the momentum at a given location is analogous to the total energy of the idealized marble moving on the surface. In this analogy, those factors represent the potential and kinetic energies of the marble, respectively. The probability of acceptance is given by the ratio between the energy at the proposed and current locations. This ratio would always be one in the idealized frictionless system, which means that the new position would always be accepted. However, in reality, the trajectories are discretised into small time intervals and this approximation causes a certain percentage of proposal rejections.

The way in which the HMC generates proposal positions results in proposal distributions specific for each location that favours the moves towards the higher probability regions of the target function. The bottom right plot in Figure 2.15 shows the proposal distributions for the positions *a0* and *a1* obtained after many testing jumps at each location.

As with the Metropolis algorithm, the HMC requires tuning of parameters for efficient sampling. In this case, the time step, the number of steps, and the variance of the distribution used to generate the initial momentum are the parameters requiring adjustment. Time steps too small will result in a high acceptance rate but will require many steps to cover the parameter domain. Conversely, time steps too large will result in a lower acceptance rate with a rough coverage of the parameter domain. The number of steps controls the length of the path followed by the rolling marble. If the number of steps is too high, the proposed jumps might be too small as the marble tries to roll back towards the starting positions. A refinement of the HMC to prevent this situation is the algorithm known as the No-U-Turn Sampler (NUTS) that eliminates the need of tuning the number of steps and step size required in the normal HMC procedure.

2.8.5 The affine-invariant ensemble algorithm

A refinement of the Metropolis-Hastings (M-H) algorithm is the affine-invariant ensemble sampling method (Foreman-Mackey et al., 2013). The procedure consists of running a group of M-H samplers (walkers) in parallel generating the moves in a way that results in an efficient coverage of the domain with a proposal distribution that is auto-tuned during the process. The proposed move of a walker is generated by stretching along the straight line connecting the walker with another randomly selected walker used to create the alignment as illustrated in Figure 2.16. In this way, as the walkers start to move towards the higher probability regions, they will attract other walkers in that direction. This procedure of generating proposal locations has two consequences; first, it transforms the variable space into an affine space where the steps from the proposal distribution are more efficient to explore the domain, and secondly, it promotes the auto-tuning of the proposal distribution as more walkers move toward the regions of high probability.

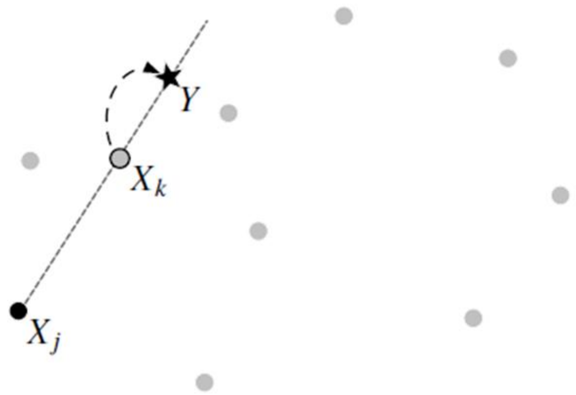

Figure 2.16 The stretch move in the proposal algorithm used in the affine-invariant ensemble sampling method. The position updating of walker x_k is based on the position of another random walker x_j. The light grey dots represent other walkers not participating in this move (Goodman and Weare, 2010)

This algorithm is very efficient with functions of highly correlated parameters, however, it has limitations in certain situations as pointed out by Foreman-Mackey et al. (2013). First, it will not perform adequately with multi-modal target functions, because the walkers can become stuck in different modes and secondly, it cannot be used with functions that contain discrete variables or that have certain types of integer constraints because it will not be possible to perform some vector operations within the algorithm.

2.8.6 Assessment of quality of the MCMC analysis results

In general, the implementation of the MCMC techniques requires adjustments of various parameters to achieve a stable solution in the form of representative independent samples from the parameters. In addition, it is common to throw away a portion of the early steps of the chain, known as the burn-in process, while the sampling sequence evolves into a stable process. An MCMC sample should be representative of the posterior distribution, should have sufficient size to ensure the accuracy of estimates and should be generated efficiently (Kruschke, 2015). There are some diagnostic checks carried out on graphs produced with the results of the analysis that serve to assess some of these requirements. Figure 2.17

shows an example of the diagnostic graphs associated with the sampling of a parameter from a posterior distribution.

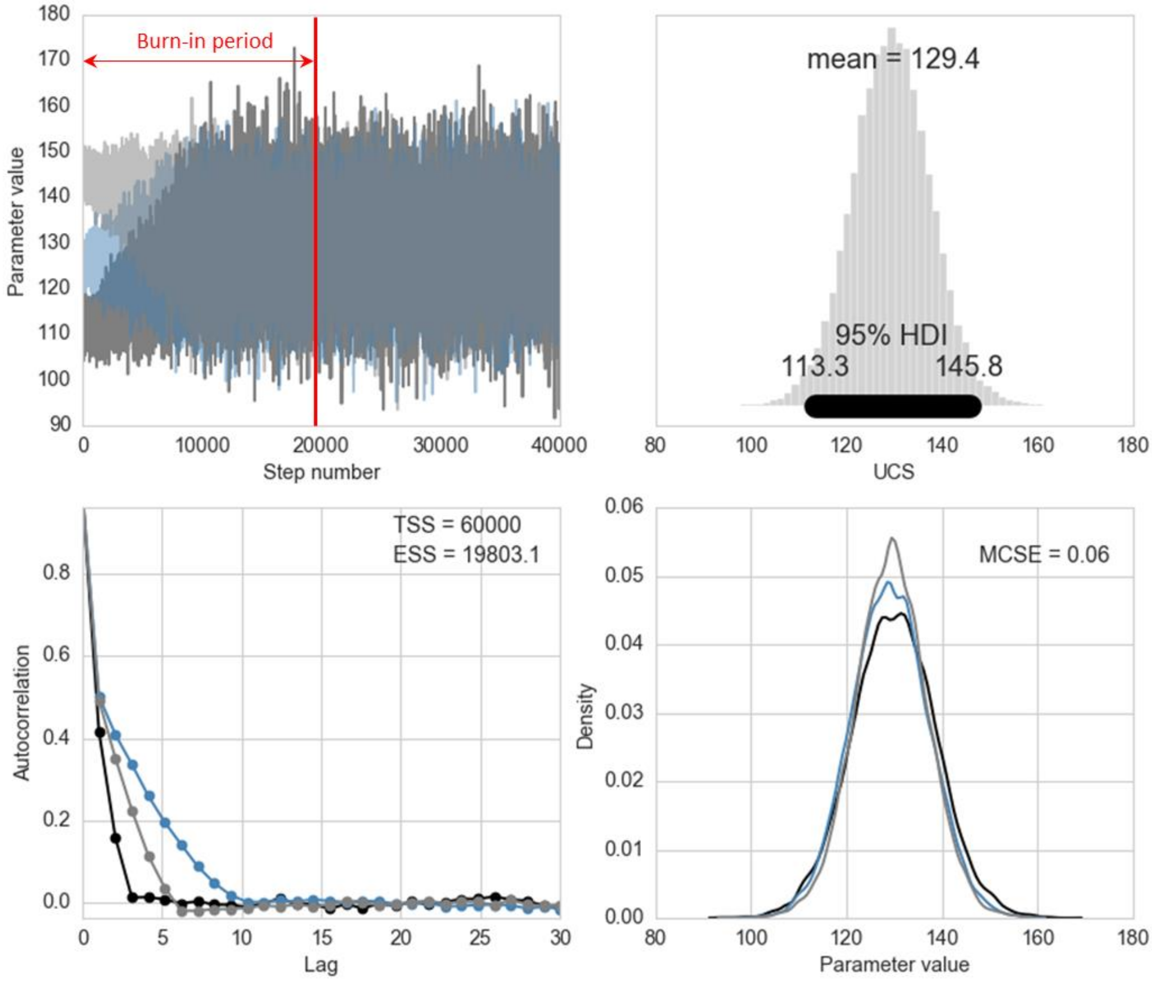

Figure 2.17 Diagnostic graphs to verify the quality of the MCMC sampling of a parameter

The top-left graph in Figure 2.17 corresponds to the trace plot where the parameter values sampled with various chains are displayed as a function of the step number. The plot shows three chains that started at different values and progressed for some time before they reached stability. The total number of steps was 40,000 but only the last 20,000 were used to define a representative sample of the parameter. The first 20,000 discarded steps correspond to the burn-in period. The histogram of the sampled values is shown in the top right graph and includes the estimated mean and the 95% HDI. The bottom left graph is the autocorrelation plot and displays the autocorrelation characteristics of the sample as a function of the lag. The autocorrelation values are calculated as the correlation between the sequence of sampled values and other sequences of the sample shifted a number of positions called the lag. The sample is perfectly correlated with itself and therefore the autocorrelation is one for a lag of zero. The autocorrelation reduces for increasing lags and autocorrelation values close to zero indicate independence of the values and therefore it is a wanted condition. The two results annotated in the autocorrelation graph are the total sample size (TSS) and the effective sample size (ESS). In this case, there are three chains with 20,000 samples each after the removal of the burn-in steps giving a total of 60,000 samples. The ESS reduces the TSS according to the amount of autocorrelation of the chains yielding in this case 19,803 samples. Finally, the bottom right graph corresponds to the density plot, which displays smoothed histograms of the values sampled with each chain. If these plots overlap closely it is an indication of similar coverage of the parameter domain with the chains suggesting representative samples. The annotated value in this plot corresponds to the Monte Carlo standard error (MCSE) calculated as the standard deviation of the sample divided by the square root of the ESS.

In general, the representativeness of the sample is evaluated with the trace plots and the density plots, and the accuracy of the estimates is evaluated with the autocorrelation plots and in particular, with the ESS which is a measure of the number of independent points defining the sample. The efficiency of the process is a function of the algorithm used and the hardware characteristics.

For the algorithms based on acceptance of moves such as the Metropolis-Hastings and Hamiltonian Monte Carlo type of methods, there are some heuristic rules used to assess the quality of the MCMC result. These rules state recommended values for the acceptance rate at the end of the sampling process, to ensure that the samples are independent and representative of the posterior distribution. For example, for the HMC an acceptance rate of 65% is commonly pursued (Kruschke, 2015, p.403) and for the affine-invariant assemble sampler, the recommendation is to have a rate between 20% and 50% (Foreman-Mackey et al., 2013, p.10). In general, an acceptance rate close to zero means that the chain was stuck for many steps at most locations, so there will be few independent points and the sample will not be representative. On the other hand, an acceptance rate close to one means that there is little influence of the target distribution on the chain walk and the sample will not be representative either.

2.8.7 Popular software for MCMC analysis

Although it is important to understand the concepts behind the various algorithms used for the MCMC analysis to assess properly the quality of results, the analyst does not have to program these algorithms. There are already elaborated open source packages in various programming languages developed by computer scientists and related specialists that can be easily incorporated into ad doc code. Figure 2.18 shows the popular options currently available as described by Vincent (2014), supplemented with information from Smith (2014).

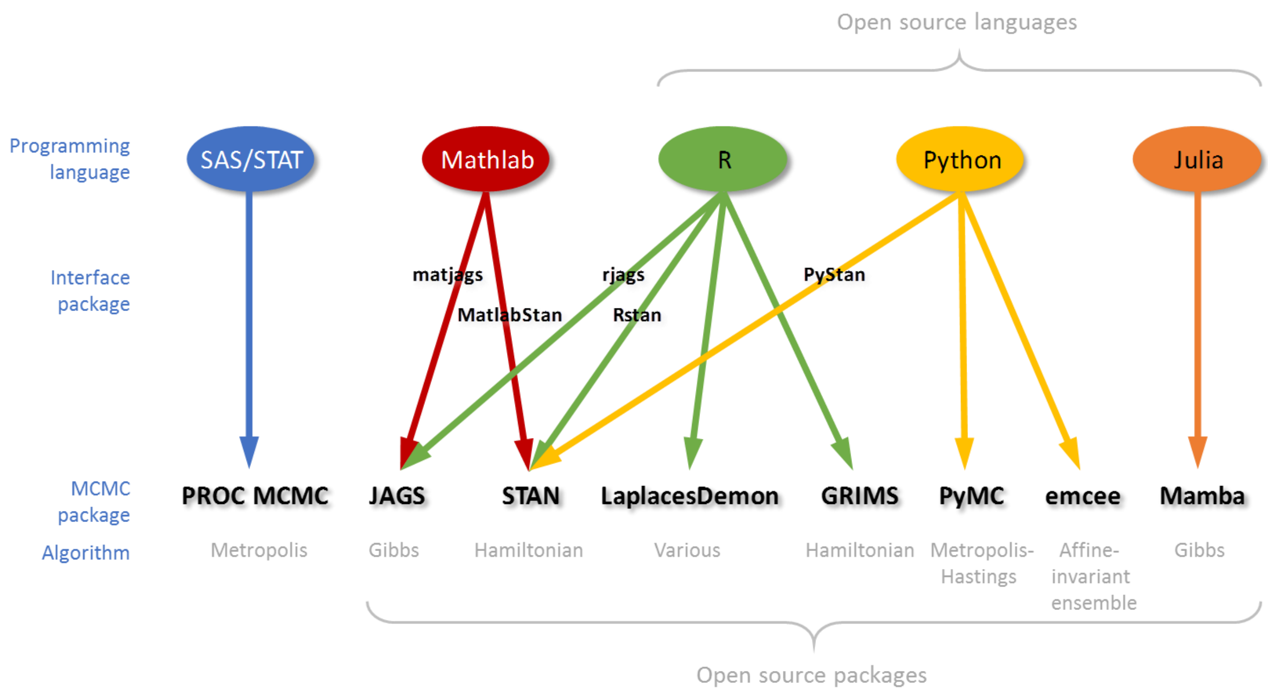

Figure 2.18 Popular software packages for MCMC analysis and the programming languages and interface utilities required to use them (Vincent, 2014, Smith, 2014)

The SAS/STAT is a commercial software system that includes an MCMC procedure based on a Metropolis algorithm. The Gibbs algorithm is incorporated within the JAGS (just another Gibbs sampler) system and can be accessed with packages written in the Mathlab and R programming languages. The system STAN (sampling through adaptive neighbourhoods) uses the HMC method and includes the NUTS algorithm that eliminates the need for tuning. The STAN system can be accessed through packages in Mathlab, R and Python programming languages. The LaplacesDemon and GRIMS packages are developed in R, the former uses a collection of various samplers and the latter is based on the HMC algorithm. The PyMC system uses the classic M-H sampler and the emcee system incorporates the affine invariant ensemble sampler. The latter two systems are pure python packages (Python Software Foundation, 2001) that can be used directly within the python code. The Mamba package uses a Gibbs sampler and is developed in the Julia open source programming language.

VanderPlas (2014b) presents a detailed comparison between the three Python systems using a relatively simple model to measure performance and features. His analysis indicates that PyStan is the more complex system with many features and options and emcee is the more basic and light, however, in terms of ease of installation and use, emcee is the best rated with PyStan the more difficult to handle. In terms of performance, the three systems are similar for relatively simple models, suggesting that the differences probably will only be relevant for complex models with many dimensions. Kruschke (2015) uses the two R systems in all the examples presented in his book. The description of the example cases suggests that both systems are powerful, although the JAGS system requires the rescaling of functions for models with highly correlated variables. The software used for the models described in this thesis was coded in the python programming language using the emcee sampler. An important point to note is that the emcee package, although described as basic in the evaluation by VanderPlas, is very powerful. The software was developed and it is used by the astrophysicist's community with complex multidimensional models that exceed the expected complexity and dimensionality of the models for geotechnical analysis.

References

Baecher, G.B. and Christian, J.T., 2003. *Reliability and statistics in geotechnical engineering.* Wiley, Chichester, UK.

Barton, N., and Choubey, V., 1977. The Shear Strength of Rock Joints in Theory and Practice. *Rock Mechanics,* 10, 1–54.

Barton, N., and Bandis, S., 1982. Effects of block size on the shear behaviour of jointed rock. In *Proceedings of 23rd US Symposium of Rock Mechanics* (eds RE Goodman and FE Heuze)*,* Berkeley, California, AIME, New York, 739-760.

Bayes, T., 1763. An essay towards solving a problem in the doctrine of chance. *Philosophical Transactions*, Royal Society of London, 53, 370–418.

Bozorgzadeh, N. and Harrison, J.P., 2014. Characterizing uniaxial compressive strength using Bayesian updating. *Proceedings 48th US Rock Mechanics/Geomechanics Symposium*, Minneapolis, 1-4 June, Paper ARMA 14-7194, 7 p.

Cai, M., Kaiser, P.K., Uno, H., Tasaka, Y. and Minami, M., 2004. Estimation of rock mass deformation modulus and strength of jointed hard rock masses using the GSI system. *International Journal of Rock Mechanics and Mining Sciences,* 41(1), 3–19.

Cao, Z., Wang, Y. and Li, D., 2016. Quantification of prior knowledge in geotechnical site characterization. *Engineering Geology*, 203, 107-116.

Contreras, L.F., 2015. An economic risk evaluation approach for pit slope optimization. *The Journal of the Southern African Institute of Mining and Metallurgy*, 115, 607-622.

Diaconis, P., 2009. The Markov Chain Monte Carlo Revolution. *Bulleting of the American Mathematical Society*, 46(2), 179–205.

Christian, J.T., 2004. Geotechnical Engineering Reliability: How Well Do We Know What We Are Doing? *Journal of Geotechnical and Geoenvironmental Engineering*, 130(10), 985–1003.

Foreman-Mackey, D., Hogg, D.W., Lang, D. and Goodman, J., 2013. emcee: The MCMC Hammer. *Publications of the Astronomical Society of Pacific*, 125(925), 306–312.

Gelman, A., Carlin, J.B., Stern, H.S., Dunson, D.B., Vehtari, A. and Rubin, D.B., 2013. *Bayesian Data Analysis*. Chapman and Hall, CRC Press.

Gregory, P., 2005. *Bayesian Logical Data Analysis for the Physical Sciences.* Cambridge; New York: Cambridge University Press.

Goodman, J. and Weare, J., 2010. Ensemble Samplers with Affine Invariance. *Communications in Applied Mathematics and Computational Science*, 5(1), Mathematical Science Publishers.

Harr, M.E., 1987. *Reliability-based design in civil engineering.* Dover Publications Inc., Mineola, New York.

Helton, J.C., Johnson, J.D. and Oberkampf, W.L., 2004. An exploration of alternative approaches to the representation of uncertainty in model predictions. *Reliability Engineering and System Safety,* 85(1–3), 39–71.

Hoek, E., 2012. *Blast Damage Factor D*. Technical note for RocNews – Winter 2012 Issue, 1–7.

Hoek, E. and Bray, J.W., 1981. *Rock slope engineering.* Third edition, The Institute of Mining and Metallurgy, London, UK.

Hoek, E. and Brown, E.T., 1997. Practical Estimates of Rock Mass Strength. *International Journal of Rock Mechanics and Mining Sciences*, 34(8), 1165–1186.

Hoek, E. and Brown, E.T., 2019. The Hoek – Brown failure criterion and GSI – 2018 edition. Journal of Rock Mechanics and Geotechnical Engineering, 11(3), 445-463.

Hoek E., Carranza-Torres C.T. and Corkum B., 2002. Hoek–Brown failure criterion—2002 edition. In R. Hammah, W. Bawden, J. Curran, M. Telesnicki (eds), *Proceedings of the Fifth North American Rock Mechanics Symposium (NARMS-TAC)*, University of Toronto Press, Toronto. 267–273.

Hoek, E., Carter, T.G. and Diederichs, M.S., 2013. Quantification of the Geological Strength Index chart. *Proceedings 47th US Rock Mechanics/Geomechanics Symposium*, San Francisco, 23-26 June, Paper ARMA 13-672, 9 p.

Hoff, P.D., 2009. *A first course in Bayesian statistical methods.* Springer Texts in Statistics.

Juang, C.H. and Zhang, J., 2017. Bayesian Methods for Geotechnical Applications - A Practical Guide. *Proceedings of Georisk 2017 on Geotechnical Risk from Theory to Practice*, 4-7 June, Denver, Colorado, USA.

Kruschke, J.K., 2015. *Doing Bayesian Data Analysis: A Tutorial with R, JAGS and STAN*, Academic Press/Elsevier.

Langford, J.C. and Diederichs, M.S., 2013. Evaluating uncertainty in intact and rockmass parameters for the purposes of reliability assessment. *Proceedings 47th US Rock Mechanics/Geomechanics Symposium*, San Francisco, 23-26 June, Paper ARMA 13-459, 9 p.

Neal, R.M., 2011. MCMC using Hamiltonian dynamics. In S Brooks, A Gelman, G Jones and X-L Meng (eds), *Handbook of Markov Chain Monte Carlo*, Chapman and Hall / CRC Press. 113–160.

Palmström, A., 1996. Characterizing rock masses by the RMi for use in practical rock engineering. *Tunnelling and Underground Space Technology*, 11.

Priest, S.D. and Hudson, J.A., 1981. Estimation of discontinuity spacings and trace length using scanline surveys. *International Journal of Rock Mechanics and Mining Sciences,* 18, 183–197.

Python Software Foundation, 2001. *Python language reference*, version 3.4 [on line]. [Accessed 20/01/2015]. https://www.python.org/.

Robert, C.P. and Casella, G., 2004. *Monte Carlo Statistical Methods*. 2nd ed. Springer, New York.

Robert, C.P. and Casella, G., 2011. A Short History of Markov Chain Monte Carlo: Subjective Recollections from Incomplete Data. *Statistical Science*, 26(1), 102–115.

Russo, G., 2009. A new rational method for calculating the GSI. *Tunnelling and Underground Space Technology*, 24, 103–111.

Shannon, C.E., 1948. A Mathematical Theory of Communication. *The Bell System Technical Journal, 27*, 379–423, 623–656.

Siu, N.O. and Kelly, D.L., 1998. Bayesian parameter estimation in probabilistic risk assessment. *Reliability Engineering and System Safety*, 62, 89–116.

Sivia, D.S. and Skilling, J., 2006. *Data Analysis. A Bayesian Tutorial*. Oxford University Press.

Smith, B.J., 2014. *Mamba: Markov chain Monte Carlo (MCMC) for Bayesian analysis in Julia* [on line]. [Accessed 08/06/2016]. https://github.com/brian-j-smith/Mamba.jl.

Sonmez, H. and Ulusay R., 1999. Modifications to the geological strength index (GSI) and their applicability to stability of slopes. *International Journal of Rock Mechanics and Mining Sciences,* 36, 743–760.

Stacey, P., 2009. Fundamentals of Slope Design. In J. Read and P. Stacey (eds), *Guidelines for Open Pit Slope Design*, CSIRO Publishing, Collingwood, Victoria. 1–14.

Steffen, O.K.H., Contreras, L.F., Terbrugge, P.J. and Venter, J., 2008. A risk evaluation approach for pit slope design. *Proceedings 42nd US Rock Mechanics/Geomechanics Symposium*, San Francisco, June 29-July 2, Paper ARMA 08-231, 18 p.

Stone, J.V., 2013. *Bayes' Rule: A Tutorial Introduction to Bayesian Analysis*, Sebtel Press.

Tribus, M., 1988. An engineer looks at Bayes. In G.J. Erickson and C.R. Smith (eds), *Maximum Entropy and Bayesian Methods in Science and Engineering*, Kluwer Academic Publishers, 1, 31–52.

VanderPlas, J., 2014a. *Frequentism and Bayesianism: A Practical Introduction*. In Phytonic Preambulations Blog [on line]. [Accessed 20/01/2015]. https://jakevdp.github.io/blog/2014/03/11/frequentism-and-bayesianism-a-practical-intro/.

VanderPlas, J., 2014b. *Frequentism and Bayesianism IV: How to be a Bayesian in Python*, in Phytonic Preambulations Blog [on line]. [Accessed 20/01/2015]. http://jakevdp.github.io/blog/2014/06/14/frequentism-and-bayesianism-4-bayesian-in-python/.

Vincent, D.B.T., 2014. *Software for MCMC.* In inference Lab blog [on line] [Accessed 08/06/2016]. http://www.inferencelab.com/mcmc_software/.

Wesseloo, J. and Read, J., 2009. Acceptance Criteria. In J. Read and P. Stacey (eds). *Guidelines for Open Pit Slope Design*, CSIRO Publishing, Collingwood, Victoria. 221-236.

Chapter 3 - Unconventional Methods to Treat Geotechnical Uncertainty in Slope Design

Luis-Fernando Contreras[a], *Marc Ruest*[a]

[a] The University of Queensland, Brisbane, Australia.

Corresponding author: luis.contreras@uq.net.au

Abstract

The definition of the geotechnical model for slope design is based on the geological, structural, rock mass and hydrogeological models. Each model is described by different sets of information and parameters and is defined at a scale of interest for the purpose of the analysis of slope behaviour. However, no clear guidelines exist in terms of the appropriate statistical methods to manage this information. Probabilistic methods are traditionally used to account for the uncertainty in engineering design, however, the base assumptions of these methods are not always fully understood, resulting in misinterpretations of results. There are two main approaches of statistical analysis known as frequentist (classical) and Bayesian, which are based on different interpretations of probability. In the classical approach, probabilities are considered as frequencies in a series of similar trials, whereas in the Bayesian approach, probabilities correspond to degrees of belief. One of the main characteristics of the Bayesian approach is that makes use of both prior information on the hypothesis (or model) being examined and the likelihood of the available data, to provide a balanced answer to the probability of that hypothesis (or model). Another aspect of the uncertainty characterization process is the understanding of the type of uncertainty present in the various components of the geotechnical model. At a broad level, there are two main types of uncertainty in geotechnical engineering, one due to random variation of the aspect evaluated (aleatory) and the second due to lack of knowledge of the subject under analysis (epistemic). The uncertainty is considered epistemic if it can be reduced with the collection of additional data or by refining models, otherwise, it is treated as natural variation. The majority of the uncertainty in the geotechnical model for slope design is epistemic, typically analysed with probabilistic methods. However, epistemic uncertainty has different aspects some of which (i.e. vagueness or non-specificity) can be represented more naturally with

alternative approaches outside the field of probability (i.e. interval analysis, possibility and evidence theories). Simple examples will be included to illustrate the merits of treating uncertainty in the mine slope design process with unconventional methods such as Bayesian statistics and non-probabilistic based approaches.

Keywords: uncertainty; probabilistic methods; Bayesian statistics; epistemic uncertainty.

3.1 Introduction

One of the major difficulties encountered by the geotechnical engineer is to deal with the uncertainty present in every aspect of the process of slope design. Uncertainty is associated with natural variation of parameters and properties, and the imprecision and unpredictability caused by insufficient information on parameters or models. Design strategies to deal with the problems associated with uncertainty include conservative design options with large factors of safety, adjustments during the implementation phases based on observations of performance, and the use of probabilistic methods that attempt to measure and account for the uncertainty in the design. However, one of the drawbacks of the probabilistic approach is related to the strong component of subjective information such as engineering judgement that is incorporated in the process without a formal framework to do so. Another weakness of the probabilistic approach is related to the misunderstanding of the basic assumptions of the classical statistical methods that commonly results in interpretations of statistical results that exceed the capabilities of these methods. Some examples that illustrate this point are the assignment of probability distributions derived from samples as unique representations of populations, or the use of confidence intervals (CIs) as a measure of data reliability. The Bayesian approach is based on a particular interpretation of probability and offers an adequate framework to treat uncertainty in the geotechnical model for slope design. It offers a formal way to combine hard data with subjective information, and provides the probability measures of the hypothesis, parameters or models given the data. These are the type of results needed by the geotechnical engineer, as opposed to the probability of data assuming that the hypothesis, parameters or models are true.

The epistemic uncertainty associated with lack of information has a multifaceted character, and there are situations where probabilistic methods are incapable of adequately representing aspects such as non-specificity, fuzziness or ambiguity. Non-probabilistic methods such as interval analysis, fuzzy set analysis and approaches based on possibility and evidence theories are indicated in these cases. The paper provides a brief description of some unconventional approaches to treat uncertainty that have the application potential during the construction of geotechnical models for slope design.

3.2 Uncertainty in the geotechnical model for slope design

The geotechnical model for slope design is particularly complex because it incorporates information from different already complex models. The slope design model is based on the geological, structural, rock mass and hydrogeological models (Stacey, 2009). Each model is described by different sets of information and parameters and is defined at a scale of interest for the analysis of slope behaviour. Intuitively, it is clear that there is uncertainty in the geotechnical model, but to have a better understanding of how this uncertainty affects the design process, it is necessary to look in more detail at its characteristics.

3.2.1 Types of uncertainty

Uncertainty is associated with various concepts such as unpredictability, imprecision, variability and so forth. At a basic level, uncertainty can be categorised into aleatory and epistemic. Baecher and Christian (2003) discussed these types of uncertainty in detail, indicating that aleatory uncertainty is associated with random variations, natural variability, occurring in the world, of external character; whereas epistemic uncertainty is associated with the unknown, derived from lack of knowledge, occurring in the mind, of internal character. The epistemic uncertainty can be reduced with the collection of additional data or by refining models based on a better understanding of the entities represented. The natural variation, on the other hand, cannot be reduced with more information, which will only serve to have a better representation of this type of uncertainty.

The sketch in Figure 3.1 is adapted from Bedi and Harrison (2013) and shows the distinction between the two types of uncertainty in terms of the available information at a particular point in time. The limit state of precise information that defines the point of irreducible uncertainty, moves through time towards the end of complete certainty as a result of technological advances. This is a consequence of a better understanding of the processes perceived initially as random. An example of this situation is the distribution of fractures in a rock mass. Baecher and Christian (2003) indicated that the separation between epistemic and aleatory uncertainty in a model is the result of a trade-off defined by the geotechnical engineer to treat the uncertainty.

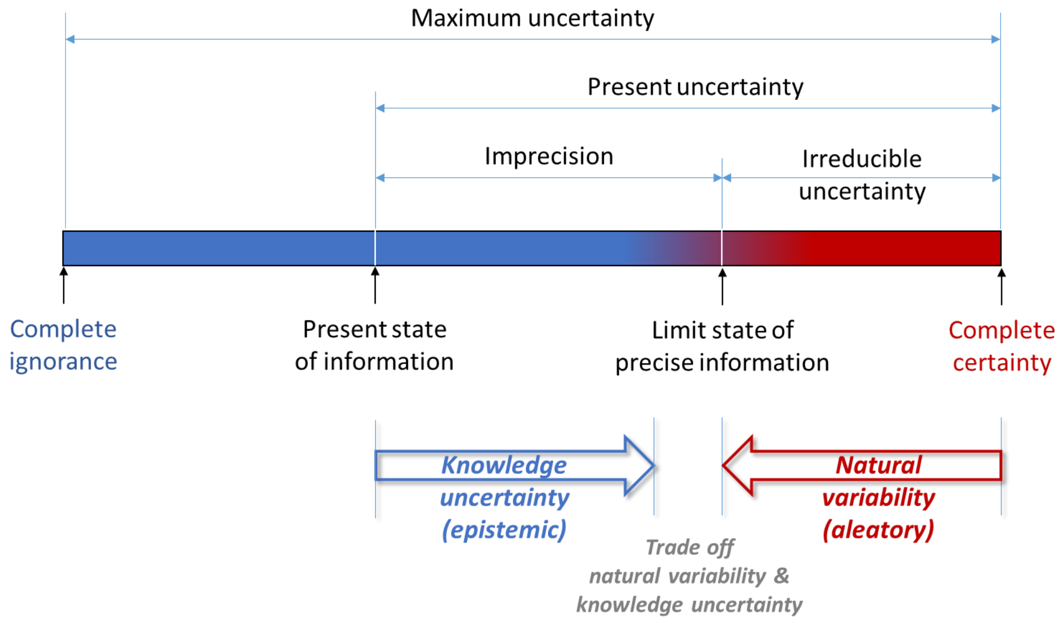

Figure 3.1 Relationship between types of uncertainty and information available (adapted from Bedi & Harrison 2013)

3.2.2 Uncertainty in the geotechnical model

The amount of geotechnical data typically available for slope design is small compared with that collected for mineral exploration and resource model estimation. Inferences on rock properties are based on limited data, uncertainty levels are perceived to be high, and the quantification of the confidence levels of model parameters is based on rudimentary methods or not evaluated at all. Moreover, the geotechnical model borrows information from other models with no measure of confidence, or with confidence levels assigned using rudimentary systems that cannot capture the complexities of spatial variations, and trends and cross-correlations in addition to data characteristics. The transfer of information across models is done in an intuitive manner, with a strong judgemental basis. The end result is that the levels of confidence of the geotechnical model and its components are unknown or defined in a rudimentary way. The implications of the lack of a suitable approach to quantify the confidence of the geotechnical model are the inability to judge whether the available data is sufficient to support the design at the various stages of project development and the difficulty to define strategies for site characterisation on a rational basis.

The uncertainty in the geotechnical model for slope design is present in all the component models in different forms. The sources of uncertainty include:

- The inherent variability of the basic properties considered as random variables (i.e. structural features, Unconfined Compression Strength (UCS), Rock Quality Designation (RQD), etc.).
- Measurement errors of the properties.
- Estimation of the statistical parameters used to represent the variables (i.e. mean, standard deviation, etc.).
- Approximations in the definition of sub-models to estimate derived variables (i.e. Hoek-Brown mi parameter from UCS, Brazilian Tensile Strength (BTS) and Triaxial Compression Strength (TCS) testing, Geological Strength Index (GSI) from the joint structure and joint condition descriptors, etc.).

A large part of the uncertainty present in the geotechnical model for slope design corresponds to epistemic uncertainty that would be susceptible to reduction with increased data collection, but this is rarely achieved due to the typical constraints in the mining environment.

3.3 Conventional ways to treat uncertainty in slope design

The situation in the geotechnical model for slope design is that the levels of information are relatively low and the range of the epistemic uncertainty as sketched in Figure 3.1 is wide, and commonly treated as aleatory uncertainty by means of assuming large variances and wide distributions of parameters. However, the statistical methods used in this process are inconsistent with these practices, as will be discussed hereafter. Common strategies to deal with uncertainty in geotechnical engineering were described by Christian (2004) and a brief description of the strategies relevant to the slope design process is presented next.

3.3.1 Conservative design

The simplest (although not the most efficient) way to account for the uncertainty in the geotechnical model is through the implementation of conservative designs. This is done by selecting higher factors of safety or low probabilities of failure in the acceptability criteria of the slope design. However, the difficulty of defining what are acceptable design values remains. Moreover, this strategy might not be effective in many mining projects where the steepest or highest slopes are often required to achieve the sought economic benefit of the project. A conservative design in this scenario likely would result in a financially unviable mine.

3.3.2 Observational method

The observational method is a common way to deal with uncertainty in geotechnical information in many types of engineering projects. The approach is part of the normal process of measuring the performance of the works as the project progresses, to verify the original assumptions and models, and to implement the pertinent design adjustments to ensure design objectives are achieved. However, there are situations in mine slope projects where changes are difficult to implement at the time they are identified as necessary, reducing the space for this strategy. For example, this is the case when the flattening of a slope is required to prevent a ramp failure, but the implementation might be unfeasible at the time the need for this measure is identified.

3.3.3 Quantification of uncertainty

Uncertainties are quantified with probabilities, which in turn can be interpreted as frequencies in a series of similar trials, or as degrees of belief. Some aspects of geotechnical engineering can be treated as random entities represented by relative frequencies and others may correspond to unique unknown states of nature better considered as degrees of belief. An example of the former is a material property evaluated with data from laboratory testing, and the latter can be represented by any form of expert opinion, for example when a geological section is constructed from site investigation data. Baecher and Christian (2003) provide a detailed discussion on the topic of duality in the interpretation of uncertainty and probability in geotechnical engineering. They indicate that both types of probabilities are present in risk and reliability analysis, and point out that the separation between them is a modelling artefact rather than an immutable property of nature.

The two alternative interpretations of probability are at the base of the two approaches of statistical analysis known as frequentist (classical) and Bayesian. In mineral exploration, the approach to deal with uncertainty is based on classical statistics characterised by the systematic collection of data and the use of geostatistics to model spatial variation. In the oil and gas industries, uncertainty is evaluated through risk analysis methods based on decision theory and Bayesian concepts. In the geotechnical engineering field for slope design, there is not a clear definition on the appropriate statistical approach to follow to quantify uncertainty. However, it is argued that Bayesian statistical methods are a better option to treat the geotechnical uncertainty in slope design, because they provide a formal framework to combine hard data, which is typically scarce, with other sources of information that may be available, including expert judgment.

3.4 Probabilistic methods to treat uncertainty

The basis of classical statistical methods is consistent with the concepts behind the aleatory type of uncertainty but less so with the epistemic uncertainty. The Bayesian statistical approach is well suited to deal with both types of uncertainty and will be of great benefit to treat the uncertainty in the geotechnical model for slope design. Unfortunately, its use in this particular area is rare, probably due to a lack of understanding of its conceptual basis.

3.4.1 Frequentist versus Bayesian statistical methods

The more relevant points of contrast between the frequentist and Bayesian approaches are summarised in Table 3.1. The first aspect constitutes one of the more important advantages of the Bayesian approach as it addresses the question of interest to the geotechnical engineer. This aspect is also at the base of the misunderstanding on the type of answer that the classical methods provide. A simple way to present Bayes' equation, using the definition of terms in Table 3.1 is:

$$p(h|d) = \frac{p(d|h)p(h)}{p(d)} \tag{3.1}$$

which can also be interpreted in the following manner (Kruschke 2015):

$$posterior = \frac{likelihood \ \times prior}{evidence} \tag{3.2}$$

Table 3.1 Key aspects of contrast between the frequentist (classical) and Bayesian approaches of statistical analysis

Aspect	Frequentist approach	Bayesian approach
Question answered with the approach	What is the probability of the data if the hypothesis (parameter or model) examined is true (*p[d|h]*)	What is the probability of the hypothesis (parameter or model) examined given the data observed (*p[h|d]*)
Information used	Only data collected with sampling (*p[d|h]*)	Prior information of any type (*p[h]*) and data from sampling (*p[d|h]*)
Characteristics of the result from the inference process	Point estimate (maximum likelihood) and standard error of the parameter (or model) evaluated	Probability distribution of the parameter (or model) evaluated
Assumptions regarding data and parameters (or models)	Data are random, parameters (or models) are fixed	Data are fixed, parameters (or models) are random
Inference method	Based on null hypothesis significance testing	Based on the updating of prior information by adding the effect of observed data to provide a posterior distribution reflecting a balance between the two inputs

The "posterior" is the answer of interest when defining the geotechnical model for design, the "likelihood" of data is the answer given by classical statistical methods, the "prior" represents the initial knowledge (or lack of it) on the hypothesis and the "evidence" of data normally treated as a normalisation factor so that the posterior integrates to 1.0. When $p(h)$ is set to a uniform distribution representing the case of no previous knowledge, the equation reduces to $p(h|d) \propto p(d|h)$ and the two approaches provide the same answer. For this reason, the frequentist method can often be viewed as a special case of the Bayesian approach for some (implicit) choice of the prior (VanderPlas 2014).

The main criticism of the Bayesian approach is related to the use of prior information which in some cases could be subjective. However, this aspect is of little relevance in the area of mine slope design, where subjective information is important and continuously incorporated into the process, although in an intuitive and non-formal way. The Bayesian approach provides a framework to use this type of information in a formal and more rational way.

3.4.2 Common misinterpretations of results from frequentist statistical methods

A consequence of the different interpretations of probability is the contrasting assumptions regarding data and parameters made by the approaches, which in turn affects how the boundaries of model parameters are determined. In the frequentist approach, CIs from data are used to define meaningful parameter boundaries, whereas in the Bayesian approach this is done with credible regions of the posterior distribution.

The CI is defined by upper and lower bound values above and below the mean of a data sample, and is associated with good estimates of the unknown population parameter investigated. The CI is calculated from a particular sample and its width depends on the number of data points in the sample, and the chosen level of confidence for the estimation. For this reason, this result is commonly used as a measure of confidence of parameter estimates, without a full understanding of the meaning. A CI is specific to a data sample and its confidence level only has meaning in repeated sampling. For example, if the 95% CI for the mean UCS of a particular rock type is constructed, it either includes the true UCS value or it does not, but it is not possible to know the situation for that particular CI. The 95% confidence means that if the sampling process were repeated numerous times, and CI's calculated for those various samples, 95% of the sample sets will have CI's containing the true UCS value. However, because the true value is an unknown fixed parameter in the frequentist framework, it is not possible to identify the sample sets containing the true UCS. The uncertainty regarding the true UCS value remains.

Figure 3.2 shows an example of repeated sampling that allows an appreciation of the meaning of the CI in the frequentist approach. The values could represent UCS results for a particular rock type, but the data was randomly generated to illustrate the point. A total of 100 data sets of 15 values each were sampled from a normal distribution with a mean of 120 and a standard deviation of 30, that represent the unknown fixed parameters of the population. Each data set has its own mean and standard deviation and the bars in Figure 3.2 correspond to the 95% CIs of the mean. However, for this particular group of data sets, 91 of the intervals contain the true mean. A larger number of data sets would be required to get a better approximation of the 95% level used for the construction of the intervals. Nevertheless, the important point with this example is that in terms of each individual data set, there is no probability associated with the inclusion of the true mean.

The interval either includes it or does not and in a real case situation, there would be only one data set and it would not be possible to estimate the true value.

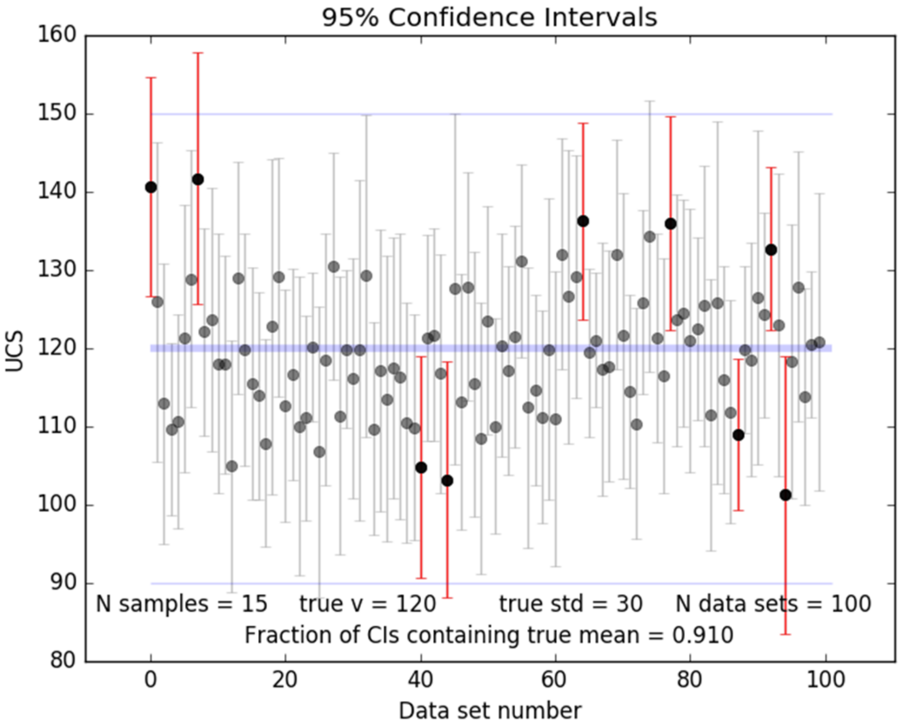

Figure 3.2 Frequentist interpretation of CIs for randomly generated UCS data sets of 15 values with a mean of 120 and a standard deviation of 30

In the Bayesian approach, the situation is different because the unknown parameter investigated is considered a random variable that is updated for every new data set. The posterior probability distribution resulting from the Bayesian updating process is used to define the highest density interval with a particular level of precision, and this interval defines the bounds of the credible region for the estimation of the parameter. In many simple situations, the results from both approaches coincide, but the meaning of the result is different. The Bayesian result has a meaning consistent with the answer that is normally sought by the analyst, whereas the frequentist result responds to a different question that is of less interest to the analyst.

Figure 3.3 compares the frequentist 95% CI for data set 27 in Figure 3.2 with the credible interval corresponding to the 95% highest density interval (HDI) of the posterior distribution. The posterior distribution is calculated with the Bayesian approach for the same data set, assuming a uniform prior distribution which is considered a non-informative prior in this case.

The results show that the likelihood of the data is not affected by the prior, yielding a result that seems to coincide with the frequentist result, although with different meanings. In this case, the Bayesian interval indicates a range for the sought mean with a 95% credibility. This is possible because in the Bayesian framework, the parameter investigated is not fixed and it changes as new data is available. The frequentist result corresponds to a point estimate of the mean and a measure of the error represented by the width of the CI, whereas the Bayesian results provide a full probability distribution for the mean based on the data used.

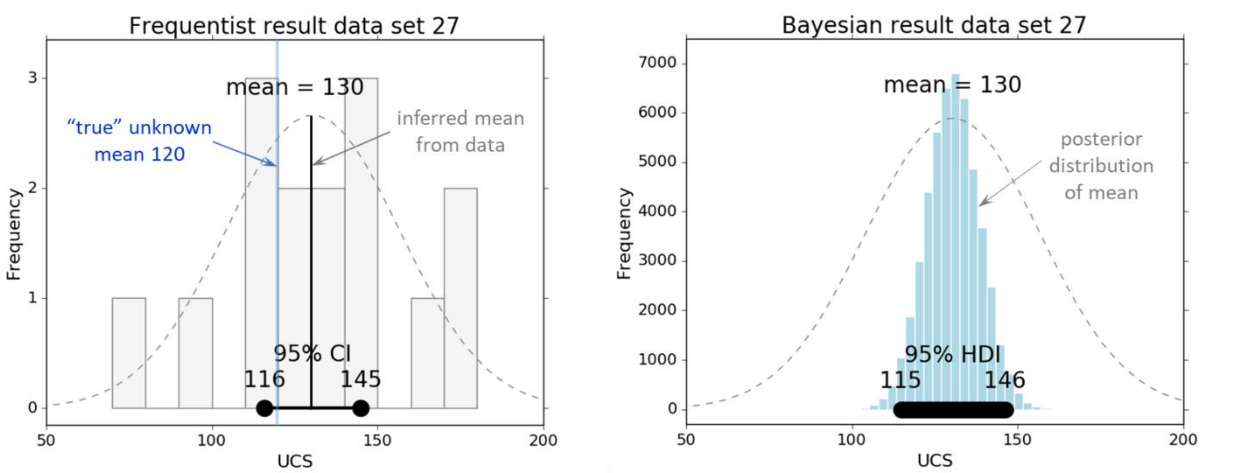

Figure 3.3 Comparison between the frequentist (left) and Bayesian (right) results for the inference of the mean UCS of data set 27 in Figure 3.2

3.4.3 Inconsistency of the frequentist approach with the epistemic uncertainty

The definition of probability within the frequentist approach is inconsistent with the definition of epistemic uncertainty. Therefore, it seems inappropriate to model this type of uncertainty by means of repetition of trials with a particular probability distribution. Some aspects of this type of uncertainty are closer to the interpretation of probability as a degree of belief that can be assigned directly to states of nature. However, a common practice in geotechnical design is to include assumptions that enable the randomisation of epistemic uncertainty, and the modelling with frequentist methods.

For this reason, the Bayesian approach seems better equipped to model uncertainty in general, including epistemic uncertainty. Subjective knowledge and expert opinion can formally be incorporated into this methodology through the selection of the appropriate priors. The frequentist approach does not allow the use of information that is not the result of a random sampling process. Nevertheless, at least within the geotechnical engineering field in open pit mining, it is not conceivable to have a slope design where some form of previous knowledge is not used in the process. However, a drawback from this practice is the difficulty to quantify the uncertainty of the design, because the inclusion of this information is based on the intuition of individuals and carried out in a rather arbitrary way.

3.4.4 A simple example of the Bayesian method

The Bayesian approach is not meant to be used in simple cases like the UCS analysis presented above, where apart from the subtle differences in their meaning, numerical results seem to coincide. The real strength of this approach is shown in situations where the models examined are multidimensional, with a multitude of parameters that need to be inferred, where the frequentist methods would be less efficient and produce results more difficult to interpret. A few recent examples of the application of Bayesian analysis in rock mechanics and slope problems include: the estimation of the rock mass deformation modulus based on model selection and Bayesian updating by Feng and Jimenez (2015), the characterisation of the UCS from the Bayesian selection of a site-specific model based on the Point Load Index (IS_{50}) by Wang and Aladejare (2015) and the back analysis of slope failure based on a Bayesian model solved with Markov Chain Monte Carlo (MCMC) analysis by Zhang et al. (2010).

The example of the Bayesian approach included in this paper to illustrate the method corresponds to a linear regression analysis to estimate the Hoek–Brown parameters σ_{ci} and m_i for intact rock from UCS, TCS and BTS test results. The main advantages of the method compared with a conventional linear regression analysis are the proper handling of the outliers, with no requirement of judgments from the analyst, and the natural assessment of the confidence level of the estimation.

The estimation of σ_{ci} and m_i as described by Hoek (2006) consists of fitting the test results on a graph of $(\sigma_1\text{-}\sigma_3)^2$ versus σ_3. The Hoek–Brown strength envelope is linear in this plot and a linear regression analysis provides the required values of σ_{ci} and m_i. The parameter σ_{ci} is calculated as the square root of the intercept and m_i as the slope divided by the calculated σ_{ci}. Hoek indicates that this method is robust, reliable and has the advantage that it gives a good visual impression of the distribution and scatter of the data.

The formula that supports this procedure is derived by rearranging the terms in the original expression of the Hoek–Brown failure criterion for rock masses, after incorporating the parameter values for the condition of intact rock. The H-B failure envelope is given by:

$$\sigma_1 = \sigma_3 + \sigma_{ci}\sqrt{m\frac{\sigma_3}{\sigma_{ci}} + s} \qquad (3.3)$$

For intact rock, s = 1.0 and the equation can be rearranged such that it forms a straight line with coordinate axes σ_3 and $(\sigma_1 - \sigma_3)^2$, as follows:

$$(\sigma_1 - \sigma_3)^2 = m_i\,\sigma_{ci}\,\sigma_3 + {\sigma_{ci}}^2 \qquad (3.4)$$

where:

σ_1, σ_3 = major and minor principal stresses

σ_{ci} = unconfined compressive strength of intact rock

m, s = parameters of the Hoek–Brown strength criterion for rock masses

m_i = parameter m of the Hoek–Brown strength criterion for intact rock

The method relies on the estimation of the direct tensile strength (DTS) values from indirect measurements with BTS tests. Perras and Diederichs (2014) suggests the use of a factor of 0.9 for metamorphic rocks, 0.8 for igneous rocks and 0.7 for sedimentary rocks.

The main difficulty with the conventional (frequentist) linear regression analysis is that it is affected by the presence of outliers, requiring different sorts of manipulation of the data set to avoid the bias they cause in the estimation. In addition, the result corresponds to a point estimation based on the data considered without proper measurement of the confidence of the estimated intercept and slope parameters.

The sketch in Figure 3.4 shows a description of the generic Bayesian model used for the linear regression analysis. The original model is described in detail by Kruschke (2015) and was implemented in a software code for statistical analysis named R. The example presented in this paper was implemented in the Python programming language (Python Software Foundation, 2001) and was modified to account for the correct direction of measurement of errors in the tensile strength tests. The method is robust in the true statistical sense because it uses a student t-distribution to model the spread of the data points in the direction of measurement of errors. The t-distribution is defined by three parameters that control the central value (mean μ), the width (scale σ) and the weight of the tails (normality v). The possibility to set heavy tails with this distribution allows for accommodating outliers without shifting the mean. The model considers prior distributions on four parameters, the intercept (β_0) and the slope (β_1) of the regression line modelled with normal distributions, and the scale (σ) and normality (v) parameters of the t-distribution modelled with uniform and exponential distributions, respectively, as sketched in Figure 3.4.

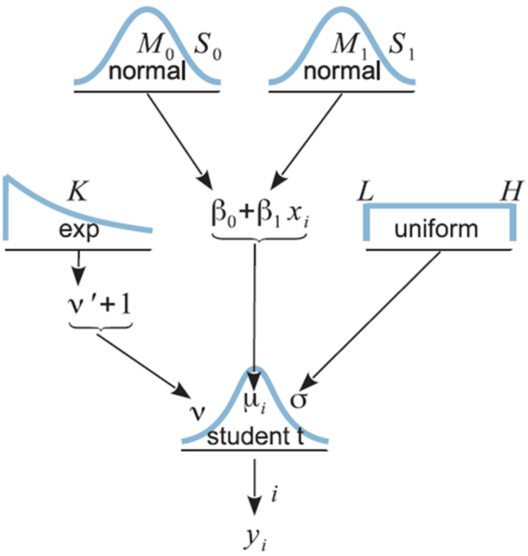

Robust Bayesian Linear Regression:
$y = \beta_0 + \beta_1 x$

Errors in y modelled with a Student dist. with parameters:

μ (mean):	central value
σ (scale) :	width
ν (normality) :	weight of tails

Prior distributions on four parameters:

Intercept β_0 :	normal distribution (M_0, S_0)
Slope β_1 :	normal distribution (M_1, S_1)
Scale σ :	uniform distribution (L, H)
Normality ν :	exponential distribution (K=1/29) shifted+1

Posterior distribution equation sampled with a MCMC process to get credible estimates of β_0, β_1, σ, ν:

$$p(\beta_0, \beta_1, \sigma, \nu \,|d) = \frac{p(d\,|\beta_0, \beta_1, \sigma, \nu) \;\; p(\beta_0, \beta_1, \sigma, \nu)}{\iint \iint p(d\,|\beta_0, \beta_1, \sigma, \nu) \;\; p(\beta_0, \beta_1, \sigma, \nu) \;\; d\beta_0 \, d\beta_1 \, d\sigma \, d\nu}$$

Figure 3.4 Conceptual basis of the robust Bayesian linear regression model used for the estimation of credible σ_{ci} and m_i values from UCS, TCS and tensile strength test results (generic model from Kruschke 2015)

The specification of the parameters of the prior distributions is based on the characteristics of the data set and consists of setting up values sufficiently vague to avoid constraining the result. The justification for the selection of these distributions as well as the selection of the prior constants is described by Kruschke (2015) and is not presented here. The Bayesian posterior distribution of the parameters sought with the regression analysis is shown at the bottom of Figure 3.4. However, the equation does not need to be expanded on further, as the various components can be incorporated into specialised packages used to sample the distribution and get credible estimates of these parameters. The sampling process is carried out with a methodology known as MCMC, which in turn can be implemented with different algorithms. The example in this paper was solved with the affine-invariant ensemble sampler algorithm implemented in the emcee Python package developed by Foreman-Mackey et al. (2013).

The σ_{ci} and m_i estimation analysis was carried out with a reduced data set of 31 points (8 UCS, 8 DTS and 15 TCS) without outliers and with the extended data set of 60 points (15 UCS, 15 DTS and 30 TCS) including a few outliers. The results of the analysis using a conventional least squares regression method (frequentist result) and the Bayesian approach are shown in Figure 3.5. The m_i results for the case with 31 data points are similar (frequentist 15.4, Bayesian 16.6); however, they differ for the case of 60 data points with a difference of 5.3 points in the value of m_i (frequentist 11.9, Bayesian 17.2) and a flatter line with the conventional regression method caused by the outliers. The Bayesian result, on the other hand, appears less affected by the outliers, showing the robustness of the method with estimated m_i values of 16.6 and 17.2 for the two data sets.

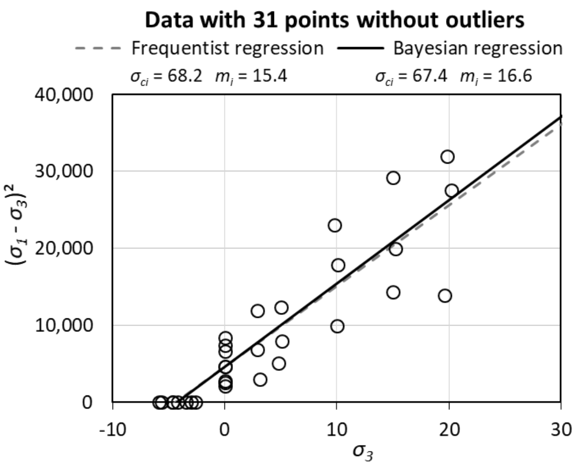

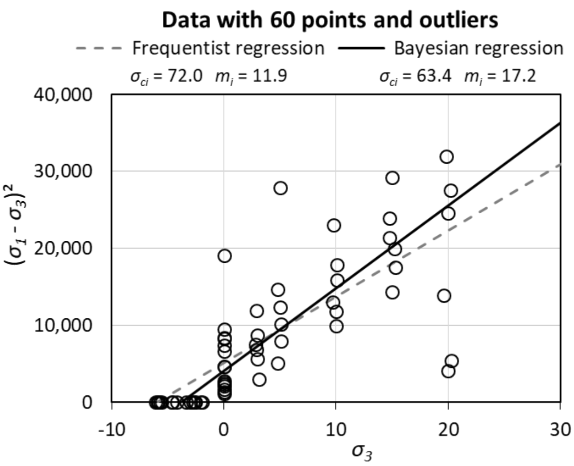

Figure 3.5 Comparison of results between frequentist and Bayesian linear regression analysis for data sets of 31 points without outliers (left) and 60 points with outliers (right)

The result of the Bayesian analysis is richer than just the regression line; it includes various diagnostic graphs, probability distributions and scatter plots of the four parameters investigated. The diagnostic graphs are intended to ensure that a proper stable solution has been obtained, the probability distributions serve to define the ranges of credible values defined by the 95% HDI and the scatter plots facilitate the identification of correlations between parameters. Due to space limitations not all of these results are included and discussed in this paper, and only a selection of them are shown in Figure 3.6 and Figure 3.7.

Figure 3.6 shows the inferred posterior distributions for σ_{ci} and m_i with the respective 95% HDIs which define the ranges of credible values for these parameters. Figure 3.6 also includes the scatter plots of sampled values of intercept versus slope, showing a low correlation between these parameters, and the respective plot of σ_{ci} versus m_i showing a marked inverse correlation between these variables. Figure 3.7 shows a plot with the 95% confidence band of the regression lines, which considers the correlation between σ_{ci} and m_i indicated in Figure 3.6. The plot also includes the data points and a selection of the t-distributions used to model the scatter (noise) in the directions of measurement of errors, depicting how they can include the outliers without shifting the mean.

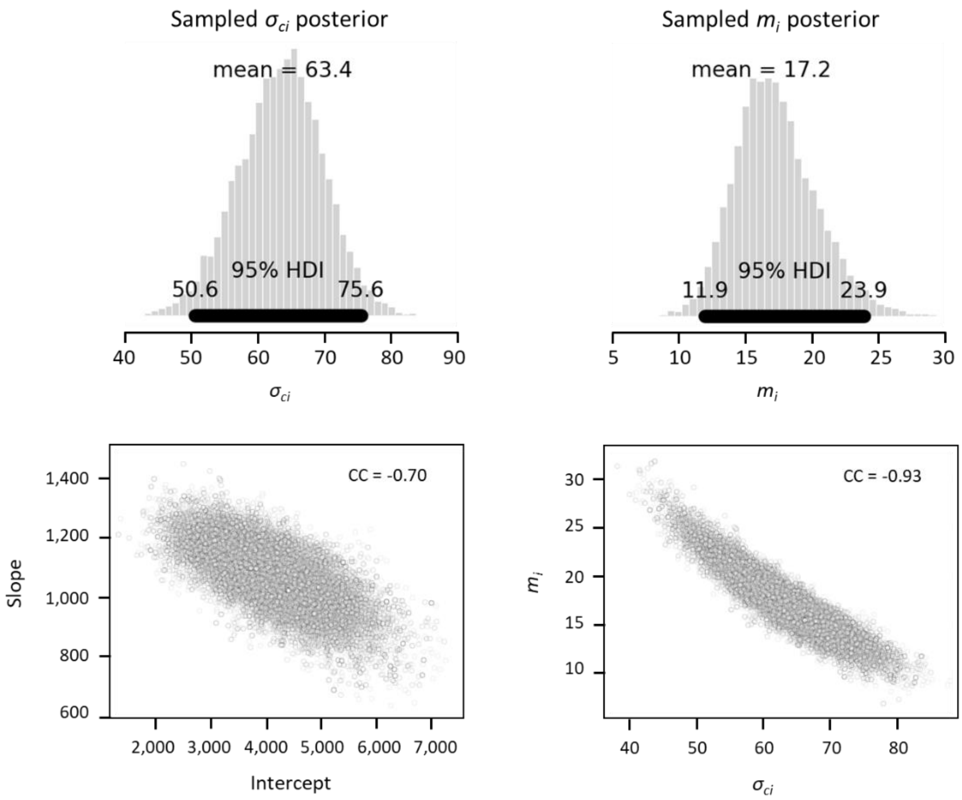

Figure 3.6 Posterior distributions of σ_{ci} and m_i with mean and 95% HDI ranges indicated (top) and scatter plots of sampled values of intercept versus slope and corresponding values of σ_{ci} versus m_i (bottom)

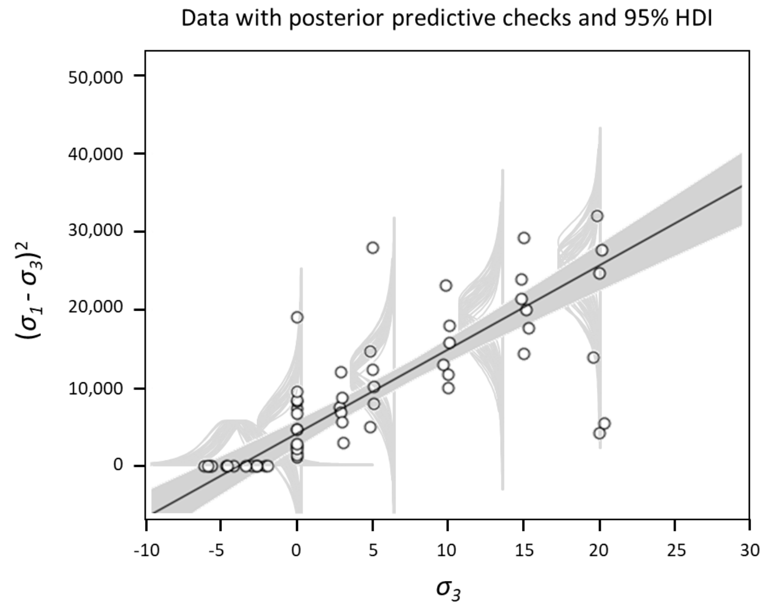

Figure 3.7 Data points with a selection of credible regression lines including the mean and t-noise distributions superimposed

3.5 Non-probabilistic methods for special cases of epistemic uncertainty

Although the Bayesian probabilistic methods are capable of dealing with the general aspects of epistemic uncertainty, there are uncertainty sub-classes whose representation would be incompatible with the principles of probability theory. A probability assignment somehow implies a sharp definition of the element assessed. This is a consequence of the probability axiom that indicates that once the probability of occurrence of an event p is defined, its probability of no occurrence is automatically stated as equal to 1-p. Alternative approaches based on theories that some authors (Klir 1989; Halpern & Fagin 1992) see as generalisations of the probability theory have been developed to deal with these situations as described hereafter.

3.5.1 The multifaceted character of epistemic uncertainty

A description of various aspects associated with imprecision in uncertainty-based information such as vagueness and ambiguity of various classes (for example non-specificity, dissonance and confusion) was given by Klir (1989). He stated mathematical arguments for the suitability of various theories available at the time to treat uncertainty.

More recently, the same author (Klir & Wierman 1999; Klir 2004) provided a more detailed taxonomy of the existing theories to treat uncertainty related to information within the framework of the generalised information theory. Zimmermann (2000) provides a less formal and more practical classification of uncertainty properties in terms of four aspects: its causes, the type of available information, the type of numerical data and the requirements of the model output. Blockley (2013) argues that any type of uncertainty can be defined in terms of three basic aspects i.e. fuzziness, incompleteness (epistemic) and randomness (aleatory), which can be represented in a tridimensional space (Fuzziness, Incompleteness and Randomness space or FIR space). Other attributes of uncertainty such as ambiguity, dubiety and conflict, can be interpreted as complex mixes of interactions in the FIR space. Figure 3.8 shows a representation of the FIR space as presented by Blockley (2013) with the interpretation of some uncertainty attributes.

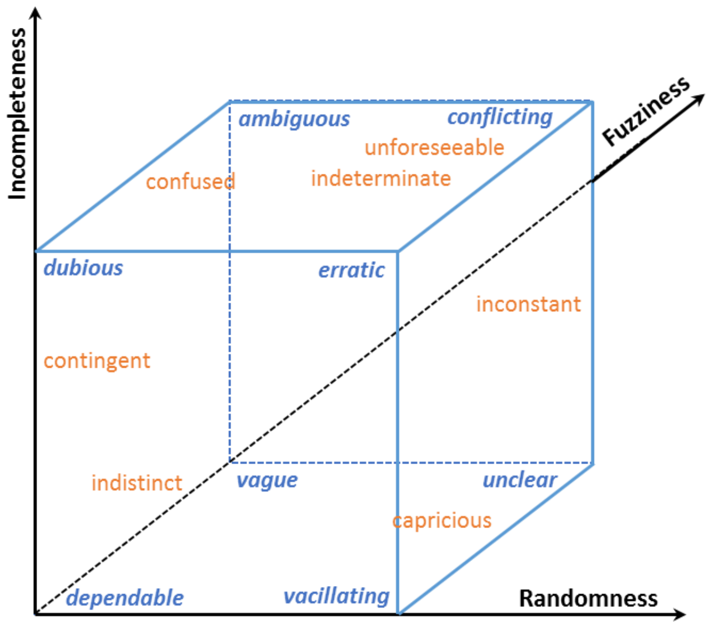

Figure 3.8 Interpretations of uncertainty attributes in the FIR space (Blockley 2013)

3.5.2 Description of non-probabilistic approaches

Some of the more common alternative approaches to represent epistemic uncertainty include interval analysis (Moore et al. 2009), evidence theory also known as Dempster-Shafer theory (Halpern & Fagin 1992) and possibility theory (Dubois & Prade 2009). A comparison of these approaches is presented by Helton et al. (2004) with some hypothetical simple problems to illustrate the main aspects of each methodology. Uncertainty characterised by fuzziness is treated with a branch of methodologies based on a fuzzy representation of uncertain variables, which is not included in this paper. However, to illustrate the group of non-probabilistic approaches to treat uncertainty, a simple hypothetical example is used to show the main features of the interval, possibility and evidence theory approaches, which are compared with the traditional probabilistic result.

A complete description of these approaches is outside the scope of this paper and the reader is referred to the documents cited above for more information on the mathematical formulations and procedures. A non-mathematical simple description of each approach is given with the aim of getting some intuition on the meaning of the results of the example included. The motivation to present these methods is to highlight certain situations where the representation of epistemic uncertainty might require techniques outside the conventional probability theory and to provide a brief description of three techniques typically used to deal with imprecision due to lack of information.

3.5.2.1 Interval analysis

This is the simplest approach, consisting of the evaluation of the propagation of the bounding values of the input parameters, with no attempt to infer the uncertainty of the result based on any assumption of the uncertainty of the input variables within the known boundary values (Helton et al. 2004).

3.5.2.2 Possibility theory approach

Possibility theory is defined by Dubois and Prade (2009, p. 6927) as “the simplest uncertainty theory devoted to the modelling of incomplete information. It is characterised by the use of two dual set functions that respectively grade the possibility and the necessity of events.” If *A* represents a particular set of information regarding an unknown value *x*, a qualitative description of these attributes would indicate that the necessity of *A*, *Nec(A)*, is a measure of the amount of uncontradicted information that supports the proposition that *A* contains the correct value for *x.* Furthermore, the possibility of *A*, *Pos(A)*, is a measure of the amount of information that does not refute the proposition that *A* contains the correct value for *x* (Helton & Sallaberry 2008). A key element of the possibility theory approach is the possibility measure (*r*), which is a function associated with the amount of likelihood that can be assigned to each element of a set.

3.5.2.3 Evidence theory approach

Helton et al. (2004, p. 42) indicate that "Evidence theory provides an alternative to the traditional manner in which probability theory is used to represent uncertainty by allowing less restrictive statements about likelihood than is the case with a full probabilistic specification of uncertainty." In this case, the two specifications of likelihood are represented by the belief and plausibility attributes of sets of information. Again, if A represents a particular set of information regarding an unknown value *x*, a qualitative description of these attributes would indicate that the belief of *A*, *Bel(A)*, corresponds to the likelihood that must be associated with *A* regarding the value of *x*; and the plausibility of *A*, *Pla(A)*, corresponds to the likelihood that could potentially be associated with *A* (Helton & Sallaberry 2008). In this case, the function associated with the amount of likelihood that can be assigned to each element of a set is the basic probability assignment (*m*). Although there are similarities between the concepts of necessity and belief, and possibility and plausibility, they are defined by different mathematical descriptions.

3.5.3 Example of non-probabilistic approaches

The example corresponds to the numerical estimation of *GSI* based on uncertain inputs of *RQD* and joint condition rating (*JC*), using the relationship proposed by Hoek at al. (2013). The condition of epistemic uncertainty in the *RQD* and *JC* values is represented in this example by assuming that only ranges of values from different sources are known with insufficient information on how these values may vary within the boundaries given. Three possible intervals for *RQD* and four for *JC* values are considered as listed at the right of Figure 3.9. Examples of sources supporting the various sets of data might include records from borehole logs, data from face mapping, back analysis of slopes performance, judgements from experts, and so forth. Figure 3.9 also shows the chart used for the calculation of *GSI* from *RQD* and *JC* values, with the shaded area indicating the range of possible *GSI* values associated with the input intervals.

The conventional probabilistic approach to define GSI would assume a uniform distribution of the property for each interval and calculate the joint probability distribution for each parameter (*RQD* and *JC*). The density of the resulting distributions will reflect the relative support of the values within the range from the various input sets. A Monte Carlo simulation of the *GSI* calculation, based on sampling the input parameters from these distributions, produce a distribution of *GSI* values. This result can be presented in the form of a reverse cumulative distribution to express the probability of exceeding a particular value, P(>*GSI*), as shown in the graphs of Figure 3.10.

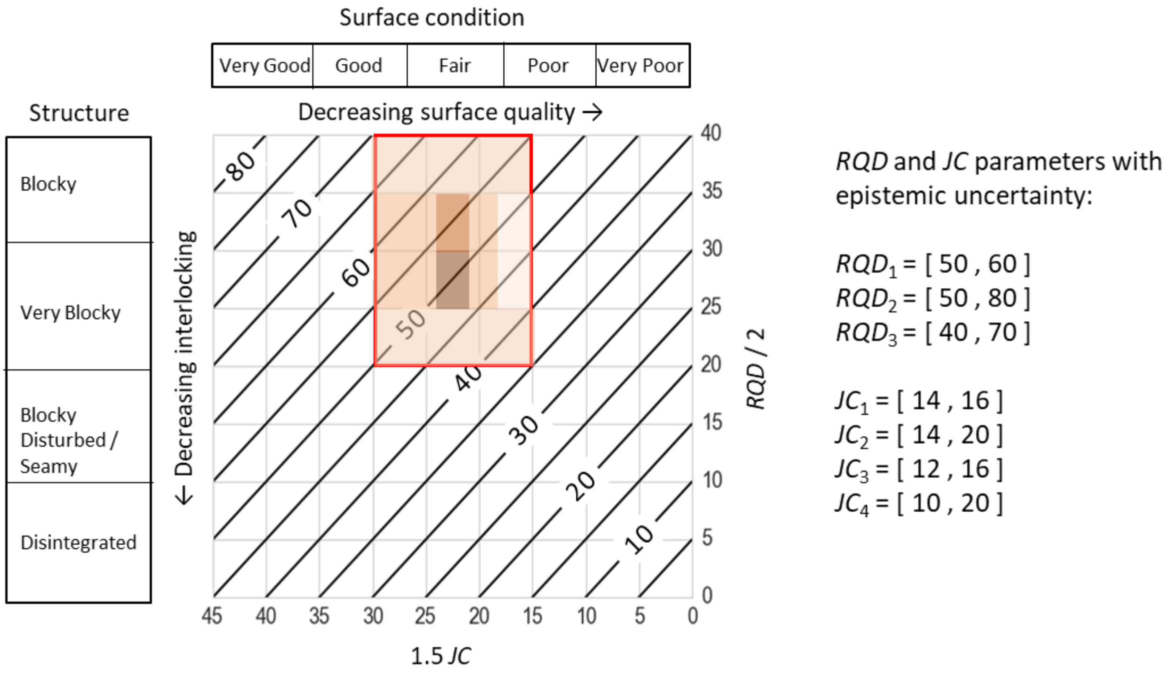

Figure 3.9 Example of treatment of epistemic uncertainty. Chart for the calculation of *GSI* from *RQD* and *JC* values (left). The shaded areas represent the likely *GSI* values proportionally to the support from the imprecise information according to the possibility theory

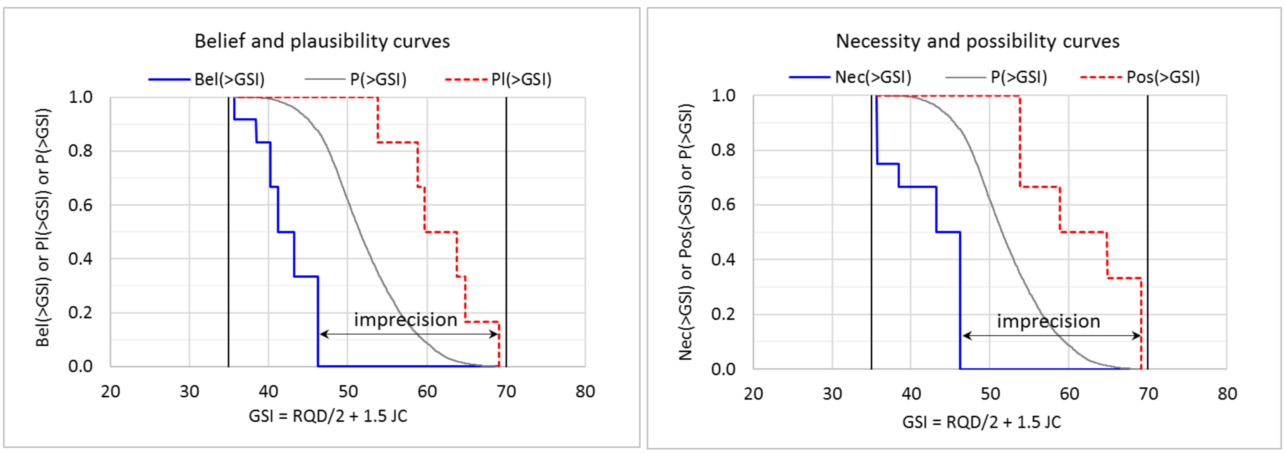

Figure 3.10 Comparison of *GSI* results using a conventional probabilistic analysis with belief and plausibility curves from evidence theory (left) and with necessity and possibility curves from possibility theory (right). The wider bounds from interval analysis are also indicated in both graphs

The graphs in Figure 3.10 indicate probabilities of 100%, 50% and 0% of exceeding *GSI* values of 36, 52 and 69, respectively. The criticism of this approach is that any type of assumption on the values of the input parameters within the boundaries provided, are not supported and effectively means adding information that does not exist. In other words, the existence of epistemic uncertainty (lack of information) is being neglected and replaced with added data to enable a randomised simulation with the model.

Figure 3.11 shows, in a simplified manner, the way in which the likelihood functions *m* (evidence theory) and *r* (possibility theory) are calculated for the variables *RQD* and *JC* from the input data. When these likelihood functions are incorporated into the *GSI* calculation model, they define distinct regions of the likelihood of *GSI* represented by the shaded areas in the *GSI* space. In the evidence theory approach, a product of the likelihoods of the input parameters is used to estimate the *GSI* likelihood, whereas in the possibility theory approach, this operation is based on the minimum logic operator. A Monte Carlo simulation was used to generate the *GSI* likelihood functions with either approach and to define belief and plausibility (evidence theory), and necessity and possibility (possibility theory) curves, which are presented in the form of reverse cumulative distributions in the graphs of Figure 3.10.

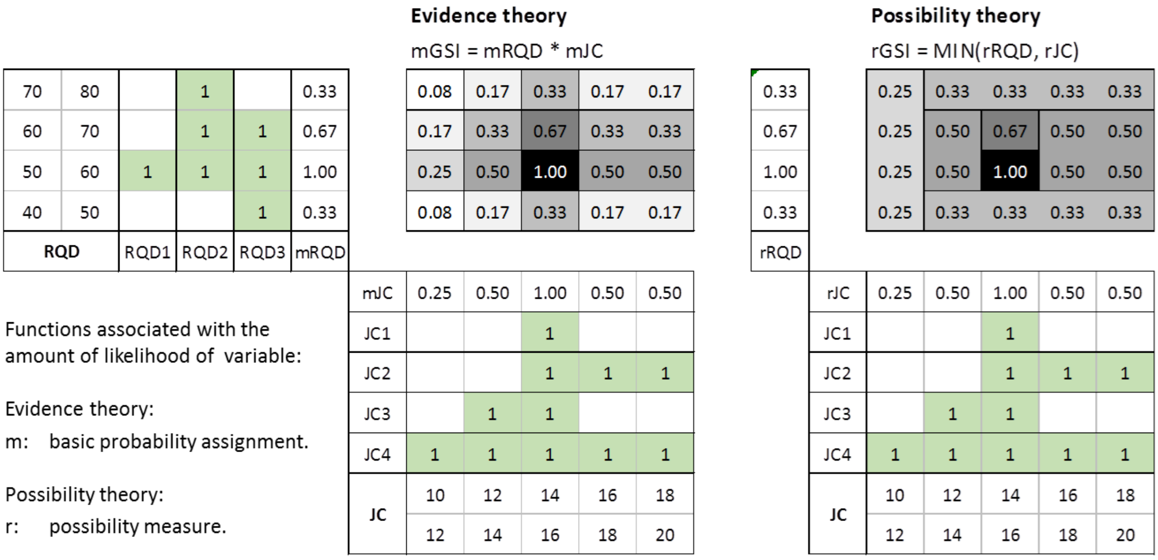

Figure 3.11 Likelihood of *GSI* values derived from imprecise information in the input parameters *RQD* and *JC*, according to evidence (centre) and possibility (right) theory approaches

The results of Figure 3.10 allow an appreciation of the concept of imprecision associated with epistemic uncertainty reflected in the gap between the two envelopes either side of the conventional probability result. For reference, Figure 3.10 also includes the result of the interval analysis, which consists in the definition of the maximum interval defined by the propagation of the bounding values of the input parameters through the *GSI* calculation model. The results of the interval analysis are conservative and might be unjustified in many situations. On the other hand, the probabilistic result might be inappropriate in many risk-based analysis, where an explicit separation between the aleatory and epistemic components of uncertainty is required to interpret results and to identify mitigation measures.

3.6 Summary and conclusion

Uncertainty is a common occurrence in geotechnical engineering and two main types of uncertainty are normally identified. These are the irreducible aleatory uncertainty associated with the natural variation of parameters, and the epistemic uncertainty related to lack of knowledge on parameters and models that can be reduced with the collection of information. The geotechnical model for slope design takes information from different complex models and typically contains a large proportion of epistemic uncertainty due to the relative scarcity of data available for design.

There are two interpretations of probability for the frequentist and Bayesian approaches of statistical analysis. Probabilistic methods are commonly used to represent and quantify uncertainty in the slope design process. However, there are no clear guidelines with regard to the appropriate methods to use in specific situations, and most of the techniques of analysis used correspond to frequentist methods. Nevertheless, the adopted methods are not always fully understood and their results are commonly misinterpreted. Common misuses of frequentist methods include the characterisation of population parameters based on reduced sampling, and the use of CIs from single data sets to measure the reliability of data. Bayesian methods can be used to represent both types of uncertainty and are especially suited for situations where data is scarce and previous knowledge exist. However, they are rarely used in the mine slope design process where they could be of great benefit. Some aspects of the epistemic uncertainty cannot be represented with probabilistic methods and alternative approaches are required in those cases. Interval analysis and methods based on evidence theory and possibility theory can provide the tools required to deal with situations where imprecision due to incomplete information exists.

Two examples of unconventional methods to treat uncertainty in the slope design process were presented. The first example corresponded to the Bayesian estimation of the mi parameter of the H-B strength criterion using a robust linear regression method for UCS, TCS and tensile strength data plotted in a $(\sigma_1 - \sigma_3)^2$ versus σ_3 space. A generic model implemented in Python code and solved with an MCMC methodology based on the affine-invariant ensemble sampler algorithm using the emcee Python package was used for this purpose. The results were useful to highlight the benefits of the method over a traditional frequentist regression method. The benefits are related to the adequate handling of the outliers in the data and the proper quantification of the confidence of the estimates. Further work will be carried out to improve the method using real data sets to validate results.

The second example consisted of the use of three non-probabilistic approaches to deal with epistemic uncertainty related to the incompleteness of information represented by sets of intervals of input parameters. The estimation of *GSI* values from *RQD* and *JC* parameters using the model by Hoek et al. 2013, was carried out with interval analysis, and procedures based on the evidence and possibility theories and included the assessment of the likelihood of the estimates. These results were compared with the conventional probability distribution curve to highlight the implications of the incompleteness aspect of the uncertainty. The results showed the importance of having a separation between the aleatory and epistemic components of uncertainty, which are of relevance for risk-based design procedures.

Acknowledgements

The first author is supported by the LOPII project and by SRK Consulting South Africa. Their support is greatly appreciated.

References

Baecher, G.B. and Christian, J.T., 2003. *Reliability and statistics in geotechnical engineering.* Wiley, Chichester, UK.

Bedi, A. and Harrison, J.P., 2013. A comparison of Bayesian techniques and non-probabilistic models in rock engineering design. *Proceedings 47th US Rock*

Mechanics/Geomechanics Symposium, San Francisco, 23-26 June, Paper ARMA 13-550, 10 p.

Blockley, D., 2013. Analysing uncertainties: Towards comparing Bayesian and interval probabilities. *Mechanical Systems and Signal Processing,* 37(1–2), 30–42.

Christian, J.T., 2004. Geotechnical Engineering Reliability: How Well Do We Know What We Are Doing? *Journal of Geotechnical and Geoenvironmental Engineering*, 130(10), 985–1003.

Dubois, D. and Prade, H., 2009. Possibility Theory. In RA Meyers (ed.), *Encyclopedia of Complexity and Systems Science*, Springer, 6927–6939.

Feng, X. and Jimenez, R., 2015. Estimation of deformation modulus of rock masses based on Bayesian model selection and Bayesian updating approach. *Engineering Geology,* 199, 19–27.

Foreman-Mackey, D., Hogg, D.W., Lang, D. and Goodman, J., 2013. emcee: The MCMC Hammer. *Publications of the Astronomical Society of Pacific*, 125(925), 306–312.

Halpern, J.Y. and Fagin, R., 1992. Two views of belief: belief as a generalized probability and belief as evidence. *Artificial Intelligence*, 54(3), 275–317.

Helton, J.C. and Sallaberry C.J., 2008. *Alternative Representations of Uncertainty* [on line]. [Accessed 20/01/2016]. http://www.stat.unm.edu/~storlie/st579/Alternative_Representation_of_Uncertainty.pdf

Helton, J.C., Johnson, J.D. and Oberkampf, W.L., 2004. An exploration of alternative approaches to the representation of uncertainty in model predictions. *Reliability Engineering and System Safety,* 85(1–3), 39–71.

Hoek, E., 2006. *Practical Rock Engineerin*g. Course notes on rock mass properties, [on line]. [Accessed 20\012016]. https://www.rocscience.com/documents/hoek/corner/12_Rock_mass_properties.pdf.

Hoek, E., Carter, T.G. and Diederichs, M.S., 2013. Quantification of the Geological Strength Index chart. *Proceedings 47th US Rock Mechanics/Geomechanics Symposium*, San Francisco, 23-26 June, Paper ARMA 13-672, 9 p.

Klir, G.J., 1989. Is there more to uncertainty than some probability theorists might have us believe?*' International Journal of General Systems,* 15(4), 347–378.

Klir, G.J., 2004. Generalized information theory: aims, results, and open problems. *Reliability Engineering and System Safety*, 85(1), 21–38.

Klir, G.J. and Wierman M.J., 1999. *Uncertainty-Based Information: Elements of Generalized Information Theory*, Physica-Verlag HD.

Kruschke, J.K., 2015. *Doing Bayesian Data Analysis: A Tutorial with R, JAGS and STAN*, Academic Press/Elsevier.

Moore, R.E., Kearfott, R.B. and Cloud, M.J., 2009. *Introduction to Interval Analysis*. Society for Industrial and Applied Mathematics, Philadelphia.

Perras, M.A. and Diederichs, M.S., 2014. A Review of the Tensile Strength of Rocks: Concepts and Testing. *Geotechnical and Geological Engineering*, 32(2), 525–546.

Python Software Foundation, 2001. *Python language reference*, version 3.4 [on line]. [Accessed 20/01/2015]. https://www.python.org/.

Stacey, P., 2009. Fundamentals of Slope Design. In J. Read and P. Stacey (eds), *Guidelines for Open Pit Slope Design*, CSIRO Publishing, Collingwood, Victoria. 1–14.

VanderPlas, J., 2014. *Frequentism and Bayesianism: A Practical Introduction*. In Phytonic Preambulations Blog [on line]. [Accessed 20/01/2015]. https://jakevdp.github.io/blog/2014/03/11/frequentism-and-bayesianism-a-practical-intro/.

Wang, Y. and Aladejare, A.E., 2015. Selection of site-specific regression model for characterization of uniaxial compressive strength of rock. *International Journal of Rock Mechanics and Mining Sciences,* 75, 73–81.

Zhang, L.L., Zhang, J., Zhang, L.M. and Tang, W.H., 2010. Back analysis of slope failure with Markov chain Monte Carlo simulation. *Computers and Geotechnics*, 37(7–8), 905–912.

Zimmermann, H.J., 2000. An application-oriented view of modelling uncertainty. *European Journal of Operational Research*, 122(2), 190–198.

Chapter 4 - Bayesian Data Analysis to Quantify the Uncertainty of Intact Rock Strength

Luis-Fernando Contreras[a], Edwin T.Brown[b], Marc Ruest[a]

[a] The University of Queensland, Brisbane, Australia.

[b] Golder Associates Pty. Ltd, Brisbane, Australia.

Corresponding author: luis.contreras@uq.net.au

Abstract

One of the main difficulties of the geotechnical design process lies in dealing with uncertainty. Uncertainty is associated with natural variation of properties, and the imprecision and unpredictability caused by insufficient information on parameters or models. Probabilistic methods are normally used to quantify uncertainty. However, the frequentist approach commonly used for this purpose has some drawbacks. First, it lacks a formal framework for incorporating knowledge not represented by data. Secondly, it has limitations in providing a proper measure of the confidence of parameters inferred from data. The Bayesian approach offers a better framework for treating uncertainty in geotechnical design. The advantages of the Bayesian approach for uncertainty quantification are highlighted in this paper with the Bayesian regression analysis of laboratory test data to infer the intact rock strength parameters σ_{ci} and m_i used in the Hoek-Brown strength criterion. Two case examples are used to illustrate different aspects of the Bayesian methodology and to contrast the approach with a frequentist approach represented by the nonlinear least squares method. The paper discusses the use of a Student's t-distribution versus a normal distribution to handle outliers, the consideration of absolute versus relative residuals, and the comparison of quality of fitting results based on standard errors and Bayes factors. Uncertainty quantification with confidence and prediction intervals of the frequentist approach is compared with that based on scatter plots and bands of fitted envelopes of the Bayesian approach. Finally, the Bayesian method is extended to consider two improvements to the fitting analysis. The first is the case in which the Hoek-Brown parameter, a, is treated as a variable to improve the fitting in the triaxial region. The second is the incorporation of

the uncertainty in the estimation of the direct tensile strength from Brazilian test results within the overall evaluation of the intact rock strength.

Keywords: uncertainty; intact rock strength; Bayesian analysis; Hoek-Brown criterion.

4.1 Introduction

One of the major difficulties encountered by the rock engineer is dealing with the uncertainties present in every aspect of the geotechnical design process. Uncertainty is associated with natural variation of properties, and the imprecision and unpredictability caused by the lack of sufficient information on parameters or models (Baecher and Christian, 2004). Design strategies to deal with the problems associated with uncertainty include conservative design options with large factors of safety, which can be adjusted during the implementation phase based on observations of performance, and the use of probabilistic methods that attempt to measure and account for uncertainty in the design (Christian, 2004).

The probabilistic methods commonly used to treat uncertainty in rock mechanics design belong to the so-called frequentist approach, but this methodology has some drawbacks (VanderPlas, 2014). First, the approach lacks a formal framework to incorporate subjective information such as engineering judgement. Secondly, it has limitations in providing a proper measure of the confidence of parameters inferred from data. The Bayesian approach provides an alternative route to the conventional probabilistic methods used in geotechnical design; some examples are presented by Miranda et al. (2009), Zhang et al. (2009, 2012), Brown (2012), Bozorgzadeh and Harrison (2014), Feng and Jimenez (2015) and Wang et al. (2016). The approach is based on a particular interpretation of probability and offers an adequate framework for the treatment of uncertainty in geotechnical design.

Probabilistic data analysis using the Bayesian approach involves numerical procedures to estimate parameters from posterior probability distributions. These distributions are the result of combining prior information with available data through Bayes' equation (Kruschke, 2015). The posterior distributions are often complex, multidimensional functions whose analysis requires the use of a class of methods called Markov chain Monte Carlo (MCMC) (Robert and Casella, 2011). These methods are used to draw representative samples of the parameters investigated, providing information on their best estimate values, variability and correlations. The understanding of the concepts behind the various algorithms used to perform MCMC analysis is important to properly assess the quality of results. However, the analyst does not have to develop the software in order to use the method. There are already elaborated open source packages in various programming languages (Foreman-Mackey et al., 2013; Smith, 2014; Vincent, 2014) developed by computer scientists and related specialists, which have been tested extensively by these communities. These packages can be easily incorporated into ad-hoc codes for different modelling applications.

The paper presents initially the concepts of geotechnical uncertainty and provides a contrast between the frequentist and Bayesian approaches to quantify uncertainty. The description of the Bayesian approach with reference to the case of the inference of parameters is used to highlight the advantages of this methodology over the frequentist approach. The Bayesian methodology is applied to estimating the intact rock strength parameters σ_{ci} and m_i of the Hoek-Brown strength criterion, through the analysis of data from compression and tensile strength tests. Two data set examples are presented to compare the Bayesian approach with the nonlinear least squares regression method representing the frequentist approach. The results of these example cases are used to discuss different aspects of the analysis, including the advantages of evaluating errors with a Student's t-distribution to handle outliers, the implications of using absolute and relative residuals, and the measure of the quality of the fitting results. The second example is used to emphasise the advantages of the uncertainty quantification with the scatter plots and bands of fitted envelopes of the Bayesian approach, in contrast to the use of confidence and prediction intervals in the frequentist method. Finally, the versatility of the Bayesian method is illustrated with two situations that require the model to be extended to include additional parameters for inference. The first case corresponds to the consideration of the Hoek-Brown parameter, *a*, as a free variable so that the fitting in the triaxial compression region is not constrained by that obtained in the tensile and uniaxial compression regions based on a two-parameter model. The second case is the inclusion of the uncertainty in the conversion from Brazilian tensile strength (BTS) to direct tensile strength (DTS) into the overall uncertainty evaluation of the intact rock strength.

The distributions of σ_{ci} and m_i resulting from the Bayesian analysis can be used as inputs for the analysis of the reliability of geotechnical structures such as slopes and tunnels. The first-order reliability method (FORM) is the most common technique used for this purpose (Low and Tang, 2007; Lu and Low, 2011; Goh and Zhang, 2012; Zhang and Goh, 2012;

Low, 2014; Liu and Low, 2017). The FORM typically considers predefined probability distributions to represent the variability of uncertain parameters and a limit state surface (LSS) defining the condition of failure of the structure. The LSS is derived from a performance function that may be available in explicit form, or alternatively, could be approximated with a response surface for complex models.

The purpose of this paper is to explain the essential differences between frequentist and Bayesian statistics in quantifying the inevitable uncertainty in experimentally-determined rock mechanics parameters. While the paper uses the parameters in the Hoek-Brown peak strength criterion for intact rock material for illustration purposes, it does not explore the relationships between those parameters or their physical meanings.

4.2 Uncertainty in geotechnical design

The geotechnical design process implies the existence of a geotechnical model. This model is understood as the collection of elements representing different aspects of a geotechnical environment (i.e. geology, rock strength, structural features, etc.). These components include models and data used to calibrate those models by adjusting certain parameters of interest. For example, the intact rock strength can be represented by the Hoek-Brown criterion defined by the σ_{ci} and m_i parameters (Hoek and Brown, 1997). The values of these parameters are defined through regression analysis of data from compression and tensile strength tests on intact rock specimens. The quantification of the uncertainty of the parameters representing particular aspects of the geotechnical model is of interest to the analyst using this information for design purposes in order to assess the reliability of the system analysed.

4.2.1 Types of uncertainty

Uncertainty is associated with various concepts such as unpredictability, imprecision and variability. At a basic level, it can be categorised into aleatory or epistemic uncertainty. Aleatory uncertainty is associated with random variations, present in natural variability, occurring in the world or having external character, whereas epistemic uncertainty is associated with the unknown, derived from lack of knowledge, occurring in the mind or having an internal character, as discussed by Baecher and Christian (2003). Therefore, epistemic uncertainty can be reduced with the collection of additional data or by refining models based on a better understanding of the entities represented. On the other hand, natural variation cannot be reduced with the availability of more information that will only serve to provide a better representation of this type of uncertainty.

4.2.2 Sources of uncertainty in geotechnical design

Uncertainty is present in all aspects of the geotechnical design process. The sources of uncertainty include:

(1) The inherent variability of the basic properties considered as random variables (e.g. uniaxial compressive strength (UCS), DTS, etc.).

(2) Measurement errors of the properties.

(3) Estimation of the statistical parameters used to represent the variables (i.e. mean, standard deviation, etc.).

(4) Approximations in the definition of sub-models to estimate derived variables (e.g. Hoek-Brown parameters σ_{ci} and m_i estimated from UCS, BTS and triaxial compressive strength (TCS) testing; geological strength index (GSI) estimated from structure and discontinuity condition descriptors).

A large part of the uncertainty present in the geotechnical design process corresponds to epistemic uncertainty that would be susceptible to reduction with increased data collection. However, this is often difficult to achieve in practice because of the constraints typically operating during the site investigation stage.

4.2.3 Quantification of uncertainty

Uncertainties may be quantified as probabilities, which in turn can be interpreted as frequencies in a series of similar trials, or as degrees of belief. Some aspects of geotechnical engineering can be treated as random entities represented by relative frequencies while others may correspond to unique unknown states of nature, better considered as degrees of belief. An example of the former is a material property evaluated with data from laboratory testing, and any form of expert opinion represents the latter (e.g. a geological section that is constructed from site investigation data). Baecher and Christian (2003) provided a detailed discussion on the topics of duality in the interpretation of uncertainty and of probability in geotechnical engineering. They indicated that both types of probability are present in risk and reliability analyses, and pointed out that the separation between them is a modelling artefact rather than an immutable property of nature.

4.3 Probabilistic methods to treat uncertainty

Two alternative interpretations of probability provide the bases of the frequentist (classical) and Bayesian approaches of statistical analysis. The conventional approach for dealing with uncertainty in geotechnical design is based on classical statistics. In this case, data are collected and used as the only element to infer parameters and models. It will be argued that Bayesian statistical methods are a better option for treating uncertainty in geotechnical design, because they provide a formal framework for combining hard data, which are typically scarce, with other sources of information that may be available, including expert judgment.

4.3.1 The frequentist approach of statistical analysis

The frequentist approach of statistical analysis is based on the interpretation of probability as frequencies of outcomes of random trials repeated many times. The trials are the essence of the random sampling process central to the approach. The objective of the analysis is to infer the characteristics of a hypothesis or model, from the relevant data collected randomly. The process involves the estimation of values of parameters that are assumed to be unknown, fixed quantities, whereas data are considered to be a set of random variables. This framework allows the definition of point estimates and errors of the parameters investigated that are data set-dependent. Common techniques of data analysis within the frequentist approach include maximum likelihood estimation, confidence intervals analysis and null hypothesis significance testing. The first is a method used for the estimation of point estimates of parameters. The second provides ranges used to assess the spread of point estimates in recurring sampling. The third is a procedure used to define whether a particular value of a parameter can be accepted or rejected based on the agreement with the trend suggested by data. Frequentist statistical methods are used by default in many areas of engineering design and in many cases without a full appreciation of the implications of their conceptual basis. Only recently has the Bayesian approach become a popular alternative in geotechnical design (Miranda et al., 2009; Zhang et al., 2009, 2012; Brown, 2012;

Bozorgzadeh and Harrison, 2014; Feng and Jimenez, 2015; Wang et al., 2016), as it is based on a conceptual framework suited for the treatment of geotechnical uncertainty.

4.3.2 The Bayesian approach of statistical analysis

The Bayesian approach of statistical analysis is based on the interpretation of probability as degrees of belief. The inference process with this approach combines existing information on the model or hypothesis to be examined, known as priors, with the data from sampling using Bayes' rule. An important aspect of the Bayesian approach is that the sought parameters of the models or hypothesis being examined are considered to be random variables, whereas data is assumed to be a fixed known quantity. The results of Bayesian analyses are probability distributions known as posteriors.

Bayes' rule was proposed by Thomas Bayes in 1763 (Bayes, 1763). Bayes' rule can be derived from basic definitions of conditional probability and allows the calculation of the probability of the hypothesis given the data $p(h|d)$, from the probabilities of the data given the hypothesis $p(d|h)$, the hypothesis $p(h)$, and the data $p(d)$.

The general form of Bayes' equation is

$$p(h\,|d) = \frac{p(d|h)p(h)}{p(d)} \tag{4.1}$$

which can also be interpreted in the following manner (Kruschke, 2015):

$$posterior = \frac{likelihood\ \times prior}{evidence} \tag{4.2}$$

The Bayes' equation is used to update knowledge of a hypothesis or model from observations represented by the data. The updating process is done by quantifying the uncertainties of the model parameters when there is no information on the characteristics of their distributions. Detailed information on Bayesian analysis at introductory to advanced levels can be found in several texts (e.g. Gregory, 2005; Sivia and Skilling, 2006; Stone, 2013; Gelman et al., 2013; Kruschke, 2015).

4.3.2.1 The posterior distribution

The "posterior" is a probability distribution that balances the knowledge provided by the prior information and the data. If sufficient data are available, data will drive the result. If the data component is weak, prior knowledge will have a strong effect. All of this is handled within the Bayesian approach in a rational manner, without external manipulation. The posterior is the answer of interest to the data analyst, but this distribution is typically complex and its evaluation requires the use of special numerical techniques.

4.3.2.2 The likelihood function

The "likelihood" function defines the probability of obtaining the observations included in the data set given the model or hypothesis under examination. The likelihood is the answer given by classical statistical methods. Figure 4.1 adapted from Kruschke (2015) shows an example of the calculation of the likelihood of a data set of three points, d = {85, 100, 115}, assuming that its variability is represented by a normal distribution with mean, μ, and standard deviation, σ. The likelihood is calculated for three values of μ (87.8, 100, 112) shown in the column plots and three values of σ (7.35, 12.2, 18.4) shown in the row plots. The probability of an individual point is represented by the vertical dotted line over the point and the probability of the data set $p(d|\mu, \sigma)$ is the product of the three individual probabilities as expressed by the likelihood function. As expected, the maximum likelihood result (7.71×10^{-6}) corresponds to the mean (μ = 100) and standard deviation (σ = 12.2) of the data points.

4.3.2.3 The prior distribution

The "prior" represents the initial knowledge, or lack of it, in the hypothesis, and therefore can be either informative or vague. Informative priors can be any type of distribution that represents adequately the existing knowledge of the model or parameter being examined. However, the usual situation is that there is little information available, so the goal becomes to encode this lack of knowledge in a non-informative or vague probability distribution to avoid constraining the results. This is done with distributions derived by applying the maximum entropy principle (Jaynes, 1957). In this case, entropy refers to disorder or randomness in the information and has a similarity with the concept of entropy in physical systems. The uniform distribution is a common maximum entropy distribution and corresponds to the situation in which only the limits of the parameter are known. The selection of the prior is an important step in Bayesian data analysis. The prior could add valuable available information to the posterior if selected adequately, or it could bias the results if it over-constrains the data.

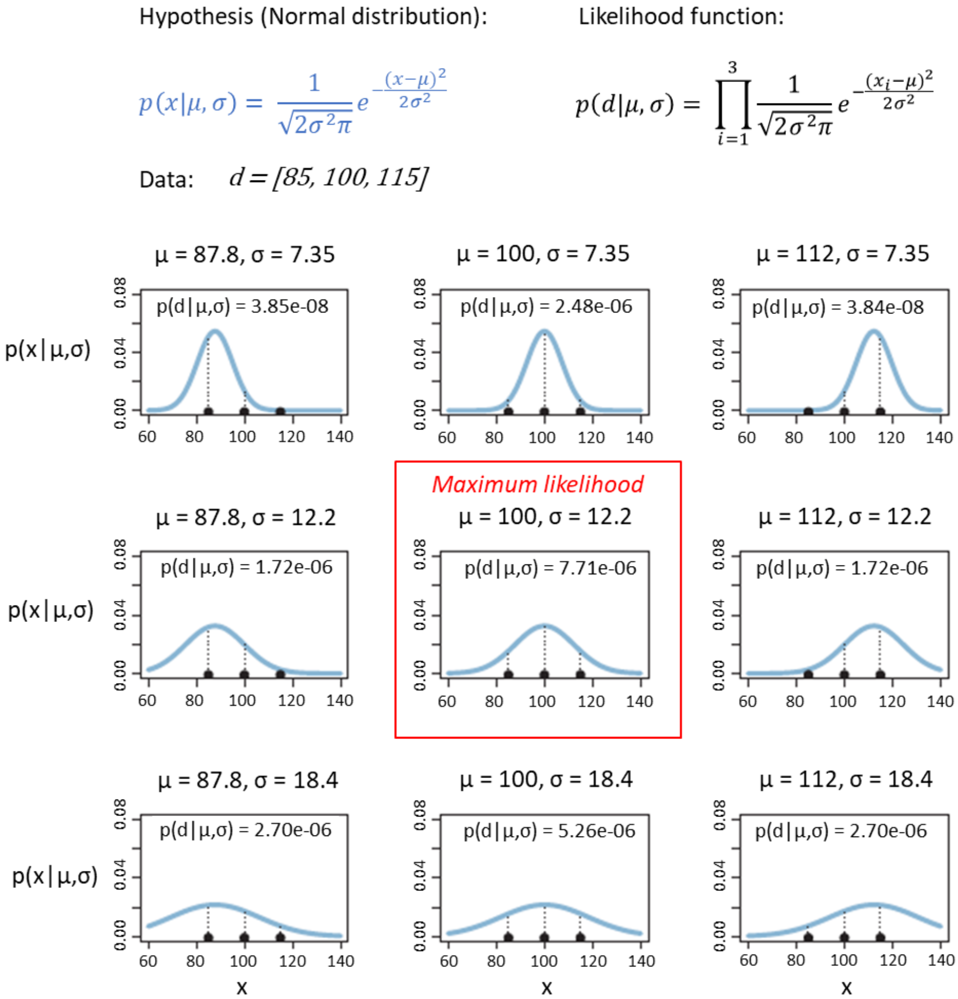

Figure 4.1 Example of the calculation of the likelihood of a data set of three points, assuming a normal distribution and testing different values of mean, μ, and standard deviation, σ. Columns show different values of μ and rows show different values of σ. The middle plot shows the maximum likelihood result (adapted from Kruschke, 2015)

4.3.2.4 The evidence function

The “evidence” part in the denominator of Bayes’ equation is normally treated as a normalisation factor so that the posterior integrates to one. It is calculated as the integral over the whole parameter space of the numerator, i.e. as the product of the likelihood function and the prior distribution. The posterior distribution does not need to be normalised when the purpose of the Bayesian analysis is the inference of the uncertain parameters using a numerical approach such as the MCMC. Therefore, the calculation of the typically complex integral in the denominator of the Bayes' equation can be omitted. The denominator is required when the objective of the analysis is the comparison of two alternative models which is done through the calculation of the Bayes factor.

4.3.3 Contrast between the frequentist and Bayesian approaches

The more relevant points of contrast between the frequentist and Bayesian approaches are summarised in Table 4.1 (Contreras and Ruest, 2016). The second aspect constitutes one of the more important advantages of the Bayesian approach as it addresses the question of interest to the geotechnical engineer. This aspect is also at the base of misunderstanding about the type of answer that classical statistical methods provide. The results of Bayesian analyses are richer and more informative than the conventional point estimates and error measurements given by the frequentist approach. The conceptual framework of the Bayesian approach is better suited to the task of the inference of model parameters.

Table 4.1 Key aspects of contrast between the frequentist (classical) and Bayesian approaches to statistical analysis (adapted from Contreras and Ruest, 2016)

Aspect	Frequentist approach	Bayesian approach
Interpretation of probability	Frequency of outcomes in repeated trials	Degrees of belief
Question answered with the approach	What is the probability of the data if the hypothesis (parameter or model) examined is true ($p[d\|h\ ]$)?	What is the probability of the hypothesis (parameter or model) examined given the data observed ($p[h\|d]$)?
Information used	Only data collected with sampling ($p[d\|h]$)	Prior information of any type ($p[H]$) and data from sampling ($p[d\|h]$)
Characteristics of the result from the inference process	Point estimate (maximum likelihood) and standard error of the parameter (or model) evaluated	Probability distribution of the parameter (or model) evaluated
Assumptions regarding data and parameters (or models)	Data are random, parameters (or models) are fixed	Data are fixed, parameters (or models) are random
Inference method	Based on maximum likelihood, confidence interval and null hypothesis significance testing	Based on the updating of prior information by adding the effect of observed data to provide a posterior distribution reflecting a balance between the two inputs

4.3.4 Example to contrast the results from the two approaches

A consequence of the different interpretations of probability is the contrasting assumptions regarding data and parameters made by the approaches. This, in turn, affects how the boundaries of model parameters are determined. In the frequentist approach, confidence intervals (CI) from data are used to define meaningful parameter boundaries, whereas in the Bayesian approach this is done with credible regions of the posterior distribution.

The CI is defined by upper and lower bound values above and below the mean of a data sample, and is associated with good estimates of the unknown population parameter investigated. The CI is calculated from a particular sample with its width depending on the number of data points in the sample, and the chosen level of confidence for the estimation. For this reason, this result is commonly used as a measure of confidence of parameter estimates without having a full understanding of its meaning. A CI is specific to a data set and its confidence level only has meaning in repeated sampling. For example, if the 95% CI for the mean UCS of a particular rock type is constructed, it either includes the true UCS value or does not, but it is not possible to know the situation for that particular CI. The 95% confidence means that if the sampling process is repeated numerous times, and CIs are calculated for those various samples, 95% of the sample sets will have CIs containing the true UCS value. However, because the true value is an unknown fixed parameter in the frequentist framework, it is not possible to identify the sample sets containing the true UCS. The uncertainty regarding the true UCS value remains.

Figure 4.2 shows an example of repeated sampling that provides an appreciation of the meaning of the CI in the frequentist approach. The values could represent UCS results for a particular rock type, but the data were randomly generated to illustrate the point. A total of 100 data sets of 15 values each were sampled from a normal distribution with a mean of 120 and a standard deviation of 30 that represent the unknown fixed parameters of the population. Each data set has its own mean and standard deviation and the bars in Figure 4.2 correspond to the 95% CIs of the mean. However, for this particular group of data sets, 91 of the intervals contain the true mean. A larger number of data sets would be required to obtain a better approximation of the 95% level used for the construction of the intervals. Nevertheless, the important point with this example is that in terms of each individual data set, there is no probability associated with the inclusion of the true mean.

The interval either includes it or does not. In a real case, there would be only one data set and it would not be possible to estimate the true value.

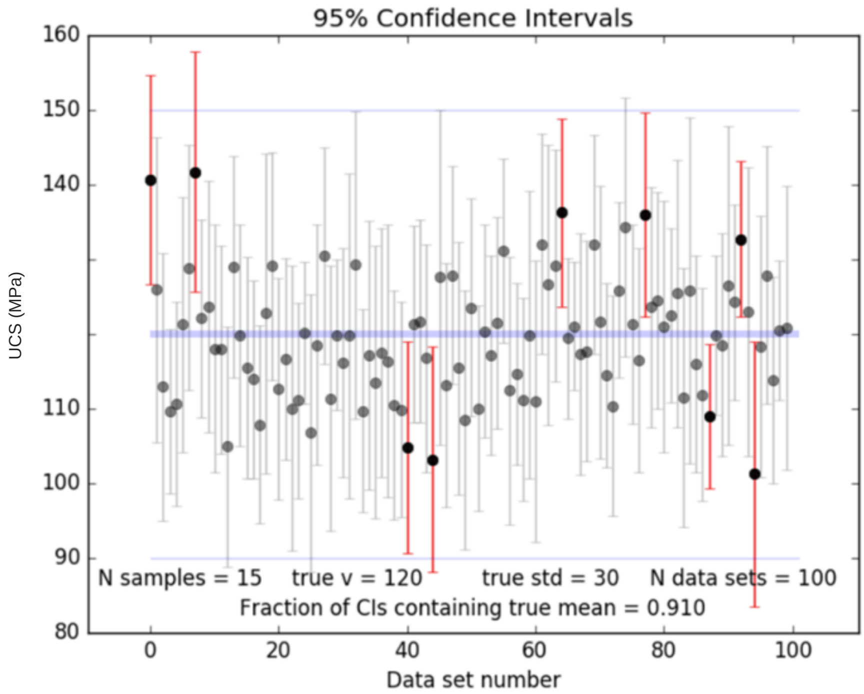

Figure 4.2 Frequentist interpretation of CIs for randomly generated UCS data sets of 15 values with a mean of 120 and a standard deviation of 30

In the Bayesian approach, the situation is different because the unknown parameter being investigated is considered to be a random variable that is updated for every new data set. The posterior probability distribution resulting from the Bayesian updating process is used to define the highest density interval with a particular level of precision. This interval defines the bounds of the credible region for the estimation of the parameter. In many simple situations, the results from both approaches coincide, but the meanings of the results are different. The Bayesian result has a meaning consistent with the answer that is normally sought by the analyst, whereas the frequentist result responds to a different question that is of less interest to the analyst.

Figure 4.3 compares the frequentist 95% CI for data set 27 in Figure 4.2 with the credible interval corresponding to the 95% highest density interval (HDI) of the posterior distribution from a Bayesian estimation of the mean. The posterior distribution is calculated for the same data set, assuming a uniform prior distribution, which is considered to be a non-informative prior in this case. The results show that the prior does not affect the likelihood of the data, yielding a result that appears to coincide with the frequentist result, although with a different meaning. In this case, the Bayesian interval indicates a range for the sought mean with a 95% credibility. This is possible because, in the Bayesian framework, the parameter investigated is not fixed but changes as new data become available. The frequentist result corresponds to a point estimate of the mean and a measure of the error represented by the width of the CI, whereas the Bayesian result provides a full probability distribution for the mean based on the data used.

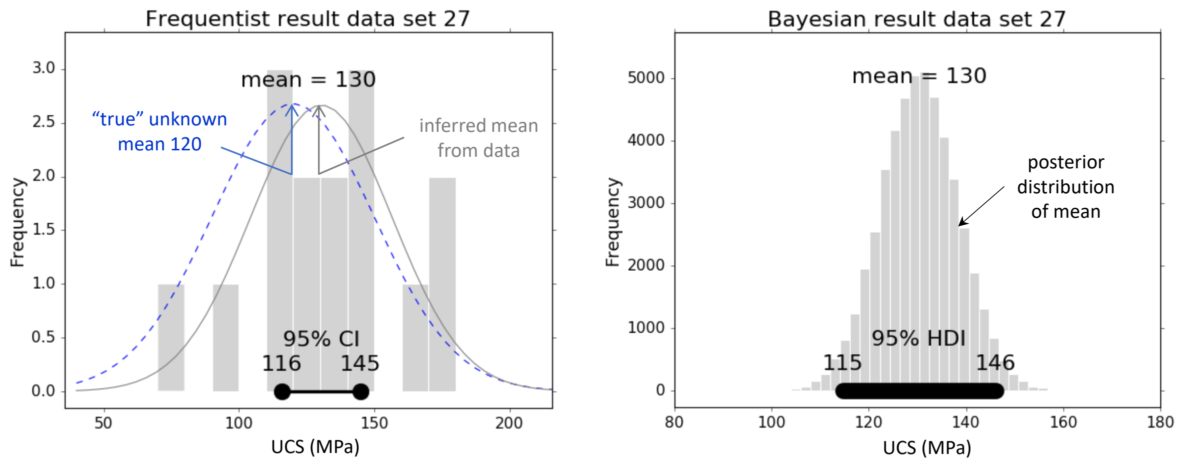

Figure 4.3 Comparison between the frequentist (left) and Bayesian (right) results for the inference of the mean UCS of data set 27 in Figure 4.2

4.4 Bayesian inference of uncertain parameters

Three elements are required for the construction of a Bayesian model for the inference of parameters. Figure 4.4 shows a conceptual representation of this model. First, there must be a model in the form of a mathematical function that represents the performance of a particular system of interest. This model includes a predictor variable, x, and the parameters for inference, θ. Secondly, there must be data that normally correspond to measurements of the actual performance of the system, y_{actual}, to compare with the model predictions, y_{model}. Thirdly, there is the prior knowledge available on the parameters; this means any type of information, for example valid ranges or credible values. These elements are combined in a probabilistic function that contains the set of uncertain parameters for inference, θ_1 to θ_k. This function effectively corresponds to a posterior probability distribution using the Bayes formula and gives probability values, p, for particular sets of uncertain parameters, θ. The objective of the analysis is to define the sets of θ that produce the largest *p* values. In other words, the objective is to define the most probable parameter values.

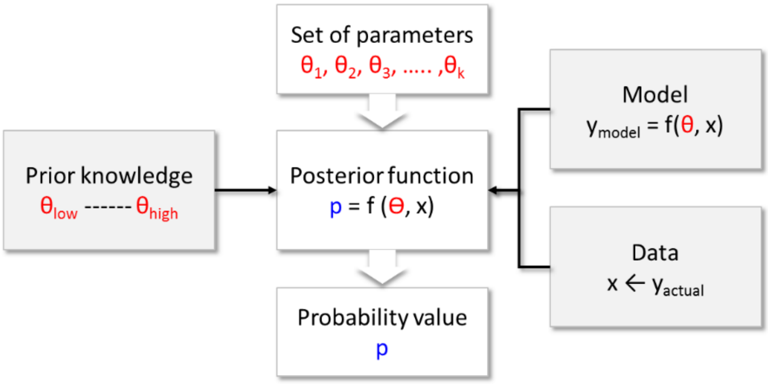

Figure 4.4 Conceptual representation of the Bayesian model for inference of parameters

4.4.1 Generic formulation of the model for Bayesian inference of parameters

Zhang et al. (2009, 2012) described the concepts of characterisation of geotechnical model uncertainty in a Bayesian framework. The following presentation uses some elements of that account but it is adapted to fit the case of the intact rock strength model discussed in Section 4.5.

A model can be represented by a function *f( )* used to predict a system response, y_{model}:

$$y_{model} = f(\theta, r) \tag{4.3}$$

The function depends on θ and *r*, which are vectors with the uncertain and certain parameters of the model, respectively. The certain parameters include the predictor variables *x*, which are those variables used to define the predicted variable *y*, whose behaviour is targeted with the model. If there are measurements of the actual system response, y_{actual}, then it is possible to define the error, ε, which accounts for model uncertainty:

$$y_{actual} = y_{model} + \varepsilon = f(\theta, r) + \varepsilon \tag{4.4}$$

The error, ε, is assumed to have a Gaussian (normal) distribution, with mean, μ, and standard deviation, σ. Alternatively, a t-distribution can be used to represent the variability of ε and to give improved handling of any outliers. In this case, an additional parameter called normality, v, is required, which controls the weight of the tails of the distribution. The t-distribution coincides with the normal distribution when v is equal to or greater than 30. For simplicity, a normal distribution is considered in the description of the method that follows.

The errors are assumed to be normally distributed around the model prediction so that we have

$$\mu = y_{model} \tag{4.5}$$

and

$$\varepsilon = y_{actual} - y_{model} = y_{actual} - f(\theta, r) \tag{4.6}$$

In this case, the standard deviation of the errors, σ, is the only so-called nuisance parameter that needs to be inferred together with the model parameters of interest in the vector, θ.

The Bayesian approach can be used to evaluate the posterior probability $p(\theta, \sigma|d)$ of the uncertain parameters used in the model given the data d on the actual performance of the system modelled:

$$p(\theta, \sigma \,|d) \;= \frac{p(d\,|\theta, \sigma) \;\; p(\theta, \sigma)}{\iint \cdots \iint p(d\,|\theta, \sigma) \;\; p(\theta, \sigma) \;\; d\theta \, d\sigma} \tag{4.7}$$

Eq. (4.7) is an extended version of the Bayes' equation shown in Eq. (4.1). Vague priors are used if there is little information on the values of the uncertain parameters. In this case, the prior term $p(\theta, \sigma)$ is defined with uniform distributions for σ and the k uncertain parameters in θ:

$$p(\theta,\, \sigma) = \; \frac{1}{\left(\sigma_{up} - \sigma_{lo}\right)} \times \prod_{j=1}^{k} \frac{1}{(\theta_{up\;j} - \theta_{lo\;j})} \tag{4.8}$$

The subscripts in this equation refer to upper (up) and lower (lo) values defining credible ranges of the uncertain parameters. The likelihood term $p(d|\,\theta, \sigma)$ is defined using a normal distribution to reflect the Gaussian variability of the errors, ε. The calculation is carried out for the n measurements of the system response:

$$p(d\,|\theta,\,\sigma) = \prod_{i=1}^{n} \frac{1}{\sqrt{2\sigma^2\pi}}\, e^{-\frac{(y_{actual\,i} - y_{model})^2}{2\sigma^2}} \tag{4.9}$$

The likelihood term is defined as the probability of the data given the uncertain parameters, but it can also be presented as the likelihood of the parameters given the data:

$$p(d\,|\theta,\,\sigma) \propto L(\theta, \sigma|d) \tag{4.10}$$

The denominator in Eq. (4.7) is calculated as the integral of the numerator across the whole parameter space. This is the normalisation term not required for inference of parameters with an MCMC procedure. This term is required for the calculation of the Bayes factor used for model comparison. The formula for the posterior distribution in Eq. (4.7) can become a complex expression if the model in Eq. (4.3) is itself a complex formula with many uncertain parameters. An efficient way of evaluating this function is by obtaining representative samples of the parameter values using the MCMC procedure.

4.4.2 The Markov Chain Monte Carlo (MCMC) method

The MCMC method is a procedure for sampling a probability distribution based on the selection of representative samples according to a random process called a Markov chain. In a Markov chain, every new step of the process depends on the current state and is completely independent of previous states (Kruschke, 2015). One of the main applications of the MCMC method is the evaluation of complex probability distribution functions of many dimensions such as those encountered in the posterior or likelihood functions of Bayesian data analysis. The Markov chain also called the random walk, in spite of being a random process, will always mimic the target distribution in the long run. The increased use of MCMC methods during the last 15 years is related to advances in computer hardware and numerical algorithms facilitating the use of these methods. There are numerous books and papers devoted to the subject of the MCMC method. For example, Diaconis (2009) provided some examples of formerly intractable problems that can now be solved using this technique. Robert and Casella (2011) presented a brief history of MCMC and provided a comprehensive treatment of MCMC techniques (Robert and Casella, 2004).

Several algorithms are used to implement an MCMC process, with the Metropolis, Gibbs and Hamiltonian algorithms being among the more commonly used ones (Kruschke, 2015). In general, all the algorithms share the following basic steps:

(1) Start with an initial guess of the set of parameters to sample.

(2) Evaluate a random jump of the set of parameters from their current values.

(3) Evaluate the probabilities of the proposed and current sets of values with the target distribution.

(4) Use the ratio between the probabilities of the proposed and current sets of values to define a criterion of acceptance of the jump. The criterion should favour moves towards the regions of higher probability, but should not eliminate the possibility of moves towards the regions of lower probability.

(5) Apply the acceptance criterion to update or retain the current values and repeat the process from step 2 until a sufficient number of sets of values (samples) are defined.

One advantage of this procedure is that it works even if the target function is not normalised to conform to the definition of a probability distribution.

4.4.3 Assessment of the quality of the MCMC analysis results

An MCMC sample should be representative of the posterior distribution, should have sufficient size to ensure the accuracy of estimates, and should be generated efficiently (Kruschke, 2015). In general, the implementation of an MCMC process requires some adjustments to achieve a stable solution in the form of representative independent samples from the parameters. It is common to discard a portion of the early steps of the chain, known as the burn-in process, while the sampling sequence evolves into a stable process. Diagnostic checks carried out on graphs produced with the results of the analysis serve to assess the quality of results. Some algorithms have heuristic rules on the acceptance rate of the steps of the chain to ensure that the samples are independent and representative of the posterior distribution. For example, for the affine-invariant assemble sampler used for the examples discussed in this paper, the recommendation is to have a rate of between 20% and 50% (Foreman-Mackey et al., 2013).

4.4.4 Software for MCMC analysis

Although it is important to understand the concepts behind the various algorithms used for the MCMC analysis to properly assess the quality of the results, the analyst does not have to programme these algorithms. There are already elaborated open source packages in various programming languages developed by computer scientists and related specialists that can be easily incorporated into ad-hoc code. Vincent (2014) listed some currently available popular packages for MCMC. The models described in this paper were coded in the Python programming language (Phyton Software Foundation, 2001) and the posterior distributions were sampled with the 'emcee' Python package developed by Foreman-Mackey et al. (2013). The software includes an algorithm known as the affine-invariant ensemble sampler characterised by the use of multiple chains running simultaneously to explore the domain of the function. The software was developed and is used by the astrophysics community with complex multidimensional models that exceed the expected complexity and dimensionality of the models normally used for geotechnical analysis.

4.5 Bayesian inference of intact rock strength parameters

4.5.1 Description of the method

The Bayesian estimation of intact rock peak strength parameters is based on the Hoek-Brown strength criterion (Hoek and Brown, 1997) defined by the following equation:

$$\sigma_1 = \sigma_3 + \sigma_{ci} \left(m_i \frac{\sigma_3}{\sigma_{ci}} + 1 \right)^{0.5} \tag{4.11}$$

where σ_{ci} is the UCS of intact rock; m_i is a constant of the intact rock material; and σ_1 and σ_3 are the major and minor principal stresses, respectively. σ_{ci} and m_i are the parameters investigated with the analysis. Using this criterion, the intact tensile strength, σ_t, is given by

$$\sigma_t = \frac{\sigma_{ci}}{2} \left(m_i - \sqrt{{m_i}^2 + 4} \right) \tag{4.12}$$

The data correspond to the results of TCS and UCS tests and DTS estimates made from BTS test results. These results correspond to measurements of one of the principal stresses at failure for particular values of the other principal stress. For example, the results of TCS and UCS tests provide measurements of the major principal stress, σ_1, at failure for fixed values of the minor principal stress, σ_3, with compression taken as positive. The DTS values correspond to σ_3 measurements at failure when σ_1 is zero. The estimation of DTS is normally based on indirect measurements made using the BTS test. Perras and Diederichs (2014) found good rock type-dependent correlations between DTS and BTS results with suggested correlation factors of α = DTS/BTS of 0.9 for metamorphic rocks, 0.8 for igneous rocks, and 0.7 for sedimentary rocks.

Langford and Diederichs (2013, 2015) discussed the estimation of Hoek-Brown intact rock strength envelopes from laboratory test results using a frequentist approach. In their latter paper, they compared three regression methods to estimate the best-fit envelope, namely, two variants of ordinary least squares with the linearised form of the Hoek-Brown strength equation, and a nonlinear regression method with the equation in its original form. These two versions of linear regression refer to the inclusion or otherwise of the adjustment for the measurement of errors in the tensile zone. The nonlinear method includes this adjustment. Langford and Diederichs (2013, 2015) considered nonlinear regression to be the preferred method of producing the best fits. In terms of uncertainty evaluation, they used the concept of prediction interval (PI) to quantify the uncertainty of data. Subsequently, they made assumptions regarding the correlation characteristics between UCS and m_i to fill the PIs with Hoek-Brown envelopes in order to assess the variability of these parameters. However, as will be discussed in Section 4.5.5, the use of PIs to assess the uncertainty of the fitted envelopes is not consistent with the standard concept of PI in the frequentist approach.

As indicated in Section 4.3.2, in the Bayesian approach, data are fixed whereas parameters are random. This characteristic results in a much clearer and sounder assessment of the uncertainty of the parameters. The result of the Bayesian analysis consists of probability distributions of σ_{ci} and m_i as well as scatter plots of sampled values providing information on their correlation characteristics. This information is used to produce the band of plausible failure envelopes reflecting the uncertainty of the intact rock strength.

The Bayesian analysis in this paper is compared with the nonlinear least squares regression method used by Langford and Diederichs (2015). Both methods consider the correct direction of measurement of errors, i.e. errors in σ_1 are calculated for UCS and TCS data, whereas errors in σ_3 are evaluated for DTS data. Figure 4.5 shows the way in which errors are measured in the Bayesian analysis. The linear regression method is not considered with the Bayesian analysis because the indirect estimation of the parameters causes some drawbacks with regard to the selection of vague priors. This is because the parameters inferred using the linear regression approach are the intercept and the slope of the Hoek-Brown linearised equation, and the vague condition of their priors is not transferred to the parameters of interest, σ_{ci} and m_i.

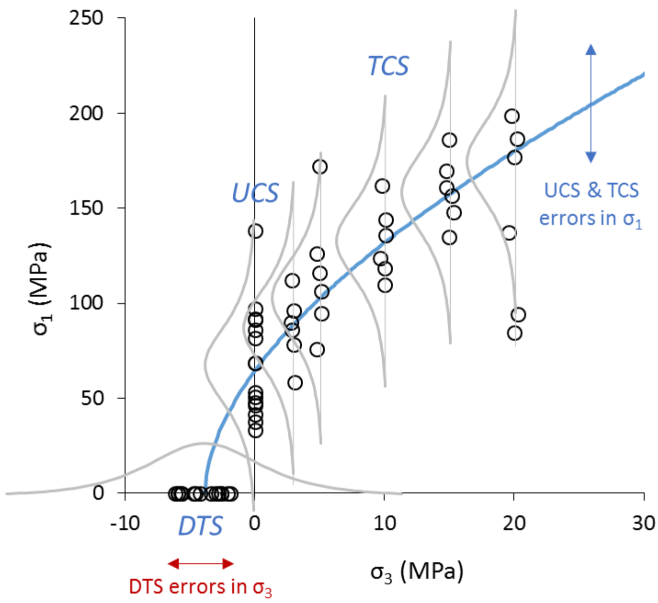

Figure 4.5 Measurement of errors in the tensile and compressive strength regions with a t distribution to handle outliers

The diagram in Figure 4.6 illustrates the structure of the Bayesian model for the robust estimation of intact rock strength parameters. The model combines the prior and the likelihood parts to define the posterior function according to Bayes' rule. The Hoek-Brown criterion represents the model whose predictions are compared with data to define errors, which are evaluated with a t-distribution to construct the likelihood function.

A problem commonly met in regression analyses is the bias in the estimation of parameters caused by the presence of outliers in the data. A way to deal with this situation is to consider a t-distribution to represent the spread of the data points in the direction of measurement of errors. The t-distribution is defined by three parameters that control the central value (mean, μ), the width (scale, σ) and the weight of the tails (normality, v). The possibility to set heavy tails with this distribution allows outliers to be accommodated without shifting the mean. This point is illustrated in Figure 4.7 (taken from Kruschke, 2015) where the advantage of the t-distribution over the normal distribution is highlighted. The use of the t-distribution for modelling errors makes the method robust in the true statistical sense.

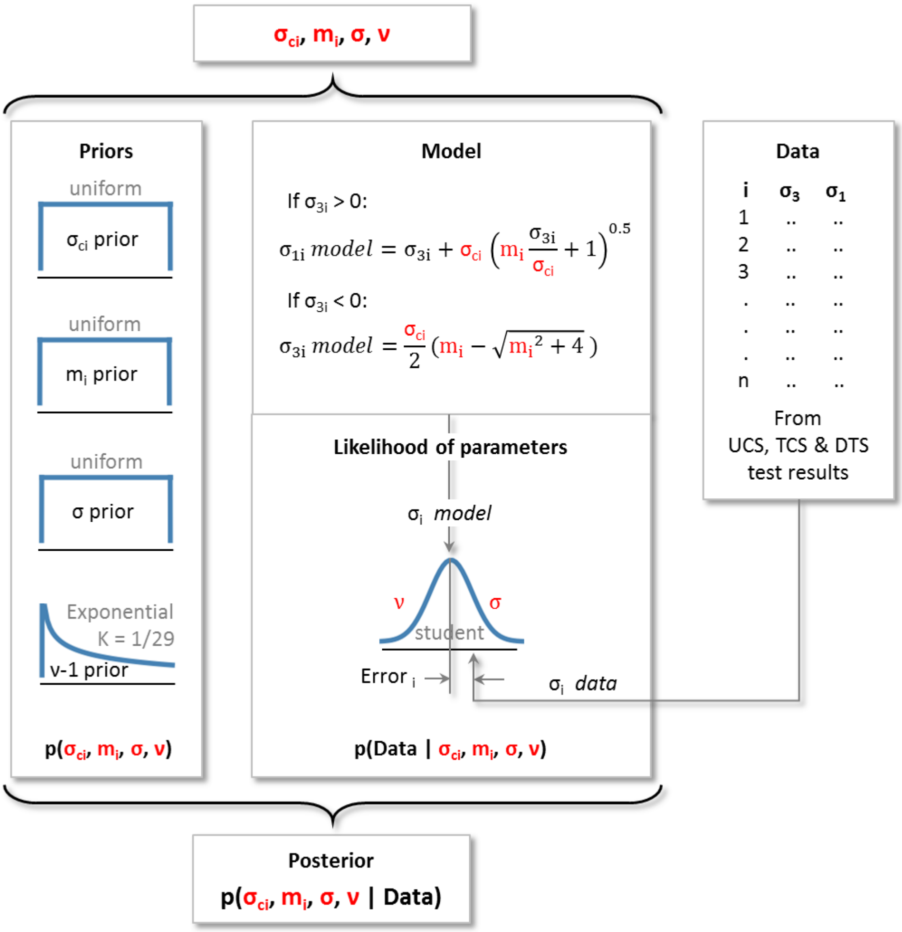

Figure 4.6 Conceptual basis of the Bayesian model for the robust estimation of the Hoek-Brown intact rock strength parameters, σ_{ci} and m_i

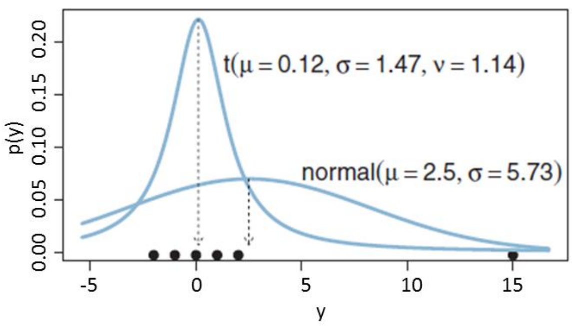

Figure 4.7 Illustration of the advantage of the t-distribution over the normal distribution to accommodate outliers in robust statistical inference (Kruschke, 2015)

The Bayesian model considers prior distributions of four parameters – the rock mechanics parameters, σ_{ci} and m_i, modelled with uniform distributions, and the scale, σ, and normality, v, parameters of the t-distribution modelled with uniform and exponential distributions, respectively, as shown in Figure 4.6. The uniform distributions are defined within valid ranges of the parameters determined by lower and upper bound values. The vague priors of the rock mechanics parameters are intended to limit their variations to plausible values without constraining the estimation within those limits. The ranges used for the examples in this paper are 10–500 MPa for σ_{ci} and 1–50 for m_i.

The range for the σ parameter is based on the characteristics of the data set with lower and upper values defined as the standard deviation of data in the y-axis (stdev. σ_1) divided and multiplied by 100, respectively. The prior for the parameter v is an exponential distribution with mean 1/29 because the majority of the changes of the t-distribution occur for values between 1 and 30. When v is greater than 30, the t-distribution coincides with the normal distribution. In this way, the full range of tail shapes of the t distribution has similar chances of being selected. The one added to the value sampled from the distribution is intended to convert the range of the exponential distribution from 0 to infinity to the valid range of v from 1 to infinity.

The details of the definition of the posterior distribution function for the conditions of analysis presented in this paper are included in Appendix A. The posterior is a cumbersome four-dimensional function that is better evaluated by sampling the parameters with an MCMC algorithm. The model was implemented in the Python programming language, using the MCMC sampler “emcee”.

Finally, in this account of the methods of analysis to be used in the illustrative examples to follow, it is important to offer a qualification about the UCS data used in the examples. It has been established that the value of the UCS parameter, σ_{ci}, used in fitting the Hoek-Brown criterion to peak strength TCS data for intact rock, should be the value obtained from the intercept of the peak strength curve with the $\sigma_3 = 0$ axis (Hoek and Brown, 1997; Bewick et al., 2015; Kaiser et al., 2015). This value may correspond to the results of well-conducted UCS tests in which shear failure occurs, but is usually higher than the UCS value obtained from tests in which splitting failure occurs. It should be noted that in the data analysed here, no attempt has been made to differentiate between samples showing these different modes of failure.

4.5.2 Example of fitting data with outliers

The methodology is illustrated using a “typical” intact rock strength data set of 60 points (15 UCS, 15 DTS and 30 TCS), including a few outliers, which was generated using random numbers between pre-defined limits. The analysis was carried out with a reduced data set of 31 points (8 UCS, 8 DTS and 15 TCS) without outliers, and with the complete data set of 60 points, in order to highlight the effect of the outliers. Figure 4.8 shows the data points together with the fitted envelopes using the nonlinear least squares (NLLS) regression method and the Bayesian approach. The NLLS method is based on the numerical estimation of the set of parameters that minimizes the squared residuals function. The Bayesian method is denoted as MCMC_S in Figure 4.8 to indicate that the MCMC sampling was done on a posterior function using a t-distribution to model the errors. The two methods shown in Figure 4.8 consider the actual (absolute) residuals for the calculation of errors. The results of the analyses are similar for the case with 31 data points but differ for the case of 60 data points with a marked effect from the outliers on the NLLS envelope. On the other hand, the Bayesian result appears to be less affected by the outliers, demonstrating the robustness of the method.

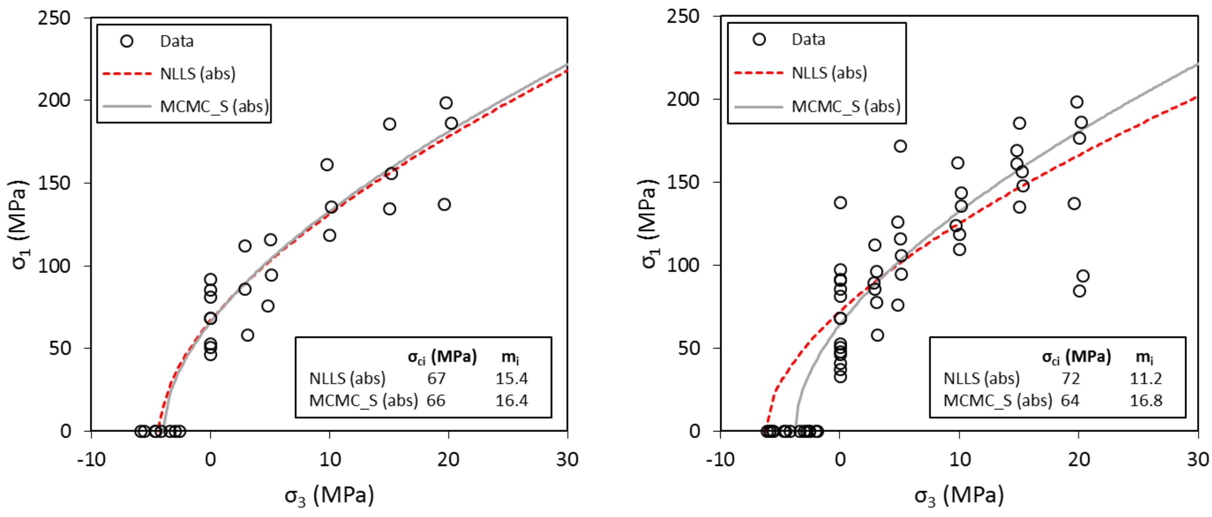

Figure 4.8 Comparison of fitted Hoek-Brown failure envelopes with nonlinear least squares (NLLS) and Bayesian sampling (MCMC_S) methods, considering absolute residuals. Data sets of 31 points without outliers (left) and 60 points with outliers (right) were used

One aspect of the data set that has an impact on the fitting result is the fact that the errors in the tensile region are one order of magnitude smaller than the errors in the compressive region. For example, the case without outliers in Figure 4.8 shows that the range of tensile strength values is about 5 MPa whereas the compressive strength values are 10 times more variable. One way of accounting for this imbalance with the Bayesian model would be to set up separate t-distributions to model tensile and compressive errors. This adjustment would imply the addition of two uncertain variables to be inferred. However, a simpler alternative also available to the frequentist method is the normalisation of errors with the respective model values. The relative residuals calculated in this way would have similar orders of magnitude in the tensile and compressive regions.

Figure 4.9 shows the data points for the case of 60 test results and the six fitted envelopes using three methods of analysis with absolute and relative residuals. The methods include the NLLS, the Bayesian sampling of a posterior function based on a t-distribution for the errors (MCMC_S), and the Bayesian sampling of a simpler function using a normal distribution to model the errors (MCMC_N). The reason for using a model with the normal instead of the t-distribution is to appreciate the real effect that the use of relative errors has on the bias caused by the outliers.

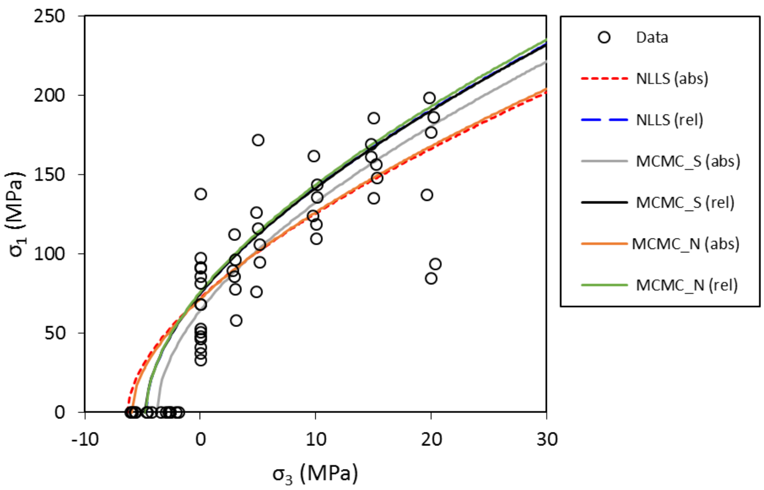

Figure 4.9 Comparison of fitted Hoek-Brown failure envelopes with nonlinear least squares (NLLS) and Bayesian sampling (MCMC_S and MCMC_N) methods, considering absolute and relative residuals and the data set of 60 points

The results in Figure 4.9 show coincidence of the envelopes defined by the three methods when the errors are normalised (relative residuals). The results of the analysis with absolute residuals show the strong effect of the outliers on the envelopes fitted with the NLLS and the Bayesian with normal distribution methods. These results also highlight the robust effect of the t-distribution in the Bayesian model indicated by the closeness of the result to the fitted envelopes using relative residuals.

4.5.3 Comparison of regression methods

The quantification of the goodness of fit with the NLLS method is based on the standard error (SE), which can be calculated for absolute and relative residuals. The SE of the fitted envelopes defined with two parameters from n data points is calculated as

$$SE = \sqrt{\frac{\Sigma(errors^2)}{n-2}} \tag{4.13}$$

The SE can also be calculated for the envelopes obtained from the Bayesian analysis. However, in this case, a more adequate indicator of the goodness of fit is the maximum likelihood value (MxL) that measures the likelihood of the estimated parameters. The MxL is calculated with the model described in Figure 4.6. Likelihood values correspond to the product of small probabilities of the individual data points; therefore, they are very small numbers. For this reason, the maximum likelihood estimations are normally reported as the logarithms of the values. The comparison of the maximum likelihood values to assess the effectiveness of the regression models is meaningful when the two competing models have the same numbers of parameters. If the models have different numbers of parameters, the appropriate way to compare the models is through the Bayes factor *K*, defined as the ratio of the evidence terms of the two competing models:

$$K = \frac{p(d|model1)}{p(d|model\ 2)} \tag{4.14}$$

The evidence term *p(d|model)* corresponds to the integration of the numerator of the Bayes posterior over the parameter domains (see Eq. (4.7)). A model with more parameters having a greater maximum likelihood due to smaller errors is not necessarily better than a model with a lesser maximum likelihood but with fewer parameters. The Bayes factor, *K*, provides the appropriate measure of the relative effectiveness of the two models.

Table 4.2 shows a summary of the results of the six regression analyses presented in Figure 4.9. The table includes the main characteristics of each regression model, the estimated parameters, the SE for absolute and relative errors, and the natural logarithm of MxL for the Bayesian analysis. As expected, the minimum SEs with absolute residuals are obtained with the methods that use the absolute residuals in the calculation process, and similarly occur with the minimum SE with relative residuals. The MxL results of the four Bayesian models indicate a better fit with the models that use relative residuals as compared with the models based on absolute residuals. A proper comparison of the effectiveness of the Bayesian models is shown in Table 4.3, which includes the Bayes factors for all the model pairs.

Table 4.2 Comparison of results of the fitting analysis

Model no.	Method	Type of residuals	Distribution of errors	No. of parameters	σ_{ci} (MPa)	m_i	SE_{abs}	SE_{rel}	Ln(MxL)
1	NLLS	Abs		2	72	11.2	26.0	0.34	
2	NLLS	Rel		2	75	15.7	28.8	0.31	
3	MCMC	Abs	Student’s	4	64	16.8	27.1	0.34	-293.0
4	MCMC	Rel	Student’s	4	75	15.6	28.8	0.31	-23.5
5	MCMC	Abs	Normal	3	72	11.7	26.0	0.33	-279.8
6	MCMC	Rel	Normal	3	76	15.9	29.4	0.31	-13.3

Table 4.3 Effectiveness of Bayesian regression models based on Bayes factor comparisons

Bayesian	MCMC_S (abs)	MCMC_S (rel)	MCMC_N (abs)	MCMC_N (rel)
MCMC_S (abs)	1	<1	123	<1
MCMC_S (rel)	>100	1	>100	<1
MCMC_N (abs)	<1	<1	1	<1
MCMC_N (rel)	>100	1.3	>100	1

A commonly used interpretation of the Bayes factor for model comparison is indicated in Table 4.4 (Kass and Raftery, 1995). According to this interpretation, the Bayes factors in

Table 4.3 indicate very strong support of the models based on relative residuals as compared to the models that use absolute residuals. In terms of the type of distribution used to model the errors, the models based on the t-distribution and the normal distribution are effectively equivalent. However, the calculated Bayes factors are specific to the data set used for the analysis. Therefore, it is concluded that the model based on the t-distribution with relative residuals is the preferred fitting method since it will provide superior handling of potential outliers in any of the test results.

Table 4.4 Interpretation of Bayes factors (Kass and Raftery, 1995)

K	Strength of evidence
< 1	Negative (supports model 2)
1 to 3	Not worth more than a bare mention
3 to 20	Positive
20 to 150	Strong
> 150	Very strong

4.5.4 Additional results from the Bayesian approach

A notable feature of the Bayesian analysis is that the parameters are defined from complete probability distributions that not only provide information on the reliability of the estimates but also indicate their correlation characteristics. In this respect, the Bayesian method can provide a complete quantification of the parameter uncertainty.

Figure 4.10 shows the scatter plots of m_i versus σ_{ci} values obtained from the Bayesian analysis using the four models implemented. The graphs at the left are from the analysis with absolute residuals and those at the right are from the analysis with relative residuals. The graphs at the top correspond to the models based on the t-distribution and those at the bottom are from models using the normal distribution to evaluate the errors. The contours define the 95 and 68 percentiles of sampled points and the crosses mark the mean values. The calculated coefficients of correlation (CC) are indicated in the upper right corner of each plot. The parameters show a negative correlation for the analysis with absolute residuals, which is a consequence of the difference in the order of magnitude of the errors in the tensile and compressive strengths. The normalisation of the errors causes the narrowing of the likely tensile strength, which translates to the reduction in the spread of the σ_{ci} and m_i values.

This effect is better appreciated in the graphs of Figure 4.11 showing the bands of envelopes corresponding to the 95% of sampled values for the cases of absolute and relative residuals. The results in Figure 4.11 and Figure 4.12 confirm the benefit of normalising the errors for the regression analysis and the indifference of the results with relative residuals to the type of distribution used to evaluate these errors.

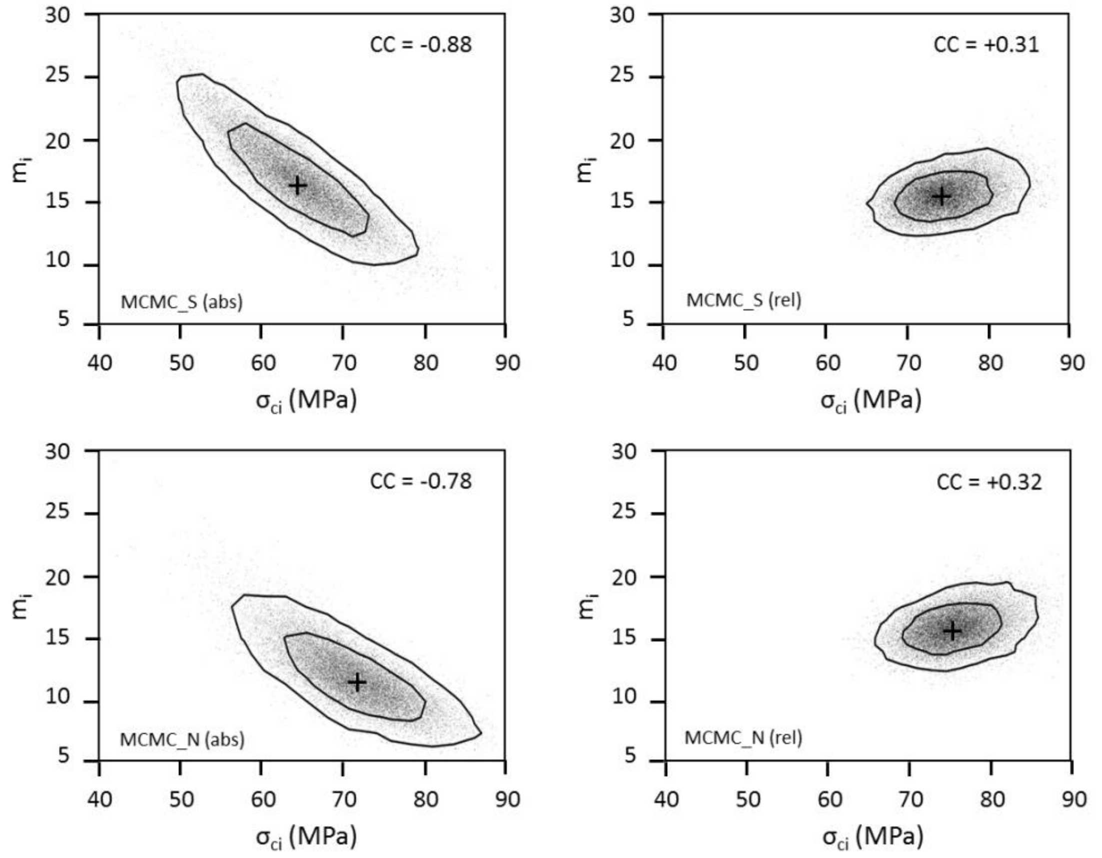

Figure 4.10 Scatter plots of mi versus σ_{ci} from the Bayesian regression analysis with absolute (left) and relative (right) residuals. Models based on t-distribution (top) and normal distribution (bottom) were used to evaluate the errors

Figure 4.12 shows the histograms of the representative samples of σ_{ci} and m_i drawn from the posterior distribution, for the case of relative residuals evaluated with the t-distribution. The histograms define the ranges of credible values corresponding to the 95% HDIs and the more likely estimates represented by the mean values (σ_{ci} = 75 MPa and m_i = 15.6).

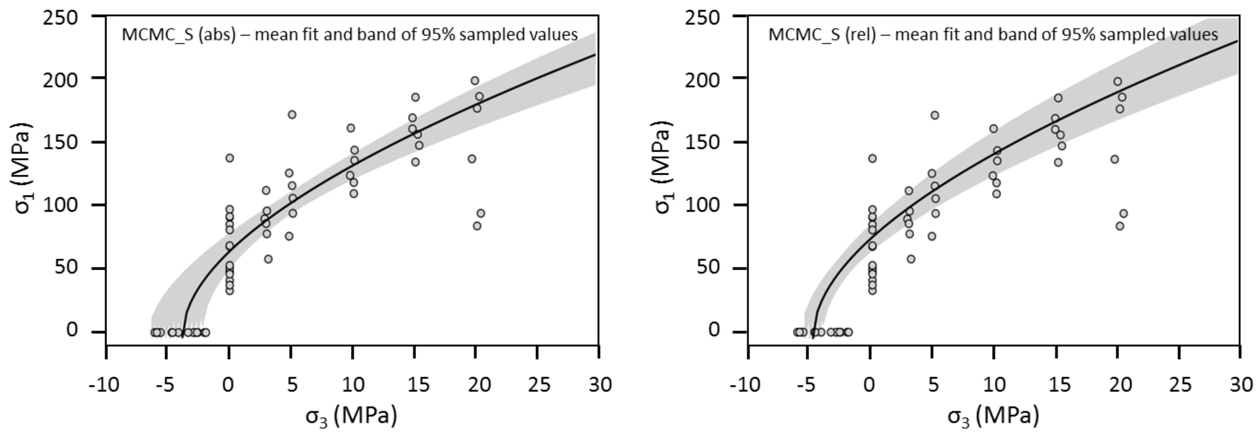

Figure 4.11 Fitted envelopes with bands corresponding to the 95% of sampled points from the analysis with absolute (left) and relative (right) residuals and the model based on the t-distribution to evaluate errors

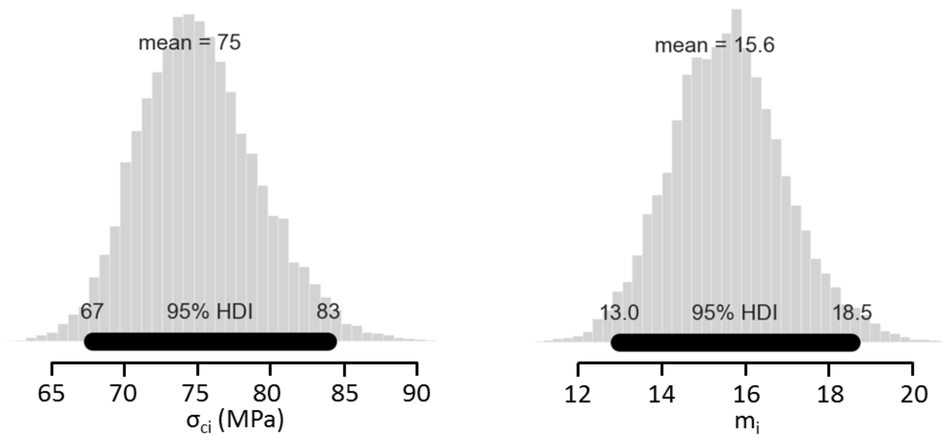

Figure 4.12 Posterior distributions of σ_{ci} and m_i with mean and 95% HDIs indicated, for the case of relative residuals evaluated with a t-distribution

Figure 4.13 shows the complete set of results of the MCMC analysis for the case of relative residuals evaluated using a t-distribution. The graph includes the scatter plots between all the parameters sampled from the posterior distribution as well as the histograms of those parameters. The graph shows not only the results of the parameters of interest, σ_{ci} and m_i, but also the nuisance parameters, σ and v, used in the model to characterise the t-distribution. The parameter v is plotted in logarithmic form to facilitate an appreciation of its variability. These plots are useful for identifying correlations and for detecting possible anomalous situations that might suggest instability of the chains or other problems with the sampling process.

The specification of the MCMC sampling process included fifty chains, also known as walkers, with two thousand steps per walker and excluding half of the steps as part of the burn-in process. An important diagnostic graph to verify the validity of the results is the trace plot shown in Figure 4.14. Trace plots show the progress of the fifty chains sampling each parameter through the total number of steps specified. They indicate that a stable process was reached in a few steps, suggesting that fewer steps may have been sufficient to sample the function. The acceptance rate of the sampling process was 0.47 which is within the limits recommended for the affine invariant assemble algorithm (Foreman-Mackey et al., 2013).

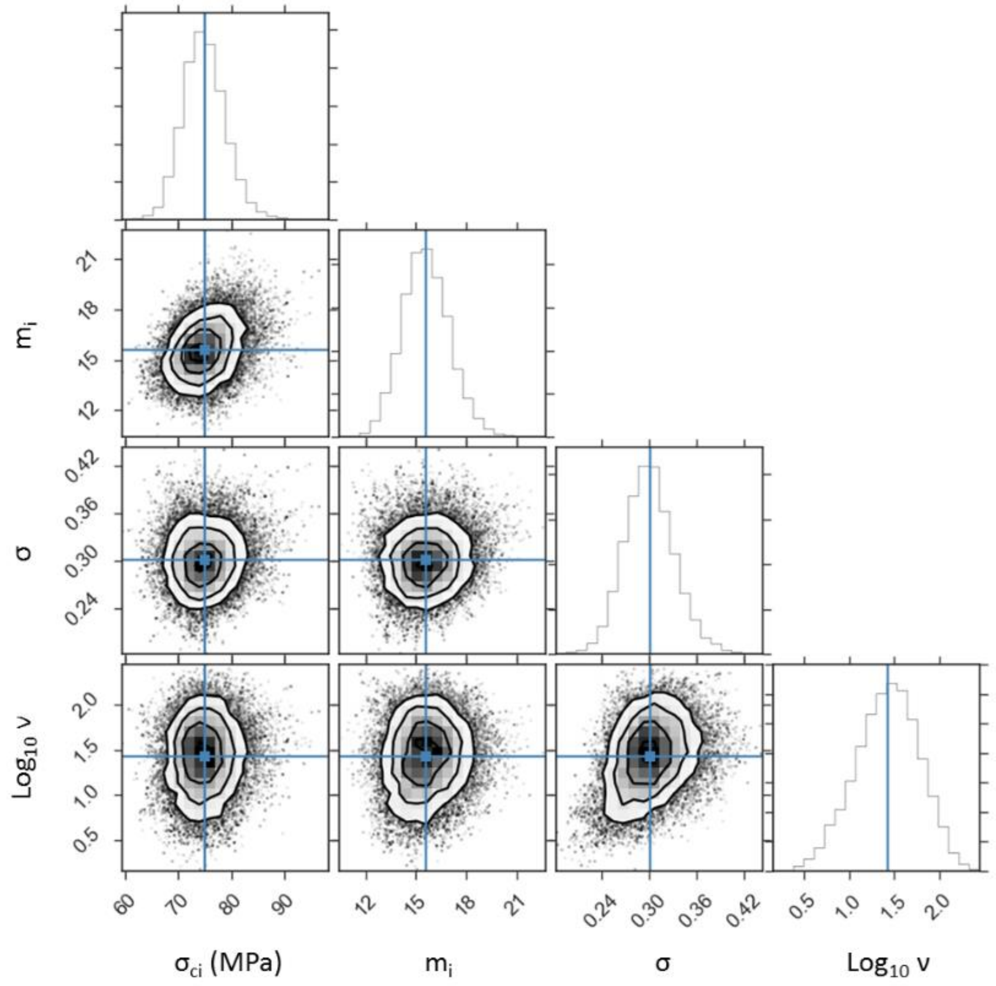

Figure 4.13 Corner graph showing the scatter plots of pairs of all the sampled parameters and their individual histograms

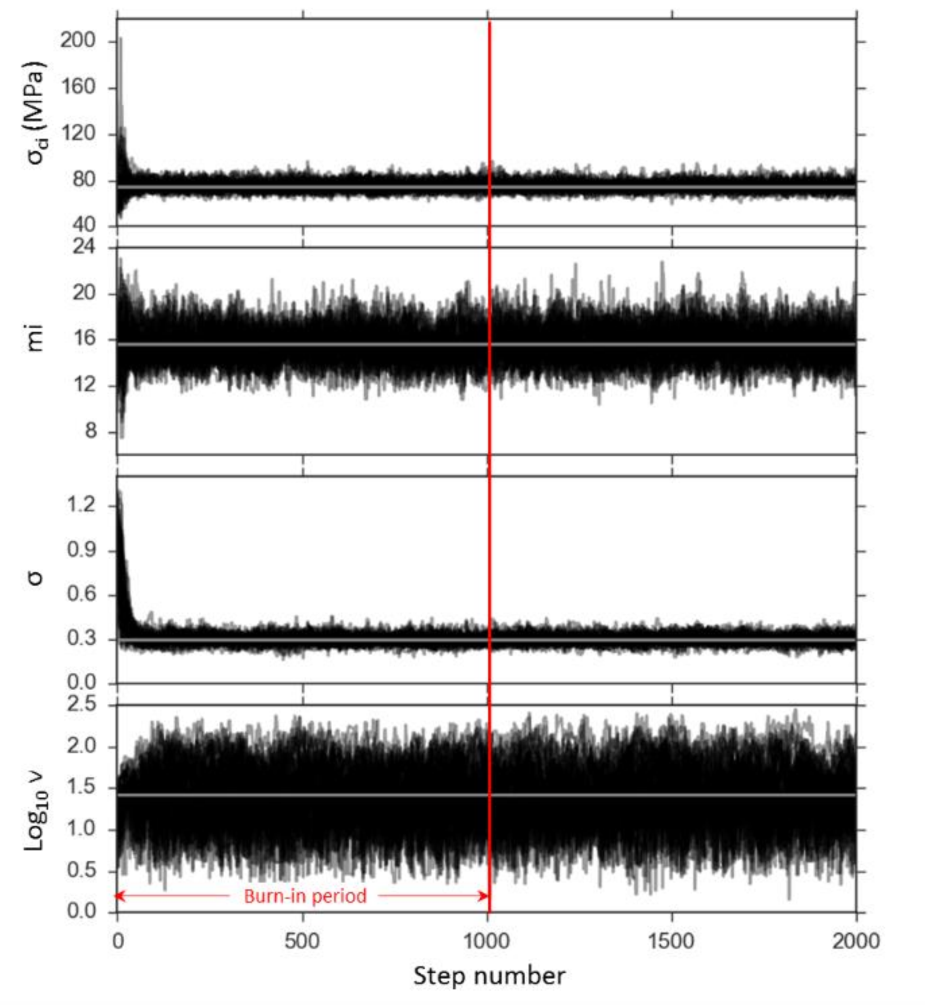

Figure 4.14 Trace plots of the MCMC chains for the four parameters sampled from the posterior distribution. Each plot includes the traces of the 50 walkers used for the sampling giving a total of one hundred thousand samples per parameter. The first fifty thousand steps correspond to the burn-in process and were excluded from the results

4.5.5 Comparison between the uncertainty evaluations with the frequentist and Bayesian approaches – a second example

Given the merits of considering relative residuals to obtain the best estimation of the intact rock strength parameters, the focus in this section is on the quantification of the uncertainty of these parameters. The example presented in the preceding sections showed coincidence between the NLLS and Bayesian results for the analysis with relative residuals. The example also served to highlight the main features of the quantification of uncertainty of the parameters inferred with the Bayesian approach. Sections 5.5 to 5.7 illustrate the contrast between the uncertainty quantification with the two approaches, by analysing a data set of

166 test results on samples of a homogenous granite in Sweden. The data set includes 70 BTS, 59 UCS and 37 TCS tests with confining pressures of between 2 MPa and 50 MPa. The tests were carried out at the Swedish National Testing and Research Institute (SP) for the Swedish Nuclear and Fuel Waste Management Company (SKB). The data were extracted from 14 publically available data reports concerning the Oskarshamn site investigation in Sweden (Jacobsson, 2004, 2005, 2006, 2007). All of the results in the data set correspond to tests on intact rock with failure modes not affected by local defects.

The two regression methods considered for the comparison of uncertainty quantification are the NLLS and the Bayesian sampling with the model based on a t-distribution to evaluate the errors (MCMC_S). In both cases, the analyses are carried out with relative residuals.

4.5.6 Confidence interval (CI) and prediction interval (PI) in the frequentist approach

The conventional way of measuring the uncertainty of a parameter estimate within the frequentist approach is to construct a CI around the inferred point estimate. In this case, the parameter is non-random and unknown. The interpretation of a 95% CI is that in repeated sampling, 95% of the intervals constructed around their respective point estimates will contain the true fixed but unknown value of the parameter. In the Hoek-Brown strength envelope case, the fitted envelope defined by the parameters σ_{ci} and m_i is the point estimate and the 95% CI is defined as follows for the compressive and tensile strength regions:

$$CI_{\ compressive} = \sigma_1 \pm \left(t_{2.5\%,\ n-2}\right) SE_r \sigma_1 \sqrt{\frac{1}{n} + \frac{(\sigma_3 - \mu_{\sigma 3\ data})^2}{\sum_{i=1}^{n}(\sigma_{3\ data\ i} - \mu_{\sigma 3\ data})^2}} \tag{4.15}$$

$$CI_{\ tensile} = \sigma_t \pm \left(t_{2.5\%,\ n-2}\right) SE_r \sigma_t \sqrt{\frac{1}{n} + \frac{(\sigma_3 - \mu_{\sigma 3\ data})^2}{\sum_{i=1}^{n}(\sigma_{3\ data\ i} - \mu_{\sigma 3\ data})^2}} \tag{4.16}$$

where σ_t is the tensile strength for the fitted strength envelope; $t_{2.5\%,\ n-2}$ is the 2.5 percentile of the t-distribution with n-2 degrees of freedom, which defines the interval that includes 95% of the area of the t-distribution with a zero mean; SE_r is the standard error as defined by Eq. (13) considering normalised (relative) errors; n is the number of data points; and μ is the mean of the σ_3 data values.

The PIs within the frequentist approach have a different meaning and refer to the uncertainty of data values which are considered to be random variables. The interpretation of a 95% PI is that there is a 95% probability that the next data value to be observed will fall within the interval. In the Hoek-Brown strength envelope case, the fitted envelope defined by the parameters σ_{ci} and m_i can be used to predict individual strength values. A 95% PI constructed around this envelope defines the limits where future strength observations will be with a 95% probability. The 95% PI is defined as follows for the compressive and tensile strength regions:

$$PI_{\ compressive} = \sigma_1 \pm \left(t_{2.5\%,\ n-2}\right) SE_r \sigma_1 \sqrt{1 + \frac{1}{n} + \frac{(\sigma_3 - \mu_{\sigma 3\ data})^2}{\sum_{i=1}^{n}(\sigma_{3\ data\ i} - \mu_{\sigma 3\ data})^2}} \tag{4.17}$$

$$PI_{\ tensile} = \sigma_t \pm \left(t_{2.5\%,\ n-2}\right) SE_r \sigma_t \sqrt{1 + \frac{1}{n} + \frac{(\sigma_3 - \mu_{\sigma 3\ data})^2}{\sum_{i=1}^{n}(\sigma_{3\ data\ i} - \mu_{\sigma 3\ data})^2}} \tag{4.18}$$

The PI and CI are centred on the fitted envelope, but the PI is wider than the CI, because the PI refers to the variability of individual data points, whereas the CI is associated with the variability of the whole envelope. In both cases, it is implied that there must be additional sampling for the levels of confidence to have a meaning. In the case of the PI, a future data point is required, whereas for the CI, many similar data sets need to be collected.

Figure 4.15 shows the data set and the results of the frequentist analysis that include the fitted envelope with the 95% CI and PI around the mean. The intervals are narrower towards the mean of the σ_3 data range. This effect is compounded with the widening of the interval relative to the model fit value that multiplies the SE_r. Langford and Diederichs (2015) used the PI to quantify the uncertainty of the fit. However, as indicated above, within the frequentist approach, the uncertainty of the fit is measured with the CI, whereas the uncertainty of the data points is associated with the PI (Hyndman, 2013).

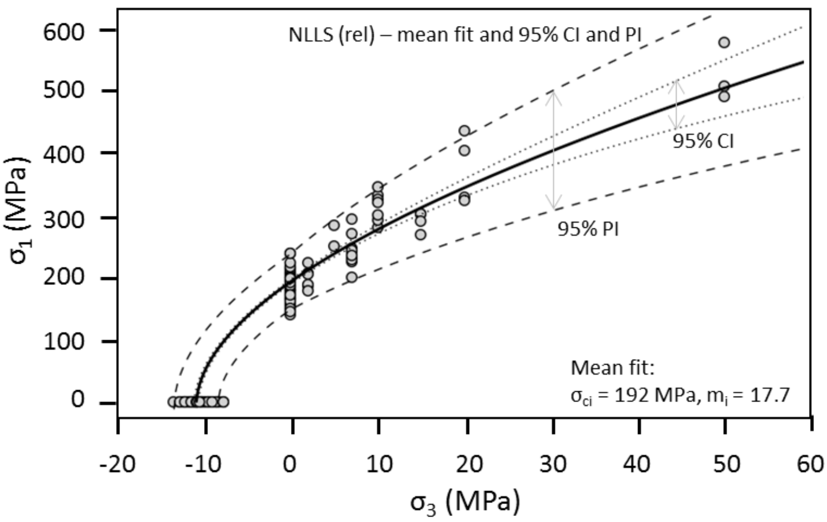

Figure 4.15 Uncertainty quantification of the Hoek-Brown intact rock strength envelope with the frequentist approach (NLLS method with relative residuals). Fitted envelope, 95% CI reflecting the uncertainty of the mean envelope and 95% PI reflecting the uncertainty of individual data points

4.5.7 Scatter plots and envelope bands in the Bayesian approach

Figure 4.16 shows the results of the fitting analysis of the data set using the Bayesian approach. In this case, the samples drawn from the posterior function with the MCMC procedure are represented in the scatter plot of m_i versus σ_{ci} on the left in Figure 4.16. This graph indicates a positive correlation between the two parameters and provides a complete description of their uncertainty. The outer contour in the scatter plot corresponds to the 95 percentile of the sampled values and the envelopes constructed with these values define the envelope band represented in the graph on the right in Figure 4.16. The narrow band suggests a sharp definition of the Hoek-Brown strength envelope supported by the 166 test results in the data set. This is not a typical number of test results available in many projects. Fewer data will result in wider uncertainty bands.

The results presented in Figure 4.15 and Figure 4.16 show coincidence in the estimation of the mean envelope, but highlight the differences in the evaluation of the uncertainty of the intact rock strength parameters. The frequentist approach provides intervals where the envelope or a data point may be found with a level of confidence. However, for this approach, the level of confidence only has meaning if repeated future sampling is carried out. The Bayesian method provides a representative sample of parameter values with the highest probability of occurrence based on the set of test results used in the analysis. The sampled values allow the definition of the range of credible envelopes for a particular level of confidence. The Bayesian method offers a richer and clearer evaluation of the uncertainty of the intact rock strength parameters.

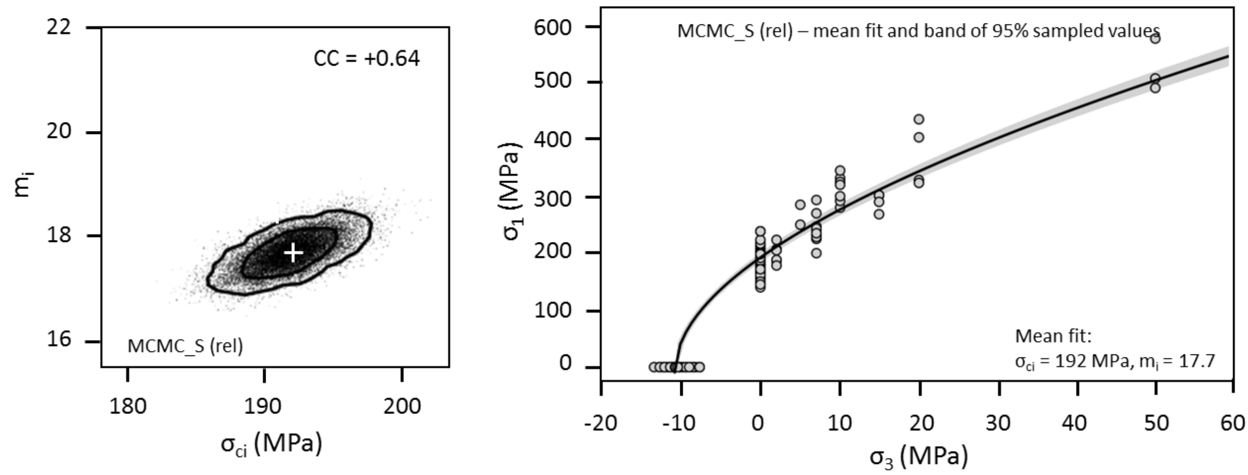

Figure 4.16 Uncertainty quantification of the Hoek-Brown intact rock strength envelope with the Bayesian approach (model based on relative residuals with t-distribution). Scatter plot of sampled values of m_i versus σ_{ci} with 68 and 95 percentile contours (left). Fitted envelope and the band of envelopes corresponding to the 95% of sampled parameter values (right)

4.5.8 Improving the fit in the triaxial region

The Hoek-Brown parameters σ_{ci} and m_i inferred from the fitting analysis define the intercepts of the peak strength envelope with the tensile and uniaxial compressive strength axes. However, the fit in the triaxial region is constrained by the assumption that the parameter, *a*, in the generalised criterion for rock masses is 0.5 for intact rock, as indicated by the exponent in Eq. (11). The Bayesian approach provides a convenient way to assess the merits of including the *a* parameter as an additional uncertain variable for inference. Langford and Diederichs (2015) described the improvement of the fit with a frequentist approach when the *a* parameter is included in the analysis. They also pointed out the practical difficulties of implementing this modification to the criterion for intact rock strength.

Figure 4.17 shows the corner plot of the three rock mechanics parameters inferred with the Bayesian analysis for the Swedish granite data set. The model considers a t-distribution to evaluate the relative errors, which adds two nuisance parameters for inference. The scatter plots show a negative correlation of the parameter *a* with both σ_{ci} and m_i. The improvement of the fit in the triaxial region when the parameter *a* is free to vary can be appreciated in the graph of Figure 4.18, in which the fitted envelope with a = 0.58 is compared to the envelope resulting from the analysis when a is fixed to 0.5. The histogram of parameter a in Figure 4.17 shows a range of probable values between 0.48 and 0.66. This variability compounded with the correlation with σ_{ci} and m_i results in a larger uncertainty in the triaxial region. Figure 4.19 shows the mean fit and the band of envelopes defined by the 95 percentile of the parameters σ_{ci}, m_i and a. This result is an indication of insufficient data points with high confining stresses to confirm the strength envelope in that stress region.

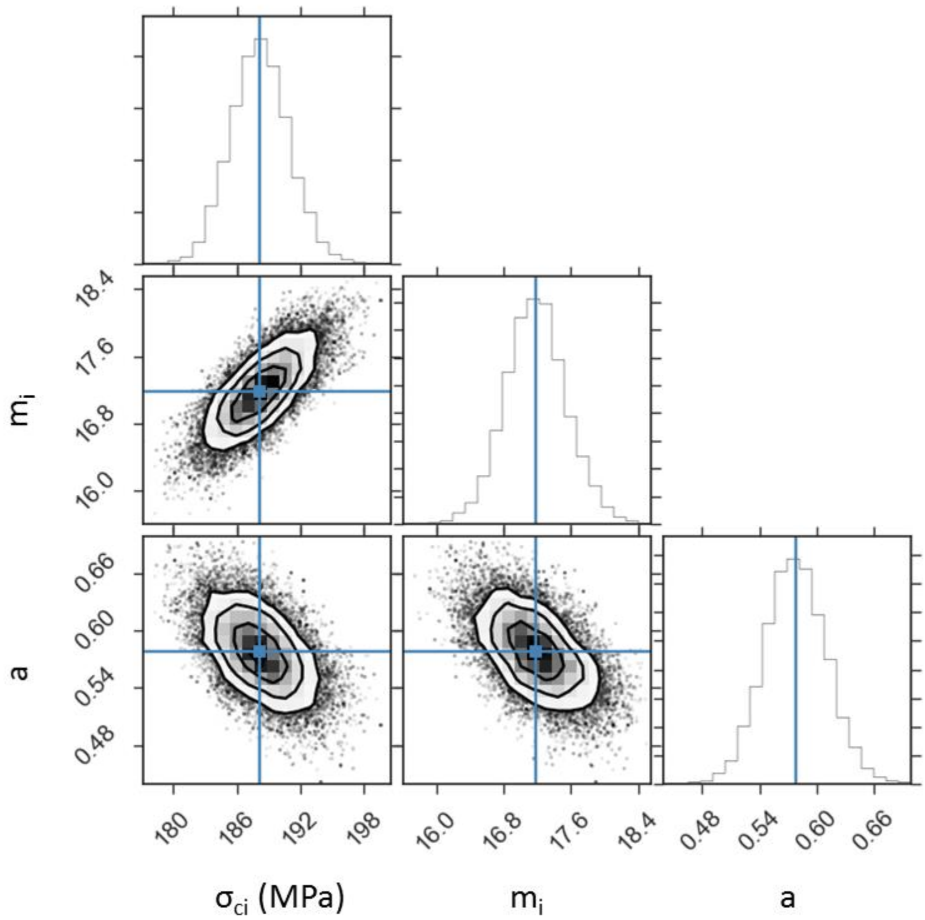

Figure 4.17 Corner plot from the analysis of the Swedish granite data set considering the Hoek-Brown parameter a as variable. The plot shows the scatter plots and histograms of the rock mechanics parameters

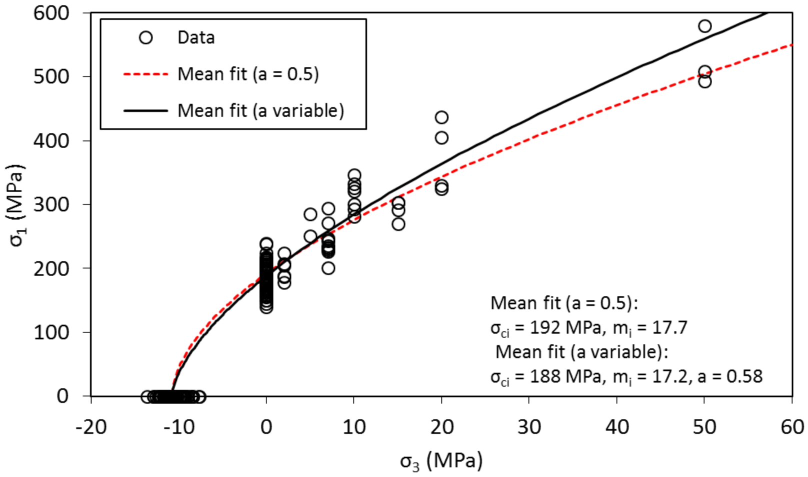

Figure 4.18 Comparison of the fitted envelopes from the analysis with the parameter *a* fixed to 0.5 and for the case in which *a* is variable

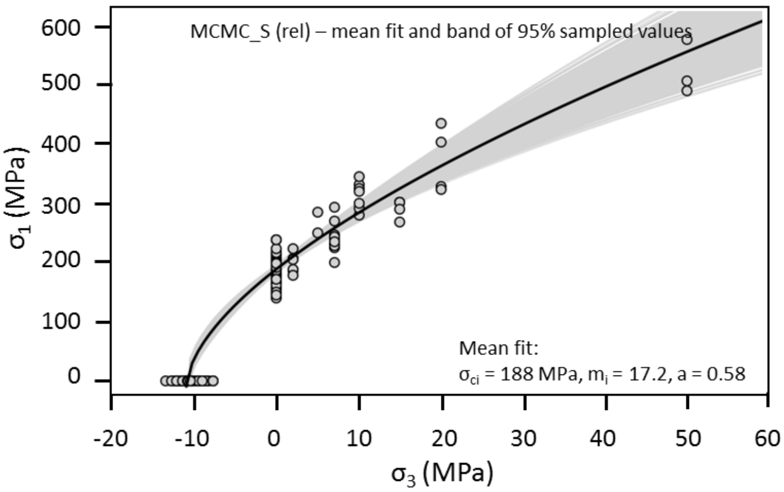

Figure 4.19 Uncertainty of the Hoek-Brown intact rock strength envelope when the parameter *a* is considered variable (model based on relative residuals with t-distribution). The band of envelopes corresponds to 95% of the sampled parameter values

4.5.9 Accounting for the uncertainty in the estimation of DTS from BTS

The test data for the Swedish granite used to illustrate the Bayesian fitting method include 70 BTS test results. These results were converted to DTS values using a factor of 0.83 derived from data for igneous rocks. This correlation factor is based on a linear regression analysis of 40 pairs of BTS and DTS test results mainly on granite samples, extracted from Perras and Diederichs (2014). The uncertainty of this correlation factor is not transferred to the fitting analysis of the strength envelope when the DTS values are calculated using a fixed conversion factor. The Bayesian model allows for the incorporation of this uncertainty, by using the data set of BTS versus DTS to define the correlation factor (α) within the posterior function. Therefore, during the sampling process, each trial value of α is used within the model to convert BTS data into DTS values required for the fitting analysis of the Hoek-Brown envelope.

The extended Bayesian model to include the uncertainty in the correlation between BTS and DTS uses two data sets, one consisting of 40 BTS versus DTS test results and the second the 166 σ_1 versus σ_3 values from BTS, UCS and TCS test results. The model uses t-distributions with parameters σ and v to evaluate relative errors in the strength envelope and normal distributions with standard deviation σ_α to evaluate absolute errors in the BTS-DTS correlation. Therefore, the model has six uncertain parameters for inference (σ_{ci}, m_i, σ, v, α, σ_α). Effectively, the Bayesian model uses the angle of the slope in radians (α_{rad}) for the inference process, to facilitate the setting of vague priors with a uniform distribution. This is because the factor α in the form of tan(α_{rad}) does not change uniformly between 0 and $\pi/2$, and a uniform distribution on this factor would favour flatter slopes.

Figure 4.20 shows the corner plot with the results of the analysis considering the uncertainty in the correlation between BTS and DTS. This figure only includes the rock mechanics parameters of immediate interest; the parameters used to define the distributions for the evaluation of errors are nuisance parameters and are not displayed. The scatter plot between α and m_i shows a strong negative correlation between these parameters. In terms of the variability of α, the analysis considers the possibility of errors in both DTS and BTS (Hogg et al., 2010). Accordingly, errors are evaluated with the normal distributions in a direction orthogonal to the fitted lines as shown in Figure 4.21. The plot in Figure 4.21 shows the band of fitted envelopes corresponding to the 95% HDI of α values sampled. The uncertainty of α is transferred within the Bayesian model and added to the uncertainty of the fitted Hoek-Brown strength envelope. Figure 4.22 shows the results of the fitting analysis where the larger spread of σ_{ci} and m_i causes a wider band of 95 percentile of envelopes. The results shown in Figure 4.22 can be contrasted with those in Figure 4.16 to illustrate the effect of including the uncertainty in the correlation between BTS and DTS on the uncertainty of the intact rock peak strength envelope.

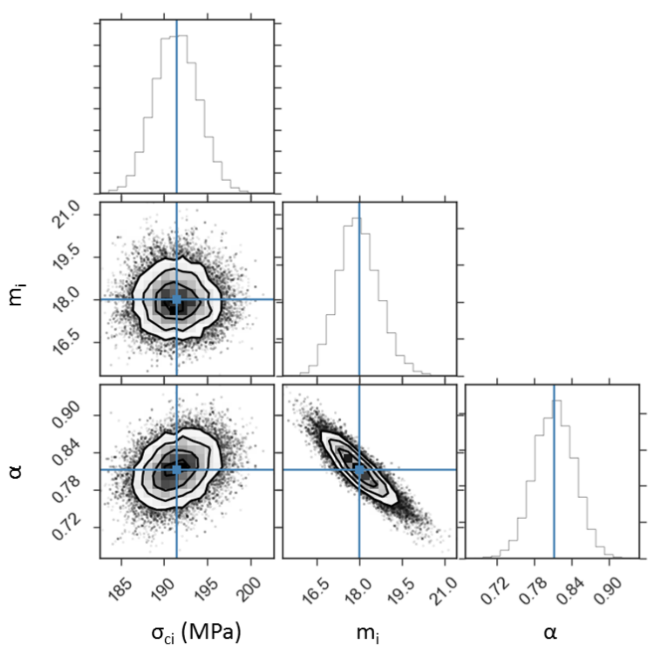

Figure 4.20 Corner plot from the analysis of the granite data set including the uncertainty in the correlation between DTS and BTS. The plot shows the scatter plots and histograms of the rock mechanics parameters

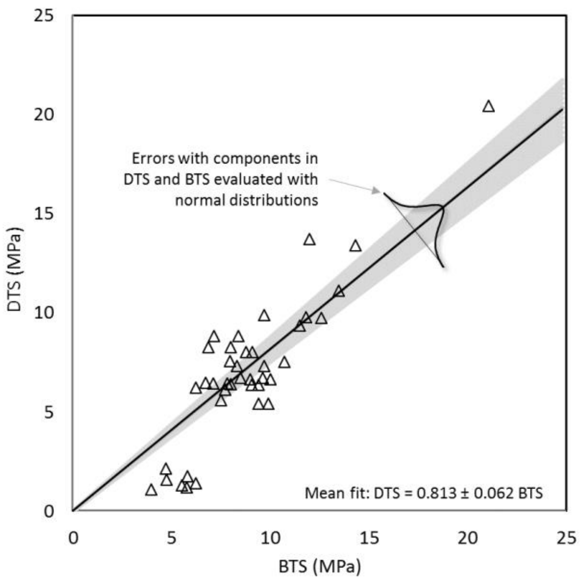

Figure 4.21 Correlation between DTS and BTS for igneous rocks (data from Perras and Diederichs, 2014). Normal distributions orthogonal to the fitted line are used to evaluate the errors with components in DTS and BTS. The mean fit corresponds to α =0.81 with a 95% HDI=±0.06, but this variability is linked to that of m_i as indicated in the scatter plot of Figure 4.20

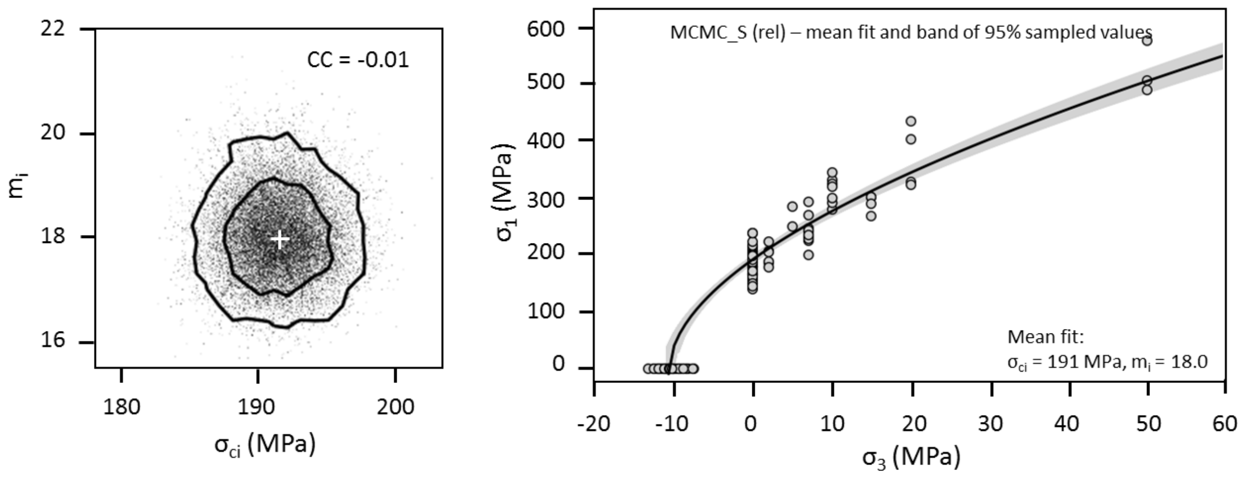

Figure 4.22 Uncertainty quantification of the Hoek-Brown intact rock strength envelope with the Bayesian approach, including the uncertainty in the correlation between BTS and DTS (model based on relative residuals with t-distribution). Scatter plot of sampled values of m_i versus σ_{ci} with 68 and 95 percentile contours (left). Fitted envelope and the band of envelopes corresponding to the 95% of sampled parameter values (right)

4.6 Summary and conclusions

Uncertainty is a common occurrence in geotechnical design with two types of uncertainty being normally identified. Aleatory uncertainty is associated with the natural variation of parameters, and epistemic uncertainty is related to the lack of knowledge on parameters and models. Epistemic uncertainty can be reduced with the collection of more information but aleatory uncertainty is irreducible.

Probabilistic methods are commonly used to represent and quantify uncertainty in geotechnical design. There are two approaches of statistical analysis based on two interpretations of probability. The frequentist approach considers probability as a frequency of outcomes in repeated trials, and treats data as a random entity and parameters or models as fixed quantities. In contrast, probability in the Bayesian approach is interpreted as degrees of belief, and considers data as fixed whereas parameters are random entities. The frequentist approach is generally used in geotechnical design to quantify uncertainty; however, the methods of analysis have limitations and the results are often misinterpreted. Frequentist methods rely only on sampling and produce point estimates and error measures. The Bayesian approach provides a better framework within which to quantify uncertainty in geotechnical design. The approach combines prior knowledge with data using Bayes' rule to define posterior probability distributions of inferred parameters. The result of Bayesian analysis is richer than the frequentist result, providing information on parameter correlations and offering a clearer quantification of the uncertainty of parameters.

The Bayesian approach was applied to the case of the Hoek-Brown intact rock strength estimation using results of compressive and tensile strength tests. The Bayesian model was used to estimate the parameters σ_{ci} and m_i with different variants of the model, including the use of absolute and relative residuals and the use of normal and t-distributions to evaluate the errors. The results of the Bayesian analysis were compared with those obtained for equivalent conditions using a frequentist approach represented by the NLLS method. The analysis of a data set including outliers highlighted the effectiveness of the t distribution to model the errors resulting in a true robust estimation. The difference in the order of magnitude of the errors in the tensile and compressive regions has an effect on the results of the analysis using absolute residuals. In this case, the larger error in the compressive region prevails and causes a larger uncertainty in the tensile strength. The use of relative residuals equates the order of magnitude of errors in the tensile and compressive regions, diminishes the effect of the outliers and reduces the uncertainty of the mean fit. The fitted envelopes obtained using the Bayesian and frequentist methods are effectively equivalent when the analysis is based on relative residuals. The relative effectiveness of the Bayesian models was evaluated using the Bayes factor. The conclusion from this analysis is that the model based on the t-distribution with relative residuals is the preferred fitting method since it provides superior handling of potential outliers in the test results.

A second example with a real data set for a homogeneous granite from Sweden was used to highlight the differences in the evaluation of the uncertainty with the two approaches. The limitations of CIs and PIs to quantify the uncertainty of the fitted envelope in the frequentist approach are contrasted with the richness of the evaluation with the scatter plots and band of envelopes in the Bayesian approach. The CI is related to the uncertainty of the mean fit but implies repeated systematic sampling for the confidence level to be meaningful. The PI is associated with the uncertainty of data points in future observations. The scatter plots and band of envelopes from the Bayesian analysis measure the uncertainty of the fitted envelope (and of the parameters σ_{ci} and m_i) based on the observed data. Future observations will be used to update the results of the analysis, but are not required to give a meaning to the present results. Finally, the strength of the Bayesian method to evaluate variations to the regression analysis was demonstrated by two analyses incorporating new features. The first is the addition of the Hoek-Brown parameter, *a*, to the inference analysis to improve the fitting in the triaxial region. The second is the consideration of the uncertainty in the factor used to convert BTS data to DTS results, by incorporating this regression analysis into the posterior function used in fitting the intact rock strength parameters.

Conflict of interest

The authors wish to confirm that there are no known conflicts of interest associated with this publication and there has been no significant financial support for this work that could have influenced its outcome.

Acknowledgements

The first author is supported by the Large Open Pit II Project through contract No. 019799 with the Geotechnical Research Centre of The University of Queensland and by SRK Consulting South Africa. Their support is greatly appreciated. We wish to thank the anonymous reviewers for their suggestions and comments made to improve the paper.

Appendix A – Mathematical formulation of posterior distributions

Tables A1 to A4 summarize the equations used for the definition of the posterior distribution for the regression analysis of intact rock strength data with the Bayesian approach. Each table corresponds to a particular set of conditions of analysis. The mathematical formulation for the cases of relative residuals with a t-distribution and absolute residuals with a normal distribution can be easily deduced from the equations presented in Tables A1 and A2.

Table A1 Equations used to define the posterior distribution for regression analysis with absolute residuals and t-distribution

Bayesian component	Equations
Prior	$p(\sigma_{ci}) = \dfrac{1}{(\sigma_{ci\ upper} - \sigma_{ci\ lower})}$ $p(m_i) = \dfrac{1}{(m_{i\ upper} - m_{i\ lower})}$ $p(\sigma) = \dfrac{1}{(100\ \mathrm{stdev}(\sigma_{1\ data}) - 0.01\ \mathrm{stdev}(\sigma_{1\ data}))}$ $p(\nu) = \dfrac{1}{29} e^{-\frac{1}{29}(\nu-1)}$ $p(\sigma_{ci}, m_i, \sigma, \nu) = p(\sigma_{ci})\ p(m_i)\ p(\sigma)\ p(\nu)$
Likelihood	If $\sigma_{3\ data} > 0$: $\sigma_{1\ model} = \sigma_{3\ data} + \sigma_{ci}\left(m_i \dfrac{\sigma_{3\ data}}{\sigma_{ci}} + 1\right)^{0.5}$ $\mathrm{error} = \sigma_{1\ data} - \sigma_{1\ model}$ If $\sigma_{3\ data} < 0$: $\sigma_{3\ model} = \dfrac{\sigma_{ci}}{2}\left(m_i - \sqrt{m_i^2 + 4}\right)$ $\mathrm{error} = \sigma_{3\ data} - \sigma_{3\ model}$ $p(\mathrm{data}\mid\sigma_{ci}, m_i, \sigma, \nu) = \prod_{j=1}^{n} \dfrac{\Gamma\left(\frac{\nu+1}{2}\right)}{\Gamma\left(\frac{\nu}{2}\right)\sqrt{\pi\nu}\sigma}\left(1 + \dfrac{1}{\nu}\left(\dfrac{\mathrm{error}_j}{\sigma}\right)^2\right)^{-\frac{(\nu+1)}{2}}$
Posterior (un-normalized)	$p(\sigma_{ci}, m_i, \sigma, \nu\mid\mathrm{data}) = p(\mathrm{data}\mid\sigma_{ci}, m_i, \sigma, \nu)\ p(\sigma_{ci}, m_i, \sigma, \nu)$

Table A2 Equations used to define the posterior distribution for regression analysis with relative residuals and normal distribution

Bayesian component	Equations
Prior	$p(\sigma_{ci}) = \dfrac{1}{(\sigma_{ci\ upper} - \sigma_{ci\ lower})}$ $p(m_i) = \dfrac{1}{(m_{i\ upper} - m_{i\ lower})}$ $p(\sigma) = \dfrac{1}{\left(100\dfrac{stdev(\sigma_{1\ data})}{mean(\sigma_{1\ data})} - 0.01\dfrac{stdev(\sigma_{1\ data})}{mean(\sigma_{1\ data})}\right)}$ $p(\sigma_{ci}, m_i, \sigma) = p(\sigma_{ci})\ p(m_i)\ p(\sigma)$
Likelihood	If $\sigma_{3\ data} > 0$: $\sigma_{1\ model} = \sigma_{3\ data} + \sigma_{ci}\left(m_i \dfrac{\sigma_{3\ data}}{\sigma_{ci}} + 1\right)^{0.5}$ $error = \dfrac{(\sigma_{1\ data} - \sigma_{1\ model})}{\sigma_{1\ model}}$ If $\sigma_{3\ data} < 0$: $\sigma_{3\ model} = \dfrac{\sigma_{ci}}{2}\left(m_i - \sqrt{m_i^2 + 4}\right)$ $error = \dfrac{(\sigma_{3\ data} - \sigma_{3\ model})}{\sigma_{3\ model}}$ $p(data\|\sigma_{ci}, m_i, \sigma) = \prod_{j=1}^{n} \dfrac{1}{\sqrt{2\sigma^2\pi}} e^{-\frac{1}{2}\left(\frac{error_j}{\sigma}\right)^2}$
Posterior (un-normalized)	$p(\sigma_{ci}, m_i, \sigma\|data) = p(data\|\sigma_{ci}, m_i, \sigma)\ p(\sigma_{ci}, m_i, \sigma)$

Table A3 Equations used to define the posterior distribution for regression analysis with relative residuals, t-distribution and Hoek-Brown parameter, *a*, as an uncertain variable

Bayesian component	**Equations**
Prior	$p(\sigma_{ci}) = \dfrac{1}{(\sigma_{ci\ upper} - \sigma_{ci\ lower})}$ $p(m_i) = \dfrac{1}{(m_{i\ upper} - m_{i\ lower})}$ $p(a) = \dfrac{1}{(a_{\ upper} - a_{\ lower})}$ $p(\sigma) = \dfrac{1}{\left(100\dfrac{stdev(\sigma_{1\ data})}{mean(\sigma_{1\ data})} - 0.01\dfrac{stdev(\sigma_{1\ data})}{mean(\sigma_{1\ data})}\right)}$ $p(\nu) = \dfrac{1}{29}e^{-\frac{1}{29}(\nu-1)}$ $p(\sigma_{ci}, m_i, a, \sigma, \nu) = p(\sigma_{ci})\ p(m_i)\ p(a)\ p(\sigma)p(\nu)$
Likelihood	If a = 0.5: $\sigma_t = \dfrac{\sigma_{ci}}{2}\left(m_i - \sqrt{m_i^2 + 4}\right)$ If a ≠ 0.5: Find σ_t from: $0 = \sigma_t + \sigma_{ci}\left(m_i\frac{\sigma_t}{\sigma_{ci}} + 1\right)^a$ If $\sigma_{3\ data}$ > 0: $\sigma_{1\ model} = \sigma_{3\ data} + \sigma_{ci}(m_i\dfrac{\sigma_{3\ data}}{\sigma_{ci}} + 1)^a$ $error = \dfrac{(\sigma_{1\ data} - \sigma_{1\ model})}{\sigma_{1\ model}}$ If $\sigma_{3\ data}$ < 0: $\sigma_{3\ model} = \sigma_t$ $error = \dfrac{(\sigma_{3\ data} - \sigma_{3\ model})}{\sigma_{3\ model}}$ $p(data\|\sigma_{ci}, m_i, a, \sigma, \nu) = \prod_{j=1}^{n}\dfrac{\Gamma\left(\frac{\nu+1}{2}\right)}{\Gamma\left(\frac{\nu}{2}\right)\sqrt{\pi\nu}\sigma}\left(1 + \dfrac{1}{\nu}\left(\dfrac{error_j}{\sigma}\right)^2\right)^{-\frac{(\nu+1)}{2}}$
Posterior (un-normalized)	$p(\sigma_{ci}, m_i, a, \sigma, \nu\|data) = p(data\|\sigma_{ci}, m_i, a, \sigma, \nu)\ p(\sigma_{ci}, m_i, a, \sigma, \nu)$

Table A4 Equations used to define the posterior distribution for regression analysis with relative residuals, t-distribution and including the uncertainty in the correlation between BTS and DTS

Bayesian component	**Equations**
Prior	$p(\sigma_{ci}) = \dfrac{1}{(\sigma_{ci\ upper} - \sigma_{ci\ lower})}$ $p(m_i) = \dfrac{1}{(m_{i\ upper} - m_{i\ lower})}$ $p(\sigma) = \dfrac{1}{\left(100\dfrac{stdev(\sigma_{1\ data})}{mean(\sigma_{1\ data})} - 0.01\dfrac{stdev(\sigma_{1\ data})}{mean(\sigma_{1\ data})}\right)}$ $p(\nu) = \dfrac{1}{29}e^{-\frac{1}{29}(\nu-1)}$ $p(\alpha_{rad}) = \dfrac{1}{(\alpha_{rad\ upper} - \alpha_{rad\ lower})}$ $SDT = \sqrt{stdev(DTS_{data})^2 + stdev(BTS_{data})^2}$ $p(\sigma_{\alpha}) = \dfrac{1}{(100\ SDT - 0.01SDT)}$ $p(\sigma_{ci}, m_i, \sigma, \nu, \alpha_{rad}, \sigma_{\alpha}) = p(\sigma_{ci})\ p(m_i)\ p(\sigma)\ p(\nu)\ p(\alpha_{rad})\ p(\sigma_{\alpha})$

Table A4 (Continued)

Bayesian component	**Equations**
Likelihood	Hoek-Brown criterion: If $\sigma_{3\ data} > 0$: $\sigma_{1\ model} = \sigma_{3\ data} + \sigma_{ci}\left(m_i \frac{\sigma_{3\ data}}{\sigma_{ci}} + 1\right)^{0.5}$ $error = \frac{(\sigma_{1\ data} - \sigma_{1\ model})}{\sigma_{1\ model}}$ If $\sigma_{3\ data} < 0$: $\sigma_{3\ model} = \frac{\sigma_{ci}}{2}\left(m_i - \sqrt{m_i^2 + 4}\right)$ $error = \frac{(\alpha\ \sigma_{3\ data} - \sigma_{3\ model})}{\sigma_{3\ model}}$ DTS versus BTS correlation: $\alpha = \mathrm{Tan}(\alpha_{rad})$ $error_{DTS\_BTS} = \mathrm{Sin}(\alpha_{rad})(\frac{DTS_{data}}{\alpha} - BTS_{data})$ $p(data\|\sigma_{ci}, m_i, \sigma, \nu, \alpha_{rad}, \sigma_\alpha) =$ $\prod_{j=1}^{n} \frac{\Gamma\left(\frac{\nu+1}{2}\right)}{\Gamma\left(\frac{\nu}{2}\right)\sqrt{\pi\nu}\sigma}\left(1 + \frac{1}{\nu}\left(\frac{error_j}{\sigma}\right)^2\right)^{-\frac{(\nu+1)}{2}} \prod_{k=1}^{m} \frac{1}{\sqrt{2{\sigma_\alpha}^2\pi}} e^{-\frac{1}{2}\left(\frac{error_{DTS\_BTS\ j}}{\sigma_\alpha}\right)^2}$
Posterior (un-normalized)	$p(\sigma_{ci}, m_i, \sigma, \nu, \alpha_{rad}, \sigma_\alpha\|data) = p(data\|\sigma_{ci}, m_i, \sigma, \nu, \alpha_{rad}, \sigma_\alpha)\ p(\sigma_{ci}, m_i, \sigma, \nu, \alpha_{rad}, \sigma_\alpha)$

Notations

σ_{ci}, m_i, a Parameters of the Hoek-Brown intact rock strength criterion

σ Standard deviation of normal distribution or scale parameter of t-distribution used to evaluate errors in the Hoek-Brown intact rock strength fitting

v Normality parameter of t-distribution used to evaluate errors in the Hoek-Brown intact rock strength fitting

σ_1, σ_3 Major and minor principal stresses

σ_t Tensile strength in the Hoek-Brown strength envelope

DTS, BTS Direct tensile strength and Brazilian tensile strength

n Number of data points for Hoek-Brown intact rock strength fitting

m Number of data points for DTS versus BTS fitting

α_{rad} Slope of DTS versus BTS fitted line in radians

α Slope of DTS versus BTS fitted line

σ_α Standard deviation of normal distribution used to evaluate errors in the DTS versus BTS fitting

$\Gamma()$ Gamma function

References

Baecher, G.B. and Christian, J.T., 2003. *Reliability and statistics in geotechnical engineering.* Wiley, Chichester, UK.

Bayes, T., 1763. An essay towards solving a problem in the doctrine of chance. *Philosophical Transactions*, Royal Society of London, 53, 370–418.

Bewick, R.P., Amann, F., Kaiser, P.K. and Martin, C.D., 2015. Interpretation of the UCS test for engineering design. *Proceedings of the 13th International Congress on Rock Mechanics: ISRM Congress 2015 – Advances in Applied & Theoretical Rock Mechanics*, Montréal, Canada. International Society for Rock Mechanics and Rock Engineering, Paper 521.

Bozorgzadeh, N. and Harrison, J.P., 2014. Characterizing uniaxial compressive strength using Bayesian updating. *Proceedings 48th US Rock Mechanics/Geomechanics Symposium*, Minneapolis, 1-4 June, Paper ARMA 14-7194, 7 p.

Brown, E.T., 2012. Risk assessment and management in underground rock engineering – An overview. *Journal of Rock Mechanics and Geotechnical Engineering,* 4(3), 193–204.

Christian, J.T., 2004. Geotechnical Engineering Reliability: How Well Do We Know What We Are Doing? *Journal of Geotechnical and Geoenvironmental Engineering*, 130(10), 985–1003.

Contreras, L.F. and Ruest, M., 2016. Unconventional methods to treat geotechnical uncertainty in slope design. In P. Dight (editor). *Proceedings of the First Asia- Pacific Slope Stability in Mining Conference*, Brisbane, Australia. Australian Centre for Geomechanics, Perth, 315–330.

Diaconis, P., 2009. The Markov Chain Monte Carlo Revolution. *Bulleting of the American Mathematical Society*, 46(2), 179–205.

Feng, X. and Jimenez, R., 2015. Estimation of deformation modulus of rock masses based on Bayesian model selection and Bayesian updating approach. *Engineering Geology,* 199, 19–27.

Foreman-Mackey, D., Hogg, D.W., Lang, D. and Goodman, J., 2013. emcee: The MCMC Hammer. *Publications of the Astronomical Society of Pacific*, 125(925), 306–312.

Gelman, A., Carlin, J.B., Stern, H.S., Dunson, D.B., Vehtari, A. and Rubin, D.B., 2013. *Bayesian Data Analysis*. Chapman and Hall, CRC Press.

Goh, A.T.C. and Zhang, W., 2012. Reliability assessment of stability of underground rock caverns. *International Journal of Rock Mechanics and Mining Sciences*, 55, 157–163.

Gregory, P., 2005. *Bayesian Logical Data Analysis for the Physical Sciences.* Cambridge; New York: Cambridge University Press.

Hoek, E. and Brown, E.T., 1997. Practical Estimates of Rock Mass Strength. *International Journal of Rock Mechanics and Mining Sciences*, 34(8), 1165–1186.

Hogg, D.W., Bovy, J. and Lang, D., 2010. Data analysis recipes: Fitting a model to data. In: *arXiv:1008.4686*. https://arxiv.org/pdf/1008.4686v1.pdf.

Hyndman, R.J., 2013. The difference between prediction intervals and confidence intervals. Hyndsight Blog [on line]. [Accessed on 20/01/2016]. http://robjhyndman.com/hyndsight/intervals/.

Jacobsson, L., 2004. Oskarshamn site investigation. Reports P-04-255, 256, 261, 262 and 263. *Swedish Nuclear and Fuel Waste Management Company (SKB)*. http://robjhyndman.com/hyndsight/intervals/.

Jacobsson, L., 2005. Oskarshamn site investigation. Reports P-05-90, 91, 96, and 128. *Swedish Nuclear and Fuel Waste Management Company (SKB)*. http://robjhyndman.com/hyndsight/intervals/.

Jacobsson, L., 2006. Oskarshamn site investigation. Reports P-06-37, 40, and 73. *Swedish Nuclear and Fuel Waste Management Company (SKB)*. http://robjhyndman.com/hyndsight/intervals/.

Jacobsson L., 2007. Oskarshamn site investigation. Reports P-07-140 and 217. *Swedish Nuclear and Fuel Waste Management Company (SKB)*. http://robjhyndman.com/hyndsight/intervals/.

Jaynes, E.T., 1957. Information theory and statistical mechanics. *The Physical Review*; 106(4), 620–630.

Kaiser, P.K., Amann, F. and Bewick, R.P., 2015. Overcoming challenges of rock mass characterization for underground construction in deep mines. *Proceedings of the 13th International Congress on Rock Mechanics: ISRM Congress 2015 – Advances in Applied & Theoretical Rock Mechanics*, Montréal, Canada. International Society for Rock Mechanics and Rock Engineering, Paper 241.

Kass, R.E. and Raftery, A.E., 1995. Bayes factors. *Journal of the American Statistical Association*; 90(430), 773–795.

Kruschke, J.K., 2015. *Doing Bayesian Data Analysis: A Tutorial with R, JAGS and STAN*, Academic Press/Elsevier.

Langford, J.C. and Diederichs, M.S., 2013. Evaluating uncertainty in intact and rockmass parameters for the purposes of reliability assessment. *Proceedings 47th US Rock Mechanics/Geomechanics Symposium*, San Francisco, 23-26 June, Paper ARMA 13-459, 9 p.

Langford, J.C. and Diederichs, M.S., 2015. Quantifying uncertainty in Hoek-Brown intact strength envelopes. *International Journal of Rock Mechanics and Mining Sciences*, 74, 91–102.

Low, B.K. and Tang, W.H., 2007. Efficient spreadsheet algorithm for first-order reliability method. *Journal of Engineering Mechanics*; 133(12), 1378–1387.

Low, B.K., 2014. FORM, SORM, and spatial modeling in geotechnical engineering. *Structural Safety,* 49, 56–64.

Liu, H. and Low, B.K., 2017. System reliability analysis of tunnels reinforced by rockbolts. *Tunnelling and Underground Space Technology*; 65, 155–166.

Lü, Q. and Low, B.K., 2011. Probabilistic analysis of underground rock excavations using response surface method and SORM. *Computers and Geotechnics*; 38(8), 1008–1021.

Miranda, T., Correia, A.G. and Sousa, L. R., 2009. Bayesian methodology for updating geomechanical parameters and uncertainty quantification. *International Journal of Rock Mechanics and Mining Sciences*; 46(7), 1144–1153.

Perras, M.A. and Diederichs, M.S., 2014. A Review of the Tensile Strength of Rocks: Concepts and Testing. *Geotechnical and Geological Engineering*, 32(2), 525–546.

Python Software Foundation, 2001. *Python language reference*, version 3.4 [on line]. [Accessed 20/01/2015]. https://www.python.org/.

Robert, C.P. and Casella, G., 2004. *Monte Carlo Statistical Methods*. 2nd ed. Springer, New York.

Robert, C.P. and Casella, G., 2011. A Short History of Markov Chain Monte Carlo: Subjective Recollections from Incomplete Data. *Statistical Science*, 26(1), 102–115.

Sivia, D. and Skilling, J., 2006. *Data analysis – a Bayesian tutorial*. Oxford: Oxford University Press.

Smith, B.J., 2014. *Mamba: Markov chain Monte Carlo (MCMC) for Bayesian analysis in Julia* [on line]. [Accessed 08/06/2016]. https://github.com/brian-j-smith/Mamba.jl.

Stone, J.V., 2013. *Bayes' Rule: A Tutorial Introduction to Bayesian Analysis*, Sebtel Press.

VanderPlas, J., 2014. *Frequentism and Bayesianism: A Practical Introduction*. In Phytonic Preambulations Blog [on line]. [Accessed 20/01/2015]. https://jakevdp.github.io/blog/2014/03/11/frequentism-and-bayesianism-a-practical-intro/.

Vincent, D.B.T., 2014. *Software for MCMC.* In inference Lab blog [on line] [Accessed 08/06/2016]. http://www.inferencelab.com/mcmc_software/.

Wang, Y., Cao, Z. and Li, D., 2016. Bayesian perspective on geotechnical variability and site characterization. *Engineering Geology*, 203, 117-125.

Zhang, W. and Goh, A., 2012. Reliability assessment on ultimate and serviceability limit states and determination of critical factor of safety for underground rock caverns. *Tunnelling and Underground Space Technology*; 32, 221–230.

Zhang, J., Tang, W.H., Zhang, L.M. and Huang, H.W., 2012. Characterising geotechnical model uncertainty by hybrid Markov chain Monte Carlo simulation. *Computers and Geotechnics*, 43, 26–36.

Zhang, J., Zhang, L.M. and Tang, W.H., 2009. Bayesian framework for characterizing geotechnical model uncertainty. *Journal of Geotechnical and Geoenvironmental Engineering ASCE,* 135(7), 932–940.

Chapter 5 - Bayesian Inference of Geotechnical Parameters for Slope Reliability Analysis

Luis-Fernando Contreras[a], *Edwin T. Brown*[b]

[a] The University of Queensland, Brisbane, Australia.

[b] Golder Associates Pty. Ltd, Brisbane, Australia.

Corresponding author: luis.contreras@uq.net.au

Abstract

Probabilistic methods are traditionally used to account for the uncertainty in engineering design. However, conventional probabilistic methods have limitations when representing uncertainty. There is an alternative approach, based on Bayesian statistical methods, that has advantages in treating uncertainty in the geotechnical model for slope design. Probabilistic data analysis using the Bayesian approach involves numerical procedures for estimating parameters from posterior probability distributions. These distributions are the result of combining prior information with available data through Bayes equation. The posterior distributions are often complex, multidimensional functions whose analysis requires the use of Markov Chain Monte Carlo (MCMC) methods. These methods are used to draw representative samples of the parameters investigated, providing information on their best estimate values, variability and correlations. The paper describes a methodology in which typical data from laboratory tests and site investigations are used to define representative distributions of the geotechnical parameters and the use of these results for the evaluation of the reliability of a slope. The first-order reliability method (FORM) is a common technique used for reliability analyses of geotechnical structures such as slopes and tunnels. The FORM typically considers predefined probability distributions to represent the variability of uncertain parameters and a limit state surface (LSS) defining the condition of failure of the structure. The LSS is derived from a performance function that may be available in explicit form, or alternatively, could be approximated with a response surface (RS) for complex models. The paper presents an example of a slope evaluated with an RS based on limit equilibrium analyses with the slope model. The example is used to highlight

the advantages of using the posterior distributions from the Bayesian analysis for the assessment of the slope reliability using the FORM approach.

Keywords: Bayesian analysis; Hoek-Brown criterion; response surface method, slope reliability

5.1 Introduction

It is generally accepted that probabilistic methods are the best way to represent uncertainty in engineering design. However, there are two approaches of analysis known as frequentist and Bayesian, which are based on different interpretations of probability. The frequentist approach relies on repeated sampling to produce point estimates and error measures of parameters. In comparison, the Bayesian approach uses prior knowledge and data to define posterior probability distributions to represent the uncertainty of parameters. Contreras et al (2018) discuss the contrast between the two approaches in terms of the inference of parameters. They argue that Bayesian methods provide a better framework for the quantification of uncertainty in slope design. The Bayesian analysis of data involves numerical procedures for estimating parameters from posterior probability distributions. The posterior distributions are often complex, multidimensional functions whose analysis requires the use of a class of methods called Markov Chain Monte Carlo (MCMC). These methods are used to draw representative samples of the parameters investigated, providing information on their best estimate values, variability and correlations.

The paper presents an example of the characterisation of rock mass strength using a Bayesian approach to data analysis and the use of these results for the evaluation of the reliability of a slope. The methodology uses the results of laboratory and site investigations for the inference of the rock strength parameters normally used in slope design. The results of the analysis consist of representative samples of the more probable values of the parameters, informing their variability and correlation characteristics. The samples define to the so-called posterior probability distributions within the Bayesian framework and correspond to a balanced result between the data used and the prior information available on the parameters. Contreras et al (2018) describe in detail the methodology with reference to the inference of the intact rock strength parameters. Other examples of Bayesian analysis in rock mechanics are given by Miranda et al. (2009), Zhang et al. (2010), Feng and Jimenez (2015) and, Wang and Aladejare (2015).

The emphasis of the present paper is on the use of the results of a Bayesian analysis of rock strength parameters for the evaluation of the reliability of slopes. There are two main approaches for the evaluation of the reliability of slopes. One is based on the variability of the factor of safety (FS) and the second is based on the variability of the uncertain parameters in the slope model. The second approach, known as first order reliability method (FORM), is a technique suitable for the use with the posterior distributions of parameters from a Bayesian analysis. The FORM typically considers predefined probability distributions to represent the variability of uncertain parameters (Low and Tang, 1997, 2004) and a limit state surface (LSS) defining the condition of failure of the structure. The LSS is derived from a performance function that may be available in explicit form, or alternatively, could be approximated with a response surface (RS) for complex models. The slope example presented in this paper considers an RS constructed with a slope model based on limit equilibrium analyses. The RS is used for direct calculation of the slope reliability from the variability of FS and for the definition of the LSS with the FORM. Different conditions of analysis are arranged in six procedures used to discuss different aspects of the analysis, highlighting their advantages and limitations. The procedures are the result of combining the two main approaches of reliability analysis with various options of representing the input parameters, i.e. beta distributions fitted to the posteriors, or Monte Carlo (MC) samples from the fitted distributions or the posterior samples from the Bayesian analysis.

5.2 Bayesian inference of geotechnical parameters

The characterisation of rock mass strength for slope design is commonly based on the Hoek-Brown (H-B) strength criterion, whose definition requires four parameters as illustrated in the diagram of Figure 5.1. The process includes the assessment of the intact rock strength, the rock mass quality and the disturbance factor. Sometimes it is convenient to use equivalent Mohr-Coulomb (M-C) parameters for particular stress levels. The estimation of parameters is based on data collected with site or laboratory investigations, which is fitted to models to obtain point estimate values and sometimes variability characteristics of these parameters. However, with the conventional approach, most of the information on parameter uncertainty is lost or crudely represented. The Bayesian approach provides an adequate method to capture the uncertainty of parameters, balancing data and knowledge in all the component sub-models.

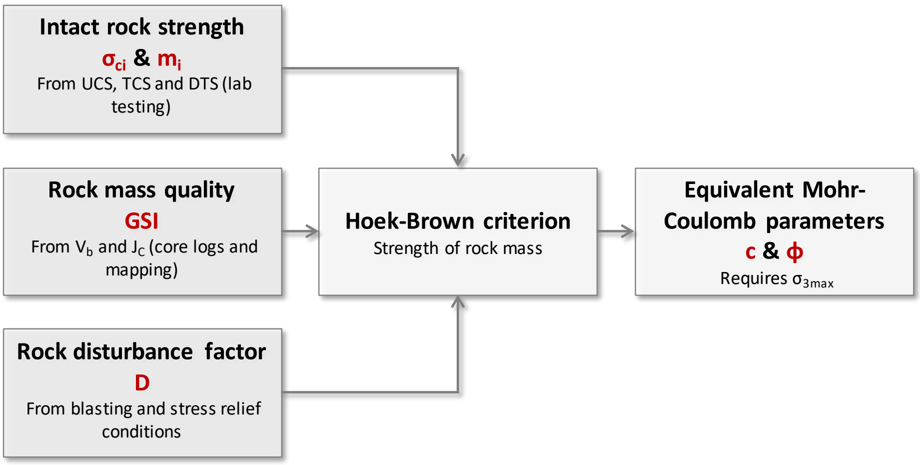

Figure 5.1 Characterisation of rock mass strength for slope design

There are several recent examples of the application of Bayesian analysis in rock mechanics and slope problems. Miranda et al. (2009) use a Bayesian approach to update the deformability modulus in a large underground structure considering two cases of initial knowledge. Zhang et al. (2010) consider the back analysis of slope failures based on a Bayesian model solved with MCMC analysis. Feng and Jimenez (2015) describe the estimation of the rock mass deformation modulus based on model comparison and Bayesian updating. Wang and Aladejare (2015) study the characterisation of the UCS from site-specific data on Point Load Index using a Bayesian method to compare alternative models and select the most appropriate.

5.2.1 Concept of Bayesian inference of parameters

The concept of Bayesian inference of parameters is illustrated in the diagram of Figure 5.2 (Contreras et al, 2018). There are three elements required in this process. First, there is a model in the form of a mathematical function that represents the performance of a particular system of interest. The model function includes predictor variables, x, and the parameters for inference, θ. Secondly, there is data that normally corresponds to measurements of the actual performance of the system to compare with the model predictions. Thirdly, there is prior knowledge of the parameters; this means any type of information, for example, valid ranges of credible values. These three elements are used to construct a probabilistic function that contains the uncertain parameters for inference θ_1 to θ_k in the vector θ. This function effectively corresponds to a posterior probability distribution using Bayes' formula and gives probability values, p, for particular sets of uncertain parameters, θ. The objective of the analysis is to define the sets of θ that produce the largest p values, in other words, to define the more probable parameter values.

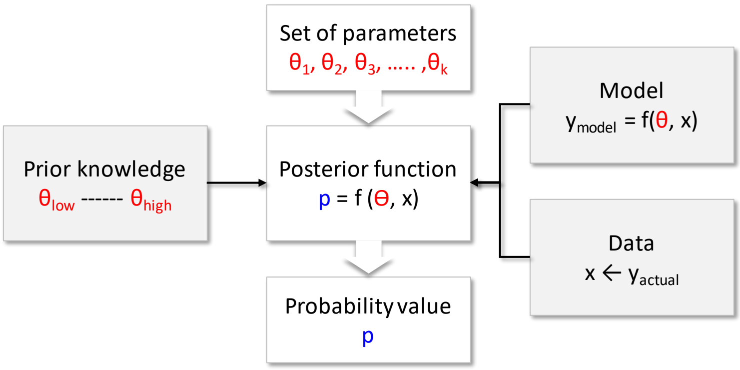

Figure 5.2 Conceptual representation of the Bayesian process for inference of parameters (Contreras et al, 2018)

The posterior distribution is a multidimensional and normally complicated function. The more efficient way of evaluating this function is by obtaining representative samples of the parameter values using the MCMC technique. The typical result of an MCMC analysis is a graph showing scatter plots of sampled values and histograms of the θ_i parameters. Contreras et al (2018) include the details on the formulation of the model for Bayesian inference of parameters, with reference to the case of intact rock strength characterisation. The Bayesian analyses presented in the present paper were implemented in the Python programming language, using the MCMC algorithm known as the affine-invariant ensemble sampler developed by Foreman-Mackey et al. (2013).

5.2.2 Intact rock strength parameters σ_{ci} and m_i

The intact rock strength is characterised with the generalised Hoek-Brown (H-B) strength criterion (Hoek and Brown, 1997) defined by the following equation:

$$\sigma_1 = \sigma_3 + \sigma_{ci}\left(m_i \frac{\sigma_3}{\sigma_{ci}} + 1\right)^a \tag{5.1}$$

where σ_{ci} is the uniaxial compressive strength of intact rock, m_i is a constant of the intact rock material, σ_1 and σ_3 are the major and minor principal stresses, respectively, and the index a takes a value of 0.5 for the rocks being considered here. Using this criterion, the intact tensile strength of the intact rock, σ_t, is given by:

$$\sigma_t = \frac{\sigma_{ci}}{2}\left(m_i - \sqrt{{m_i}^2 + 4}\right) \tag{5.2}$$

Eq. (5.1) and Eq. (5.2) correspond to the model function for the Bayesian analysis, with σ_{ci} and m_i the parameters for inference. The data corresponds to the results of triaxial (TCS) and uniaxial (UCS) compression strength tests, and estimates of direct tensile strength (DTS) made from Brazilian tensile strength (BTS) tests results. The prior information is provided with uniform distributions defining plausible ranges of variation of the parameters investigated, without constraining the estimation within those ranges. The ranges used for the example in this paper are 10 MPa to 500 MPa for σ_{ci} and 1 to 50 for m_i.

The posterior probability function uses Bayes' equation to combine the prior probability of parameters with the likelihood of data. The likelihood calculation uses the model function for the evaluation of errors. The differences between the predictions with the model function and actual data values define errors, which are evaluated with Student's t-distributions. In this way, small errors result in large probability values and vice versa. The t-distribution is similar to the normal distribution but has an additional parameter that controls the shape of the tails allowing a better handling of outliers. The posterior function takes a set of parameters as input and yields a probability value.

The methodology is illustrated using a typical intact rock strength data set of 31 points (8 UCS, 8 DTS and 15 TCS), that was generated using random numbers between pre-defined limits. The data set is assumed to correspond to an igneous rock. Figure 5.3 shows the data points and describes the way in which errors are evaluated with t-distributions in the Bayesian analysis. The estimation of DTS is normally based on indirect measurements with BTS tests. Perras and Diederichs (2014) found that the correlation between DTS and BTS is rock type dependent, and suggested correlation factors of α = DTS/BTS of 0.9 for metamorphic rocks, 0.8 for igneous rocks and 0.7 for sedimentary rocks.

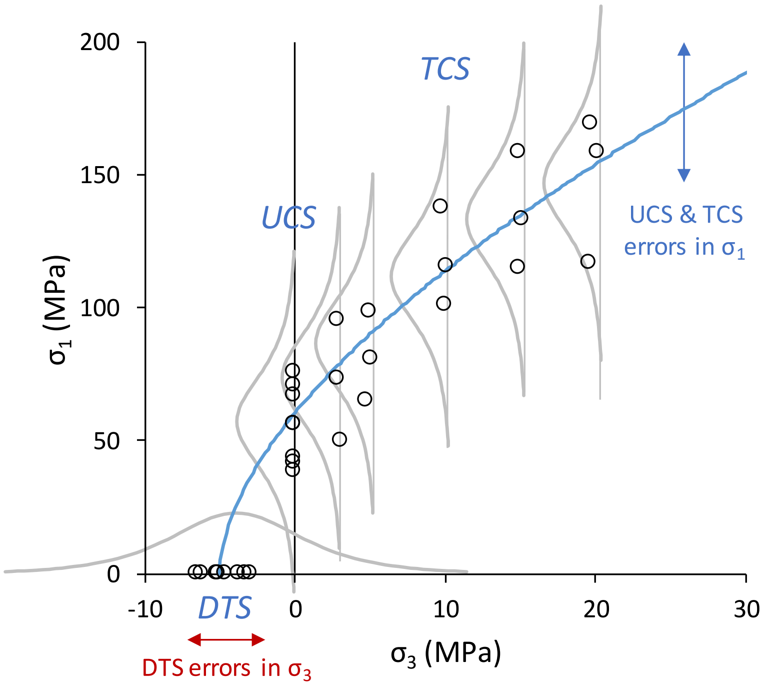

Figure 5.3 Measurement of errors in the tensile and compressive strength regions with a t-distribution to handle outliers (Contreras et al, 2018)

For the case of igneous rocks, α is based on a linear regression analysis of 40 pairs of BTS and DTS test results mainly on granite samples, as shown in Figure 5.4. The uncertainty of this correlation factor is not transferred to the fitting analysis of the strength envelope when the DTS values are calculated using a fixed value. The Bayesian model allows for the incorporation of this uncertainty, by using the data set of BTS versus DTS to define α within the posterior function. Therefore, during the sampling process, each trial value of α is used within the model to convert BTS data into DTS values required for the fitting analysis of the H-B envelope.

The example of Bayesian inference of intact rock strength parameters presented in this paper uses two data sets, one consisting of 31 σ_1 versus σ_3 values from BTS, UCS and TCS test results (Figure 5.3) and the second the 40 BTS versus DTS test results for igneous rocks (Figure 5.4). The analysis considers t-distributions to evaluate relative errors in the strength envelope and normal distributions to evaluate absolute errors in the BTS-DTS correlation. Contreras et al (2018) give the details of this analysis.

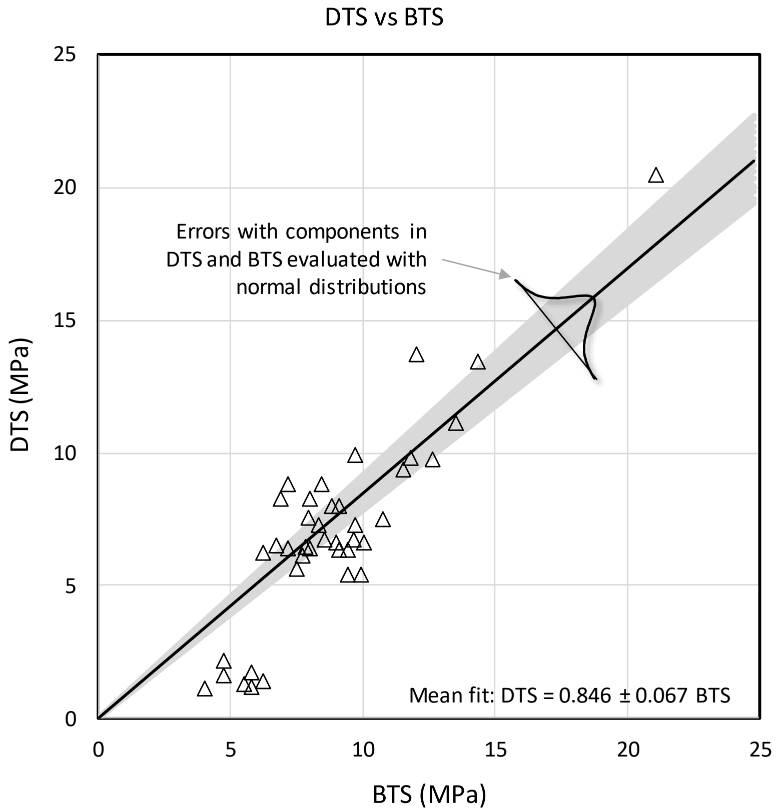

Figure 5.4 Correlation between DTS and BTS for igneous rocks (data from Perras and Diederichs, 2014). Normal distributions orthogonal to the fitted line are used to evaluate the errors with components in DTS and BTS. The mean fit corresponds to α = 0.85 with a 95%HDI = ±0.07, but this variability is linked to that of mi as indicated in the scatter plot of Figure 5.5

Figure 5.5 shows the corner plot with the results of the intact rock strength analysis including the uncertainty in the correlation between BTS and DTS. In general, the scatter plots show a low correlation between the inferred parameters. In terms of the variability of α, the analysis considers the possibility of errors in both DTS and BTS. Accordingly, errors are evaluated with the normal distributions in a direction orthogonal to the fitted lines (Figure 5.4). The plot in Figure 5.4 shows the band of fitted envelopes corresponding to the 95% highest density interval (HDI) of α values sampled. The uncertainty of α is transferred within the Bayesian model and added to the uncertainty of the fitted H-B strength envelope.

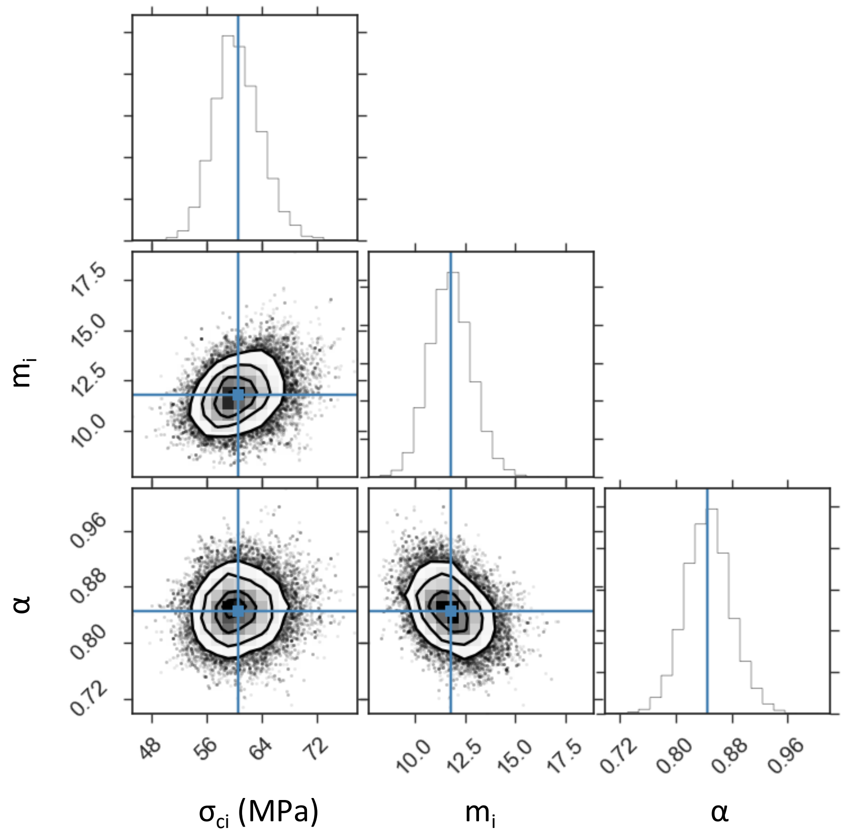

Figure 5.5 Corner plot from the analysis of the intact rock strength data including the uncertainty in the correlation between DTS and BTS. The plot shows the scatter plots and histograms of the rock mechanics parameters

Figure 5.6 shows more details of the histograms of sampled values of σ_{ci} and m_i from the posterior probability function. The histograms represent the posterior distributions of the inferred parameters. The 95% HDIs define the ranges of credible values and the mean values (σ_{ci} = 60.5 MPa, m_i = 11.8) represent the more likely estimates. Figure 5.7 shows the scatter plot of the 50,000 sampled values of σ_{ci} and m_i with the 68 and 95 percentile contours. The sampled values produce a spread of H-B envelopes around the mean fit as indicated in the graph of σ_1 versus σ_3 to the right of Figure 5.7. The plot includes the data points and the band of envelopes reflecting the uncertainty of parameters corresponds to the 95% HDI.

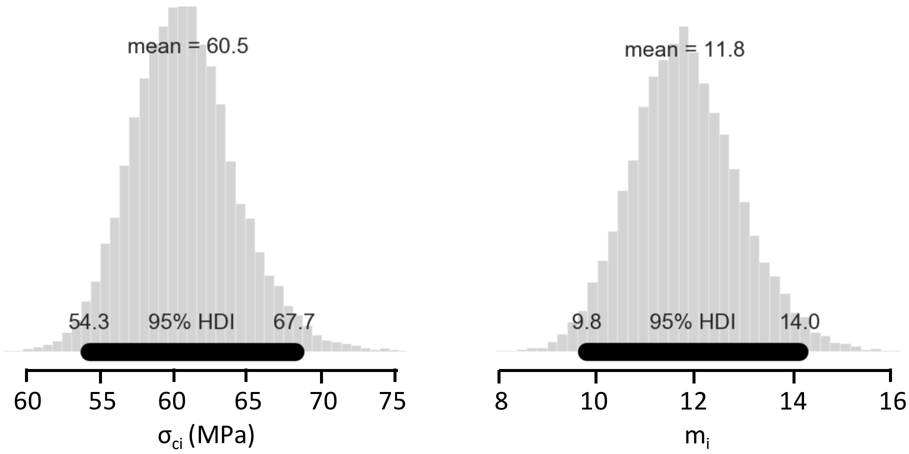

Figure 5.6 Posterior distributions of σ_{ci} and m_i with mean and 95% HDIs indicated

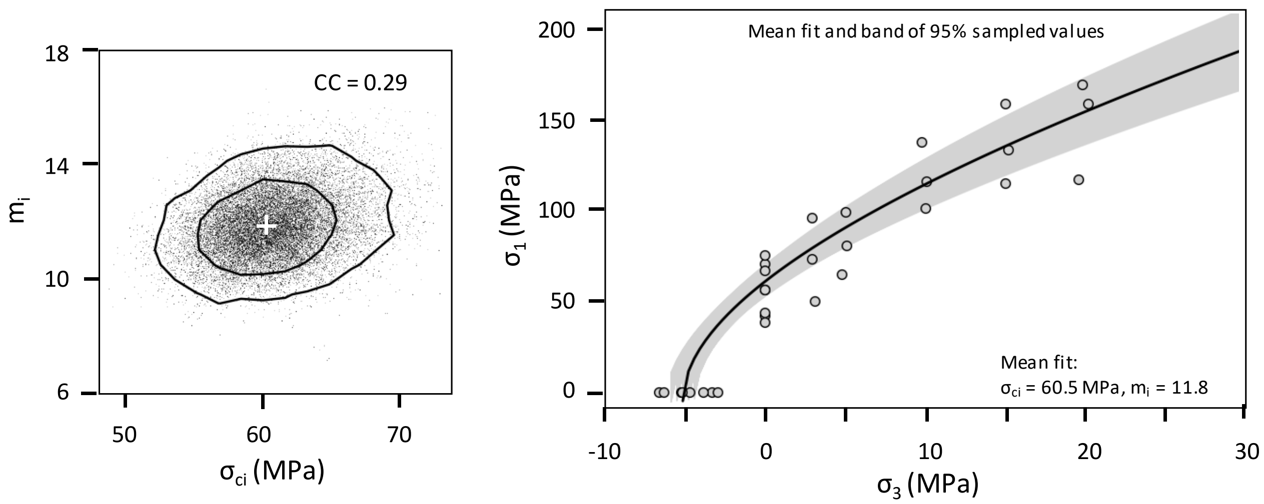

Figure 5.7 Scatter plot of sampled values of m_i versus σ_{ci} with 68 and 95 percentile contours (left) and mean fitted envelope with the band of envelopes corresponding to the 95 percentile of sampled parameter values

5.2.3 Geological strength index GSI

The GSI index carries the information on rock mass quality within the H-B failure criterion for rock masses. The index was originally linked to the 1976 version of Bieniawski's rock mass rating (RMR) index. However, Hoek and Brown (1997) redefined the index as an independent parameter with the chart shown in Figure 5.8. The chart includes qualitative descriptions of rock mass structure and joint conditions in the vertical and horizontal axis, respectively. This definition was intended to solve some drawbacks of deriving the *GSI* value from Bieniawski's *RMR*. First, the *RMR* included the intact rock strength and water conditions aspects, which are treated separately in the H-B criterion. Secondly, the ratings of the *RMR* components were continuously updated demanding adjustments to the GSI definition. For example, if *RMR* was based on the 1989 ratings, *GSI* was calculated as RMR_{89} minus 5 points.

The chart in Figure 5.8 is used to estimate credible ranges of *GSI* with a typical precision of ± 5 points; however, one drawback of this method is the strong subjective component in the estimation, which introduces an additional uncertainty due to the human factor. Several authors have proposed alternative charts for the quantitative estimation of *GSI* based on measured factors as a way of reducing the subjectivity of the estimation.

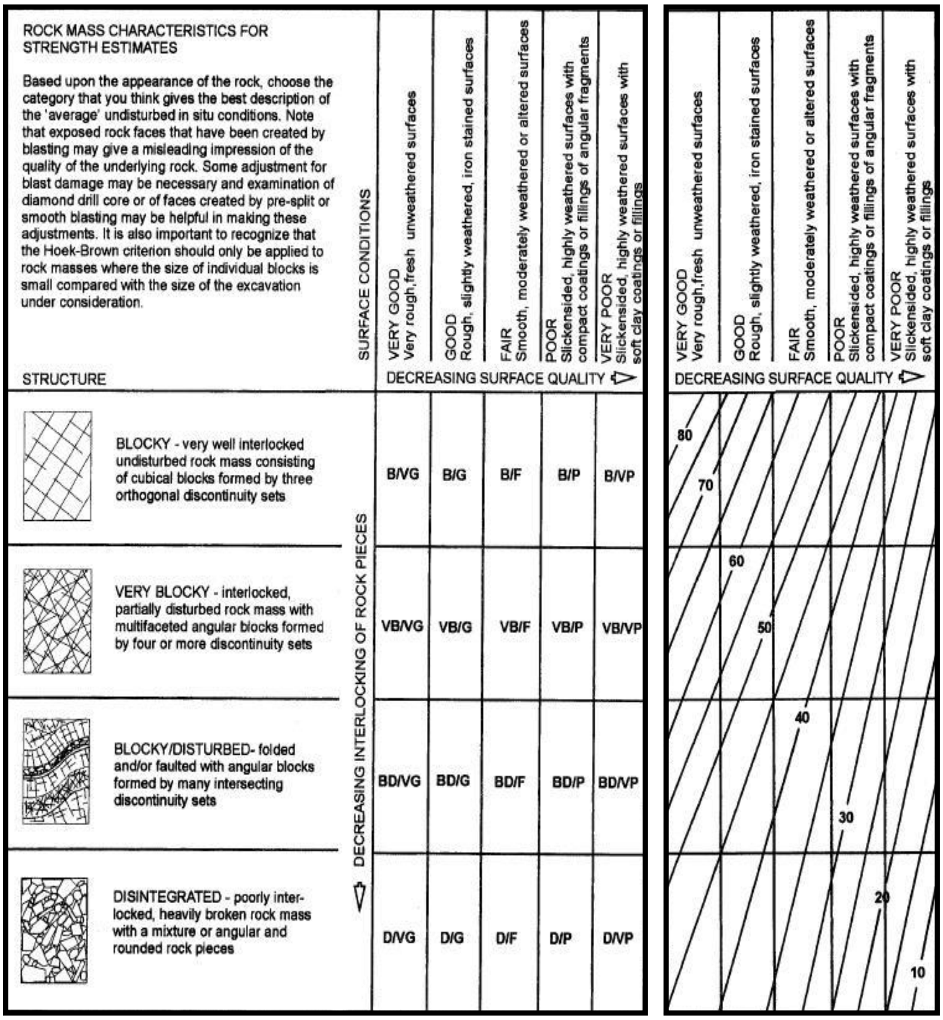

Figure 5.8 Charts with the original definition of GSI (Hoek and Brown, 1997, based on Hoek, 1994)

Sonmez and Ulusay (1999) propose a chart based on ad hoc structure and joint condition ratings for the vertical and horizontal scales, respectively. Cai et al. (2004) use the block volume (V_b) in the vertical axis to define structure and the joint condition factor (J_C) from Palmström (1996) in the horizontal axis. Russo (2009) proposes an alternative chart based on Palmström (1996) definitions of the block volume and joint condition factor for the vertical and horizontal axes, respectively. The most recent proposal by Hoek et al (2013) uses a chart based on *RQD*/2 as a measure of structure and the joint condition rating of the 1989 version of Bieniawski's *RMR* (Bieniawski, 1989) to assess surface conditions. However, none of the quantitative charts has gained general acceptance because they do not appear to fit the historical records in all situations. This is probably due to the fact that besides *GSI*, the H-B system includes the disturbance factor *D*, which is a second parameter with a strong subjective component. Each mine operation handles these parameters in different ways and uses them together to calibrate slope performance.

The Bayesian inference of *GSI* requires a model whose results can be compared with actual measurements through a probabilistic function. A comparative analysis of all the GSI calculation methods carried out by Duran (2016) indicates that the method of Cai et al (2014) appears to provide the best results. Cai et al's (2004) *GSI* chart can be interpreted as a surface defined by a two-dimensional function as follows (Cai and Kaiser, 2006):

$$GSI = \frac{26.5 + 8.79 lnJ_C + 0.9 lnV_b}{1 + 0.0151 lnJ_C - 0.0253 lnV_b} \tag{5.3}$$

Figure 5.9 shows the chart and its geometrical interpretation. In this case, the variables are V_b and J_C, and the parameters subject to estimation are the five coefficients ρ_0 to ρ_4. These parameters take the values 26.5, 8.79, 0.9, 0.0151 and -0.0253, respectively, in Cai et al's (2004) proposed chart model.

In order to illustrate the Bayesian estimation of *GSI* parameters, a synthetic data set of 50 measurements of *GSI* covering the whole chart area was randomly generated as shown in the plot to the right of Figure 5.9. A random Gaussian variation centred at Cai et al's (2004) chart plane, with a standard deviation of 5, was incorporated to the data points as illustrated in the graph to the left of Figure 5.10. The data set represents the result of a hypothetical face mapping exercise in which V_b and J_C estimates are collected independently from *GSI* determinations with the original chart in Figure 5.8. The data set is used for calibration of the chart by means of obtaining credible estimates of the coefficients ρ_0 to ρ_4. In this example, the estimated values from the 50 calibration points should be close to the original Cai et al (2004) values used to generate the data. The data for calibration of the chart may also include information from various project sites where measurements of the input factors are available together with *GSI* determinations from the performance of the rock mass.

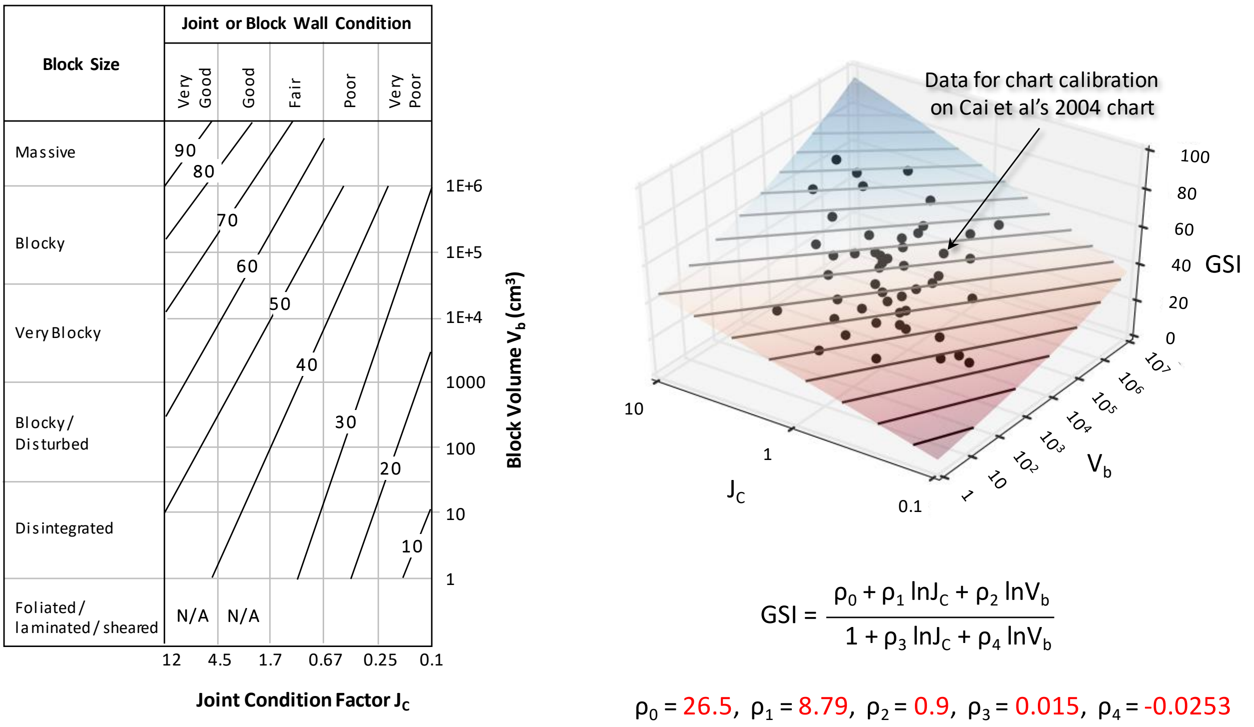

Figure 5.9 Proposed chart (Cai et al, 2004) for the numerical estimation of *GSI* from V_b and J_C indexes (left) and interpretation of the chart as a two dimensional model with variables V_b and J_C and parameters ρ_0 to ρ_4 subject to estimation from data (right). The dots correspond to a synthetic data set of 50 measurements

The Bayesian model is based on a comparison of the *GSI* values calculated with the chart with those representing actual measurements. The particular *GSI* model used for this exercise considers priors of ρ_0 to ρ_4 represented by uniform distributions with ranges around the Cai et al's (2004) chart values. The differences between model and actual values are represented with a t-distribution with scale σ and normality v used as additional estimation parameters. A side view of the fitted chart is shown at the right of Figure 5.10 with the calibration points used in the analysis. The Bayesian analysis was implemented in the Python programming language and the results are summarised in the scatter plots and histograms of ρ_0 to ρ_4 shown in Figure 5.11. These results suggest that for this particular data set, there are many possible combinations of the coefficients ρ_0 to ρ_4, including that from Cai et al's (2004) chart, that would be equally plausible.

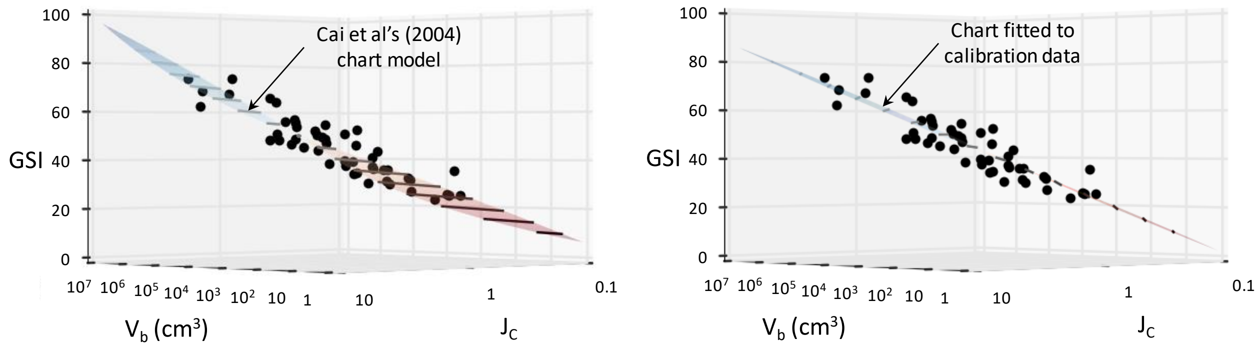

Figure 5.10 Random Gaussian spread with a standard deviation of 5 centred at Cai et al's (2004) chart model used to generate the calibration data set shown in Figure 5.9 (left) and calibration data set with the fitted chart (right)

A second synthetic data set of 100 points clustered around a *GSI* of 40 was generated to represent the data collected with core logging for the slope design. In this case, only V_b and J_C measurements are available for the estimation of *GSI* for design with the chart. The graph to the left of Figure 5.12 shows the data points on the mean fitted chart. The chart is constructed with the mean coefficients from the posterior distributions in Figure 5.11. Each set of ρ_i coefficients represents a plausible chart, which is used to generate a mean value of *GSI* from the data points.

The variability of the chart is illustrated in the graph to the left of Figure 5.12 with the outlines of a selection of those plausible charts. The histogram of the mean values of *GSI* calculated in this manner is shown at the right of Figure 5.12, with the mean and the 95% HDI indicated. The distribution of GSI_{mean} values in Figure 5.12 represents the uncertainty of this parameter and can be used for the analysis of the reliability of the slope.

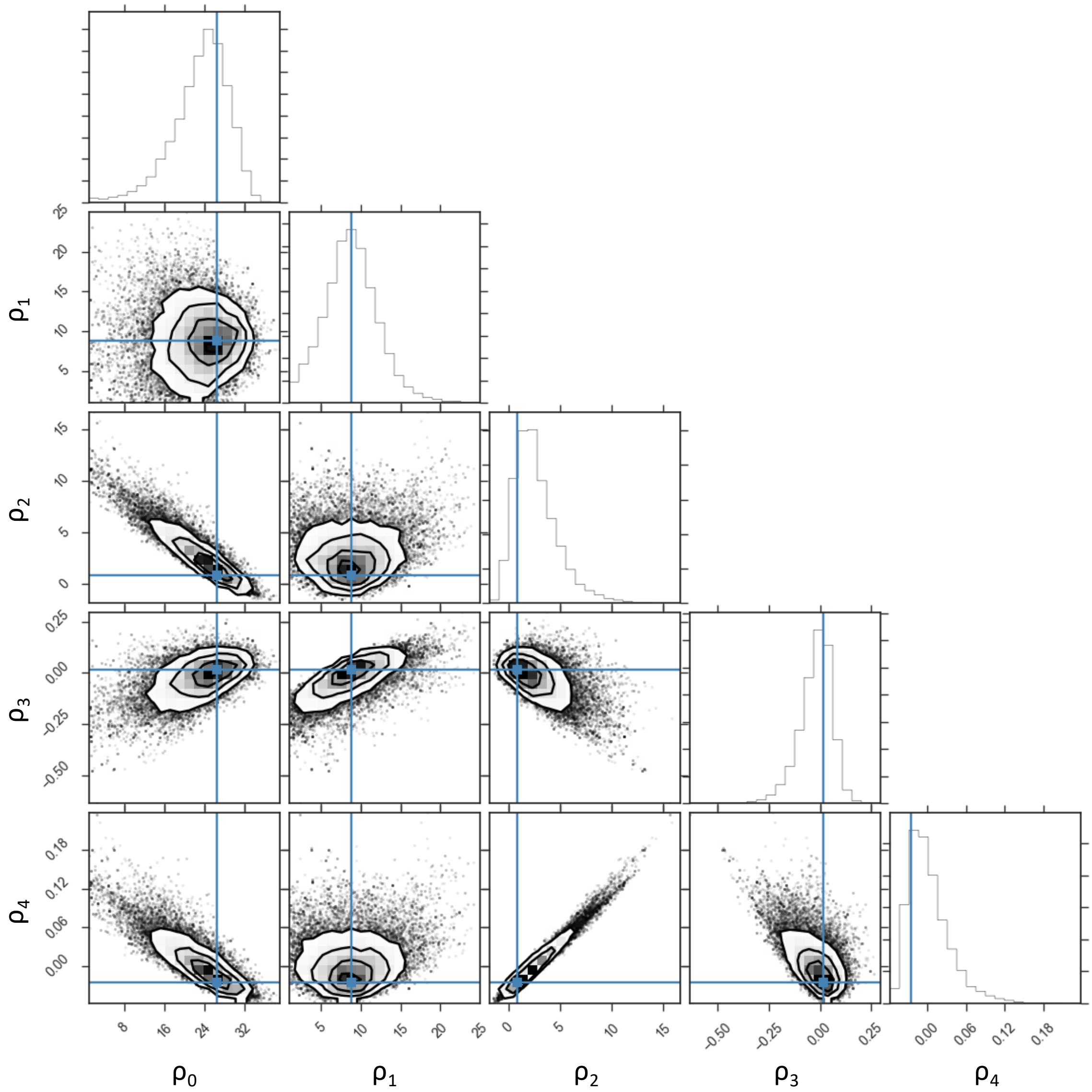

Figure 5.11 Result of the Bayesian analysis of calibration data. The corner plot shows the scatter plots and histograms of the coefficients ρ_0 to ρ_4 hat best represent the calibration data with Cai et al's model function. The marked central points correspond to the original Cai et al's (2004) chart values

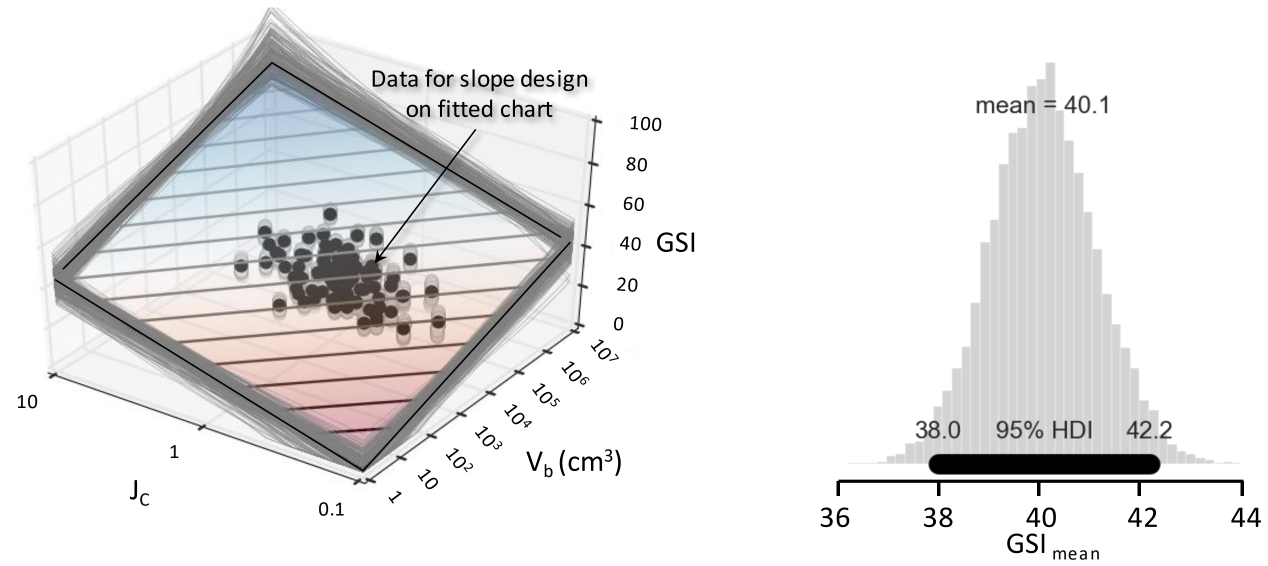

Figure 5.12 Synthetic data set of 50 measurements of V_b and J_C in a local region of *GSI* 40, displayed on the chart fitted to the calibration observations (left). Histogram of mean values of *GSI* from the 50 data points (right). Each value in the histogram corresponds to a set of chart coefficients from the MCMC analysis as indicated in Figure 5.11. The outlines of a selection of plausible charts causing the variability of the mean values of GSI are displayed on the isometric view of the chart on the left

5.2.4 Disturbance factor D

The rock mass disturbance factor (*D*) is based on the assessment of the damage from blasting and stress relief close to the surface of the excavation. At deeper levels, the *D* factor is associated with the disturbance from the stress relief caused by the excavation of the slopes. The *D* factor typically takes values from 0.7 to 1.0 in slopes, although values outside this range are possible. Larger values represent more disturbance and are assigned to zones closer to the surface of the excavation. The *D* factor has a great effect on the estimated strength of the rock mass. Therefore, different combinations of *GSI* and *D* values could produce the same estimated strength. The subjective component in the estimation of *GSI* and *D* complicates the validation of *GSI* estimates using measurements of slope performance. The Bayesian analysis can be used to obtain parameter estimates with the right balance between data and adjudications.

5.2.5 Equivalent Mohr-Coulomb parameters c and ϕ

The characterisation of the rock mass strength with the H-B model requires four parameters (σ_{ci}, m_i, *GSI,* and *D*). Sometimes it is convenient to estimate equivalent M-C parameters represented by the cohesion, *c* and friction angle, ϕ. However, the approximation of the non-linear H-B model with the linear M-C criterion requires the definition of the level of confining stresses where the equivalence is calculated. The calculation of equivalent M-C parameters is carried out in this paper because there are some advantages of using a two-parameter model in terms of visualising some aspects of the reliability and RS analysis discussed in Sections 5.3 and 5.4. The expressions given by Hoek et al (2002) were used to calculate the equivalent *c* and ϕ values from the H-B parameters defined with the Bayesian analysis. The scatter plot and the posterior distributions of the equivalent M-C parameters are shown in Figure 5.13.

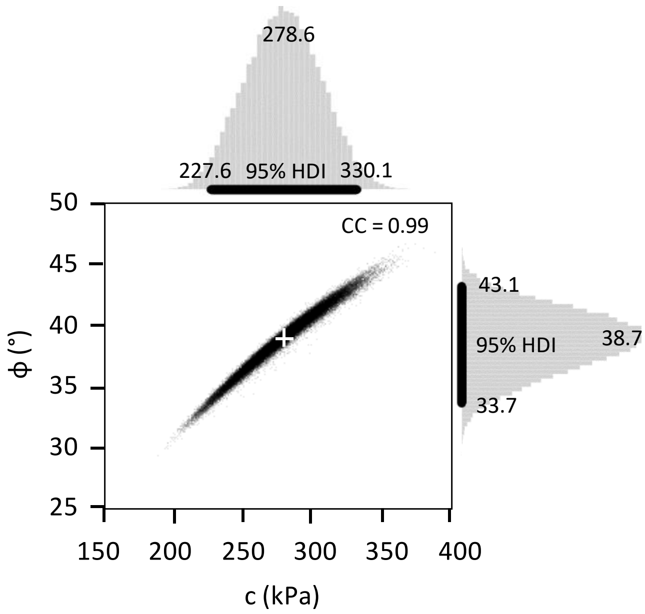

Figure 5.13 Scatter plot of equivalent *c* and ϕ and the respective posterior distributions with mean and 95% HDIs indicated

The H-B parameters are in general uncorrelated or with low correlation coefficients. However, the calculated M-C parameters have a strong positive correlation. This result sometimes surprises geotechnical engineers with soil mechanics experience, because it is common to find a negative correlation between *c* and ϕ in soils. However, the result for a rock mass is consistent with the situation in soil mechanics when the M-C equivalence is calculated for different zones of increased confining stresses as illustrated in Figure 5.14.

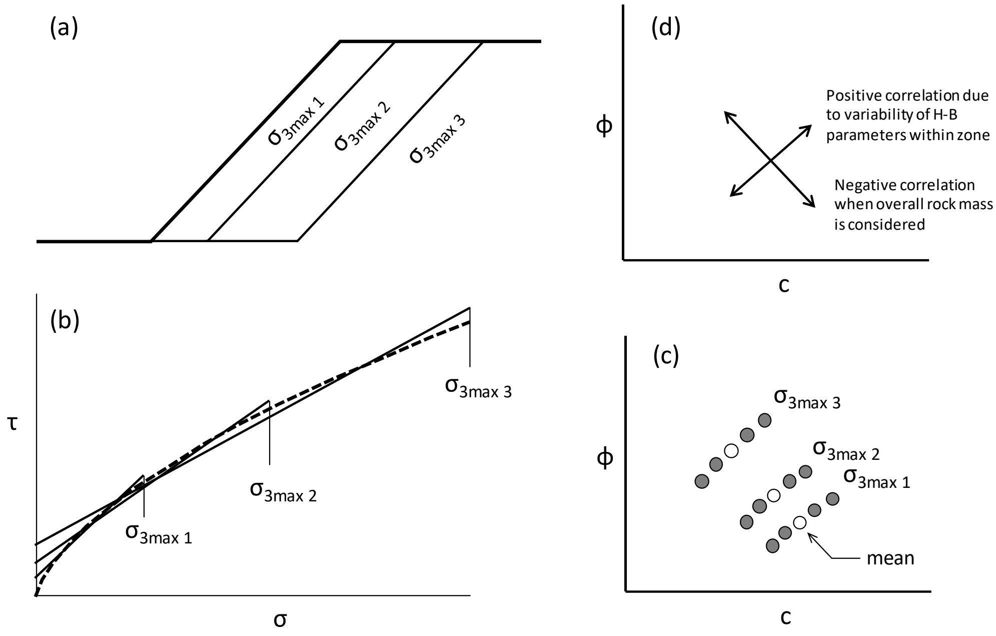

Figure 5.14 Correlation characteristics of equivalent M-C parameters for a slope in a rock mass modelled with H-B parameters. (a) Zones of similar confining stresses within the slope. (b) H-B strength envelope and equivalent M-C envelopes for the three zones of the slope. (c) Variability of *c* and ϕ for the three equivalent M-C envelopes. (d) Interpretation of the correlation characteristics within each zone and for the overall rock mass

The increase of the average confining stress with the depth from the slope face (Figure 5.14a), results in larger *c* and smaller ϕ values to match the increasingly flatter H-B strength envelope (Figure 5.14b). The variability of the H-B parameters causes a positive correlation between *c* and ϕ values. However, when the results from all the slope zones are considered, it is possible to observe a negative correlation similar to that seen in soils (Figure 5.14c and Figure 5.14d).

5.2.6 The Bayesian approach in the context of the geotechnical model for slope design

The ability of the Bayesian approach to combine information from various sources and to provide a good measure of the uncertainty of parameters and models can be used to improve the methods used to define geotechnical models for slope design. Wang et al. (2015) provide a general perspective on the use of Bayesian methods to represent uncertainty during the site characterisation process. Figure 5.15 shows a diagram from Straub and Papaioannou (2015) that illustrates the way in which Bayesian methods can be incorporated into the typical geotechnical investigation process to update the parameters. The approach uses information from site and laboratory investigations as well as the measurements of performance of the built structures. The methods described by Straub and Papaioannou are presented in the context of soil mechanics problems such as foundations and retaining walls, but they can equally be applied to the case of mine slopes.

The approach outlined in Figure 5.15 can be adapted to the case of the geotechnical model for slope design, where data from laboratory tests and site investigations can be used in conjunction with slope performance observations to update the geotechnical parameters. The process could provide the best possible estimates consistent with the information available at any time. This approach is well suited to the continuous process of design, implementation, measuring of performance and feedback followed during the development of the mine.

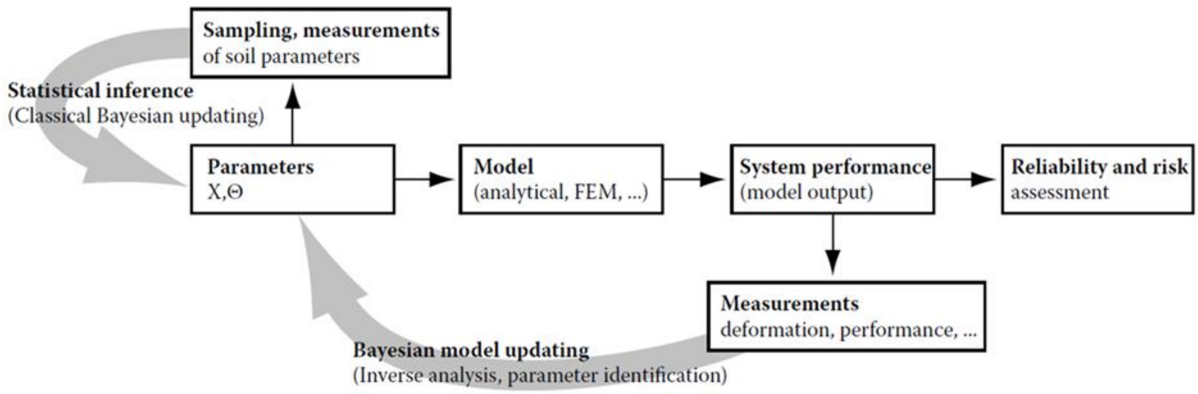

Figure 5.15 The Bayesian updating process in the context of geotechnical models (Straub and Papaioannou, 2015)

The methods described in the present paper deal with the classical Bayesian updating and the use of this information for the assessment of the reliability of the slope.

5.3 Analysis of reliability of a slope

The analysis of the reliability of a slope is one of the possible applications of the results of the Bayesian analysis for inference of the geotechnical parameters for slope design. In this context, reliability can be defined as the probability of successful performance of the slope and corresponds to the complement of the probability of failure (PF). In geotechnical practice, it is common to define the reliability index (β) in terms of the variability characteristics of the FS (Baecher and Christian, 2003) using the following equation:

$$\beta = \frac{FS_{mean} - 1}{FS_{stdev}} \tag{5.4}$$

where FS_{mean} and FS_{stdev} are the mean and standard deviation of the FS. An alternative definition of β corresponds to the structural engineering measure proposed by Hasofer and Lind (1974), which is based on the variability characteristics of the uncertain variables rather than the FS. In this case, β can be interpreted as the minimum distance in a dimensionless space between the peak of the multivariate distribution of the uncertain parameters and a function defining the failure condition. The method of analysis based on this definition of reliability is commonly known as the first order reliability method or FORM.

5.3.1 Reliability analysis with FORM

The FORM approach is explained in detail by Baecher and Christian (2003), and Duncan and Sleep (2015). Low and Tang (1997) developed an efficient procedure to apply the FORM based on reinterpreting β as an expanding ellipsoid centred in the peak multivariate distribution of input parameters and touching the limit state surface representing failure. The procedure uses tools normally available in spreadsheets, it is applicable to correlated or uncorrelated variables, and it is able to handle other distributions besides the traditional normal and lognormal. The procedure is described in detail with application examples in rock mechanics problems by Low and Tang (2007), Low (2008) and Goh and Zhang (2012).

The mathematical expression to calculate β according to the interpretation of Low and Tang (1997) is

$$\beta = min_{x\in \boldsymbol{F}} \sqrt{\left[\frac{\boldsymbol{x_i} - \boldsymbol{\mu_i}}{\boldsymbol{\sigma_i}}\right]^T \boldsymbol{R}^{-1} \left[\frac{\boldsymbol{x_i} - \boldsymbol{\mu_i}}{\boldsymbol{\sigma_i}}\right]} \tag{5.5}$$

where $\boldsymbol{x_i}$ are the uncertain variables, $\boldsymbol{\mu_i}$ and $\boldsymbol{\sigma_i}$ are their respective means and standard deviations, and $\boldsymbol{R}$ is the correlation matrix. The set of $\boldsymbol{x_i}$ values that minimizes Eq. (5.5) and satisfies the condition of failure ($\mathbf{x} \in \boldsymbol{F}$), correspond to the design point. This interpretation is illustrated in Figure 5.16 for the case of two variables represented by the cohesion (c) and friction angle (ϕ) with a negative correlation. The figure shows an ellipsoid centred at the mean values of c and ϕ that touches the limit state surface (LSS) at the design point.

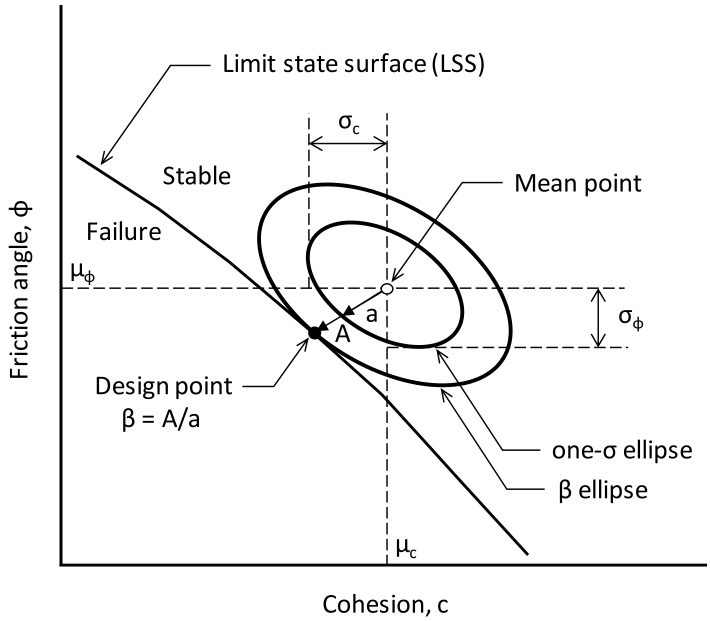

Figure 5.16 Interpretation of the reliability index β for a two-variable case corresponding to c and ϕ negatively correlated (Low, 2014)

Eq. (5.5) applies to the situation of variables with normal distributions. For other types of distributions, the methodology to calculate β requires a modification where the non-normal distributions are replaced by equivalent normal distributions centred at the equivalent normal mean values. The modified equation is

$$\beta = min_{\boldsymbol{x} \in \boldsymbol{F}} \sqrt{\left[\frac{\boldsymbol{x_i} - \boldsymbol{\mu_i}^N}{\boldsymbol{\sigma_i}^N}\right]^T \boldsymbol{R}^{-1} \left[\frac{\boldsymbol{x_i} - \boldsymbol{\mu_i}^N}{\boldsymbol{\sigma_i}^N}\right]} \tag{5.6}$$

where $\boldsymbol{\mu_i}^N$ and $\boldsymbol{\sigma_i}^N$ are the mean and standard deviation of the equivalent normal distributions. Low and Tang (2007), present this equation in the form

$$\beta = min_{\boldsymbol{x} \in \boldsymbol{F}} \sqrt{[\boldsymbol{n}]^T \boldsymbol{R}^{-1} [\boldsymbol{n}]} \tag{5.7}$$

where [$\boldsymbol{n}$] is the vector with the equivalent standard normal values n_i, which can be calculated in the following manner

$$n_i = \Phi^{-1}[F(\boldsymbol{x_i})] \tag{5.8}$$

where $\Phi^{-1}[\cdot]$ is the inverse of the standard normal cumulative distribution (CDF) and $F(x_i)$ is the original non-normal CDF evaluated at x_i. The square root term in Eq. (5.7) can be interpreted as the distance in units of directional standard deviations from the mean to the point evaluated. The procedure proposed by Low and Tang (2004, 2007) is implemented in an Excel spreadsheet and includes a menu of probability distributions that can be converted to equivalent normal distributions. The technique offers three alternative ways of minimizing β subject to the constraint of the LSS, using the solver built-in in Excel.

5.3.2 Use of posterior distributions with the FORM

The methodology proposed by Low and Tang (2004, 2007) requires the probability distributions of the geotechnical parameters as inputs. It is customary to fit probability distributions to observed data hoping that they represent adequately the variability of the geotechnical parameters. However, the posterior distributions of parameters resulting from a Bayesian analysis of data provide a better representation of their uncertainty. The posterior distributions can be used for the reliability analysis with the FORM, using the same concepts described by Low and Tang (2004, 2007), with some added benefits derived from working with a populated parameter sample rather than with a theoretical probability distribution. For example, the calculation of the performance function (i.e. FS) and the square root term in Eq. (5.7) can be done for every point of the sample. In this way, the constrained minimization reduces to screening the points where the performance function indicates failure (FS = 1) and the selection of the point with the minimum value of the square root term in Eq. (5.7).

The use of a posterior distribution for the reliability analysis with the FORM described by Low and Tang (2004, 2007) is illustrated in Figure 5.17. The plot in Figure 5.17 shows a typical scatter plot of c and ϕ values resulting from a Bayesian analysis of data from a soil deposit indicating a negative correlation between these parameters. The sample includes 50,000 values of c and ϕ defining the posterior probability distribution, with mean values of 50 kPa and 30°, respectively. The points provide sufficient information to define the CDF values of any point in the sample, as well as the correlation matrix (R) of the parameters. Therefore, Eq. (5.7) and Eq. (5.8) can be used to calculate, at every point of the sample, the distance term whose minimum value represents the β index.

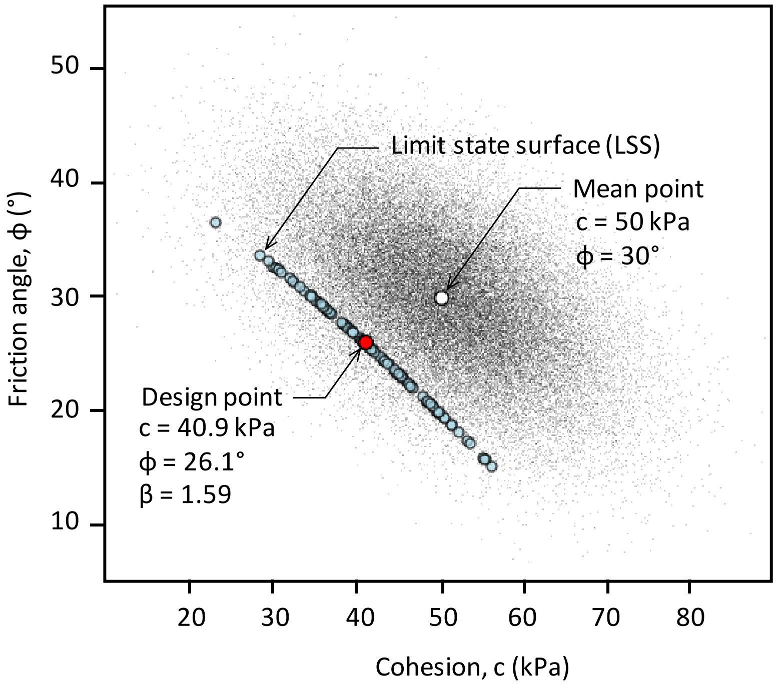

Figure 5.17 Calculation of the reliability index β for the infinite slope example with the FORM as described by Low and Tang (2004, 2007), using the posterior distributions of *c* and ϕ with a negative correlation

To illustrate the method, the sampled *c* and ϕ values plotted in Figure 5.17 are used with an example of the reliability calculation of an infinite slope. The slope has a 30° angle (ψ), with soil depth (d_s) of 10 m, water level 2 m below the surface (d_w = 8 m), saturated water content (w) of 30%, dry unit weight of soil (γ_d) of 15 kN/m^3, and unit weight of water (γ_w) of 10 kN/m^3. The performance function of the slope corresponds to the expression to calculate the FS as follows:

$$FS = \frac{(\gamma_d d_s + (1-w)\gamma_w d_w) cos\psi \; tan\varphi + c/cos\psi}{(\gamma_d d_s + (1-w)\gamma_w d_w) sin\psi + \gamma_w d_w sin\psi} \tag{5.9}$$

The FS is calculated with Eq. (5.9) for every point in the sample. The screened points from the posterior sample where *FS* = 1.0 are shown in the plot as blue dots and they define the LSS. The red point (c = 40.9 kPa, ϕ = 26.1°) corresponds to the minimum distance term and defines the design point with β = 1.59.

5.4 Performance function of the slope with response surface

Typically, the performance function of the slope is not available in an explicit form as in the example of the infinite slope. The slope models used for mine design are usually complex, assembled in matrix form for the solution with numerical methods and therefore cannot be used directly for the reliability analysis with the FORM. However, one option is to create a surrogate model expressed in polynomial form by fitting mathematical models to observations consisting of results of planned runs with the numerical models. These runs are arranged to cover the expected ranges of variation of the uncertain input parameters. This methodology is often referred to as the response surface methodology. The development of the methodology was originally motivated by the need to model responses from physical experiments (Box and Draper, 2007) to extract the maximum knowledge from the experimental process. The methodology was later extended to the evaluation of numerical models.

A wide variety of methods may be used to construct surrogate models from a limited number of observations such as polynomial regression, radial basis function models, kriging and support vector regression (Forrester et al, 2008). They vary in accuracy, efficiency and simplicity and their performance is determined by the characteristics of the problem such as non-linearity, number of dimensions, number of observations and domain scale (Jin et al, 2000). However, the polynomial regression method is the most commonly used in geotechnical engineering to approximate the slope performance function. Two common types of polynomial methods are the quadratic polynomial without cross terms and the product of the quadratic functions defined for each variable.

5.4.1 Quadratic polynomial without cross terms

The RS based on a polynomial regression usually considers a second-order polynomial function as follows:

$$y = b_0 + \sum_{i=1}^{n} b_i x_i + \sum_{i=1}^{n-1} \sum_{j=i+1}^{n} b_{ij} x_i x_j + \sum_{i=1}^{n} b_{ii} {x_i}^2 \qquad (5.10)$$

where *y* is the response of interest, *x* is a vector representing the n uncertain variables and b_i, b_{ij} and b_{ii} correspond to the unknown coefficients that need to be determined to fit the function to the observation values. The number of coefficients is $(n+1)(n+2)/2$, which defines the minimum number of observations required to determine the coefficients. A common practice used to reduce the number of observations required to fit the polynomic function is to drop the cross terms in Eq. (5.10), which reduces the number of coefficients to $2n+1$. In this case, the observations correspond to model results obtained by changing one variable at a time at two level positions located on both sides of the mean value. The central point corresponding to the mean of all variables is also included in the analysis. This arrangement of observation points is known as a central design. It is particularly well-suited for situations where the variables are uncorrelated because no observations resulting from the interaction of variables are included in the process.

Other common arrangements of observation points used to create surrogate models with the RS method are the 2^n factorial design, the central composite design and the 3^n factorial design. As suggested by the name, the 2^n factorial design uses the 2^n combinations of two levels of values per variable. However, the 2^n factorial design requires a first order polynomial for the solution. The central composite design considers the observation points from the central design and the 2^n factorial design together. The 3^n factorial design considers all the combinations of three levels of values per variable.

The polynomial function in Eq. (5.10) can be expressed in matrix form as follows:

$$Y = XB \tag{5.11}$$

where Y is the vector of k observation points, X is a matrix of the x_i terms taking the values of the uncertain variables used to get each observation point in Y, and B is a vector of coefficients b. The matrix X has k rows by p columns, where p is the number of terms of the polynomial function. The solution of the system requires that $k \geq p$ and $p = (n+1)(n+2)/2$ for a complete second-order polynomial, or $p = 2n+1$ if the polynomial excludes the cross terms. When $k > p$ the solution of the system is based on a least-squares analysis aimed at minimizing the residuals $|XB - Y|$. The matrix representation of the least squares solution is:

$$B = (X^T X)^{-1} X^T Y \tag{5.12}$$

The calculation of the coefficients is normally carried out with the input variables and responses normalised to their mean values. A central design arrangement of observation points fitted with a polynomial function without cross terms results in a function that matches the observation points because the number of points (k = $2n$+1) is equal to the number of coefficients (p) of the function.

5.4.2 Product of quadratic functions

Steffen et al. (2008) describe an alternative RS procedure for the calculation of the PF in mine slope design. The technique uses a central design arrangement of values of FS calculated with a slope model. The input variables x_i and the FS responses are normalized to their mean values, defining the input factors ξ and the response factors δ as follows:

$$\xi_i = \frac{x_i}{x_{i\,mean}} \tag{5.13}$$

$$\delta_i = \frac{FS_i}{FS_{mean}} \tag{5.14}$$

The trends of δ versus ξ for each uncertain variable are fitted with second order polynomial functions

$$\delta_i = a_i{\xi_i}^2 + b_i\xi_i + c_i \tag{5.15}$$

The group of n polynomial functions of δ versus ξ constitutes the RS and can be used as a replacement of the model to estimate FS values for any combination of input variables using:

$$FS = FS_{mean}\, \delta_1(\xi_1)\, \delta_2(\xi_2) \ldots .\, \delta_n(\xi_n) \tag{5.16}$$

Figure 5.18 illustrates the methodology for a situation with four uncertain variables used for the calculation of the FS of a slope. The curves represent the response of the FS to variations of each of the uncertain variables. The respective quadratic polynomial function is indicated at the top of each graph. The method effectively corresponds to the fitting of a polynomial function of order 2^n which is the result of incorporating the n quadratic polynomial functions given by Eq. (5.15) into Eq. (5.16). The graphs were constructed using the data listed in Table 5.1. The intervals of variation of the input parameters defining the '+' and '-' cases correspond to the bounds of the 95% HDI of the posterior probability distributions of σ_{ci}, m_i and GSI described in Section 5.2. The factor D is modelled with a triangular distribution and in this case, the points of analysis correspond to the maximum and minimum values. The slope stability analyses correspond to the case example described in Section 5.5.

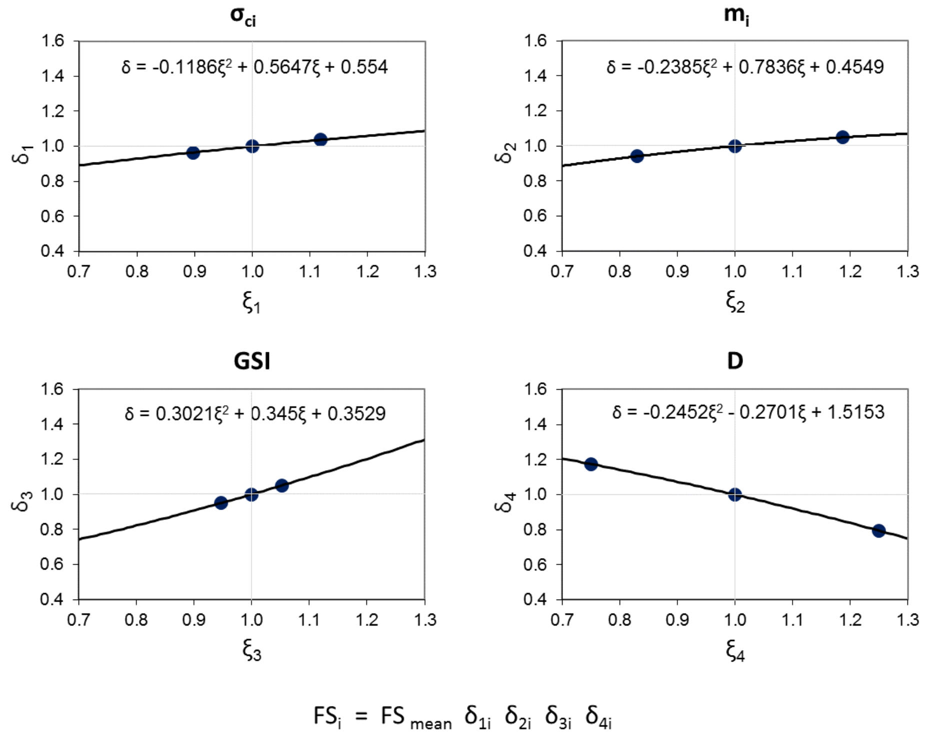

Figure 5.18 Illustration of derived influence coefficients δ for RS of FS from data in Table 5.1.

Table 5.1 Input values and FS results for construction of RS.

No.	Uncertain variable	Input values			FS		
		'-' case	mean	'+' case	'-' case	mean	'+' case
Hoek-Brown strength model							
1	σ_{ci} (MPa)	54.3	60.5	67.7	1.17	1.21	1.25
2	m_i	9.8	11.8	14.0	1.14	1.21	1.27
3	*GSI*	38.0	40.1	42.2	1.15	1.21	1.27
4	*D*	0.60	0.80	1.00	1.42	1.21	0.96
Mohr-Coulomb strength model							
1	*c* (kPa)	227.6	278.6	330.1	1.11	1.19	1.26
2	ϕ (°)	33.7	38.7	43.1	1.06	1.19	1.31

5.4.3 Comparison of RS predictions of FS

The effectiveness of the two RS methods described in this paper is evaluated with a comparative analysis of the errors in the predictions of FS, using the actual FS results from the slope model as the reference. The slope stability evaluation consisted of a probabilistic analysis of the slope example described in Section 5.5 using the program Slide from Rocscience. The MC trials included 100,000 samples drawn from beta distributions fitted to the respective posterior distributions described in Section 5.2. Table 5.2 summarises the input data used for the stability analysis with the slope model. The FS were also calculated with the RSs constructed with the two methods described in this paper, using the same MC trial inputs of the slope model analysis. These results were used to calculate the errors in the prediction of FS with the RS method.

Table 5.2 Input data for slope stability analyses with program Slide

No.	Uncertain variable	Distribution	Mean	Standard deviation	Relative minimum	Relative maximum	CC
Hoek-Brown strength parameters							
1	σ_{ci} (MPa)	Beta	60.5	3.5	10.5	12.5	
2	m_i	Beta	11.8	1.1	3.6	4.0	
3	*GSI*	Beta	40.1	1.1	3.7	3.9	
4	*D*	Triangular	0.80		0.2	0.2	
Mohr-Coulomb strength parameters							
1	c (kPa)	Beta	278.6	26.6	76.6	81.4	0.99
2	ϕ (°)	Beta	38.7	2.5	8.7	6.3	

Note: CC – Coefficient of correlation

Figure 5.19 shows a summary of the results of the analysis of errors in the FS prediction with the RS for the case of the slope in a rock mass characterised with the four H-B strength parameters. Figure 5.20 shows similar results for the case of the slope with M-C parameters. RSa corresponds to the polynomial function without cross terms solved with Eq. (5.12). RSb corresponds to the product of quadratic functions described by Eq. (5.16) and represented in Figure 5.18 for the H-B model case. The RSs are based on observations with a central design arrangement, i.e. nine points for the H-B model case and five points for the M-C model case.

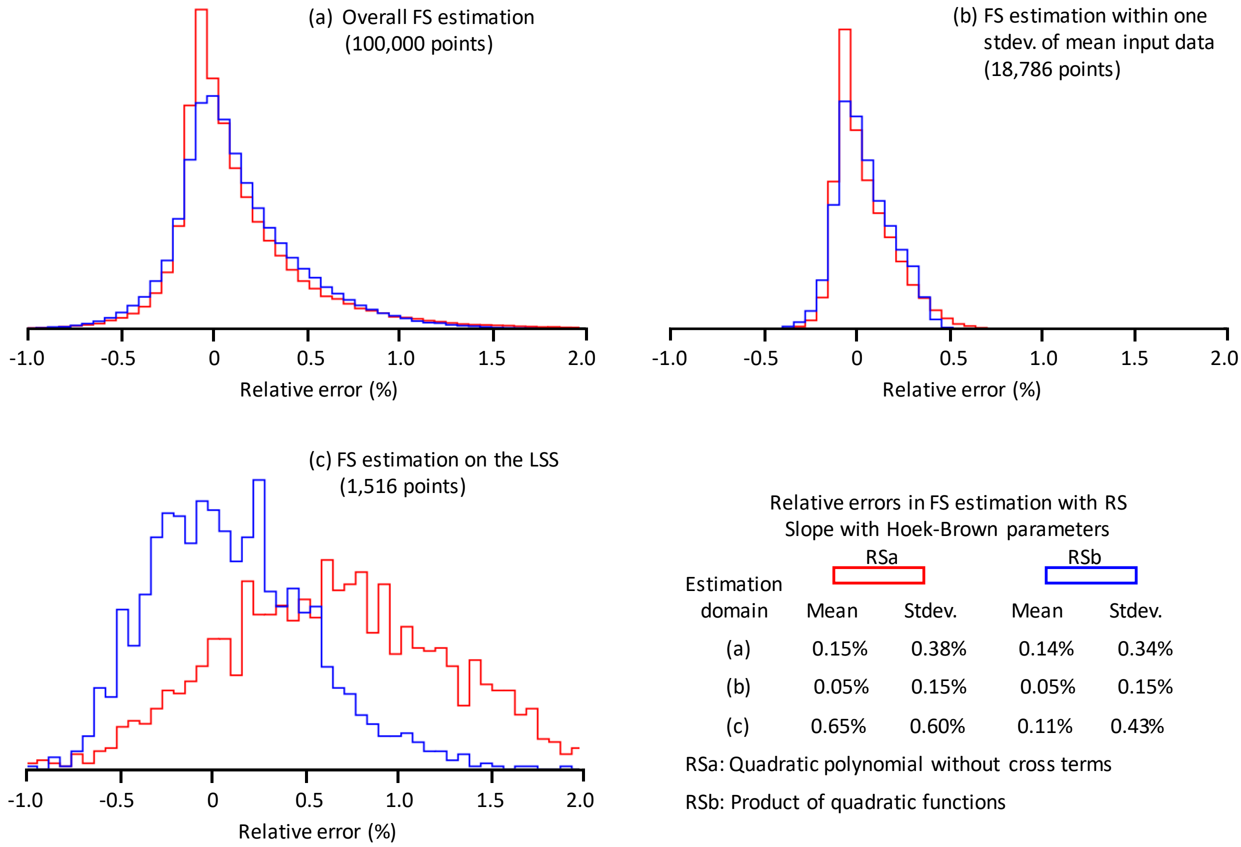

Figure 5.19 Distributions of the relative errors in FS prediction with RSa and RSb at the MC trial points of the slope stability analysis. Slope modelled with H-B parameters. (a) Errors for all the MC trials, (b) errors for the data points within one standard deviation of the mean and (c) errors for the points on the LSS. The table on the lower right corner summarizes the errors mean and standard deviation values

The graph (a) in Figure 5.19 and Figure 5.20 shows the histograms of the errors over the whole domain of the input parameters. The distribution of errors with the two RSs is similar, with a slight advantage of RSb over RSa for the M-C model case. Both RSs appear to underestimate the FS as indicated by the skewness of the distributions towards the positive errors and this effect is more marked in the M-C model case. Typically, the central design points are defined with variations of ± one standard deviation from the mean. However, a wider range was used for the present work, which is based on the 95% HDI bounds from the posterior distributions. For this reason, the precision of the prediction in a region closer to the centre of the RS was investigated. The graph (b) in Figure 5.19 and Figure 5.20 corresponds to histograms of errors for the data points within one standard deviation of the mean values. In this region, again RSb shows a slight advantage over RSa for the M-C model case. The graph (c) in Figure 5.19 and Figure 5.20 represents the distribution of errors in the domain region where *FS* = 1.0. This is an important evaluation because the FORM analysis uses the RS for the estimation of the LSS where the design point is sought. In this case, there is a clear advantage of the RSb over RSa as suggested by the comparatively smaller bias and narrower distribution of errors shown by the histograms. In general, the errors with RSb are small, with values between -0.5% and 1.0% for the H-B model case, and between 0% and 1.0% with the M-C model case.

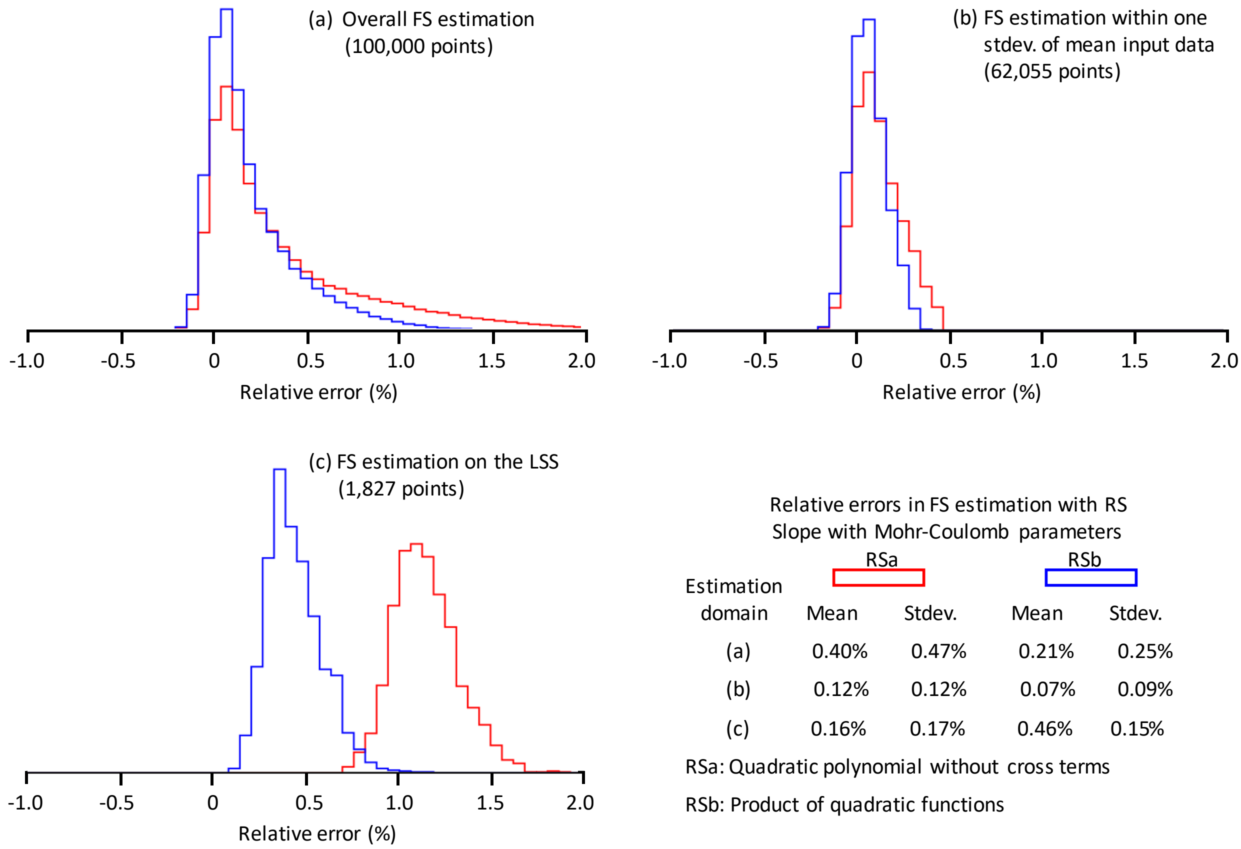

Figure 5.20 Distributions of the relative errors in FS prediction with RSa and RSb at the MC trial points of the slope stability analysis. Slope modelled with M-C parameters. (a) Errors for all the MC trials, (b) errors for the data points within one standard deviation of the mean and (c) errors for the points on the LSS. The table on the lower right corner summarizes the errors mean and standard deviation values

Based on the previous results, the RS method selected for the analysis of the reliability of the slope described in this paper is the product of quadratic functions reflecting the sensitivity of each variable. The procedure is easily incorporated into the code for the FORM analysis with posterior distributions and the number of model runs with a central design is relatively small.

5.4.4 Use of RS for the analysis of reliability with FORM

The purpose of the RS in the context of the present work is to have an explicit way of calculating the FS of the slope for every set of geotechnical parameters in the posterior probability distributions. In this way the points where *FS* = 1.0 within a specified precision range define the LSS that separates the stable and failure regions of the parameter space. The design point defining the reliability of the slope can be found in this subset of the posterior distributions. However, due to the errors in the FS prediction with the RS, the actual FS at the calculated design point might be different from one. Therefore, the procedure needs to be repeated with a new RS centred at a new point near the calculated design point, until there is consistency in the result. The convergence of the process is facilitated by defining the new RS centre from linear interpolation using the following equation (adapted from Bucher and Bourgund, 1990):

$$x_1 = x_0 + (x^* - x_0)\frac{(FS_0 - 1)}{(FS_0 - FS^*)} \tag{5.17}$$

where x_1 is the new midpoint for the new RS, x_0 is the initial midpoint (mean), x^* is the calculated design point, FS_0 is the FS at the initial midpoint and FS^* is the FS at the design point calculated with the slope model. The reliability index calculated with the second RS centred near the design point should converge to a stable solution, unless the LSS is highly nonlinear, in which case the use of the second order reliability method (SORM) is more appropriate. Tang et al (2013) describe this iterative procedure to improve the efficiency of the reliability analysis with various RS methods and sampling techniques.

5.5 Illustrative example

The reliability analysis using the posterior distributions of the geotechnical parameters is illustrated with an example of a 52° mine slope with a height of 210 m, excavated in a rock mass characterised with an H-B strength criterion. The characteristics of the slope, the groundwater surface and the mean rock mass strength properties are indicated in Figure 5.21. The stability of the slope was evaluated with the program Slide from Rocscience using the limit equilibrium method.

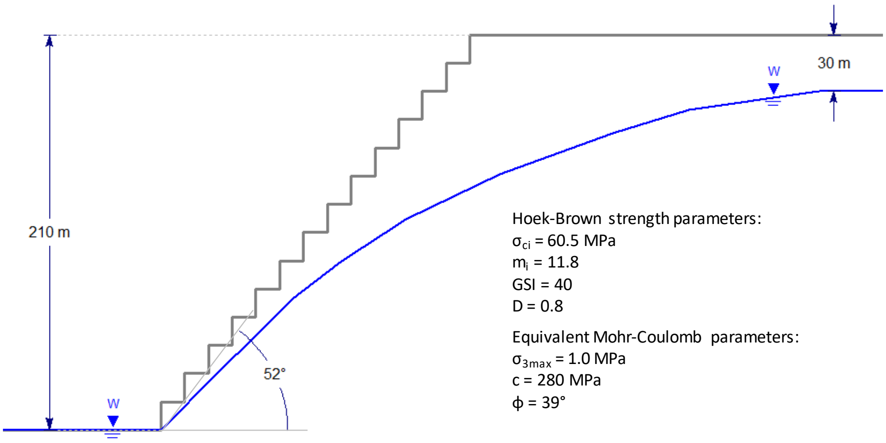

Figure 5.21 Geometry of the slope for the example of the analysis of reliability. The homogeneous rock mass is characterised by H-B strength parameters (σ_{ci}, m_i, GSI, D) and the respective equivalent M-C parameters (c, ϕ)

The uncertainty of the strength parameters σ_{ci}, m_i and GSI is represented by the posterior probability distributions derived from the Bayesian analysis of data described in Section 5.2. The variability of the factor D is represented by a set of values drawn from a triangular distribution to have a sample of equal size to the posterior distributions of the other parameters. The slope reliability evaluation is carried out for the two strength models, H-B with four parameters and M-C with two parameters to facilitate the visualization of certain aspects of the procedure. The purpose of this example is to illustrate various ways of using the results of the Bayesian analysis described in Section 5.2 to evaluate the reliability of the slope. The reliability calculations were implemented in the Python programming language.

The slope reliability analysis using the FORM approach is examined with three variants of the method. The first variant corresponds to the constrained minimization using the beta distribution functions with the spreadsheet from Low and Tang (2007). The second variant uses the MC trial inputs from the slope model analysis derived from the same beta distributions. The third variant uses the MCMC samples from the Bayesian analysis of Section 5.2. Table 5.3 shows the main results of the analysis for the slope characterised with the H-B parameters. The analyses include two iterations to ensure that the design point is on the LSS as predicted with the RS. The first iteration uses RS1 centred at the mean values and constructed with a central design arrangement of points and the second iteration uses RS2 centred at a point close to the design point from iteration 1.

Table 5.3 Summary of results of FORM analyses of the slope with H-B parameters

Iteration	RS	Centre of RS				Design point						
		σ_{ci} (MPa)	m_i	*GSI*	*D*	FS RS	β	σ_{ci}* (MPa)	m_i*	*GSI**	*D**	FS model
Beta distributions with Low and Tang (2007) spreadsheet												
1	RS1	60.5	11.8	40.1	0.80	1.000	1.85	58.9	11.0	39.5	0.93	0.998
2	RS2	59.0	11.1	39.5	0.93	1.000	1.84	59.0	11.1	39.4	0.93	1.000
MC trials from beta distributions												
1	RS1	60.5	11.8	40.1	0.80	1.001	1.84	59.0	11.0	39.5	0.93	1.003
2	RS2	59.0	11.0	39.5	0.93	0.999	1.84	59.0	11.0	39.5	0.93	1.003
MCMC samples from Bayesian analysis												
1	RS1	60.5	11.8	40.1	0.80	1.001	1.85	59.5	11.2	39.5	0.94	0.992
2	RS2	59.6	11.2	39.5	0.93	1.001	1.85	58.9	10.9	39.3	0.92	1.007

For the analysis based on the MCMC samples, every set of input parameters in the posterior distributions is used to calculate an FS with the RS1 and the distance term with Eq. (5.7) and Eq. (5.8). Screening the points where *FS* = 1.0 with a tolerance of ±0.001 identifies the location of the LSS in the parameter space. The point in the LSS with the minimum distance to the mean defines the design point represented in this case by σ_{ci}*=59.5MPa, m_i*=11.2, *GSI**=39.5 and *D**=0.94. However, the Slide slope model indicates an *FS* = 0.992 at this point, which is partly due to the prediction error with RS1. Therefore, Eq. (5.17) is used to calculate the centre for a new RS named RS2, which is used for the second iteration of the analysis. The results of the second iteration are shown in Figure 5.22.

Figure 5.22 shows the scatter plots of the input parameters and the FS values calculated with the RS2 in iteration 2. The plots include the mean value of each parameter and the points on the LSS represented by the blue dots. The LSS cannot be associated with a particular geometrical shape because it is defined in a four-dimensional space. The design point is indicated with the red dots.

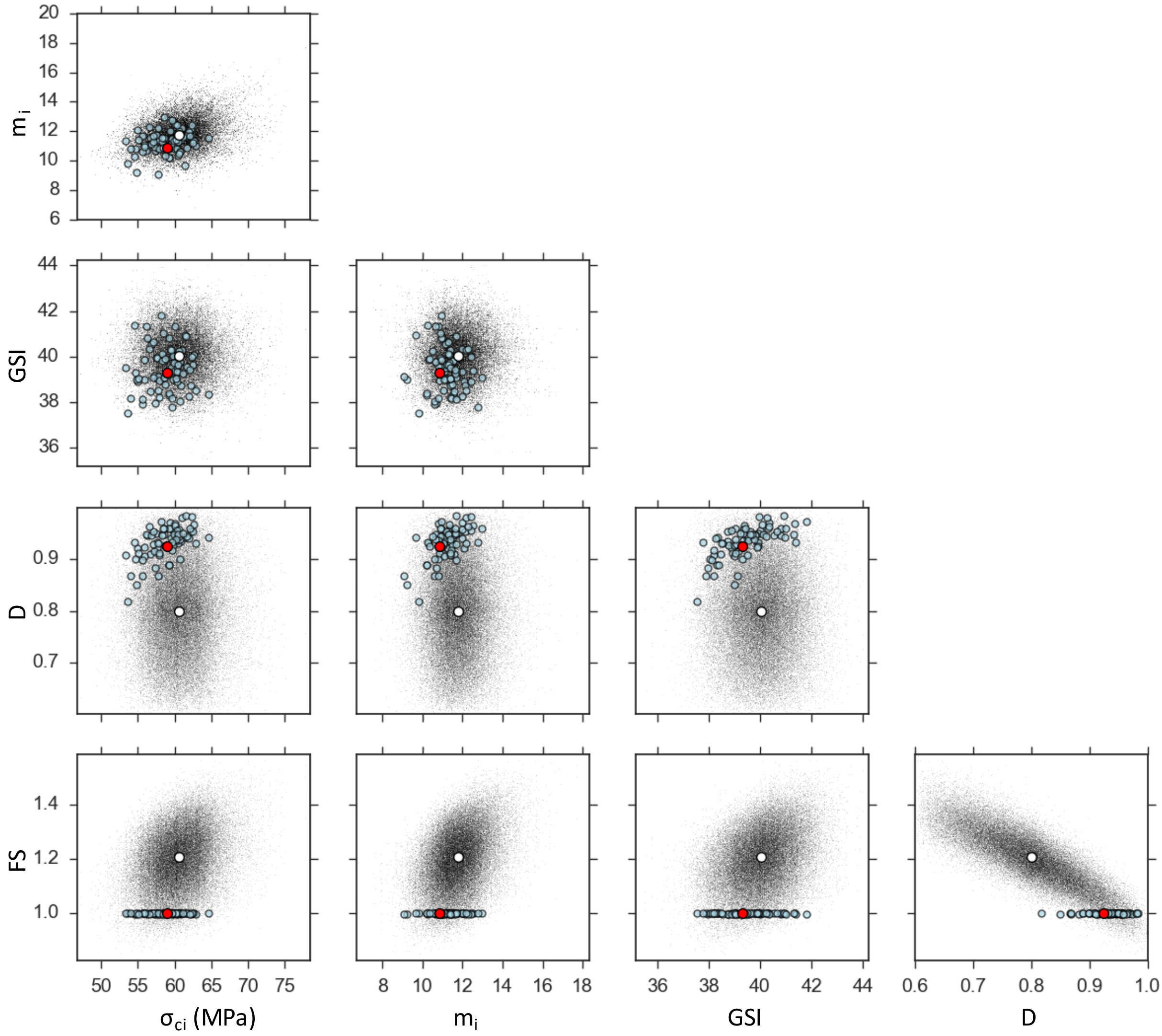

Figure 5.22 Scatter plots of the H-B strength parameters and FS values, including the mean values (white dots), the points on the LSS (blue dots) and the design point (red dots). The results correspond to the second iteration of analysis considering an RS centred in the calculated design point from the first iteration

The visualisation of the results of the FORM analysis is facilitated with the two-dimensional model using the M-C parameters. Table 5.4 shows the relevant results of the three variants of the analysis for this model case. Figure 5.23 shows a comparison of the RSs used for each iteration of the analysis. RS1 is generated with the five points centred at the mean values of c and ϕ, whereas RS2 is based on a closer arrangement of points centred at the design point identified with the first iteration.

Table 5.4 Summary of results of FORM analysis of the slope with M-C parameters

Iteration	RS	Centre of RS		Design point				
		c (kPa)	ϕ (°)	FS RS	β	c^* (kPa)	ϕ^* (°)	FS model
Beta distributions with Low and Tang (2007) spreadsheet								
1	RS1	278.6	38.7	1.000	1.80	231.6	34.1	0.996
2	RS2	232.5	34.2	1.000	1.80	231.8	34.2	1.001
MC trials from beta distributions								
1	RS1	278.6	38.7	1.001	1.80	231.7	34.2	0.994
2	RS2	233.1	34.3	1.001	1.80	231.7	34.2	0.998
MCMC samples from Bayesian analysis								
1	RS1	278.6	38.7	1.001	1.76	231.9	34.2	1.000
2	RS2	231.9	34.2	1.001	1.76	232.1	34.2	1.001

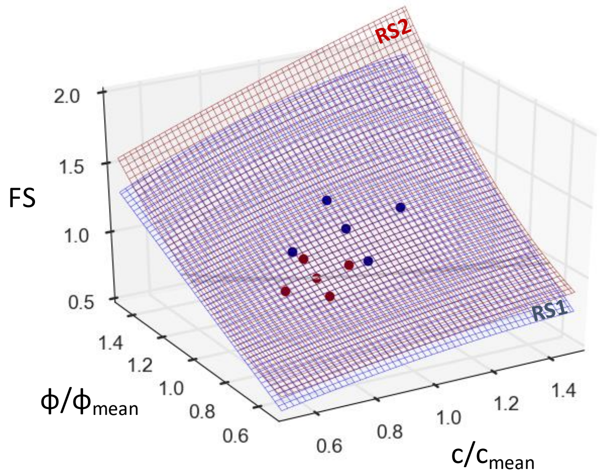

Figure 5.23 Comparison of RSs, RS1 centred at the mean values and RS2 centred at the design point from the second iteration of analysis

Figure 5.24 shows the scatter plots of c, ϕ and FS from the second iteration of the analysis based on the MCMC samples. The LSS is defined in these plots only at the location of the sampled values. Figure 5.25 shows a comparison between the MC trial values drawn from the beta distributions and the original MCMC samples from the posterior distributions. The graphs are presented in a normalized space and correspond to the second iteration of the analyses. Although in both cases there is a high correlation between c and ϕ there are differences in the density of points near the LSS, which contributes to the small differences in the results.

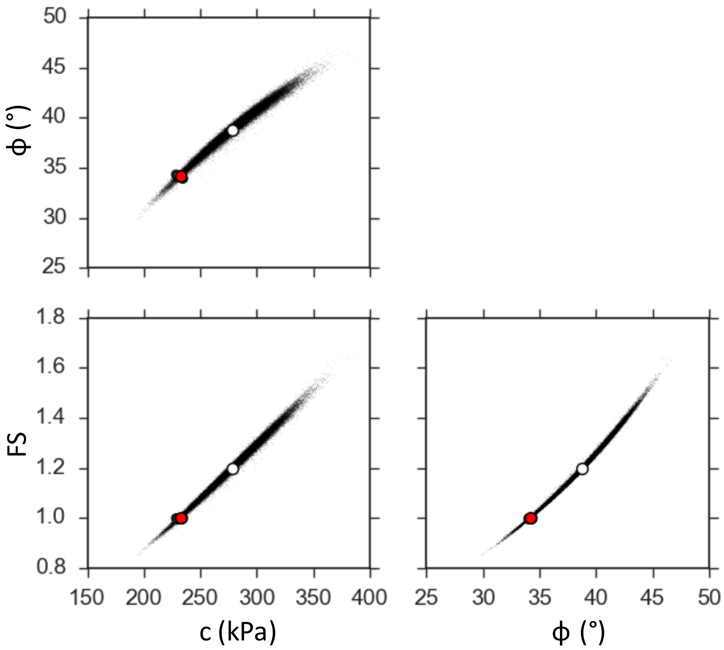

Figure 5.24 Scatter plots of the M-C strength parameters and FS values, including the mean values (white dots), the points on the LSS (blue dots) and the design point (red dots). The results correspond to the second iteration of analysis considering an RS centred in the calculated design point from the first iteration

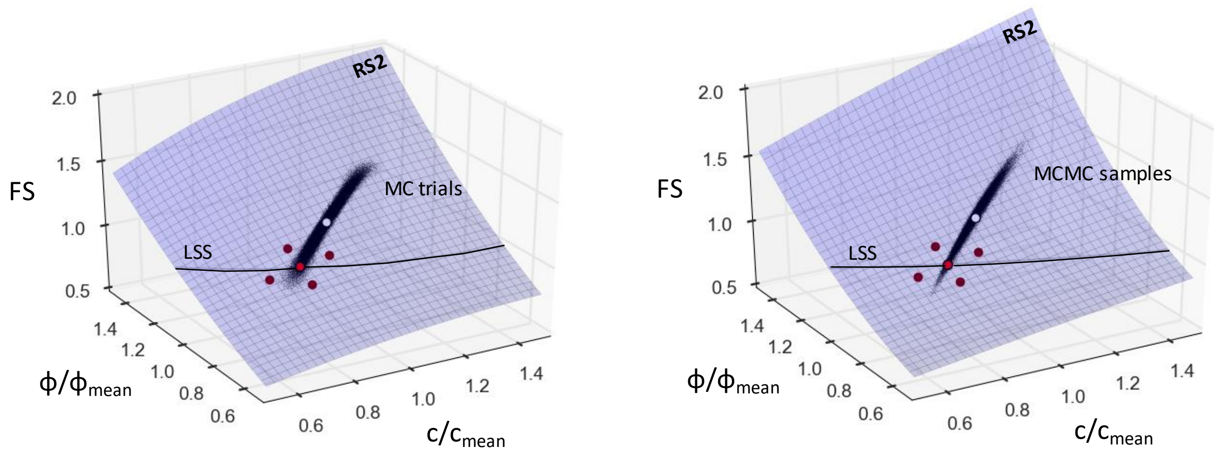

Figure 5.25 Comparison of normalised values of c and ϕ from MC trials (left) and from the MCMC samples (right) showing a high correlation. The sampled values are shown on the RS2 centred at the design point on the LSS

Table 5.5 shows a summary of the results of the six procedures of analysis of reliability used with the two cases of rock mass characterisation of the slope example. The procedures include:

1. MC analysis with the slope model based on the limit equilibrium method.
2. MC analysis with the RS based on the product of quadratic functions using the trial inputs from procedure 1.
3. Similar to procedure 2 but using the MCMC samples from the Bayesian analysis instead of the MC trial inputs.
4. FORM analysis with two iterations using the method of Low and Tang (2007) with the beta distributions used in procedure 1.
5. FORM analysis with two iterations using the MC trial inputs from procedure 1.
6. Similar to procedure 5 but using the MCMC samples from the Bayesian analysis instead of the MC trial inputs.

Table 5.5 Summary of results of reliability analysis

No.	Procedure	Input distribution	FS_{det}	FS_{mean}	PF	β	n	Δ_{PF}	Δ_{β}
				Hoek-Brown model					
1	Slide + MC trials	Beta (1)	1.207	1.203	2.79%	1.915	100,000	±0.10%	±0.016
2	RS + MC trials	Beta (1)	1.207	1.201	2.86%	1.880	100,000	±0.10%	±0.016
3	RS+MCMCpoints	Posterior (2)	1.205	1.199	3.06%	1.842	50,000	±0.15%	±0.022
4	FORM+ beta dist.	Beta (3)	1.207		3.32%	1.836			
5	FORM+ MC trials	Beta (1)	1.207		3.29%	1.840	100,000	±0.11%	±0.015
6	FORM+MCMCpoints	Posterior (2)	1.207		3.22%	1.849	50,000	±0.15%	±0.021
				Mohr-Coulomb model					
1	Slide + MC trials	Beta (1)	1.194	1.196	3.18%	1.835	100,000	±0.11%	±0.015
2	RS + MC trials	Beta (1)	1.194	1.194	3.59%	1.836	100,000	±0.12%	±0.015
3	RS + MCMC points	Posterior (2)	1.194	1.194	3.81%	1.825	50,000	±0.17%	±0.020
4	FORM + beta dist.	Beta (3)	1.194		3.63%	1.795			
5	FORM + MC trials	Beta (1)	1.194		3.56%	1.804	100,000	±0.11%	±0.015
6	FORM+MCMCpoints	Posterior (2)	1.194		3.90%	1.762	50,000	±0.17%	±0.020

Notes:

(1) Sampled with the MC method (2) Sampled with the MCMC algorithm (3) Defined with function

Procedures 1, 2 and 3 are based on defining the characteristics of the distribution of FS to estimate β and PF independently. These procedures yield a mean value of FS, besides the usual deterministic result. Procedures 4, 5 and 6 use the variability characteristics of the input parameters to calculate β and the PF value is estimated from β assuming an equivalent unitary normal distribution for FS. The number of MC trials or the number of MCMC samples, denoted as *n*, were used to calculate the maximum absolute errors Δ, in the estimation of PF and β for a 95% confidence level, using the following expressions:

$$\Delta_{PF} = z_{\alpha/2}\sqrt{\frac{(1-PF)PF}{n}} \tag{18}$$

$$\Delta_{\beta} = \frac{\Phi^{-1}(PF+\Delta_{PF}) - \Phi^{-1}(PF-\Delta_{PF})}{2} \tag{19}$$

where $z_{\alpha/2}$ is the value of the standard normal distribution where the probability is half the complement of the confidence level (2.5%), and $\phi^{-1}(\cdot)$ is the inverse of the standard normal distribution. Figure 5.26 shows plots of the results of PF and β with the estimated maximum errors associated with the number of trials or points in the posteriors. The reason to calculate these errors is to have a better appreciation for the differences between the various procedures, not affected by the number of trials or sample points of the iterative procedures.

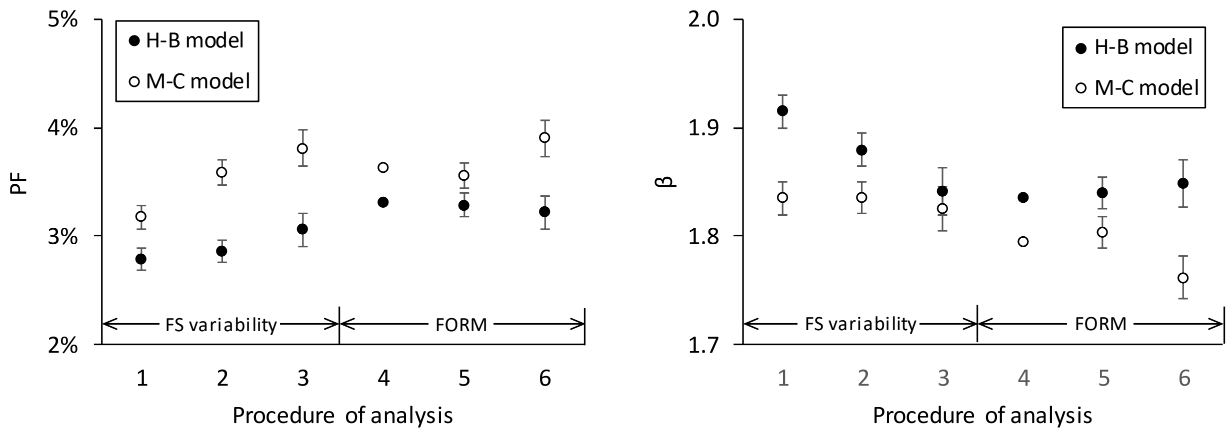

Figure 5.26 Results of PF (left) and β (right) from the procedures listed in Table 5.5, with the estimated errors associated with the number of sampled inputs where applicable

The estimated maximum errors associated with the number of sampling points are small compared to the differences due to the procedure of analysis. In general, the analyses based on sampling from fitted distributions produce smaller PF and larger β values than those using the original posteriors, for comparable procedures of analysis (i.e. comparison of results from procedures 2 with 3 and from procedures 5 with 6). However, the authors argue that the posterior distribution samples from the Bayesian analysis provide a more accurate representation of the uncertainty of the input parameters than that given by the fitted beta distributions. The structure of the posterior samples carries the information provided by the data used in the analysis, but this structure is not reproduced in complete detail with the MC sampling as shown in Figure 5.25 for the *c* versus ϕ samples. For the H-B model case, the slight correlation between σ_{ci} and m_i shown in the scatter plot of Figure 5.7 could not be included in the slope model analysis due to limitations of the Slide program to account for this feature.

The reasonable differences between the results from procedures 1 and 2 suggest an acceptable performance of the RS as a surrogate model. There is good agreement between the results from procedures 4, 5 and 6, which are based on the FORM. These results confirm the consistency of the adaptation of the FORM for the use with sampled distributions rather than with functions describing those distributions. There are slight differences between results from procedures based on the variability of FS and those based on a FORM analysis i.e. procedure 2 compared with 5, and procedure 3 with 6. None of the procedures has all the desirable features that would make it the procedure of choice with the expected best results. However, it is suggested that the FORM applied to the MCMC samples (procedure 6) combines the best set of conditions of analysis to provide consistent measures of the reliability of the slope. The procedure uses the best representation of the uncertainty of the input parameters and does not depend on the precision of the RS over the whole parameter domain. The RS is only used to estimate FS on the LSS near the design point and it can be conveniently constructed with few model runs. Moreover, the results from procedure 6 have good agreement with those from the conventional FORM analysis using the distribution functions (procedure 4).

5.6 Summary and conclusion

The Bayesian approach was applied for the inference of the H-B rock mass strength parameters using typical data from laboratory testing and site investigation results. The results of the Bayesian analysis of data includes the sets of representative samples of parameter values drawn from posterior distributions with an MCMC algorithm. The rock mass strength characterisation included the intact rock strength parameters σ_{ci} and m_i, and the rock mass quality parameter *GSI*. The disturbance factor *D* is not supported by measurements and was modelled with a triangular distribution between 0.6 and 1.0 with a mean of 0.8. Equivalent M-C parameters *c* and ϕ were calculated for the analysis of a slope with confining stresses represented by σ_{3max} = 1.0 MPa. The use of the 2-parameter M-C model equivalent to the 4-parameter H-B model was intended to facilitate the visualization of certain aspects of the reliability analysis with the FORM and to include an analysis case with correlated parameters.

The use of the results of rock mass characterisation with a Bayesian approach was illustrated with the reliability analysis of a 52° slope with a height of 210 m excavated in this rock mass. Two RS methods based on polynomial fitting of a central design arrangement of points were compared in terms of the effectiveness to predict FS values on the LSS. The method based on the product of quadratic functions for each uncertain variable was found to have advantages over the second order polynomial function without cross terms and was selected for the analysis of the reliability of the slope. The central design includes 9 runs with the slope model for the H-B case and 5 runs for the M-C case. There are two main approaches of reliability analysis; one based on the variability characteristics of the FS and the second on the variability characteristics of the uncertain parameters. The latter corresponds to the method of analysis known as FORM. The two approaches were used with different representations of the input parameters, including the posterior samples from the Bayesian analysis of data, to conform six procedures of reliability evaluation aimed at evaluating the effect of specific aspects of the analysis.

The slope stability analysis with the program Slide was carried out by sampling from beta distributions fitted to the posterior samples from the Bayesian analysis. The MC sampling from the beta distributions included 100,000 trials, whereas the posterior samples from the MCMC sampling had 50,000 points. The conventional FORM analysis is based on the constrained minimization of a function that uses the characteristics of the beta distributions. However, the use of the FORM with the distribution samples is straight forward as the FS and distance to the mean is calculated for every point of the sample. The constrained minimization is reduced to screening the samples where *FS* = 1 and finding the design point as that with the minimum distance to the mean. The results of the analyses with the FORM were consistent, confirming the validity of the adaptation of the method for the use with sampled distributions rather than with functions describing those distributions.

In general, the analyses based on sampling from fitted distributions resulted in slight differences, with smaller PF and larger β values than those using the original posteriors. It was argued that the posterior distribution samples from the Bayesian analysis provide a more accurate representation of the uncertainty of the input parameters than that given by the fitted beta distributions. The structure of the posterior samples carries the information provided by the data used in the analysis, but this structure is not reproduced in complete detail with the MC sampling.

There are slight differences between results from procedures based on the variability of FS and those based on a FORM analysis. None of the procedures has all the desirable features that would make it the procedure of choice with the expected best results. However, it is suggested that the FORM approach applied to the MCMC samples (procedure 6) has the best set of conditions of analysis to provide consistent measures of the reliability of the slope. The procedure uses the best representation of the uncertainty of the input parameters and does not depend on the precision of the RS over the whole parameter domain. The RS is only used to estimate FS on the LSS near the design point and can be conveniently constructed with few model runs.

Acknowledgements

The first author is supported by the LOPII project and by SRK Consulting South Africa. Their support is greatly appreciated.

References

Baecher, G.B. and Christian, J.T., 2003. *Reliability and statistics in geotechnical engineering.* Wiley, Chichester, UK.

Bieniawski, Z.T., 1989. *Engineering rock mass classifications*. New York, Wiley Interscience.

Bucher, C.G. and Bourgund, U., 1990. A fast and efficient response surface approach for structural reliability problems. *Structural Safety*, 7(1), 57–66.

Box, G.E.P. and Draper, N.R., 2007. *Response Surfaces, Mixtures, and Ridge Analyses*. 2nd edition, Wiley Series in Probability and Statistics, Hoboken, New Jersey.

Cai, M., Kaiser, P.K., Uno, H., Tasaka, Y. and Minami, M., 2004. Estimation of rock mass deformation modulus and strength of jointed hard rock masses using the GSI system. *International Journal of Rock Mechanics and Mining Sciences*, 41(1), 3–19.

Cai, M. and Kaiser, P.K., 2006. Visualization of rock mass classification systems. *Geotechnical and Geological Engineering*, 24, 1089–1102.

Contreras L.F., Brown E.T. and Ruest M., 2018. Bayesian data analysis to quantify the uncertainty of intact rock strength. *Journal of Rock Mechanics and Geotechnical Engineering*, 10(1), 11-31.

Duncan, J.M. and Sleep, M.D., 2015. Evaluating reliability in geotechnical engineering. *Risk and Reliability in Geotechnical Engineering*. K.K. Phoon and J. Ching (editors). CRC Press, Boca Raton, 131–179.

Duran A., 2016. Rock mass assessment – what goes wrong? In P. Dight (editor). *Proceedings of the First Asia- Pacific Slope Stability in Mining Conference*, Brisbane, Australia. Australian Centre for Geomechanics, Perth, 493-506.

Feng, X. and Jimenez, R., 2015. Estimation of deformation modulus of rock masses based on Bayesian model selection and Bayesian updating approach. *Engineering Geology,* 199, 19–27.

Foreman-Mackey, D., Hogg, D.W., Lang, D. and Goodman, J., 2013. emcee: The MCMC Hammer. *Publications of the Astronomical Society of Pacific*, 125(925), 306–312.

Forrester, A.I.J., Sobester, A. and Keane, A.J., 2008. *Engineering Design via Surrogate Modelling: A Practical Guide*. John Wiley and Sons, Ltd.

Goh A.T.C. and Zhang W., 2012. Reliability assessment of stability of underground rock caverns. *International Journal of Rock Mechanics and Mining Sciences*, 55, 157–163.

Hasofer, A. M., and Lind, N., 1974. An exact and invariant first-order reliability format. *Journal of Engineering Mechanics*, ASCE, 100(1), 111-121.

Hoek, E., 1994. Strength of rock and rock masses. *International Society for Rock Mechanics News Journal*, 2(2), 4-16.

Hoek E. and Brown E.T., 1997. Practical estimates of rock mass strength. *International Journal of Rock Mechanics and Mining Sciences*, 34(8), 1165–1186.

Hoek E., Carranza-Torres C. and Corkum B., 2002. Hoek-Brown failure criterion – 2002 edition. *Proceedings of the fifth North American rock mechanics symposium*, Toronto, Canada, 1, 267–273.

Hoek, E., Carter, T.G. and Diederichs, M.S., 2013. Quantification of the Geological Strength Index Chart. *Proceedings of the 47th US Rock Mechanics / Geomechanics Symposium*, San Francisco, 23-26 June, Paper ARMA 13–672, 8 p.

Jin, R., Chen, W. and Simpson, T.W., 2001. Comparative studies of metamodeling techniques under multiple modelling criteria. *Structural and multidisciplinary optimization*, 23(1), 1-13.

Low, B. K. and Tang, W. H., 1997. Efficient reliability evaluation using spreadsheet. *Journal of Engineering Mechanics*, ASCE, 123(7), 749–752.

Low, B.K. and Tang, W. H., 2004. Reliability analysis using object-oriented constrained optimization. *Structural Safety*, Elsevier Science Ltd., Amsterdam, 26(1), 69–89.

Low B.K. and Tang W.H., 2007. Efficient spreadsheet algorithm for first-order reliability method. *Journal of Engineering Mechanics*, ASCE, 133(12), 1378–1387.

Low, B. K., 2008. Efficient probabilistic algorithm illustrated for a rock slope. *Rock Mechanics and Rock Engineering*, 41(5), 715–734.

Miranda, T., Correia, A.G. and Sousa, L. R., 2009. Bayesian methodology for updating geomechanical parameters and uncertainty quantification. *International Journal of Rock Mechanics and Mining Sciences*; 46(7), 1144–1153.

Palmström, A., 1996. Characterizing rock masses by the RMi for use in practical rock engineering. *Journal of Tunnelling and Underground Space Technology*, 11(2), 175-188.

Perras, M.A. and Diederichs, M.S., 2014. A Review of the Tensile Strength of Rocks: Concepts and Testing. *Geotechnical and Geological Engineering*, 32(2), 525–546.

Python Software Foundation, 2001. *Python language reference*, version 3.4 [on line]. [Accessed 20/01/2015]. https://www.python.org/.

Rocscience Inc., 2016. Slide v7.0 – Two-Dimensional Limit-Equilibrium Analysis of Soil and Rock Slopes.

Russo, G., 2009. A new rational method for calculating the GSI. *Journal of Tunnelling and Underground Space Technology*, 24(1), 103–111.

Sonmez, H. and Ulusay R., 1999. Modifications to the geological strength index (GSI) and their applicability to stability of slopes. *International Journal of Rock Mechanics and Mining Sciences*, 36, 743–760.

Steffen, O.K.H., Contreras, L.F., Terbrugge, P.J. and Venter, J., 2008. A risk evaluation approach for pit slope design. *Proceedings of the 42nd US Rock Mechanics Symposium* *and 2nd US-Canada Rock Mechanics Symposium*, San Francisco, 29 June - 2 July, Paper ARMA 08–231, 18 p.

Straub, D. and Papaioannou, I., 2015. Bayesian analysis for learning and updating geotechnical parameters and models with measurements. *Risk and Reliability in Geotechnical Engineering*. K.K. Phoon and J. Ching (editors). CRC Press, Boca Raton, 221–264.

Tan, X., Shen, M., Hou, X., Li, D. and Hu N., 2013. Response Surface Method of Reliability Analysis and its Applications in Slope Stability Analysis. *Geotechnical and Geological Engineering*, 31(4), 1011-1025.

Wang, Y. and Aladejare A.E., 2015. Selection of site-specific regression model for characterization of uniaxial compressive strength of rock. *International Journal of Rock Mechanics and Mining Sciences,* 75, 73–81.

Wang Y., Cao Z. and Li D., 2015. Bayesian perspective on geotechnical variability and site characterization. *Engineering Geology*, 203, 117-125.

Zhang, L.L., Zhang, J., Zhang, L.M. and Tang, W.H., 2010. Back analysis of slope failure with Markov chain Monte Carlo simulation. *Computers and Geotechnics*, 37(7–8), 905-912.

Chapter 6 - Slope Reliability and Back Analysis of Failure with Geotechnical Parameters Estimated Using Bayesian Inference

Luis-Fernando Contreras[a], Edwin T. Brown[b]

[a] The University of Queensland, Brisbane, Australia.

[b] Golder Associates Pty. Ltd, Brisbane, Australia.

Corresponding author: luis.contreras@uq.net.au

Abstract

A Bayesian approach is proposed for the inference of the geotechnical parameters used in slope design. The methodology involves the construction of posterior probability distributions that combine prior information on the parameter values with typical data from laboratory tests and site investigations used in design. The posterior distributions are often complex, multidimensional functions whose analysis requires the use of Markov Chain Monte Carlo (MCMC) methods. These procedures are used to draw representative samples of the parameters investigated, providing information on their best estimate values, variability and correlations. The paper describes the methodology to define the posterior distributions of the input parameters for slope design and the use of these results for the evaluation of the reliability of a slope with the first order reliability method (FORM). The analysis of reliability corresponds to a forward analysis of stability of the slope where the factor of safety (FS) is calculated with a surrogate model from the more likely values of the input parameters. The Bayesian model is also used to update the estimation of the input parameters based on the back analysis of slope failure. In this case, the condition FS=1.0 is treated as a data point that is compared with the model prediction of FS. The analysis requires a sufficient number of observations of failure to outbalance the effect of the initial input parameters. The parameters are updated according to their uncertainty, which is determined by the amount of data supporting them. The methodology is illustrated with an example of a rock slope characterised with a Hoek-Brown rock mass strength. The example is used to highlight the advantages of using Bayesian methods for the slope reliability

analysis and to show the effects of data support on the results of the updating process from the back analysis of failure.

Keywords: Bayesian analysis; Hoek-Brown criterion; slope reliability; back analysis of failure

6.1 Introduction

Probabilistic methods are normally used to represent uncertainty in engineering design. However, there are two interpretations of probability, which give rise to the two main approaches to statistical analysis known as frequentist and Bayesian. Contreras et al. (2018) discuss the contrast between the two approaches in terms of the inference of parameters for mine slope design, highlighting the advantages of using Bayesian methods in this context. The Bayesian analysis includes the construction of a probabilistic function using data, models and previous information on the values of the parameters. The function is called a posterior distribution within the Bayesian framework and it is evaluated with a Markov Chain Monte Carlo (MCMC) procedure in order to obtain representative samples of the parameters investigated. The posterior samples represent a balanced result between the data used and the prior information available on the parameters. Contreras et al. (2018) described in detail the methodology with reference to the inference of the intact rock strength parameters, and Contreras and Brown (2018) discussed the analysis of the reliability of the slope with the results from a Bayesian analysis of data. Other examples of Bayesian analysis in rock mechanics are given by Miranda et al. (2009), Zhang et al. (2010), Feng and Jimenez (2015), Wang and Aladejare (2016) and Aladejare and Wang (2017).

The paper discusses three aspects of the slope design process. First, the Bayesian inference of the rock mass strength parameters required for the slope stability analysis; secondly, the use of these results for the evaluation of the reliability of the slope; and thirdly, the Bayesian updating of the parameters based on observations of slope failure. Contreras and Brown (2018) covered the first two aspects in detail. Part of that material has been updated and it is summarised in the present paper to facilitate the presentation of the steps of the slope design process.

The main changes in the paper relative to the material presented by Contreras and Brown (2018) are:

- Section 6.2.1 includes a simplified presentation of the formulae for the implementation of the Bayesian inference procedure.
- Section 6.2.2 includes the update of the inference of the intact rock strength parameters considering the latest developments to appear in the next version of the Hoek-Brown (H-B) criterion (Hoek and Brown, 2019). This means excluding tensile strength data and using the tensile cut-off instead.
- Section 6.2.2 also includes a simplified presentation of the likelihood formula and a brief discussion on the relationship between data quantity and uncertainty of the intact rock strength estimation.
- Section 6.2.3 incorporates an update to the Geological Strength Index (GSI) chart calibration using a simpler three-parameter model, instead of the five-parameter model of the original Cai et al. 2004 chart and includes a simplified presentation of the likelihood formula for chart calibration.
- Section 6.3 excludes the comparison of various methods of slope reliability analyses and uses the first order reliability method (FORM) validated by Contreras and Brown (2018).
- Section 6.4 excludes the comparison of methods of response surface (RS) analysis and uses the method recommended by Contreras and Brown (2018) on the basis of the comparison.
- Section 6.5 includes a description of the Bayesian back analysis of slope failure as a way to update the parameters from observations of slope performance, and discusses the relationship between data support, parameter uncertainty and updating the results.

6.2 Bayesian inference of geotechnical parameters for slope design

The methodology commonly used for the rock mass strength characterisation for slope design is based on the H-B criterion as illustrated in Figure 6.1 (Contreras and Brown, 2018). The intact rock strength is defined by the H-B parameters σ_{ci} and m_i, derived from uniaxial (UCS) and triaxial (TCS) compression strength test data. The *GSI* is based on charts describing the structural characteristics of the rock mass on the vertical axis and the joint conditions on the horizontal axis. The chart used in this paper is based on the block volume (V_b) and the joint condition rating (J_C) from Palmström (1996), as described by Cai et al. (2004). The rock mass disturbance factor (D) represents the reduction of strength due to damage from blasting close to the surface of the excavation or from stress relief at deeper levels. It is common to calculate equivalent Mohr-Coulomb (M-C) parameters for particular stress levels to simplify the analysis of stability with a two-parameter strength model, which allows the visualisation of certain aspects of the slope reliability calculation.

The conventional method to estimate the geotechnical parameters used in slope design considers fitting data to models to obtain point estimates and sometimes variability characteristics of these parameters. However, this approach has limitations in providing adequate representation of the uncertainty of parameters (Contreras et al. 2018). In contrast, the uncertainty of parameters quantified with the Bayesian approach reflects the balance between the data and prior knowledge used in the analysis.

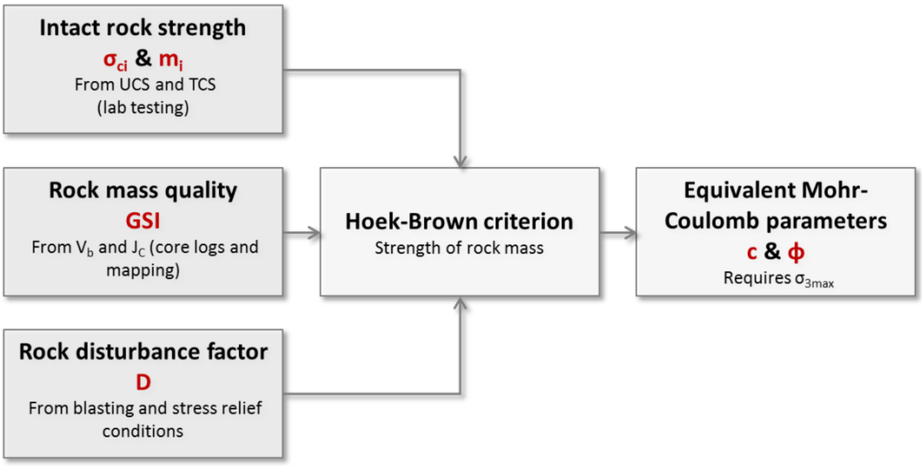

Figure 6.1 Characterisation of rock mass strength for slope design (Contreras and Brown, 2018)

6.2.1 Concept of Bayesian inference of parameters

The concept of Bayesian inference of parameters is illustrated in Figure 6.2 (Contreras and Brown, 2018). This diagram describes the structure of the posterior probability function constructed with Bayes' formula. The posterior function includes a model function, the data and the prior knowledge of the parameters for inference. The model function provides a model prediction, y_{model}, of the performance of the system it represents, based on the parameters for inference, θ, and the predictor variables, x. The data correspond to actual measurements of performance of the system, y_{actual}, to compare with the model predictions. The prior knowledge refers to available information on the parameter values and typically corresponds to valid ranges defined by low and high bound values. The posterior function takes as input a set of parameters for inference θ_1 to θ_k and yields a probability value, p, for that set. The evaluation of the posterior function gives, as a result, the sets of θ associated with the largest p values, in other words, the more probable parameter values.

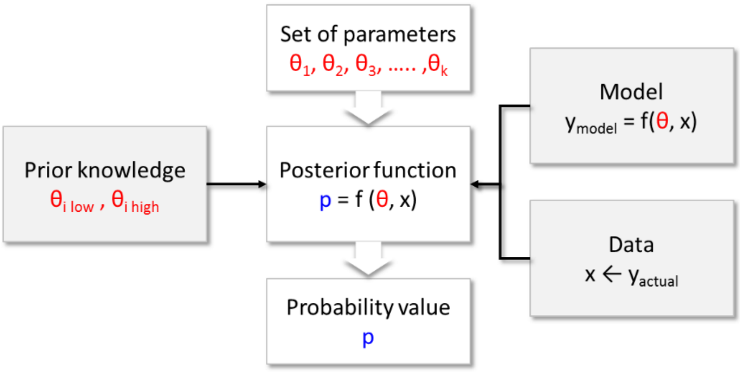

Figure 6.2 Conceptual representation of the Bayesian process for inference of parameters (Contreras and Brown, 2018)

The posterior function according to the Bayes rule defines the probability of the parameters for inference contained in the vector $\boldsymbol{\theta}$ as follows:

$$p(\boldsymbol{\theta}|data) = k\ L(\boldsymbol{\theta}|data)p(\boldsymbol{\theta}) \tag{6.1}$$

where $L(\boldsymbol{\theta}|data)$ is the likelihood of the parameters given the data, $p(\boldsymbol{\theta})$ corresponds to the prior distributions of those parameters and k is a normalisation factor so that the posterior function integrates to one. The value of k is not required for the inference of parameters with an MCMC procedure. The vector $\boldsymbol{\theta}$ contains the parameters of interest included in the model function and the parameters defining the Student or normal distributions commonly used to model the errors. If a normal distribution with standard deviation σ is used to evaluate the errors and the probability density function (pdf) of the normal distribution at x is expressed as N_{pdf} (x, mean, standard deviation), then the likelihood function for a data set with n values is:

$$L(\boldsymbol{\theta}|data) = \prod_{j=1}^{n} N_{pdf}(y_{actual\ j}; y_{model}; \sigma) \tag{6.2}$$

If the priors are represented by uniform distributions, then:

$$p(\theta) = \frac{1}{(\theta_{1\ high} - \theta_{1\ low})} \frac{1}{(\theta_{2\ high} - \theta_{2\ low})} \ldots \ldots \frac{1}{(\theta_{k\ high} - \theta_{k\ low})} \tag{6.3}$$

The evaluation of the posterior function is carried out with MCMC procedures due to the high dimensionality and complexity of the function. The result of the MCMC analysis consists of representative samples of the parameter values, which are normally displayed in a graph that collects the scatter plots and histograms of the sampled values. The Bayesian analyses presented in the paper were implemented in the Python programming language, using the MCMC algorithm known as the affine-invariant ensemble sampler developed by Foreman-Mackey et al. (2013). Additional information of the Bayesian approach can be found in Baecher (2017) and Juang and Zhang, (2017).

6.2.2 Bayesian inference of intact rock strength parameters σ_{ci} and m_i

The Bayesian inference of the intact rock strength parameters is discussed in detail by Contreras et al. (2018) and Contreras and Brown (2018). The intact rock strength is characterised with the Hoek-Brown (H-B) strength criterion (Hoek and Brown, 1997) defined by the following equation:

$$\sigma_1 = \sigma_3 + \sigma_{ci}\left(m_i \frac{\sigma_3}{\sigma_{ci}} + 1\right)^{0.5} \tag{6.4}$$

where σ_{ci} is the uniaxial compressive strength of intact rock, m_i is a constant of the intact rock material, σ_1 and σ_3 are the major and minor principal stresses, respectively. The latest edition of the Hoek-Brown strength criterion (Hoek & Brown, 2019) indicates that the criterion is not applicable to tensile failure and recommends using the tensile cut-off proposed by Hoek and Martin (2014) as a practical solution to define the strength envelope for design purposes. The tensile cut-off suggested by Hoek and Brown (2018) is given by the ratio between σ_{ci} and the intact tensile strength of the rock, σ_t, as follows:

$$\frac{\sigma_{ci}}{|\sigma_t|} = 0.81m_i + 7 \tag{6.5}$$

The components of the Bayesian model described in Figure 6.2 are the function model represented by Eq. (6.4) with σ_{ci} and m_i being the parameters for inference; the data represented by the results of TCS and UCS tests; and the prior information consisting of uniform distributions defining plausible ranges of variation of the parameters. A typical intact rock strength data set of 23 points (8 UCS and 15 TCS) was randomly generated to illustrate the methodology. The example presented in this paper considers prior ranges between 10 MPa and 200 MPa for σ_{ci}, and between 1 and 40 for m_i.

The core calculation within the posterior probability function is the evaluation of errors within the likelihood function. The errors are defined as the difference between the actual data values and the H-B model predictions using a particular set of parameters. The errors are evaluated with Student's t-distributions for better handling of outliers. Small errors result in high probability values and vice versa. The t-distribution is defined by three parameters; hence, the pdf at x can be expressed as t_{pdf} (x; mean; scale; normality). The likelihood function L_1 for the intact rock strength estimation is:

$$L_1\left(\sigma_{ci}, m_i, \sigma_s, \nu_s \middle| (UCS, TCS)_j\right) = \prod_{j=1}^{n1} t_{pdf}(\sigma_{1j}\ from\ UCS, TCS; \sigma_{1\ j} from\ eq. 4; \sigma_s; \nu_s) \tag{6.6}$$

In this case, x is defined by the UCS and TCS data points, $n1$ is the number of data points, the mean is determined by the H-B model given by Eq. (6.4), σ_s is the scale and ν_s is the normality parameter of the t-distribution. Figure 6.3 shows the data points and explains the way in which errors are evaluated with the t-distribution in the Bayesian analysis.

The results of the intact rock strength analysis are summarised in the corner plot of Figure 6.4. The scatter plot shows the correlation between the inferred parameters and the histograms define the ranges of likely values. The intact rock strength analysis was carried out for three stages with increased levels of data to show the relationship between data quantity and the uncertainty of the estimation. The data correspond to simulated compression test results representing typical values of intact strength of a particular rock type. The data sets included 10 (5 UCS + 5 TCS), 18 (8 UCS + 10 TCS) and 23 (8 UCS + 15 TCS) data points and the results of the fitting analysis are shown in Figure 6.5.

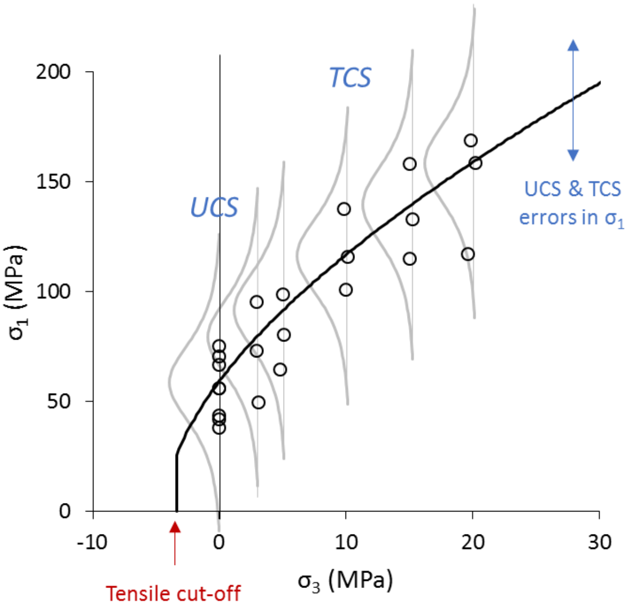

Figure 6.3 Measurement of errors with a t-distribution to handle outliers (adapted from Contreras and Brown, 2018)

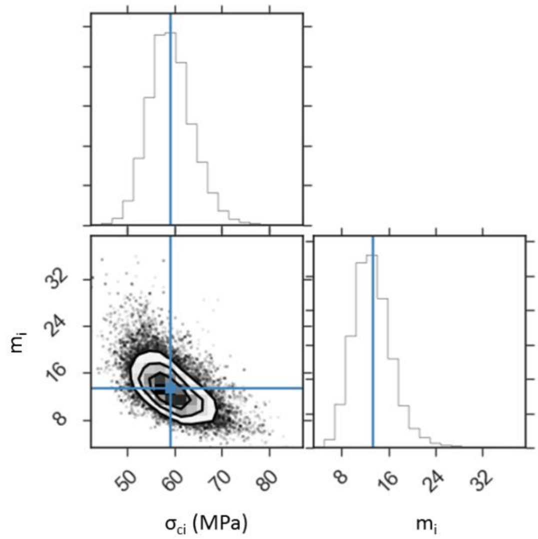

Figure 6.4 Corner plot from the analysis of the intact rock strength data. The plot shows the scatter plot of σci and mi and the histograms of these parameters

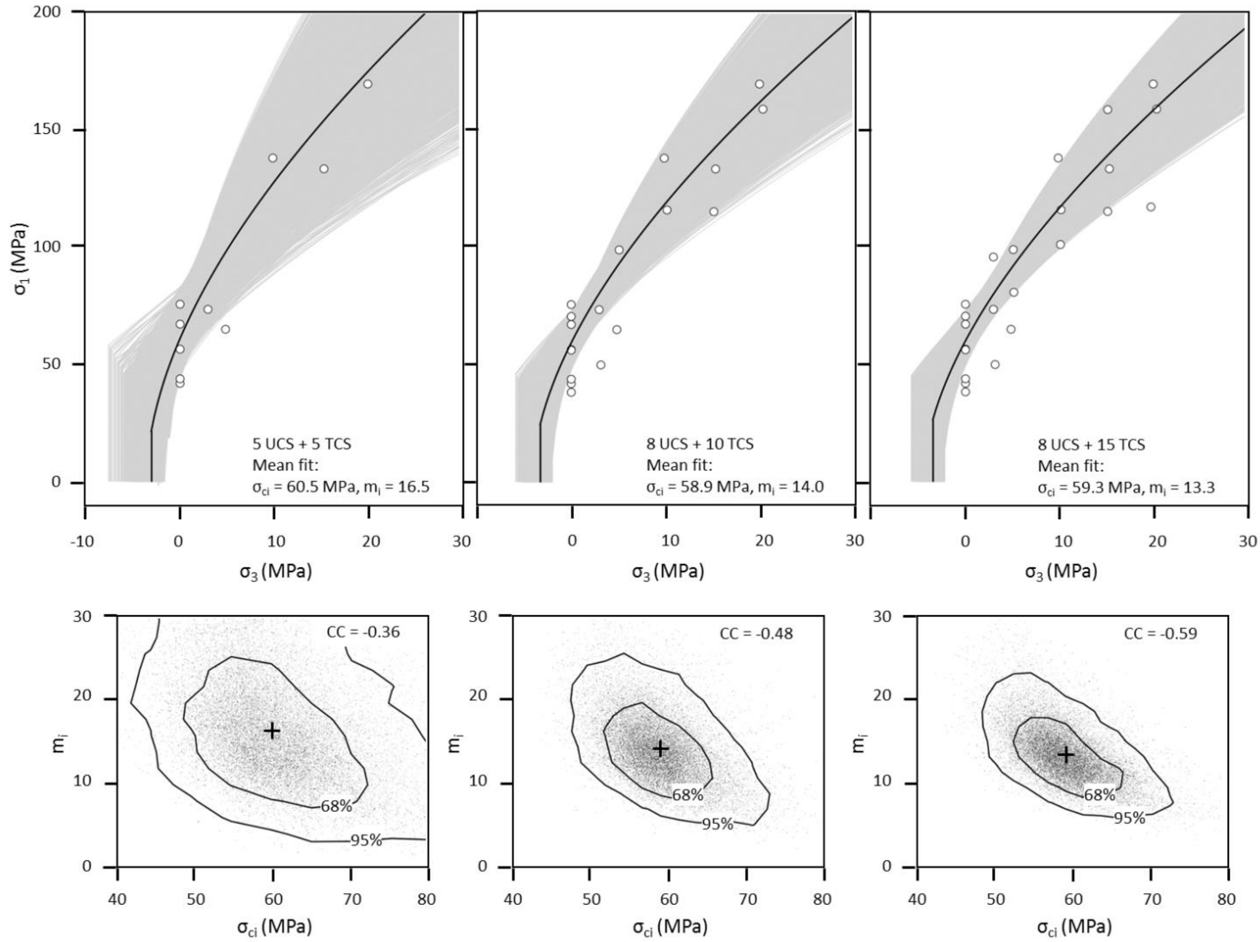

Figure 6.5 Mean fitted envelopes with bands including the 95 percentile of sampled parameter values for three levels of data (top) and the corresponding scatter plots of m_i versus σ_{ci} from the Bayesian regression analysis with 68 and 95 percentile contours and coefficients of correlation CC (bottom)

The graphs of σ_1 versus σ_3 at the top of Figure 6.5 show the data points and the band of envelopes corresponding to the 95% highest density intervals (HDIs) reflecting the uncertainty of parameters. The 95% HDIs define the ranges of credible values and the mean values represent the more likely estimates. The scatter plots of the 50,000 sampled values of σ_{ci} and m_i with the 68 and 95 percentile contours are shown at the bottom of Figure 6.5. These results show the reduction in the uncertainty of the estimated envelopes with the increase of the number of TCS results used for the regression analysis. This reduction is particularly noticeable in the high confining stress region. In the low confining stress region, the intercept of the envelope associated with σ_{ci} is well defined with relatively few UCS data points.

Figure 6.6 shows a comparison of the mean fitted envelopes from the analysis with the three levels of data. The envelopes are close in the low confining stress region and the differences are associated with the number of TCS data points used in the analysis. These results suggest that at least 10 TCS data points are required in this particular case to define a reliable mean envelope. A sufficient number of TCS results is required to outbalance the effect of the vague priors of σ_{ci} and m_i as seems to be the case for the second and third stages with 10 and 15 TCS results, respectively.

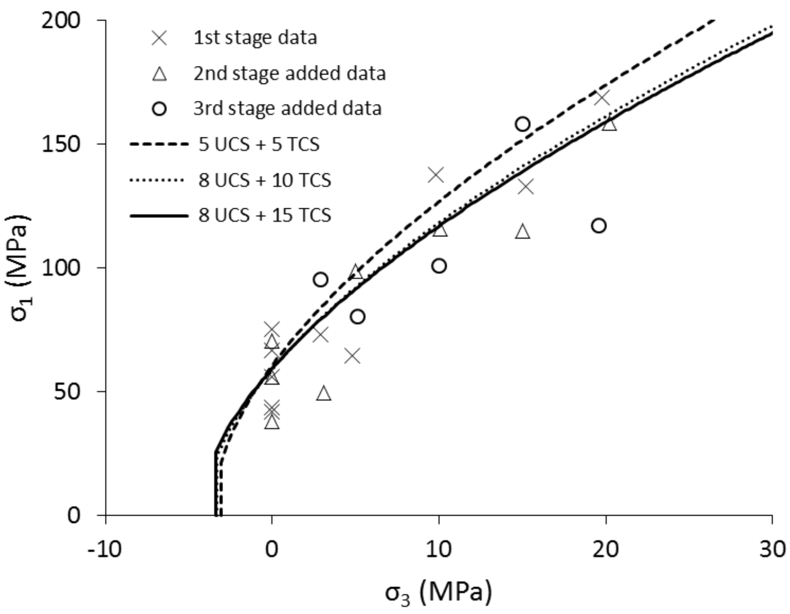

Figure 6.6 Mean fitted envelopes for three stages with increased levels of data

6.2.3 Bayesian inference of GSI chart parameters

The Bayesian inference of the GSI chart parameters is discussed by Contreras and Brown (2018). The GSI index describes the rock mass quality within the H-B failure criterion for rock masses. Hoek and Brown (1997) defined the index as an independent parameter with the look-up chart shown in Figure 6.7. The chart includes qualitative descriptions of rock mass structure and joint conditions on the vertical and horizontal axes, respectively. The chart is used to estimate credible ranges of GSI with a typical precision of ±5 points. The main drawback of this method of estimation is the subjectivity that increases the uncertainty of the index due to the human factor. Several authors have proposed alternative charts for the quantitative evaluation of GSI based on measured factors as a way of reducing the subjectivity of the estimation (Sonmez and Ulusay, 1999; Cai et al. 2004; Russo, 2009; Hoek et al., 2013). Unfortunately, none of the quantitative charts has gained general acceptance because they do not appear to fit the historical records in all cases. One possible cause of this situation is that the H-B system includes two subjective parameters, namely GSI and D, which are handled differently by different mine operations. In many cases, these parameters become eventually used as calibration parameters of slope performance.

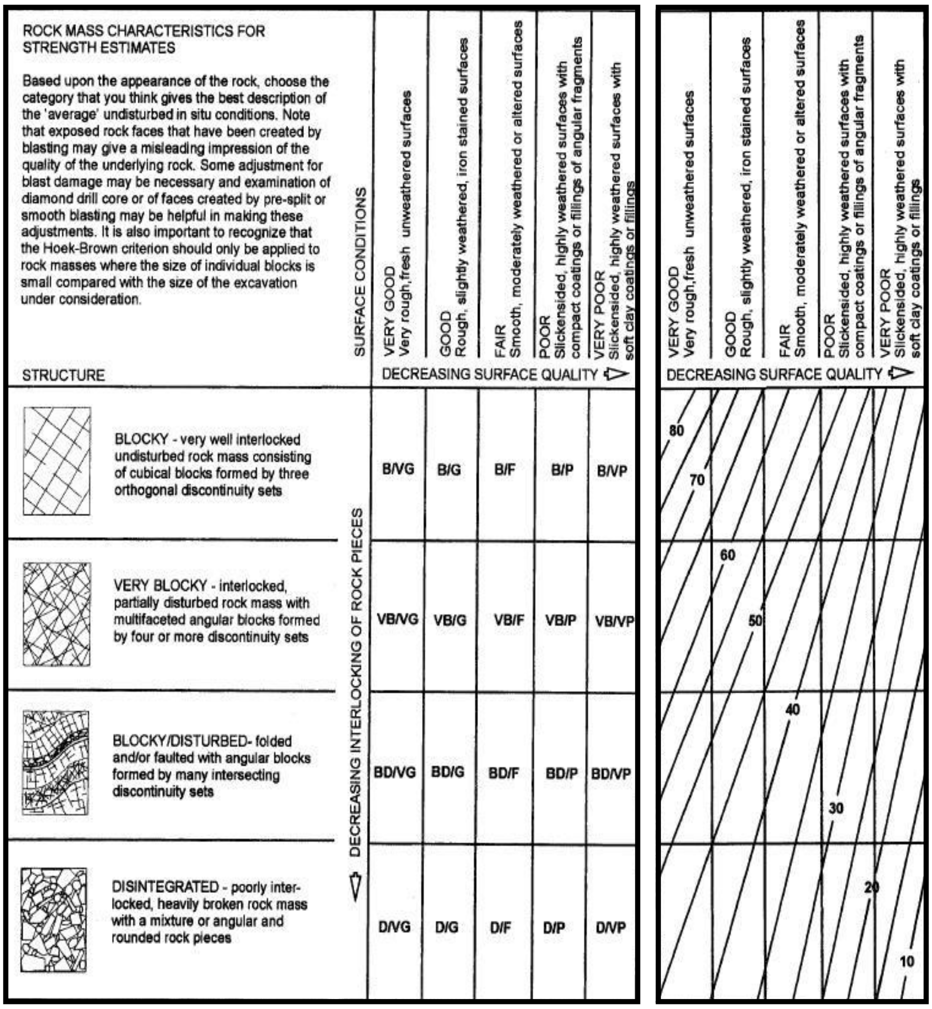

Figure 6.7 Charts with the original definition of GSI (Hoek and Brown, 1997, based on Hoek, 1994)

The Bayesian inference of GSI requires a model whose results can be compared with actual measurements through a probabilistic function. Contreras and Brown (2018) consider the chart proposed by Cai et al. (2004) to describe the Bayesian inference of GSI because it is the chart that appears to provide the best results (Duran, 2016). Cai et al. (2004)'s GSI chart corresponds to a surface defined by the following two-dimensional function with parameters J_C and V_b (Cai and Kaiser, 2006):

$$GSI = \frac{26.5 + 8.79 lnJ_C + 0.9 lnV_b}{1 + 0.0151 lnJ_C - 0.0253 lnV_b} \quad (6.7)$$

Contreras and Brown (2018) use Eq. (6.7) to describe the Bayesian regression analysis for calibration of the chart with site-specific data. In this case, the five coefficients defining the chart surface are inferred with the Bayesian approach. The uncertainty of the chart is then used to define the variability of the mean GSI of a particular rock unit based on J_C and V_b data collected for design. Cai and Kaiser (2006) point out that the chart represented by Eq. (6.7) is very close to a planar surface; therefore, for the purpose of a regression analysis with site specific data it is acceptable to use a simplified chart model based on three parameters as follows:

$$GSI = \rho_0 + \rho_1 lnJ_C + \rho_2 lnV_b \quad (6.8)$$

where ρ_0, ρ_1 and ρ_2 are the coefficients.

A planar surface estimated from Eq. (6.8) is a good approximation of the Cai et al (2004) model chart calibrated to local conditions. Figure 6.8 shows the Cai et al. (2004) chart and its geometrical interpretation. The Bayesian estimation of GSI using the three-parameter model chart is illustrated with the same calibration data set of 50 measurements used by Contreras and Brown (2018), as shown in the graphs on the right of Figure 6.8 and the left of Figure 6.9. The data set represents the result of a hypothetical face mapping exercise in which V_b and J_C estimates are collected independently from GSI determinations with the original look-up chart in Figure 6.7. The Bayesian analysis uses the data set and the model predictions with Eq. (6.8) to derive credible estimates of the coefficients ρ_0, ρ_1 and ρ_2. In a real case situation, the data for calibration of the chart may also include information from various project sites where measurements of the input factors are available together with GSI determinations from the performance of the rock mass.

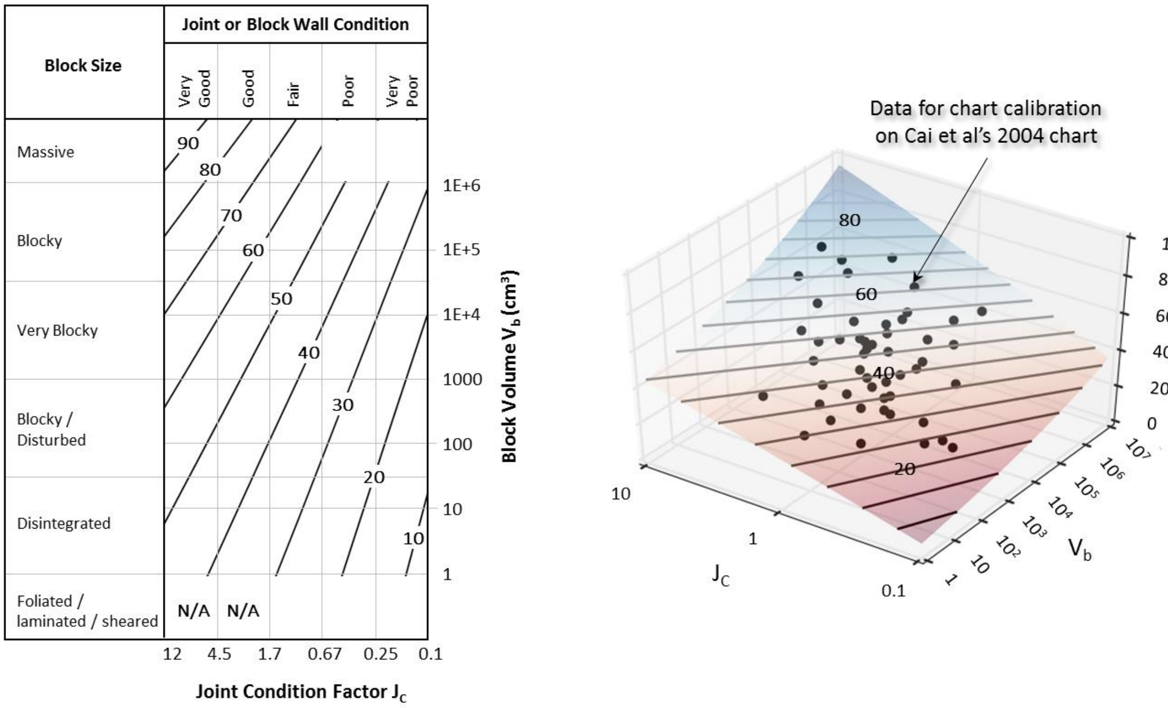

Figure 6.8 Chart (Cai et al., 2004) for the numerical estimation of GSI from Vb and JC indices (left) and interpretation of the chart as an approximate planar surface in a logarithmic space of the variables *Vb* and J_C (right). The dots correspond to a synthetic data set of 50 measurements used for calibration of the chart (Contreras and Brown, 2018)

The posterior function combines the likelihood function with the prior information. The difference between the actual GSI measurements and the model predictions using particular sets of chart parameters define the errors, which are evaluated with t-distributions within the likelihood function. The t-distribution is defined by three parameters and the pdf at *x* can be expressed as t_{pdf} (*x*; mean; scale; normality). The likelihood function L_2 for the inference of the GSI chart parameters is:

$$L_2\left(\rho_0, \rho_1, \rho_2, \sigma_g, \nu_g \middle| (J_c, V_b, GSI)_{cal\ j}\right) = \prod_{j=1}^{n2} t_{pdf}(GSI_j\ from\ calibration\ data; GSI_j from\ eq.8; \sigma_g; \nu_g) \quad (6.9)$$

In this case, *x* is defined by the chart calibration data points, *n2* is the number of data points, the mean is determined by the three-parameter chart model in Eq. (6.8), σ_g is the scale and v_g the normality parameter of the t-distribution. The priors of ρ_0, ρ_1 and ρ_2 are represented by uniform distributions with wide ranges around the values in the numerator of Eq. (6.7) to avoid constraining the results. The Bayesian analysis was implemented in the Python programming language and the MCMC sampling was carried out with the emcee sampler. The results are summarised in the scatter plots and histograms of ρ_0, ρ_1 and ρ_2 shown in Figure 6.10.

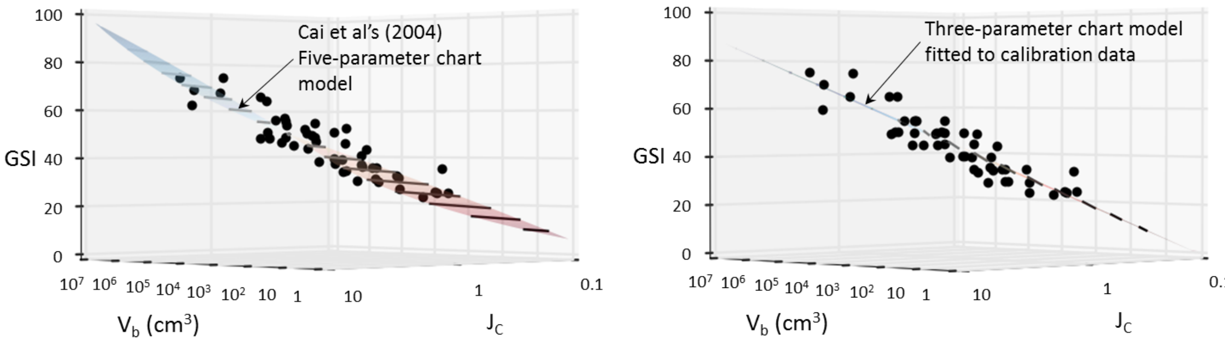

Figure 6.9 Random Gaussian spread with a standard deviation of 5 centred at Cai et al.'s (2004) chart model used to generate the calibration data set shown in Figure 6.9 (left) and calibration data set with the three-parameter fitted chart (right)

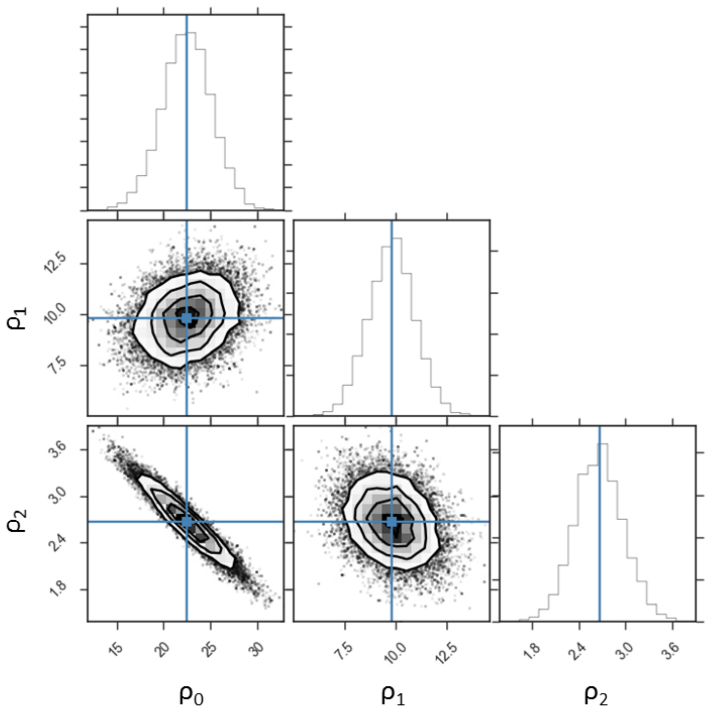

Figure 6.10 Result of the Bayesian analysis of calibration data. The corner plot shows the scatter plots and histograms of the coefficients ρ_0, ρ_1 and ρ_2 that best represent the calibration data with the three-parameter chart model function

Once the uncertainty of the chart has been defined with the calibration analysis, the results can be used to determine the variability of GSI for design. The analysis is illustrated using the same synthetic data set of 100 points used by Contreras and Brown (2018) for the analysis with the five-parameter model. The data set represents the data normally collected with core logging for the slope design; therefore, only V_b and J_C measurements are available for the estimation of GSI for design with the chart. The graph to the left of Figure 6.11 shows the data points on the mean fitted chart, which is constructed with the mean coefficients from the posterior distributions in Figure 6.10. The posterior samples have 50,000 sets of ρ_i coefficients and each set represents a plausible chart, which is used to generate a mean value of GSI from the *n3* data points as follows:

$$GSI_{mean} = \frac{1}{n3}\sum_{j=1}^{n3} GSI_j \ from \ eq. 8 \ with \ (J_c, V_b)_{design \ j} \tag{6.10}$$

The histogram of the mean values of GSI calculated in this manner is shown at the right of Figure 6.11, with the mean and the 95% HDI indicated. The distribution of GSI_{mean} values in Figure 6.11 represents the uncertainty of this parameter and can be used for the analysis of the reliability of the slope.

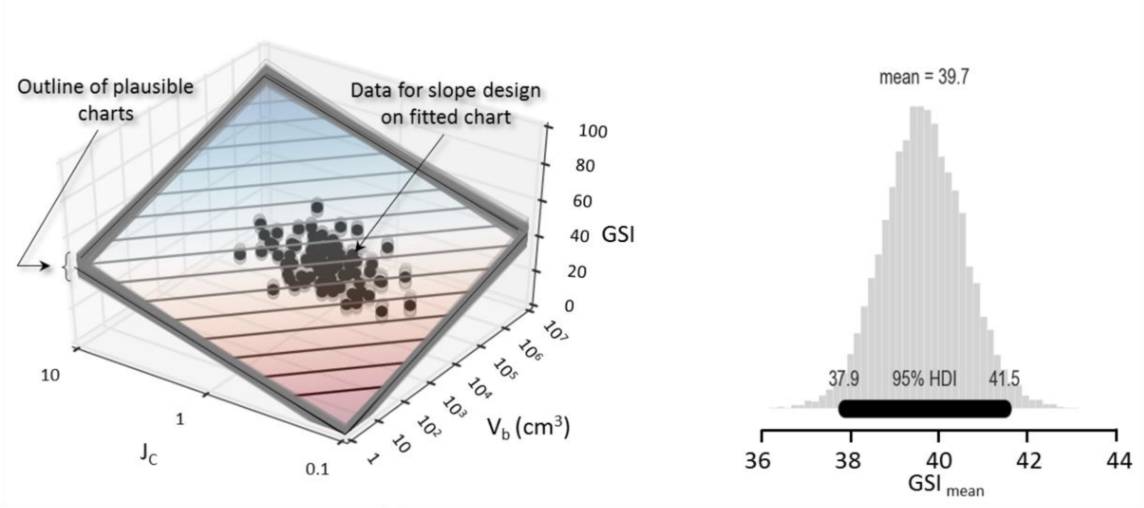

Figure 6.11 Synthetic data set of 100 measurements of Vb and JC in a local region of GSI 40, displayed on the chart fitted to the calibration observations (left). Histogram of mean values of GSI from the 100 data points with the 95% HDI indicated (right). Each value in the histogram corresponds to a set of chart coefficients from the MCMC analysis as indicated in Figure 6.11. The outlines of a selection of plausible charts causing the variability of the mean values of GSI are displayed on the isometric view of the chart on the left

6.2.4 Disturbance factor *D*

The *D* factor is based on the assessment of the damage from blasting close to the surface of the excavation. At deeper levels, *D* is associated with the disturbance from the stress relief caused by the excavation of the slopes. Typically, *D* takes values from 0.7 to 1.0 in slopes, although values outside this range are possible. Larger values represent more disturbance and are assigned to zones closer to the surface of the excavation. This parameter is not supported by data and it is commonly assessed from observation of the conditions of the excavation faces. The variability of *D* is represented in this paper by a triangular distribution between 0.6 and 1.0 with mean of 0.8. This distribution corresponds to prior information within the Bayesian framework that is not complemented with data. A set of 50,000 values were drawn from the distribution with a common Monte Carlo (MC) procedure to mimic a posterior sample of the same size as that of the inferred posteriors of the other H-B parameters.

6.2.5 Equivalent Mohr-Coulomb parameters *c* and ϕ

The equivalent M-C parameters represented by cohesion, *c* and friction angle, ϕ were calculated with the expressions given by Hoek et al. (2002). Due to the non-linearity of the H-B criterion, the analysis requires the range of confining stresses for which the equivalence is calculated. A maximum confining stress of 1.0 MPa was considered for the slope example presented in this paper. Figure 6.12 shows the scatter plot and histograms of *c* and ϕ equivalent to the H-B parameters defined with the Bayesian analysis. The advantage of using the equivalent M-C parameters is that the rock mass can be characterised with two instead of four parameters, which allows the visualisation of certain aspects of the slope reliability calculation.

The H-B parameters are in general uncorrelated or with low correlation coefficients. However, the calculated M-C parameters have a strong positive correlation. Although it is common to find a negative correlation between *c* and ϕ in soils, the result shown in Figure 6.12 is the expected situation in rock mechanics. Contreras and Brown (2018) discuss why the positive correlation for a rock mass is consistent with the situation in soil mechanics.

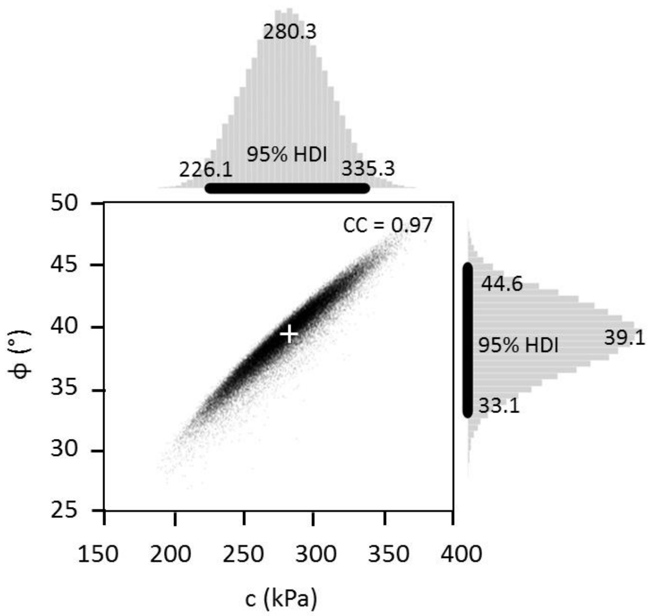

Figure 6.12 Scatter plot of equivalent c and ϕ and the respective posterior distributions with mean and 95% HDIs indicated

6.3 Analysis of reliability of a slope

Contreras and Brown (2018) described in detail the analysis of the reliability of a slope using the geotechnical parameters inferred with the Bayesian approach. The reliability of the slope is represented by the reliability index (β), which is a parameter that measures how distant the mean condition of the slope is from the failure situation. There are two methods of evaluating β, one is based on the variability characteristics of the factor of safety (FS) and the second based on the variability characteristics of the uncertain variables. The first method is the conventional procedure (Abramson et al., 2002) used in geotechnical programs and is the method used within the program Slide for slope stability analysis. The second method is known as the structural engineering method proposed by Hasofer and Lind (1974), also known as the FORM (Low and Tang, 1997, 2007; Baecher and Christian, 2003; Low, 2008; Goh and Zhang, 2012; Duncan and Sleep, 2015).

Low and Tang (1997) developed an efficient procedure to apply the FORM based on the interpretation of β shown in Figure 6.13 for the case of two variables represented by the cohesion (c) and friction angle (ϕ). The figure shows an ellipsoid centred at the mean values of c and ϕ that touches the limit state surface (LSS) at the design point. The mathematical expression to calculate β according to this interpretation is

$$\beta = min_{\boldsymbol{x}\in\boldsymbol{F}}\sqrt{\left[\frac{\boldsymbol{x_i}-\boldsymbol{\mu_i}}{\boldsymbol{\sigma_i}}\right]^T \boldsymbol{R}^{-1} \left[\frac{\boldsymbol{x_i}-\boldsymbol{\mu_i}}{\boldsymbol{\sigma_i}}\right]} \tag{6.11}$$

where $\boldsymbol{x}_i$ is the set of uncertain variables; $\boldsymbol{\mu}_i$ and $\boldsymbol{\sigma}_i$ are the sets of their respective means and standard deviations, respectively; $\boldsymbol{R}$ is the correlation matrix; and $\boldsymbol{F}$ is the failure domain. The set of $\boldsymbol{x}_i$ values that minimizes Eq. (6.11) and satisfies the condition of failure ($\boldsymbol{x} \in \boldsymbol{F}$) corresponds to the design point.

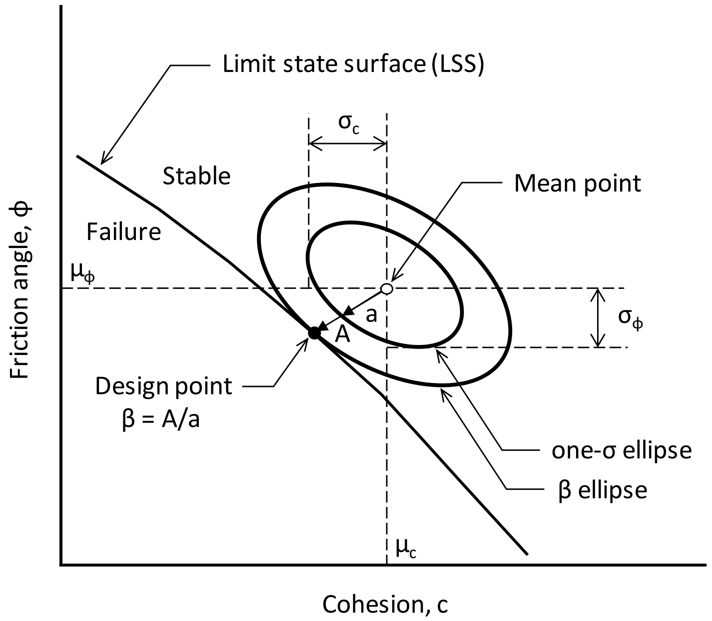

Figure 6.13 Interpretation of the reliability index β for a two-variable case corresponding to c and ϕ negatively correlated (Low, 2008)

In case of non-normal distributions, they need to be replaced by equivalent normal distributions centred at the equivalent normal mean values and the modified equation is

$$\beta = min_{\boldsymbol{x}\in\boldsymbol{F}}\sqrt{\left[\frac{\boldsymbol{x_i}-\boldsymbol{\mu_i}^N}{\boldsymbol{\sigma_i}^N}\right]^T \boldsymbol{R}^{-1} \left[\frac{\boldsymbol{x_i}-\boldsymbol{\mu_i}^N}{\boldsymbol{\sigma_i}^N}\right]} \tag{6.12}$$

where $\boldsymbol{\mu}_i^N$ and $\boldsymbol{\sigma}_i^N$ are the mean and standard deviation of the equivalent normal distributions, respectively. Eq. (6.12) can be written as (Low and Tang, 2007):

$$\beta = min_{\boldsymbol{x}\in\boldsymbol{F}}\sqrt{[\boldsymbol{n}]^T \boldsymbol{R}^{-1} [\boldsymbol{n}]} \tag{6.13}$$

where $[\boldsymbol{n}]$ is the vector with the equivalent standard normal values n_i, which can be calculated by

$$n_i = \Phi^{-1}[F(\boldsymbol{x_i})] \tag{6.14}$$

where Φ^{-1} is the inverse of the standard normal cumulative distribution function (CDF) and $F(\boldsymbol{x}_i)$ is the original non-normal CDF evaluated at $\boldsymbol{x}_i$. The procedure proposed by Low and Tang (2004, 2007) is implemented in an Excel spreadsheet and the constrained minimization of Eq. (6.13) to calculate β uses the solver built-in in Excel.

The conventional way to apply the FORM procedure proposed by Low and Tang (2004, 2007) requires, as inputs, the probability distributions representing the variability of the geotechnical parameters. However, the procedure can also be applied to the posterior distributions of the geotechnical parameters estimated with a Bayesian analysis as described by Contreras and Brown (2018). In this case, the FS and the square root term in Eq. (6.13) can be calculated for every point of the sample. In this way, the constrained minimisation reduces to screening the points where $FS = 1$ and selecting the point with the minimum value of the square root term.

The plot in Figure 6.14 illustrates the application of the method to the posterior samples of the equivalent M-C parameters shown in Figure 6.12. The sample includes 50,000 sets of c and ϕ, with mean values of 280 kPa and 39°, respectively. The points provide sufficient information to define the CDF values of any point in the sample, as well as the correlation matrix ($\boldsymbol{R}$) of the parameters. Therefore, Eqs. (6.13) and (6.14) can be used to calculate, at every point of the sample, the distance term whose minimum value represents the β index.

The sampled c and ϕ values plotted in Figure 6.14 are used to calculate the reliability of the slope of the example case described in Section 6.5. The performance function of the slope is represented by a polynomial function derived with the RS methodology as described in Section 6.4. The FS is calculated with this function for every point in the sample. The screened points from the sample where $FS = 1$ are shown in the plot as blue dots and they define the LSS. The red point ($c = 234$ kPa, $\phi = 34°$) corresponds to the minimum distance term and defines the design point with $\beta = 1.62$.

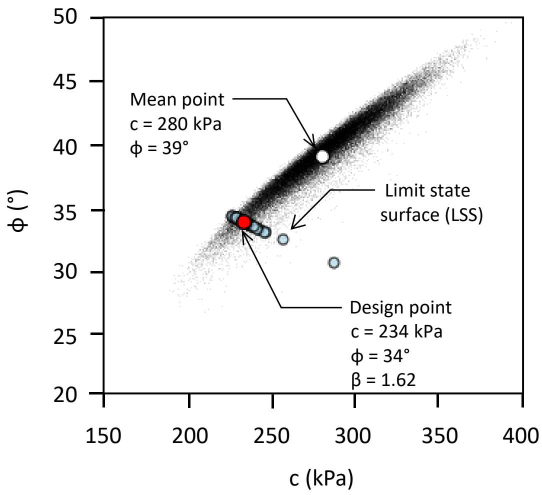

Figure 6.14 Calculation of the reliability index β with the FORM as described by Low and Tang (2004, 2007), using the posterior distributions of *c* and ϕ from the equivalent H-B parameters inferred with a Bayesian analysis

6.4 Performance function of the slope with response surface

The analysis of reliability with the FORM procedure using the MCMC posterior samples requires the slope stability model in an explicit form. This requirement can be satisfied by creating a surrogate model expressed in polynomial form using the RS methodology. The procedure is based on fitting polynomial functions to a limited number of results of planned runs with the main model. There are various types of methods used to construct surrogate models with the RS methodology; those methods more commonly used in geotechnical engineering are based on polynomial regression. Two common types of polynomial methods are the quadratic polynomial without cross terms and the product of the quadratic functions defined for each variable. Contreras and Brown (2018) compared the two methods in terms of the errors in the predictions of FS for the same case example described in this paper. The results indicate that the product of quadratic functions is the more effective method of producing smaller errors in the prediction of FS values.

The RS method based on the product of quadratic functions is described by Steffen et al. (2008) in the context of the probability of failure (PF) calculation in mine slope design. The technique uses an arrangement of values of FS calculated with a slope model resulting from changing one variable at a time from its mean value. The input variables x_i and the FS_i

responses are normalised to their mean values, defining the input factors ξ_i and the response factors δ_i as follows:

$$\xi_i = \frac{x_i}{x_{i\,mean}} \tag{6.15}$$

$$\delta_i = \frac{FS_i}{FS_{mean}} \tag{6.16}$$

The trends of δ versus ξ for each uncertain variable are fitted with the second order polynomial function:

$$\delta_i = a_i {\xi_i}^2 + b_i \xi_i + c_i \tag{6.17}$$

The group of n polynomial functions of δ_i versus ξ_i constitutes the RS and can be used as a replacement of the model to estimate FS values for any combination of input variables using

$$FS = FS_{mean}\, \delta_1(\xi_1)\, \delta_2(\xi_2) \ldots .\, \delta_n(\xi_n) \tag{6.18}$$

Figure 6.15 illustrates the methodology for a situation with the four uncertain variables from the H-B criterion used for the calculation of the FS of a slope. The curves represent the response of the FS to variations of each of the uncertain variables. The respective quadratic polynomial function is indicated at the top of each graph. The graphs were constructed using the data listed in Table 6.1. The intervals of variation of the input parameters defining the '+' and '-' cases correspond to the bounds of the 95% HDI of the posterior probability distributions of σ_{ci}, m_i and GSI described in Section 6.2. The factor D is modelled with a triangular distribution and in this case, the points of analysis correspond to the maximum and minimum values. The slope stability analyses correspond to the case example described in Section 6.5.

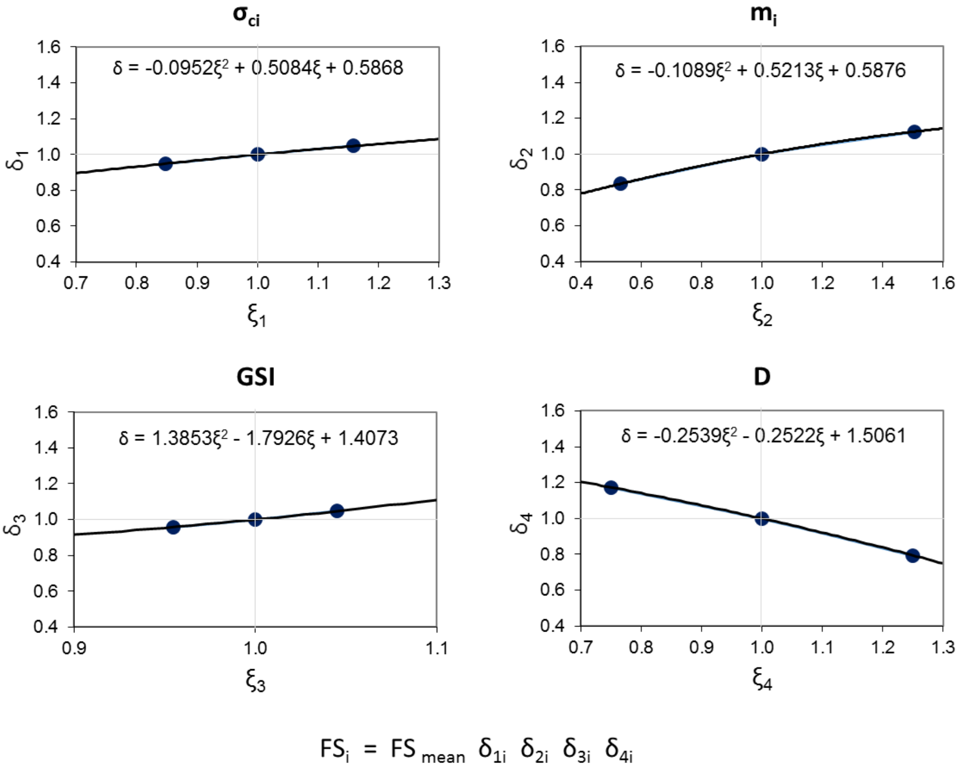

Figure 6.15 Illustration of derived influence coefficients δ_i for RS of FS from data in Table 6.1

The RS is used within the FORM process to calculate the FS of the slope for every set of input parameters. However, the RS is centred at the mean values and an error in the estimation is expected at points not close to the mean, for example where the LSS is located. For this reason, the FORM calculation is repeated with a new RS centred at a point close to the calculated design point from the previous iteration. This procedure is repeated until there is consistency between the actual FS and the RS prediction at the design point. The convergence of the process is facilitated by defining the new RS centre from linear interpolation using the following equation (Contreras and Brown, 2018, adapted from Bucher and Bourgund, 1990):

$$x_1 = x_0 + (x^* - x_0)\frac{(FS_0 - 1)}{(FS_0 - FS^*)} \tag{6.19}$$

where x_1 is the new midpoint for the new RS, x_0 is the initial midpoint (mean), x^* is the calculated design point, FS_0 is the FS at the initial midpoint, and FS^* is the FS at the design point calculated with the slope model. The reliability index calculated with the second RS centred near the design point generally converges to a stable solution.

Table 6.1 Input values and FS results for construction of RS

Model	Uncertain variable	Input values			FS		
		'-' case	mean	'+' case	'-' case	mean	'+' case
H-B	σ_{ci} (MPa)	50.3	59.3	68.7	1.17	1.23	1.29
	m_i	7.1	13.3	20.0	1.03	1.23	1.38
	GSI	37.9	39.7	41.5	1.18	1.23	1.29
	D	0.60	0.80	1.00	1.44	1.23	0.98
M-C	*c* (kPa)	226.1	280.3	335.3	1.11	1.20	1.29
	ϕ (°)	33.1	39.1	44.6	1.05	1.20	1.36

6.5 Back analysis of slope failure

The reliability analysis of the slope corresponds to a forward analysis where the expected performance of the slope is estimated from the input parameters and the slope model. The Bayesian approach can also be used to incorporate the observed performance of the slope to improve the estimation of the input parameters. This is the case of a back analysis of slope failure where the condition FS = 1 can be incorporated into the analysis as observed data. In this case, the more likely values of the input parameters are sampled from a posterior function that includes the posteriors from the intact rock strength analysis, the GSI chart calibration and the FS calculation.

The posterior function according to the Bayes' rule defines the probability of the parameters for inference contained in the vector $\boldsymbol{\theta}$ as expressed in Eq. (6.1). In the back analysis of failure case, $\boldsymbol{\theta} = (\sigma_{\mathrm{ci}}, m_{\mathrm{i}}, \sigma_{\mathrm{s}}, v_{\mathrm{s}}, \rho_0, \rho_1, \rho_2, \sigma_{\mathrm{g}}, v_{\mathrm{g}}, D, \sigma_{\mathrm{f}})$, which includes the geotechnical parameters described in Section 6.2, and the parameters of the Student's t and normal distributions used to model the errors. The likelihood functions L_1 corresponding to the intact rock strength estimation and L_2 to the GSI chart calibration, are defined by Eqs. (6.6) and (6.9), respectively. The likelihood functions L_1 and L_2 use *t*-distributions to evaluate the errors. The likelihood function L_3 describing the observations of failure in the FS calculation is based on a normal distribution to evaluate the errors. The normal distribution is defined by two parameters and its pdf at x can be expressed as N_{pdf} (x, mean, standard deviation). Hence, L_3 is written as

$$L_3\left(\sigma_{ci}, m_i, GSI_{mean}, D, \sigma_f \middle| FS1_j\right) = \prod_{j=1}^{n4} N_{pdf}(FS1_j\ from\ observations; FSfrom\ RS\ Eq.(18); \sigma_f) \tag{6.20}$$

where *FS*1 represents the observation of a failure event and *n*4 corresponds to the number of observations of this event. The compounded posterior function used for the inference of parameters with the back analysis of the slope failure is expressed as follows:

$$p(\theta|data) = k\ L_1 L_2 L_3\ p(\theta) \tag{6.21}$$

The prior probabilities of the parameters are represented by uniform distributions defined with the boundaries of credible ranges of variation of each parameter. The disturbance factor *D* is defined with a triangular distribution as described in Section 6.2.4. The posterior function in Eq. (6.21) is evaluated with an MCMC procedure to obtain representative samples of the parameters in $\boldsymbol{\theta}$.

6.6 Illustrative example

The use of the geotechnical parameters inferred with the Bayesian approach is demonstrated with the reliability analysis and the back analysis of failure of the slope shown in Figure 6.16. This example was used by Contreras and Brown (2018) to compare various procedures of reliability evaluation. The same example is included in the present paper in order to update various aspects of the rock mass characterisation process and to extend the analysis to the updating of parameters from observed slope performance. The slope is 210 m high, with a 52° overall angle and it is excavated in a rock mass characterised with an H-B strength criterion.

The stability analysis was based on the limit equilibrium method and was carried out with the program Slide from Rocscience (2016). The analyses include deterministic calculations of FS for the construction of the RS and the probabilistic analysis of reference to compare with the FORM evaluation. The probabilistic analysis includes 100,000 MC trials with inputs drawn from beta distributions fitted to the respective posterior distributions described in Section 6.2. Table 6.2 summarises the input data used for the stability analysis with the program Slide. The FS was also calculated with the RS described in Section 6.4, using the same MC trial inputs of the slope model analysis to verify the efficacy of the RS as a surrogate slope model.

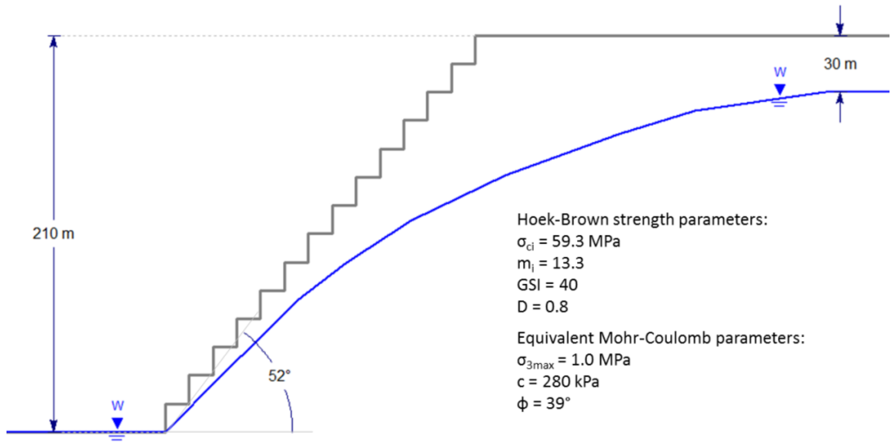

Figure 6.16 Geometry of the slope for the example of the analysis of reliability. The homogeneous rock mass is characterised by H-B strength parameters σ_{ci}, m_i, *GSI* and *D*; and the respective equivalent M-C parameters *c* and ϕ (Contreras and Brown, 2018)

Table 6.2 Input data for slope stability analyses with program Slide

Model	Uncertain variable	Distribution	Mean	Standard deviation	Relative minimum	Relative maximum	CC
H-B	σ_{ci} (MPa)	Beta	59.3	4.7	15.3	18.7	0.00
	m_i	Beta	13.3	3.5	8.3	13.7	
	GSI	Beta	39.7	0.9	3.5	3.1	
	D	Triangular	0.80		0.2	0.2	
M-C	*c* (kPa)	Beta	280.3	28.3	90.3	89.7	0.99
	ϕ (°)	Beta	39.1	3.0	10.1	8.9	

Note: CC – Coefficient of correlation

6.6.1 Analysis of the reliability of the slope

Contreras and Brown (2018) examined the slope reliability analysis with the FORM approach using different variants of the method. They validated the procedure using the MCMC samples from a Bayesian analysis presented in this paper. Table 6.3 shows the main results of the analysis for the slope characterised with the H-B parameters. The analyses include two iterations to ensure that the design point is on the LSS as predicted with the RS. The first iteration uses RS1 which is constructed with points arranged around the mean values, and the second iteration uses RS2 which is based on points arranged around the design point from iteration 1. The scatter plots shown in Figure 6.17 correspond to the results of the second iteration and include the mean values, the LSS and the design point. The distance between the mean and design points provides a visual indication of the available contribution from each parameter to the strength of the rock mass. The results of Figure 6.19 suggest that D and m_i are the parameters with more capacity for stability.

Table 6.3 Summary of results of FORM analyses of the slope with H-B parameters

Iteration	RS	Centre of RS				Design point						
		σ_{ci} (MPa)	m_i	GSI	D	FS RS	β	σ_{ci}* (MPa)	m_i*	GSI*	D*	FS model
1	RS1	59.3	13.3	39.7	0.80	0.999	1.72	60.1	10.4	39.2	0.92	0.996
2	RS2	60.1	10.5	39.2	0.92	1.001	1.78	61.1	9.0	39.5	0.89	1.003

Note: The parameters followed by an asterisk correspond to the design point.

Similarly, the results of the FORM analysis with the equivalent M-C parameters are shown in Table 6.4 and Figure 6.18. The visualisation of the elements of the FORM analysis is much simpler with the two-dimensional rock strength model. In this case, the more relevant feature of the results is the high correlation between c and ϕ and the clear outlining of the LSS. The similarity between the distances from the design point to the mean indicates a balanced contribution from both parameters to the stability of the slope.

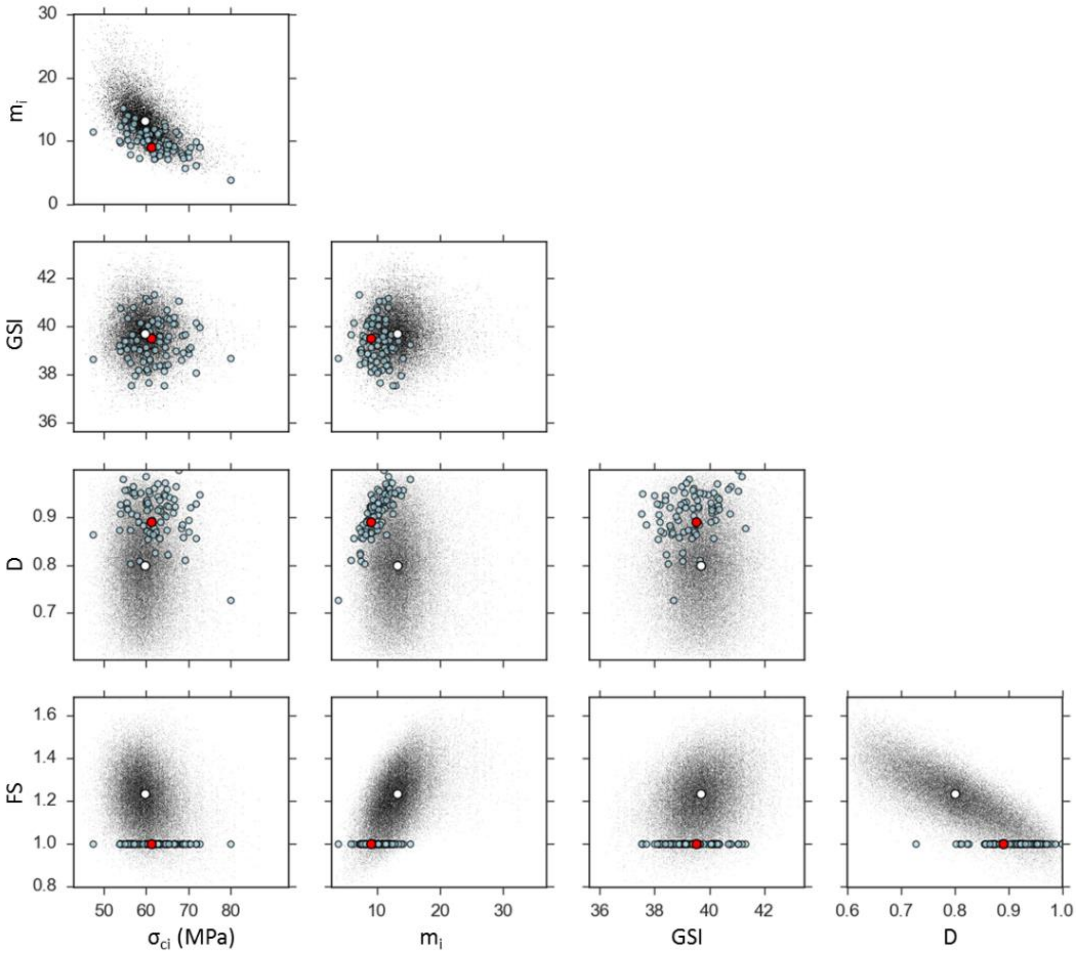

Figure 6.17 Scatter plots of the H-B strength parameters and FS values, including the mean values (white dots), the points on the LSS (blue dots) and the design point (red dots). The results correspond to the second iteration of analysis considering an RS centred in the calculated design point from the first iteration (Contreras and Brown, 2018)

Table 6.4 Summary of results of FORM analysis of the slope with M-C parameters

Iteration	RS	Centre of RS		Design point				
		c (kPa)	ϕ (°)	FS RS	β	c^* (kPa)	ϕ^* (°)	FS model
1	RS1	280.3	39.1	1.001	1.68	233.5	34.0	0.999
2	RS2	233.7	34.0	1.001	1.62	234.6	34.2	1.014

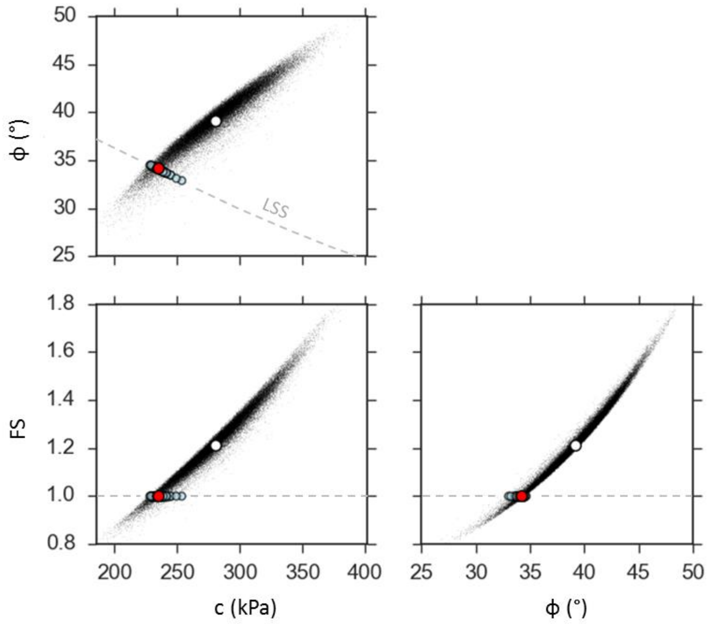

Figure 6.18 Scatter plots of the M-C strength parameters and FS values, including the mean values (white dots), the points on the LSS (blue dots) and the design point (red dots). The results correspond to the second iteration of analysis considering an RS centred in the calculated design point from the first iteration (Contreras and Brown, 2018)

Table 6.5 shows a summary of the results of the reliability analyses for the two strength models considered. The direct calculations of PF and β from the probabilistic analysis with the program Slide (procedure 1) is compared with the FORM analysis using the MCMC samples from the Bayesian inference of parameters (procedure 4). The MC trials from procedure 1 were also used with the RS model to verify its efficacy as a surrogate slope model (procedure 2). The MCMC samples were also used for the direct calculation of PF and β with the RS (procedure 3) to validate the results with the FORM approach.

The results from procedures 1 and 2 are similar, suggesting an acceptable performance of the RS as a surrogate model. These procedures are based on the MC trials with the slope model, which cannot represent the correlation between σ_{ci} and m_i due to limitations of the program Slide. This situation may be a factor contributing to the difference with the result based on the MCMC samples, for the H-B model case. However, the results from all the procedures have a good agreement for the M-C model case. The results from procedures 3 and 4 are similar in all cases, indicating the adequate performance of the FORM approach. The argument in favour of the results based on the posterior samples from the Bayesian analysis is that they correspond to a more accurate representation of the uncertainty of the input parameters as compared with the case of the fitted beta distributions used to draw samples with the MC procedure in Slide. The weakness of the procedures based on the MCMC samples is that they use a surrogate model to represent slope performance; however, the effect of this drawback is minimised in the FORM approach with the iterative procedure used to update the RS so that the new RS is centred closely to the design point.

Table 6.5 Summary of results of reliability analysis

Model	No.	Procedure	Input distribution	CC	FS_{det}	FS_{mean}	PF	β
H-B	1	Slide + MC trials	Beta [a]	0	1.229	1.216	6.03%	1.561
	2	RS + MC trials	Beta [a]	0	1.229	1.217	6.01%	1.536
	3	RS + MCMC points	Posterior [b]	-0.59	1.229	1.214	4.01%	1.711
	6	FORM + MCMC points	Posterior [b]	-0.59	1.229		3.76%	1.779
M-C	1	Slide + MC trials	Beta [a]	0.97	1.201	1.204	4.77%	1.648
	2	RS + MC trials	Beta [a]	0.97	1.201	1.206	4.49%	1.646
	3	RS + MCMC points	Posterior [b]	0.97	1.201	1.207	4.66%	1.644
	6	FORM + MCMC points	Posterior [b]	0.97	1.201		5.23%	1.623

[a] Sampled with the MC method; [b] Sampled with the MCMC algorithm.

6.6.2 Back analysis of slope failure

The reliability analysis described in the previous section corresponds to a forward stability analysis of the slope where the FS is calculated with a surrogate model from the more likely values of the input parameters. These values are defined within the Bayesian framework as a balanced outcome between prior information and data. Figure 6.19 shows the scatter plots and histograms of the input parameters and the calculated FS of the slope example. This plot is equivalent to the corner plot in Figure 6.17, where the sample points have been replaced by density contours. The Bayesian model can also be used to update the estimation of the input parameters based on the performance of the slope for the situation when slope failure is observed. In this case, the condition $FS = 1$ is treated as a data point that can be compared with the model prediction of FS. Figure 6.20 shows the scatter plots and histograms of the input parameters and the FS of the slope for a back analysis of slope failure supported by 10 observations of this event.

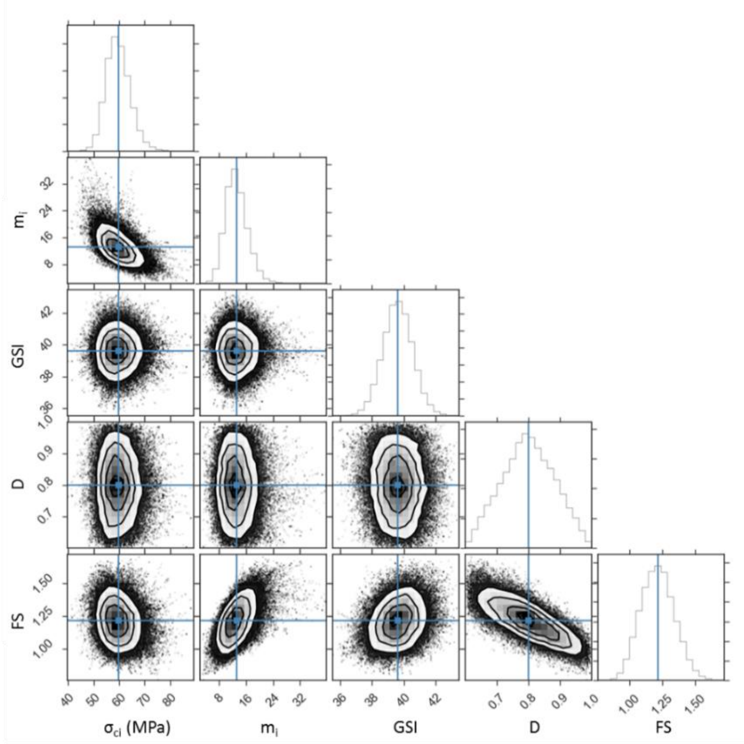

Figure 6.19 Scatter plots and histograms from the forward stability analysis of the slope based on the Bayesian inference of geotechnical parameters

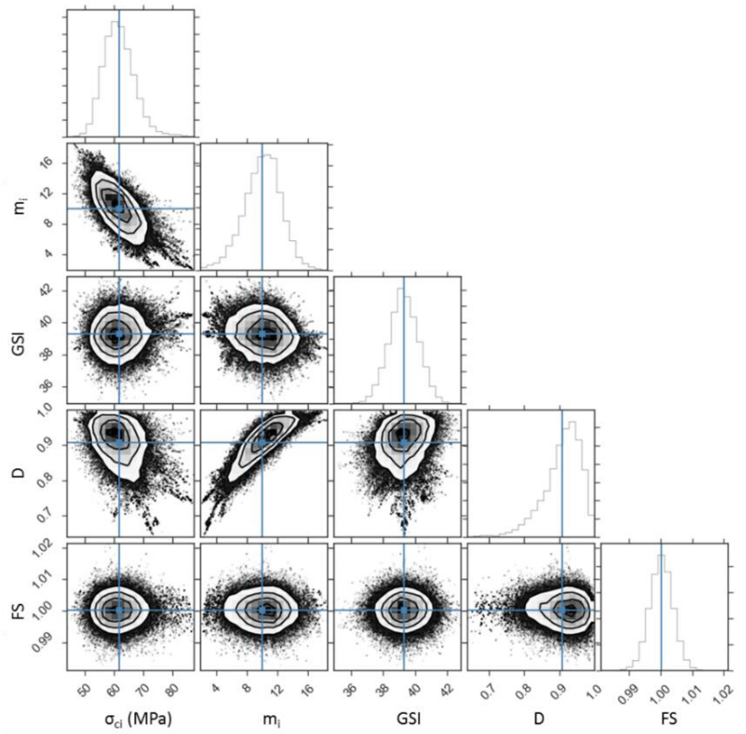

Figure 6.20 Scatter plots and histograms from the back analysis of slope failure including the Bayesian updating of geotechnical parameters for the case of 10 observations of slope failure

The back analysis of slope failure requires a sufficient number of observations to outbalance the effect of the initial input parameters. The input parameters are updated according to their uncertainty, which is determined by the amount of data supporting them. For example, factor *D* is based on prior information, without any data support, and for this reason, it is the parameter that is more affected by the updating process. Nevertheless, the other parameters sustain minor adjustments based on their data support. The plot in Figure 6.21 shows the relationship between the number of slope failure observations included in the analysis and the variability of the calculated FS. The forward analysis corresponds to the case of zero observations of failure and the graph indicates that for this example, at least five observations of failure are required to enforce the slope failure condition.

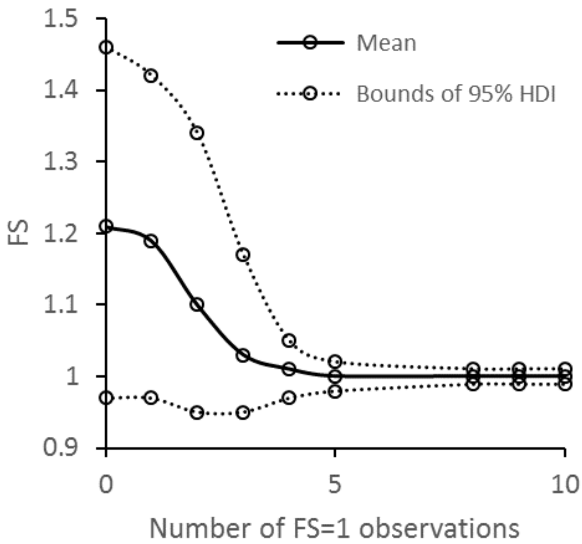

Figure 6.21 Relationship between the number of observations of failure and the variability of the FS from the back analysis of slope failure. At least five observations are required to outbalance the effect of the initial input parameters

The updating of the input parameters from the back analysis of failure can be better appreciated with their histograms as shown in Figure 6.22. The graph includes the distributions of the parameters used in the forward analysis and the updated distributions when the failure condition is imposed with 10 observations of failure. The analysis corresponds to the case where the intact rock strength estimation is based on 23 data points (8 UCS + 15 TCS), as described in Section 6.2.2. The prior distributions of these parameters are also included in the graph. The main adjustment occurs in the factor *D*, which is not supported by data. The second major adjustment occurs in the parameter m_i, which is supported by TCS data. The GSI is slightly affected by the updating process, suggesting adequate data support. The σ_{ci} parameter is hardly modified, indicating that the number of UCS values provides strong support of this parameter.

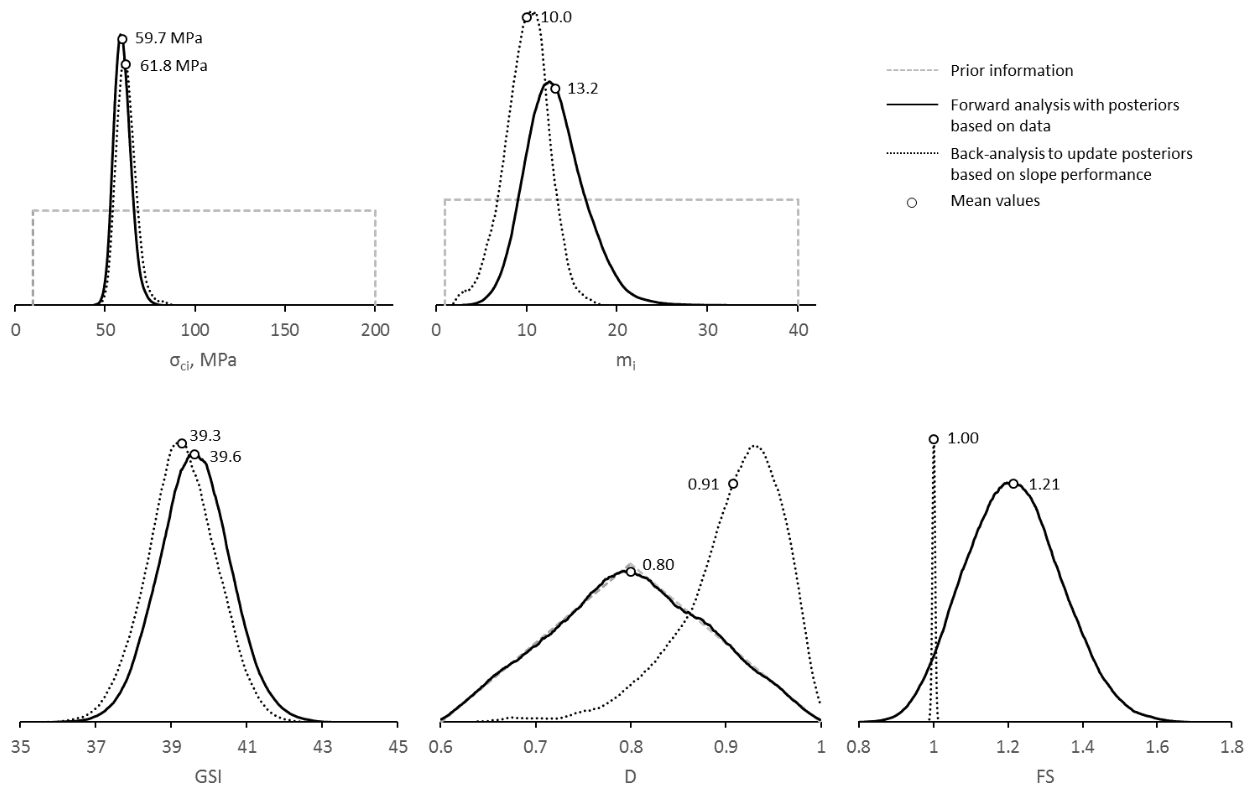

Figure 6.22 Histograms of input parameters and FS, including the forward analysis of stability and the back analysis based on 10 observations of slope failure. Intact rock strength parameters based on 23 data points (8 UCS + 15 TCS)

The effect of data support on the updating process can be appreciated in Figure 6.23, which includes the histograms of parameters from the forward and back analyses of failure for the case where the intact rock strength parameters are supported by 10 data points (5 UCS + 5 TCS), as described in Section 6.2.2. In this case, there is a larger uncertainty in the H-B envelope, which is manifested in the wider spread of m_i values as compared with the case shown in Figure 6.22. For this reason, a larger adjustment of m_i occurs during the updating process, highlighting the relationship that exists between data support, the uncertainty of the parameter and its updating potential.

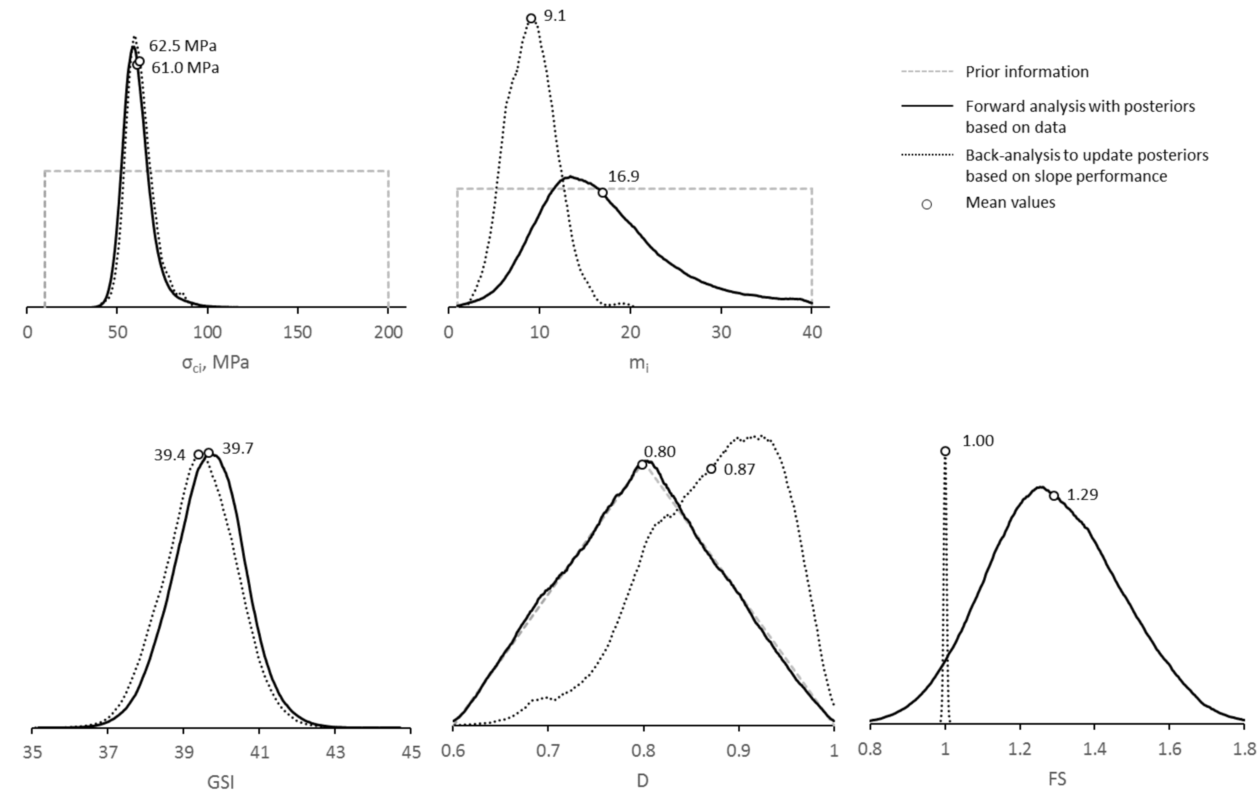

Figure 6.23 Histograms of input parameters and FS, including the forward analysis of stability and the back analysis based on 10 observations of slope failure. Intact rock strength parameters based on 10 data points (5 UCS + 5 TCS)

The Bayesian back analysis of slope failure can be used for the calibration of parameters that are difficult to quantify such as the factor *D*, provided that there is good data support for the remaining parameters. The methodology is also useful to identify deficiencies in data support indicated by larger adjustments from the updating process.

6.7 Conclusions

The Bayesian inference of the geotechnical parameters has advantages over the conventional methods of statistical analysis used for this purpose. The Bayesian approach provides an adequate quantification of the uncertainty of the rock mass strength parameters used for slope design. The results of the analysis include representative samples of σci, mi and GSImean values, with information on their variability and correlations. The methodology also shows the relationship between data quantity and the uncertainty of the inferred parameters. The posterior samples of the H-B parameters from the Bayesian analysis can be used to create posterior samples of equivalent M-C parameters c and φ for a specified maximum confining stress level. The result carries the high correlation structure typical of the M-C parameters.

The conventional FORM analysis of reliability considers predefined probability distributions to represent the variability of the uncertain parameters and it is based on a constrained minimisation of a function. The distributions are commonly the result of a fitting analysis where data or samples of parameter values are used as the source information. In contrast, the FORM method presented in this paper for the slope reliability assessment uses the posterior distributions from the Bayesian analysis to represent the input parameters and the FS and distance to the mean are calculated for every point of the sample. In this way, the constrained minimization is reduced to screening the samples where $FS = 1.0$ and finding the point with the minimum distance to the mean. The method uses a surrogate slope model defined with the RS methodology as the performance function to define the LSS.

There are slight differences between the results from the analysis with the program Slide and the FORM, for the H-B model case. The analyses based on MC sampling from fitted distributions resulted in smaller PF and larger β values than those using the original MCMC posteriors. The argument in favour of the results based on the posterior samples from the Bayesian analysis is that they correspond to a more accurate representation of the uncertainty of the input parameters as compared with the case of the fitted beta distributions used to draw samples with the MC procedure in Slide. The structure of the posterior samples carries the information provided by the data used in the analysis, but this structure is not reproduced in complete detail with the MC sampling due to limitations of the program Slide to represent the correlation between σci and mi. In contrast, the results from both procedures have a good agreement for the M-C model case.

The Bayesian approach is also used to update the estimation of the input parameters from the back analysis of slope failure. In this case, the condition $FS = 1.0$ is treated as a data point that can be compared with the model prediction of FS. The back analysis of slope failure requires a sufficient number of observations of slope failure to outbalance the effect of the initial input parameters. For the slope example presented in this paper, at least five observations of failure are required to enforce the failure condition. The input parameters are updated according to their uncertainty, which is determined by the amount of data supporting them. For example, the D factor is based on prior information, without any data support, and for this reason, it is the parameter that is more affected by the updating process. The influence of data support on the results of the updating process was confirmed for the slope example case by comparing the updating results for the cases of intact rock strength supported by 10 and 23 data points. The example of parameter updating from back analysis of slope failure illustrates the relationship that exists between data support, uncertainty of the parameter and its updating potential. The methodology is useful for the calibration of the D factor, which is difficult to quantify, and for the identification of deficiencies in data support indicated by larger adjustments from the updating process.

The examples of slope reliability and back analysis of failure presented in this paper serve to illustrate the potential of the Bayesian approach for the inference of geotechnical parameters. The methodology combines prior information, data from laboratory and site investigations, and observed performance of the slope, to provide a balanced result.

Conflicts of interest

The authors wish to confirm that there are no known conflicts of interest associated with this publication and there has been no significant financial support for this work that could have influenced its outcome.

Acknowledgements

The first author is supported by the Large Open Pit II project through contract no. 019799 with the Geotechnical Research Centre of The University of Queensland and by SRK Consulting South Africa. Their support is greatly appreciated.

List of abbreviations

CDF	Cumulative distribution function
FORM	First order reliability method
FS	Factor of safety
GSI	Geological Strength Index
H-B	Hoek-Brown (strength criterion or parameters)
HDI	Highest density interval

LSS	Limit state surface
M-C	Mohr-Coulomb (strength criterion or parameters)
MC	Monte Carlo
MCMC	Markov chain Monte Carlo
pdf	Probability density function
PF	Probability of failure
RS	Response surface
TCS	Triaxial compression strength
UCS	Uniaxial compression strength

References

Abramson, L.W., Lee, T.S., Sharma, S. and Boyce, G.M., 2002. *Slope Stability and Stabilization Methods*. Second Edition, John Wiley and Sons, New York.

Aladejare, A.E. and Wang, Y., 2017. Influence of rock property correlation on reliability analysis of rock slope stability: from property characterization to reliability analysis. *Geoscience Frontiers*. https://doi.org/10.1016/j.gsf.2017.10.003.

Baecher, G.B., 2017. Bayesian thinking in geotechnical applications. *Proceedings of Georisk 2017 on Geotechnical Risk from Theory to Practice*, 4-7 June, Denver, Colorado, USA.

Baecher, G.B. and Christian, J.T., 2003. *Reliability and statistics in geotechnical engineering.* Wiley, Chichester, UK.

Bucher, C.G. and Bourgund, U., 1990. A fast and efficient response surface approach for structural reliability problems. *Structural Safety*, 7(1), 57–66.

Cai, M., Kaiser, P.K., Uno, H., Tasaka, Y. and Minami, M., 2004. Estimation of rock mass deformation modulus and strength of jointed hard rock masses using the GSI system. *International Journal of Rock Mechanics and Mining Sciences*, 41(1), 3–19.

Cai, M. and Kaiser, P.K., 2006. Visualization of rock mass classification systems. *Geotechnical and Geological Engineering*, 24, 1089–1102.

Contreras L.F., Brown E.T. and Ruest M., 2018. Bayesian data analysis to quantify the uncertainty of intact rock strength. *Journal of Rock Mechanics and Geotechnical Engineering*, 10(1), 11-31.

Contreras, L.F. and Brown, E.T., 2018. Bayesian inference of geotechnical parameters for slope reliability analysis. *Slope Stability Symposium 2018*, Seville, Spain. Bco Congresos, 1998-2026.

Duncan, J.M. and Sleep, M.D., 2015. Evaluating reliability in geotechnical engineering. *Risk and Reliability in Geotechnical Engineering*. K.K. Phoon and J. Ching (editors). CRC Press, Boca Raton, 131–179.

Duran A., 2016. Rock mass assessment – what goes wrong? In P. Dight (editor). *Proceedings of the First Asia- Pacific Slope Stability in Mining Conference*, Brisbane, Australia. Australian Centre for Geomechanics, Perth, 493-506.

Feng, X. and Jimenez, R., 2015. Estimation of deformation modulus of rock masses based on Bayesian model selection and Bayesian updating approach. *Engineering Geology,* 199, 19–27.

Foreman-Mackey, D., Hogg, D.W., Lang, D. and Goodman, J., 2013. emcee: The MCMC Hammer. *Publications of the Astronomical Society of Pacific*, 125(925), 306–312.

Goh A.T.C. and Zhang W., 2012. Reliability assessment of stability of underground rock caverns. *International Journal of Rock Mechanics and Mining Sciences*, 55, 157–163.

Hasofer, A. M., and Lind, N., 1974. An exact and invariant first-order reliability format. *Journal of Engineering Mechanics*, ASCE, 100(1), 111-121.

Hoek, E., 1994. Strength of rock and rock masses. *International Society for Rock Mechanics News Journal*, 2(2), 4-16.

Hoek E. and Brown E.T., 1997. Practical estimates of rock mass strength. *International Journal of Rock Mechanics and Mining Sciences*, 34(8), 1165–1186.

Hoek E., Carranza-Torres C. and Corkum B., 2002. Hoek-Brown failure criterion – 2002 edition. *Proceedings of the fifth North American rock mechanics symposium*, Toronto, Canada, 1, 267–273.

Hoek, E., Carter, T.G. and Diederichs, M.S., 2013. Quantification of the Geological Strength Index Chart. *Proceedings of the 47th US Rock Mechanics / Geomechanics Symposium*, San Francisco, 23-26 June, Paper ARMA 13–672, 8 p.

Hoek, E. and Martin, D., 2014. Fracture initiation and propagation in intact rock – A review. *Journal of Rock Mechanics and Geotechnical Engineering*, 6(4), 287-300.

Juang, C.H. and Zhang, J., 2017. Bayesian Methods for Geotechnical Applications - A Practical Guide. *Proceedings of Georisk 2017 on Geotechnical Risk from Theory to Practice*, 4-7 June, Denver, Colorado, USA.

Low, B. K. and Tang, W. H., 1997. Efficient reliability evaluation using spreadsheet. *Journal of Engineering Mechanics*, ASCE, 123(7), 749–752.

Low, B.K. and Tang, W. H., 2004. Reliability analysis using object-oriented constrained optimization. *Structural Safety*, Elsevier Science Ltd., Amsterdam, 26(1), 69–89.

Low B.K. and Tang W.H., 2007. Efficient spreadsheet algorithm for first-order reliability method. *Journal of Engineering Mechanics*, ASCE, 133(12), 1378–1387.

Low, B. K., 2008. Efficient probabilistic algorithm illustrated for a rock slope. *Rock Mechanics and Rock Engineering*, 41(5), 715–734.

Miranda, T., Correia, A.G. and Sousa, L. R., 2009. Bayesian methodology for updating geomechanical parameters and uncertainty quantification. *International Journal of Rock Mechanics and Mining Sciences*; 46(7), 1144–1153.

Palmström, A., 1996. Characterizing rock masses by the RMi for use in practical rock engineering. *Journal of Tunnelling and Underground Space Technology*, 11(2), 175-188.

Python Software Foundation, 2001. *Python language reference*, version 3.4 [on line]. [Accessed 20/01/2015]. https://www.python.org/.

Rocscience Inc., 2016. Slide v7.0 – Two-Dimensional Limit-Equilibrium Analysis of Soil and Rock Slopes.

Russo, G., 2009. A new rational method for calculating the GSI. *Journal of Tunnelling and Underground Space Technology*, 24(1), 103–111.

Sonmez, H. and Ulusay R., 1999. Modifications to the geological strength index (GSI) and their applicability to stability of slopes. *International Journal of Rock Mechanics and Mining Sciences*, 36, 743–760.

Steffen, O.K.H., Contreras, L.F., Terbrugge, P.J. and Venter, J., 2008. A risk evaluation approach for pit slope design. *Proceedings of the 42nd US Rock Mechanics Symposium and 2nd US-Canada Rock Mechanics Symposium*, San Francisco, 29 June - 2 July, Paper ARMA 08–231, 18 p.

Wang, Y. and Aladejare, A.E., 2016. Evaluating variability and uncertainty of Geological Strength Index at a specific site. *Rock Mechanics and Rock Engineering*, 49(9), 3559-3573.

Zhang, L.L., Zhang, J., Zhang, L.M. and Tang, W.H., 2010. Back analysis of slope failure with Markov chain Monte Carlo simulation. *Computers and Geotechnics*, 37(7–8), 905-912.

Chapter 7 - Conclusions and Future Research

7.1 Conclusions

The overall objective of the PhD thesis was to explore the Bayesian approach of statistical analysis for the inference of parameters and to assess its applicability for the characterisation of the geotechnical model for slope design in open pit mining. The main tasks for the attainment of this objective included the understanding of the conceptual basis of the approach, the comparison with the conventional classical approach used in slope design, and the application of the approach to simple problems found in the slope design process. The outcome of these tasks is reflected in the four papers included in Chapters 3 to 6.

The Bayesian approach is normally presented in the literature using a formal mathematical framework, which has precluded its diffusion within the mining geotechnical community. Therefore, the presentation of the approach in the thesis favours intuitive descriptions aiming to a wider audience of geotechnical practitioners. The specific outcomes of the topics treated in the papers were summarised in the previous chapter and can also be found in the conclusions section of each paper. The most significant overall conclusions from the work presented in the thesis are summarised as follows.

(1) The Bayesian approach of statistical analysis is more suitable for the quantification of the geotechnical uncertainty in slope design as compared with the classical approach (frequentist). The two approaches are based on different definitions of probability and different sets of assumptions that suit different types of uncertainty. The scarcity of data is a common occurrence in the slope design process and the corresponding knowledge uncertainty (epistemic) derived from this situation is better treated with Bayesian methods. In contrast, classical methods are meant to treat aleatory uncertainty (natural variation), which implies the availability of abundant information for its characterisation.

(2) The use of the classical approach of statistical analysis is generalized in the mine slope design process mainly because it is perceived as the only available option. In addition, most geotechnical engineers have a rudimentary understanding of the

conceptual framework of the approach, which normally causes the misinterpretation of its results. A notorious example of this situation is the incorrect interpretation of the CI, whose actual meaning differs from that normally assigned by the analyst based on his/her needs. Interestingly, the wished interpretation of the CI in the classical approach is the actual interpretation of the HDI in the Bayesian approach. This observation supports the statement that the Bayesian approach addresses the question of interest to the geotechnical engineer.

(3) One of the more attractive features of the Bayesian approach for the inference of geotechnical parameters is the possibility of using other sources of information not represented by data, in addition to the conventional data sets. This means that subjective information such as expert opinion or engineering judgement can be incorporated formally into the slope design process. In contrast, the classical approach of statistical analysis only allows the use of data, which ideally should be the result of a random sampling process to have meaningful results.

(4) The Bayesian model for the inference of parameters is not constrained by the number of uncertain variables. Therefore, the data sets, geotechnical parameters and prior information conventionally used in the mine slope design process can be encoded in a posterior pdf that captures the interdependencies between all the parameters. The samples drawn from this distribution with an MCMC procedure are a good representation of the geotechnical parameters for design, reflecting the balance between data and prior information.

(5) The method for the Bayesian inference of parameters can be applied to a range of situations from single rock properties and basic characterisation models through to higher-level models that combine the simpler models. Examples of these types of applications include inference of the mean UCS (paper-I), inference of the intact H-B strength parameters σ_{ci} and m_i (paper-II), inference of the GSI chart parameters (papers III and IV) and inference of the H-B rock mass strength parameters using observations of slope performance (paper-IV).

(6) The results of the Bayesian analysis enable a rational assessment of the sufficiency of data at different stages of project development. The results reflect the balance between prior information and data; therefore, if data is weak the prior knowledge

dominates the result. As more data is collected the Bayesian results move toward stable values that are unaffected by the prior component. The prior serves in this case to test the strength of data and this behaviour provides the analyst with a good reference to judge the adequacy of the data set.

7.2 Future research

The research work presented in the thesis enabled the identification of specific benefits of using the Bayesian approach for the inference of the geotechnical parameters for slope design in open pit mining. However, some of these benefits need more evaluation as explained in this section.

The specific benefits of using the approach for mine slope design are:

(1) It allows the formal use of prior knowledge (engineering judgement, expert opinion).

(2) It provides richer and intuitive quantification of the confidence of parameters (i.e. HDI from posterior distribution is better than CI).

(3) It facilitates the adequate handling of outliers without subjective manipulation of data sets.

(4) It produces results where the correlation between parameters is an output, not an assumption.

(5) It enables a rational assessment of the sufficiency of data from the updating process (e.g. by checking the balance between prior knowledge and data at different stages).

(6) It allows the construction of hierarchical models that incorporate multiple sub-models with numerous parameters into a single high-level model to improve the updating process (e.g. rock mass characterisation sub-models embedded into slope stability model).

(7) It can make use of data from slope performance for model calibration to support the inference of geotechnical parameters (e.g. observations of slope failure or slope displacements).

All these benefits have been discussed in varying degrees of detail, including illustrative examples, in the papers of Chapters 3 to 6. However, points (5) to (7) require further evaluation using data sets from actual mine sites as a necessary step to define criteria to judge data requirements and to develop more elaborated models for inference of parameters. These topics are described in more detail next.

7.2.1 Assessment of sufficiency of data

The relationship between data quantity and the uncertainty of the inferred parameters was illustrated for the case of the H-B intact strength parameters σ_{ci} and m_i, in the example presented in Section 6.2.2. The graphs in Figure 7.1 correspond to that example and show the changes in the mean value and the width of the 95% HDI of the inferred parameters for an increase in the number of data points from five to twenty-three. The data points include UCS and TCS test results, which have a predominant influence on σ_{ci} and m_i, respectively. These graphs show that the mean values and the variability of the parameters tend to a stable situation after a certain number of data points, which is a behaviour that could be used to assess the sufficiency of data. The issue of determining the minimum number of laboratory tests required to define the mechanical properties of rocks was investigated by Gill et al. (2005) using concepts of classical statistics.

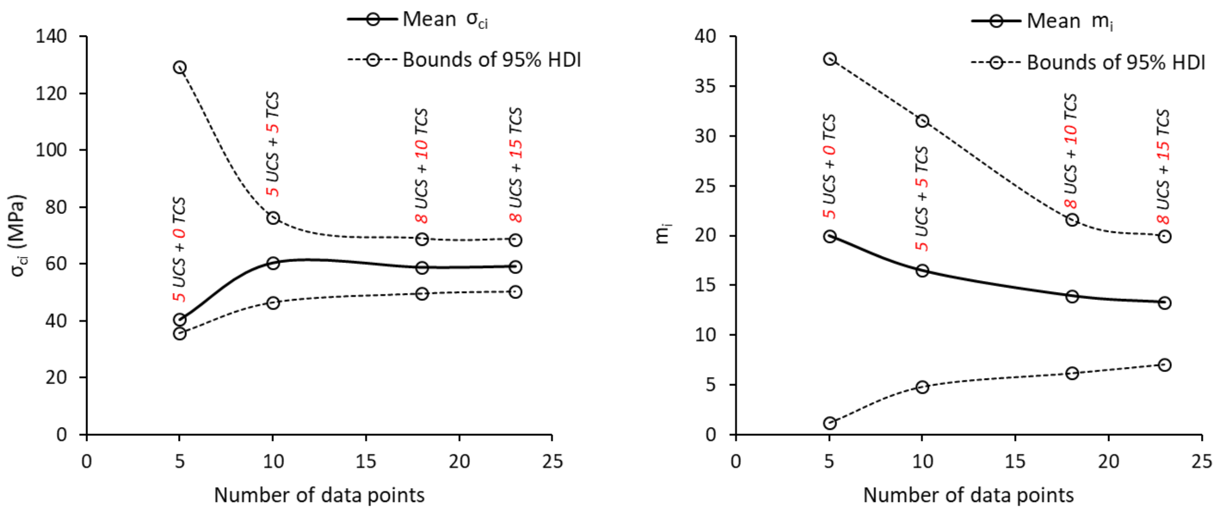

Figure 7.1 Relationship between the number of data points and the variability of the intact H-B rock strength parameters σ_{ci} and m_i from the example presented in Section 6.2.2

The graphs in Figure 7.1 provide a qualitative reference to define the sufficiency of laboratory testing data for the characterisation of the intact rock strength. However, they could also be useful to derive specific criteria to assess the number of test results required for a particular project stage. For example, the percentages of change of the mean and width of HDI could serve as a measure of the degree of convergence of the estimates. Table 7.1 shows the percentages of change relative to the previous data stage, normalised to the number of added data points, for the intact rock strength parameters inferred according to the stages depicted in Figure 7.1.

Table 7.1 Percentages of change of inferred parameters with the number of data points

Data stage	No. data points	Type of data	% change σ_{ci}		% change m_i	
			mean	HDI width	mean	HDI width
1	5	5UCS+0TCS				
2	10	5UCS+5TCS	6.6%	-21%	-4.2%	-12%
3	18	8UCS+10TCS	-0.3%	-2%	-2.3%	-10%
4	23	8UCS+15TCS	0.1%	-0%	-1.0%	-4%

The study of the relationship between parameter variability and data quantity, including the definition of criteria to assess the sufficiency of data, could be a topic for further research. This study could include analyses similar to that presented in Figure 7.1, using different databases and considering other geotechnical parameters.

7.2.2 Hierarchical model for inference of parameters from slope performance

The concept of Bayesian updating of geotechnical parameters described in Section 2.6.6 can be applied to the geotechnical model for slope design. In this case, classical Bayesian updating can be used for the estimation of parameters such as *UCS*, σ_{ci}, m_i, *GSI*, base friction angle (Φ_b), joint roughness coefficient (*JRC*) and joint compressive strength (*JCS*). These analyses imply the fitting of data from laboratory or in-situ measurements to predictions with the pertinent models such as Hoek-Brown intact rock strength, *GSI* and Barton-Bandis joint strength. The Bayesian updating model based on slope performance can be implemented by comparing the deformation measurements routinely taken during the mine operation, with predictions encoded in a polynomic function defined with a response surface methodology. This slope performance model is a hierarchical Bayesian model that includes the rock characterisation models as component sub-models.

Figure 7.2 illustrates how the Bayesian updating of geotechnical parameters can be incorporated into the conventional mine slope design process. This concept is developed further in the diagram of Figure 7.3, which shows the structure of the component modules of the overall hierarchical model. The major components include the intact rock strength, the rock mass quality and the joint strength modules that feed information into the slope performance model. Each module includes one or more sub-models for the estimation of specific parameters. Every sub-model comprises the prior information on the target parameters, the model function and the data set to fit the function. The data sets can be global or local as required. For example, if the objective is to define the factor α_1 that relates *UCS* and *PLT*, a global database can be used to establish an ad hoc factor. The estimated α_1 factor not only honours the data but also accounts for the constraints imposed by the other components of the model. The approach of using global databases linked to the overall model to re-evaluate parameters provides estimates tailored for the project under evaluation. These parameters would otherwise be pre-defined deterministic values.

The intact rock strength module in Figure 7.3 uses the Hoek-Brown strength criterion to fit data from *UCS* and *TCS* testing with the purpose of estimating σ_{ci} and m_i and their correlation characteristics. The local database of *PLT* is used to supplement the UCS data set using the correlation factor estimated from the global database.

The rock mass quality module uses the definition of the *GSI* system to fit measurements of V_b and J_C to *GSI* data collected for calibration purposes. The estimated factors ρ_1, ρ_2, and ρ_3 are used with a local database of V_b and J_C measurements to supplement the *GSI* database. The rock mass quality result corresponds to the mean *GSI* used for the slope stability analysis.

The joint strength module uses the Mohr-Coulomb strength criterion to fit data from direct shear tests on saw-cut surfaces, yielding estimates of the base friction angle (Φ_b) as a result. These estimates are used by the second model in the module that uses the Barton-Bandis joint strength criterion to fit data from direct shear tests on natural joints to get estimates of *JRC* and *JCS*.

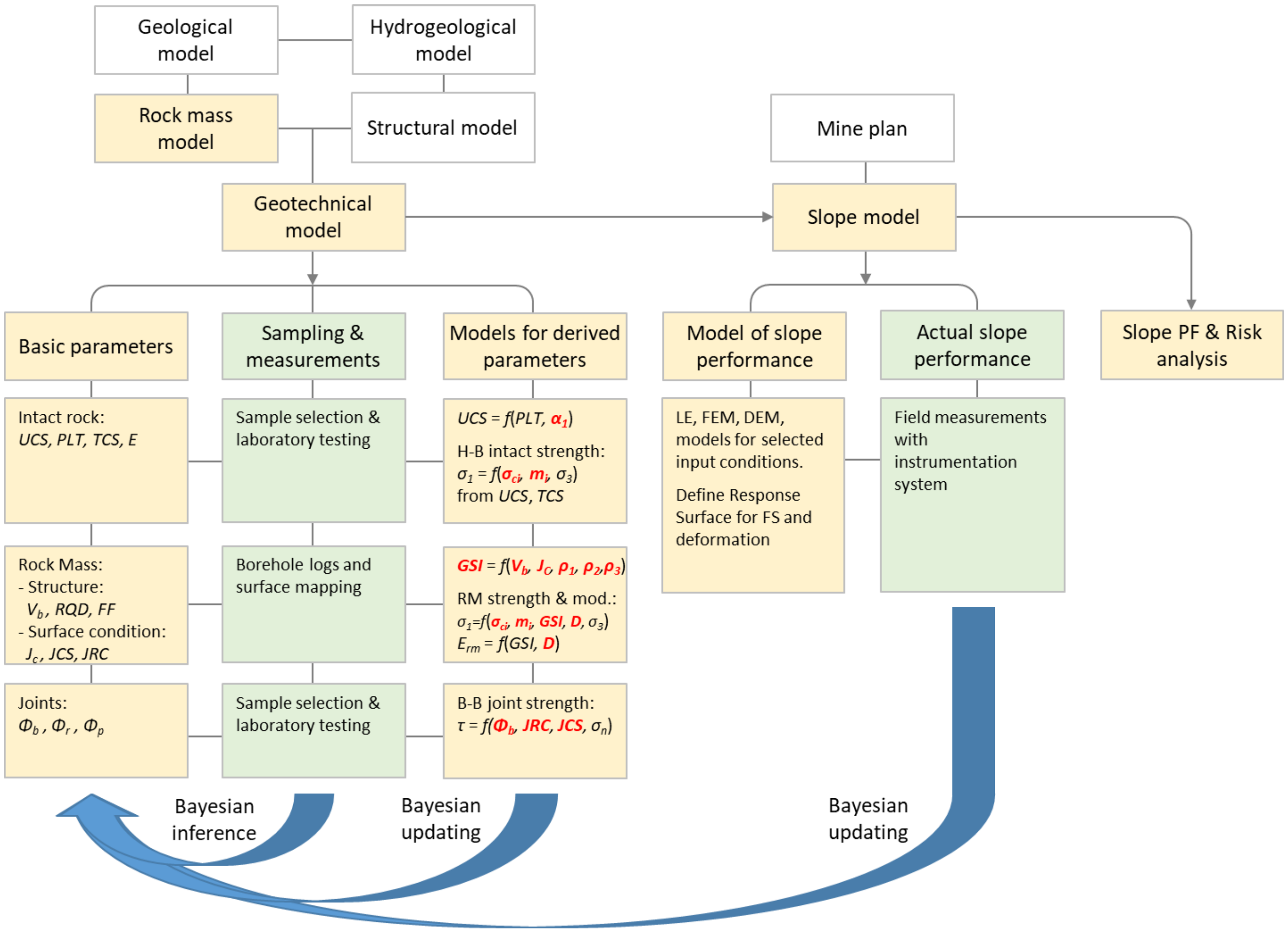

Figure 7.2 Bayesian updating of geotechnical parameters in the mine slope design process

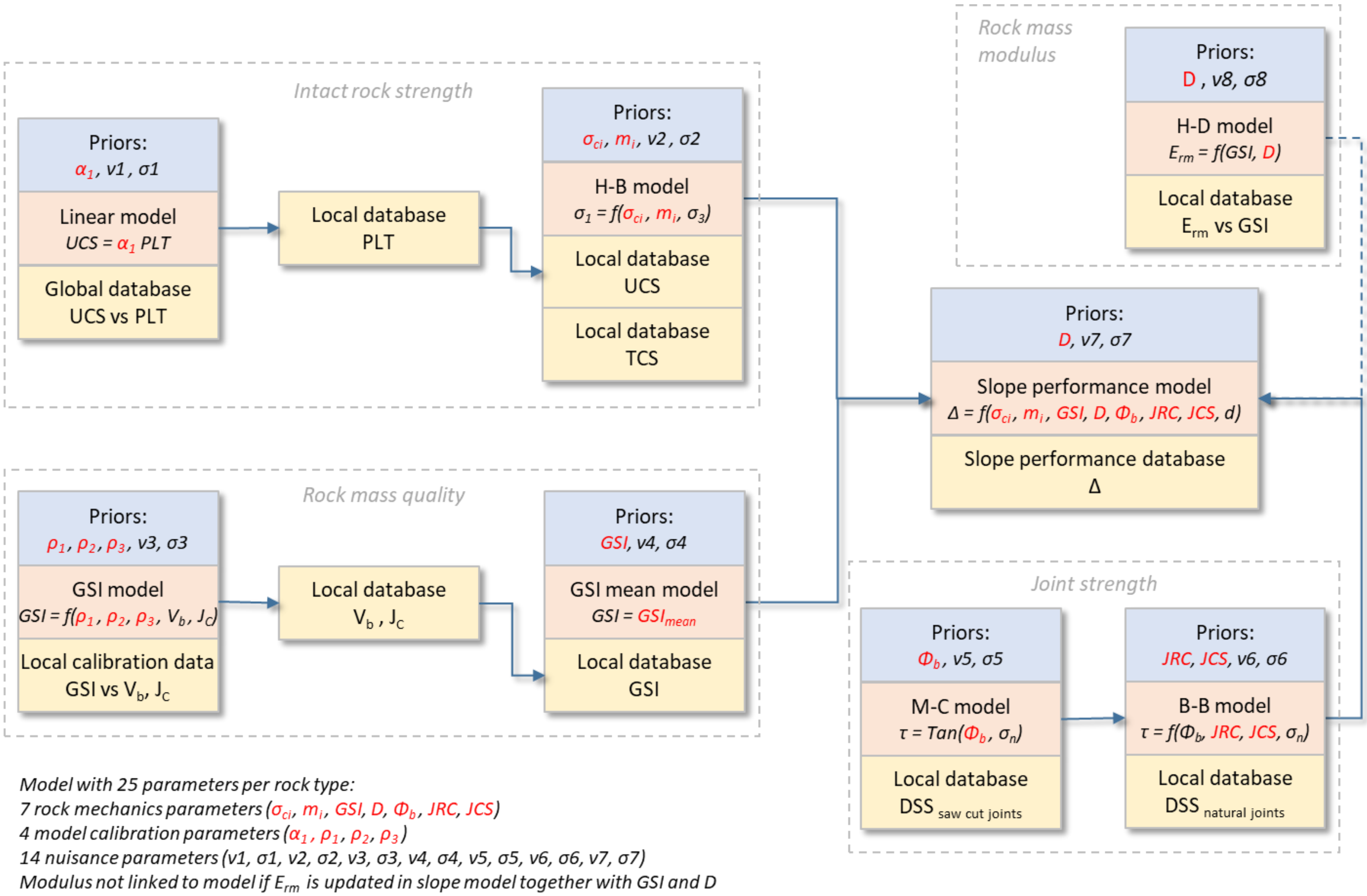

Figure 7.3 Component sub-models of the hierarchical model for Bayesian updating of geotechnical parameters

The slope performance model defined with the response surface methodology uses the rock parameters estimated with the various sub-models as outlined in Figure 7.3. The predictions with the slope performance model are compared with actual field measurements and this process introduces an additional constraint that is informed back into the component sub-models, resulting in a better estimation of the geotechnical parameters. Juang et al. (2013) describe a similar approach to update soil parameters using field measurements of deformation of braced excavations.

An important factor having an influence on the predicted deformations of the slope is the modulus of deformation of the rock mass (E_{rm}). The conventional way to estimate the modulus of deformation for the mine slope design is based on the empirical correlation proposed by Hoek and Diederichs (2006), which relates modulus measurements with various rock mass properties. The modulus depends on *GSI* and *D* when the simplified correlation is considered. If there is a local database of E_{rm} versus *GSI*, the modulus correlation can be used as an additional criterion to estimate *D*. In this case, the rock mass modulus module in Figure 7.3 should be linked with the slope performance model. If local modulus data is not available then the rock mass modulus should be updated consistently with changes of *GSI* and *D* within the slope analysis.

The model outlined in Figure 7.3 considers 25 parameters including seven rock mechanics parameters (σ_{ci}, m_i, *GSI, D,* Φ_b*, JRC, JCS*), four model calibration parameters ($\alpha_1, \rho_1, \rho_2, \rho_3$) and fourteen nuisance parameters (v_i and σ_i for i = 1 to 7 to model the errors with Student t-distributions).

The sub-models depicted in this diagram can be implemented in the appropriate computer code and can be tested independently before they are incorporated into the overall model. The intact rock strength sub-model is completed and it was described in papers II and IV. The rock mass quality sub-model is completed and it was described in papers III and IV. A simple slope performance model including the two previous sub-models was described in Paper-IV, considering a single rock unit and the slope performance represented by observations of failure. A topic for further research could include the development of the hierarchical model described conceptually in Figure 7.3, including the joint strength module. This model could be tested with actual datasets of slopes with multiple geotechnical units.

References

Gill, D.E., Corthesy, R. and Leite, M.H., 2005. Determining the minimal number of specimens for laboratory testing of rock properties. *Engineering Geology*, 78, 29–51.

Hoek, E. and Diederichs, M.S., 2006. Empirical estimation of rock mass modulus. *International Journal of Rock Mechanics and Mining Sciences*, 43, 203–215.

Juang, C.H., Luo, Z., Atamturktur, S. and Huang, H., 2013. Bayesian Updating of Soil Parameters for Braced Excavations Using Field Observations. *Journal of Geotechnical and Geoenvironmental Engineering*, ASCE, 139(3), 395–406.